Power electronics

Oliver Wallscheid

Universität Siegen / IAS Interconnected Automation Systems

Table of contents

Table of contents

What are power electronics?

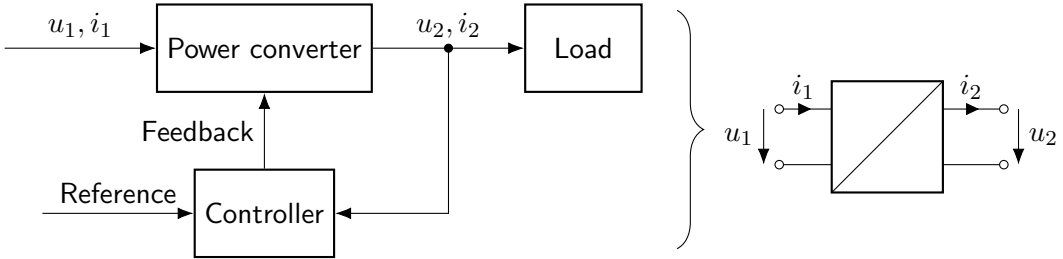

Fig. 1.1: High-level block diagram of a power electronic system

Power electronics – a definition

Power electronics is a multidisciplinary branch of electrical engineering. It focuses on processing, controlling, and converting electric power. Power electronics manipulate voltages and currents to deliver a defined power to electrical equipment and devices.

Power electronics vs. microelectronics

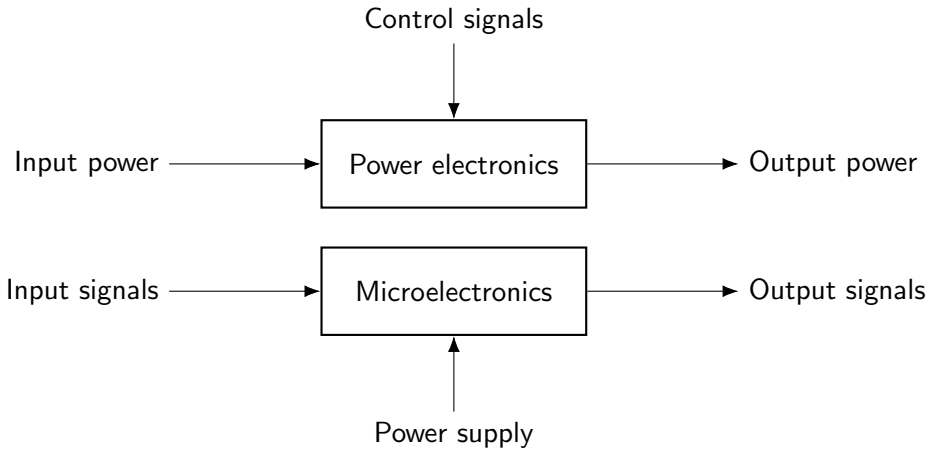

Fig. 1.2: Power electronics vs. microelectronics

Typical voltage and current manipulation tasks of power electronics

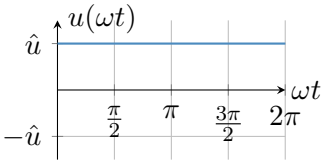

rectifier ↑ ↓ inverter

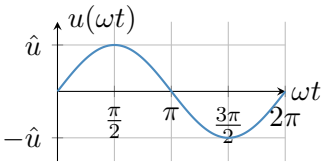

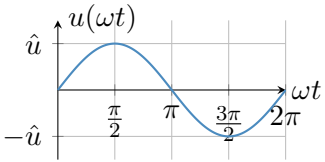

frequency ↕ phase ↕ amplitude

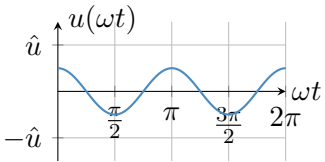

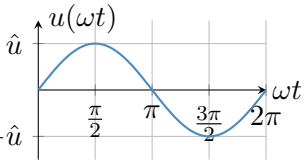

number of phases ↕

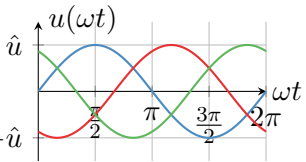

Power electronic application examples: residential

(a) Home appliances (source: pxhere, CC0 1.0)

(b) Smartphone charger (source: rawpixel, CC0 1.0)

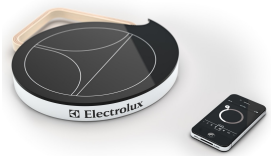

(c) Induction plate (source: flickr, Electrolux, CC BY-SA-NC 2.0)

(d) LED rectifier (source: Wikimedia Commons, D. Tribble, CC BY-SA 4.0)

Power electronic application examples: industrial

(a) Uninterruptible power supply (source: Wikimedia Commons, Stevebwallace, CC BY-SA 4.0)

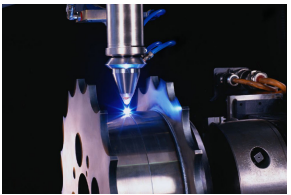

(b) Welding power supply (source: Wikimedia Commons, Trumpf GmbH, CC BY-SA 3.0)

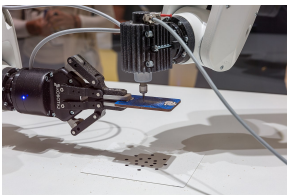

(c) Industrial drives / automation (source: Wikimedia Commons, M. Blume, CC BY-SA 4.0)

(d) Conveyor belt drive (source: Wikimedia Commons, K. Hannessen, CC BY-SA 4.0)

Power electronic application examples: energy system

(a) Wind power plants (source: pxhere, CC0 1.0)

(b) PV power plants (source: pxhere, CC0 1.0)

(c) Battery storage systems (source: flickr, Portland General Electric, CC BY-ND 2.0)

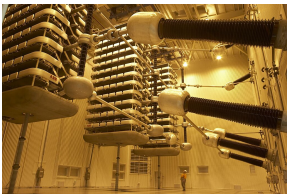

(d) High voltage DC transmission (source: Wikimedia Commons, Marshelec, CC BY-SA 3.0)

Power electronic application examples: transportation

(a) Train drive (source: Wikimedia Commons, T. Wolf, CC0 1.0)

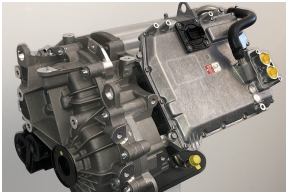

(b) Electric vehicle drive (source: Wikimedia Commons, Caprolactam123, CC BY-SA 4.0)

(c) Electric scooter (source: Wikimedia Commons, Raju, CC BY-SA 4.0)

(d) Electic ship (source: Wikimedia Commons, Wikimalte, CC BY-SA 4.0)

A broad range of nominal power ratings

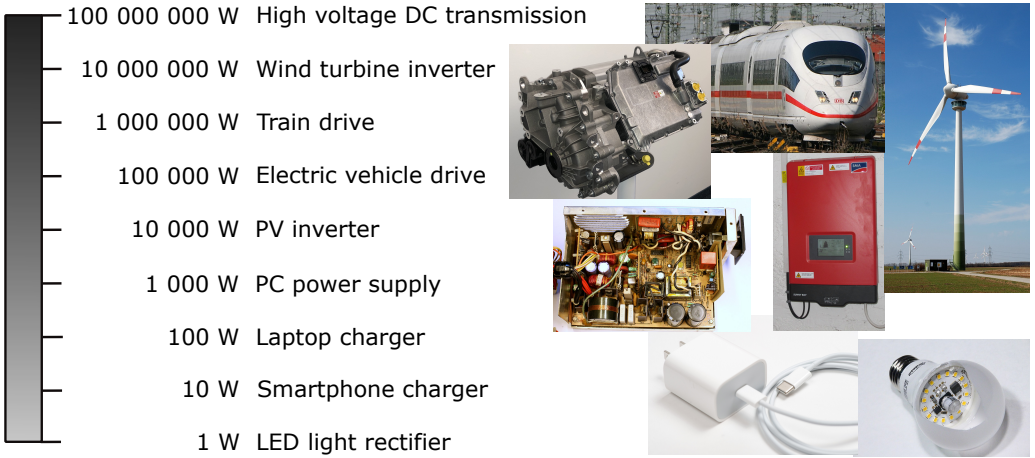

Fig. 1.7: Power range overview (figure sources: T. Wolf, KoeppiK, Caprolactam123, D. Hawgood, Mister rf, D. Tribble and rawpixel under varying CC licenses)

Typical power electronic objectives

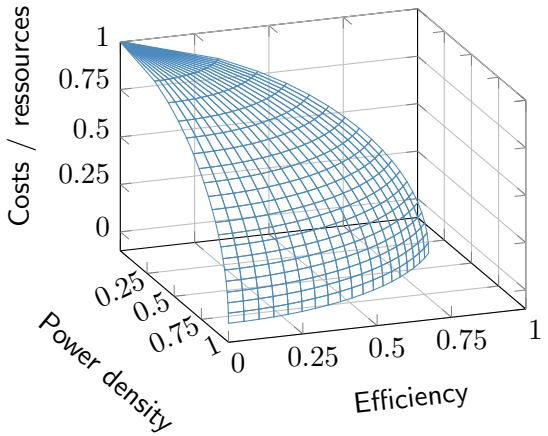

Fig. 1.8: Illustration of typical, conflicting power electronic (normalized) objectives via a Pareto front

Table of contents

Terminology: work vs. energy

Work

Work is the integral of the power over a time integral (or force over distance) and is a measure of the energy transfer.

Energy

Energy is the capacity to do work, that is, a quantity depending on the state of a system at a given point of time.

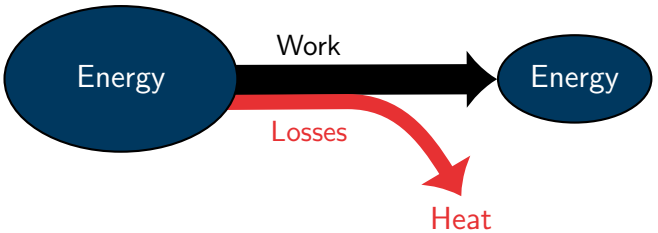

Fig. 1.9: Illustration addressing the work vs. energy terminology (simplified Sankey diagram)

Power balance of an electrical energy conversion system

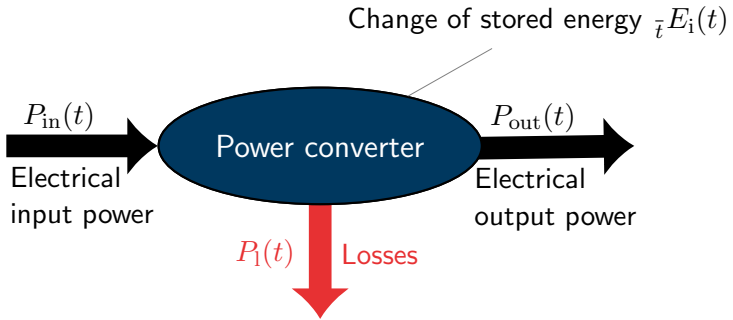

Fig. 1.10: Power balance of an energy conversion system

The power balance

$$P_\mathrm{in}(t) = P_\mathrm{l}(t) + \frac{}{t}E_\mathrm{i}(t) + P_\mathrm{out}(t) \tag{1.1}$$

must hold for any point in time as energy is conserved, that is, not created or destroyed.

Efficiency

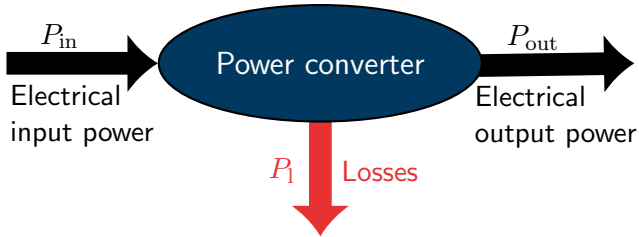

Fig. 1.11: Power balance of an energy conversion system in steady state

The power balance in steady state $\left({}^{\mathrm{d}x(t)}/_{\mathrm{d}t} = 0\right)$ is

$$P_{\mathrm{in}} = P_{\mathrm{out}} + P_{\mathrm{l}} \tag{1.2}$$

and leads to the definition of the efficiency

$$\eta = \frac{P_{\mathrm{out}}}{P_{\mathrm{in}}} = \frac{P_{\mathrm{out}}}{P_{\mathrm{out}} + P_{\mathrm{l}}}. \tag{1.3}$$

Four quadrants of operation

Depending on the current and voltage signs, the power P can be positive or negative. This leads to four quadrants of operation:

- Quadrants I & III: $P \geq 0$,
  (Power transfer from input to output)
- Quadrants II & IV: $P \leq 0$.
  (Power transfer from output to input)

How many quadrants a power converter can operate in depends on the topology and control strategy, i.e., is an important design criterion.

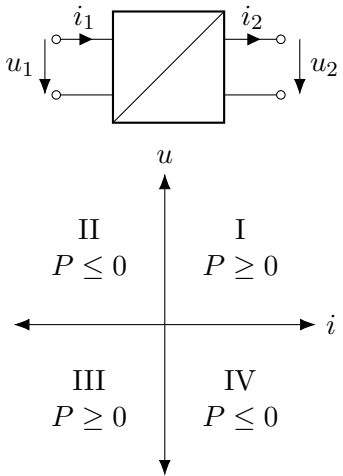

Fig. 1.12: Four quadrants of energy conversion

Why efficiency matters: a computer supply example

	Power supply A 80 PLUS Gold	Power supply B 80 PLUS Titanium
Input power	$250\,\mathrm{W}$	
Efficiency	$89\,\%$	$94\,\%$
Power loss	$27.5\,\mathrm{W}$	$15\,\mathrm{W}$
Operating hours per year	$8\,\mathrm{h} \times 220 = 1760\,\mathrm{h}$	
Cumulated loss work per year	$48.4\,\mathrm{kWh}$	$26.4\,\mathrm{kWh}$
Electricity cost for yearly losses	$14.52\,€$	$7.92\,€$
Cumulated loss work in Germany	$1.936\,\mathrm{TWh}$	$1.056\,\mathrm{TWh}$
Electricity cost for yearly losses in Germany	$580.8\,\mathrm{M€}$	$316.8\,\mathrm{M€}$

Tab. 1.1: Comparison of two computer power supplies (further assumptions: effective nominal power calculation, electricity price $0.3\,€/\mathrm{kWh}$, $40 \cdot 10^6$ computers in Germany)

Why efficiency matters: a wind power plant example

	Wind power plant A	Wind power plant B
Input power	5 MW	
Efficiency	97 %	97.1 %
Power loss	150 kW	145 kW
Nominal power operating hours per year	3000 h	
Cumulated loss work per year	450 MWh	435 MWh
Cumulated loss work (lifetime)	9.0 GWh	8.7 GWh
Lost sales proceeds due to losses per year	22.5 k€	21.75 k€
Lost sales proceeds due to losses (lifetime)	450 k€	435 k€
Cumulated loss work (lifetime, Germany)	9.0 TWh	8.7 TWh
Lost sales proceeds (lifetime, Germany)	450 M€	435 M€

Tab. 1.2: Comparison of two wind power plants (further assumptions: electricity sales price $0.05\,€/\mathrm{kWh}$, 20 years of life time, 1000 newly constructed wind power plants per year in Germany)

Table of contents

Linear power conversion

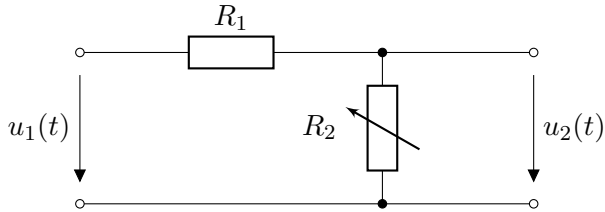

Fig. 1.13: Adjustable resistive voltage divider as step-down converter

With Kirchhoff's voltage law, the output voltage $u_2(t)$ is

$$u_2(t) = u_1(t)\frac{R_2}{R_1 + R_2}. \tag{1.4}$$

By adjusting the resistance R_2, the output voltage can be controlled. However, this method is inefficient as the power loss is independent of the output power and given by

$$P_l(t) = \frac{u_1^2(t)}{R_1 + R_2}. \tag{1.5}$$

Linear power conversion (cont.)

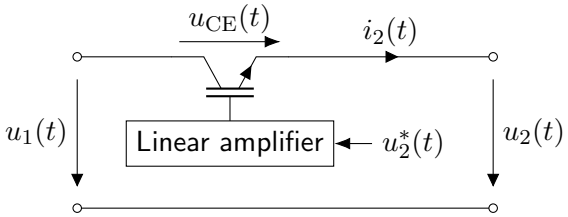

Fig. 1.14: Transistor-based step-down converter

For a transistor-based step-down converter, the output voltage is $u_2(t) = u_1(t) - u_{\mathrm{CE}}(t)$ leading to the power losses

$$P_{\mathrm{l}}(t) = u_{\mathrm{CE}}(t) i_2(t). \tag{1.6}$$

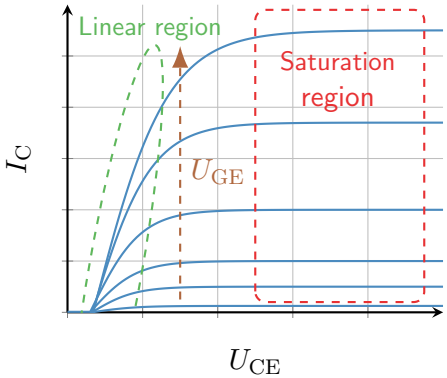

Fig. 1.15: Output characteristics of an insulated-gate bipolar transistor (IGBT)

Switching power conversion

Alternative idea: switch either fully on or off. The average output voltage $\overline{u}_2$ is controlled by the duty cycle (assuming that $u_1(t) = \overline{u}_1$ is constant)

$$D = \frac{T_{\text{on}}}{T_{\text{s}}}, \qquad \overline{u}_2 = \frac{1}{T_{\text{s}}} \int_0^{T_{\text{s}}} u_2(t)t = D\overline{u}_1. \tag{1.7}$$

As the switching losses are typically small, the overall efficiency is (much) higher compared to linear power conversion.

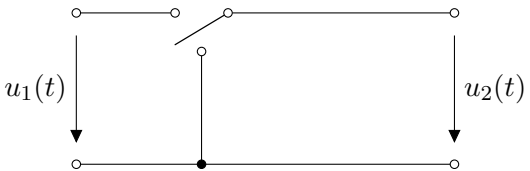

Fig. 1.16: Ideal switch-based step-down converter

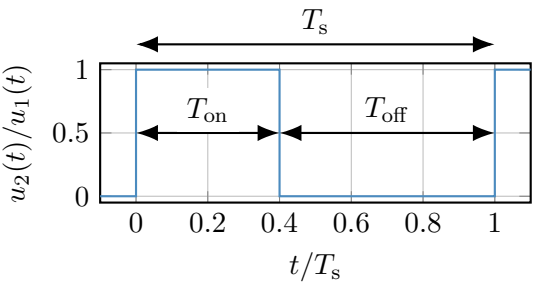

Fig. 1.17: Switching output voltage from Fig. 1.16

Switching power conversion: switching losses

Switching process is not free of power loss:

$$\overline{P}_\mathrm{l} = \frac{1}{T_\mathrm{s}} \int_0^{T_\mathrm{s}} u_\mathrm{s}(t) i_\mathrm{s}(t) t.$$

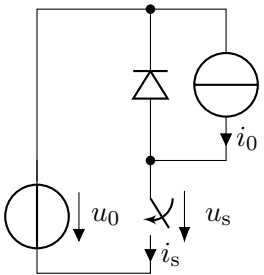

Fig. 1.18: Idealized switching loss model

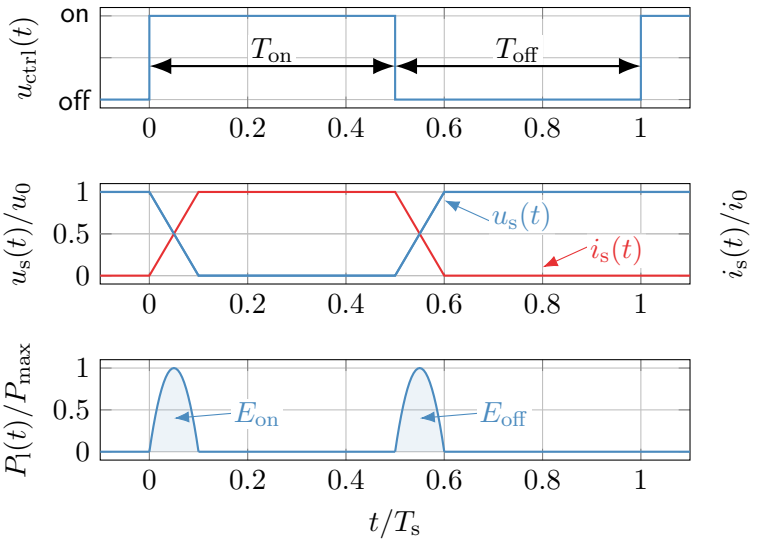

Switching power conversion: soft switching

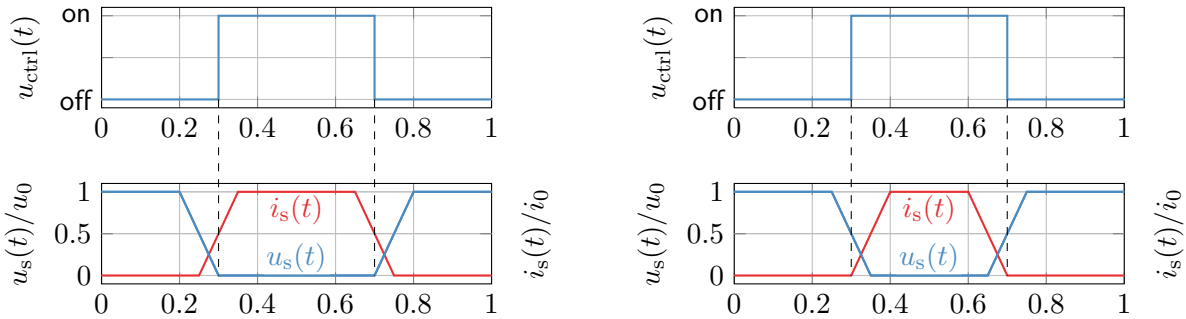

(a) Zero-voltage switching (ZVS)

(b) Zero-current switching (ZCS)

Fig. 1.19: Soft switching: reducing switching losses by turning on or off the switch when it does not transfer any power (note: above's voltage and current shapes are heavily idealized and require an appropriate circuit design besides the actual switch to enable soft switching)

Switching power conversion: passive components as filters / energy buffers

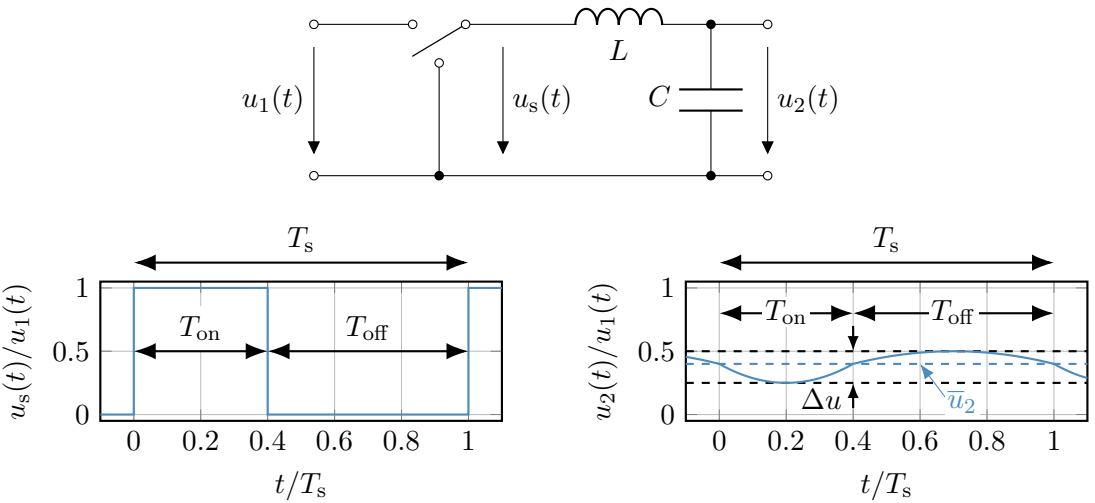

Fig. 1.20: Exemplary voltage signals for a switched power conversion system with output filter

Feasible and infeasible filter topologies

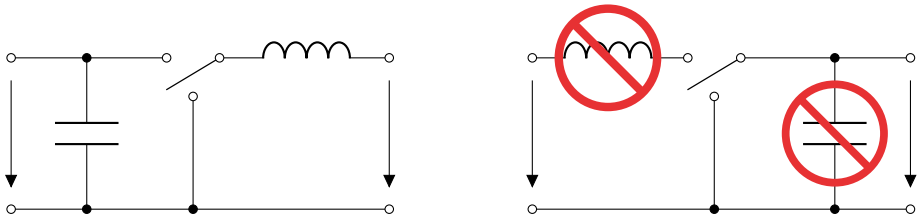

(a) Feasible filter topology

(b) Infeasible filter topology

Fig. 1.21: Basic filter topologies for switched power conversion

Short and open circuit situations

Prevent the following situations as they can lead to sparkover and damage:

- Short circuit of capacitor: current peak,
- Open circuit of inductor: voltage peak.

Important power electronic devices and idealized characteristics

Diode

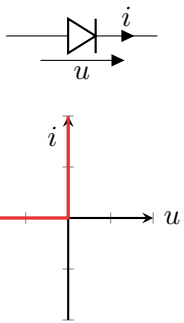

Thyristor

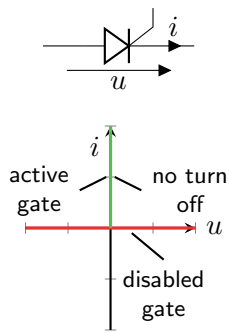

TRIAC (triode for alternating current)

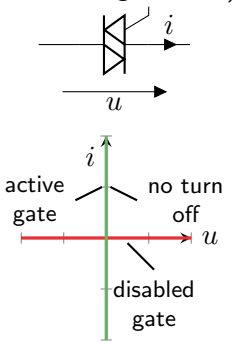

GTO (gate turn-off thyristor)

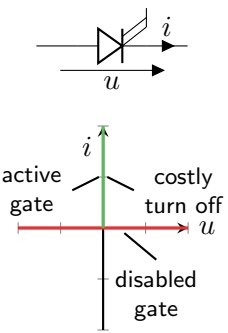

Important power electronic devices and idealized characteristics (cont.)

Bipolar junction transistor

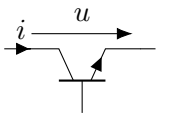

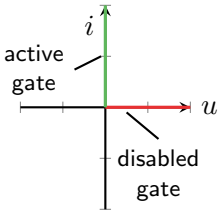

MOSFET [1] (with body diody)

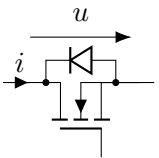

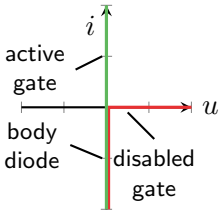

IGBT

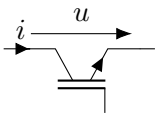

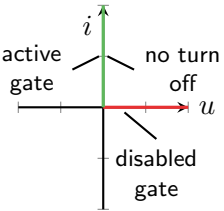

IGBT (with series diode)

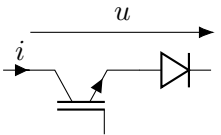

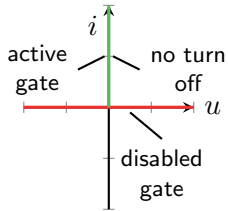

[1] metal-oxide-semiconductor field-effect transistor

Important power electronic devices and idealized characteristics (cont.)

4Q switch

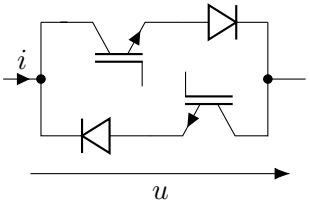

Capacitor

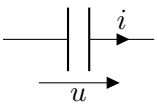

Inductor

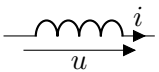

Transformer

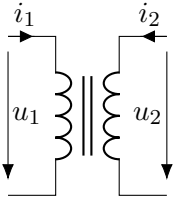

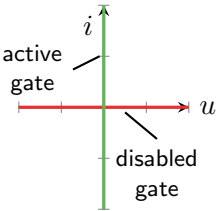

$$i(t) = C\frac{\mathrm{d}}{\mathrm{d}t}u(t) \qquad u(t) = L\frac{\mathrm{d}}{\mathrm{d}t}i(t) \qquad \boldsymbol{u}(t) = \boldsymbol{L}\frac{\mathrm{d}}{\mathrm{d}t}\boldsymbol{i}(t)$$

Important power electronic devices and idealized characteristics (cont.)

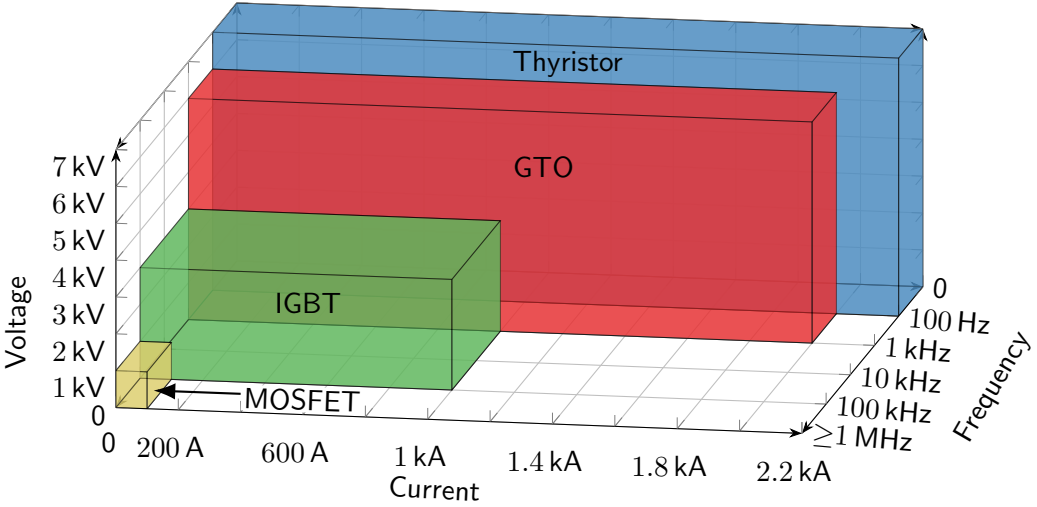

Fig. 1.22: Power electronic devices and their typical operating ranges

Internal device resistance

Besides the switching losses, power electronic devices have an internal resistance R_i that causes conduction losses. Designing such components for a low resistance is crucial, however, there is typically a conflict with weight and volume constraints.

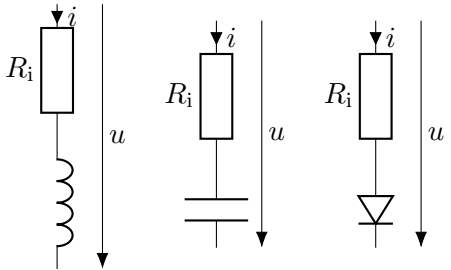

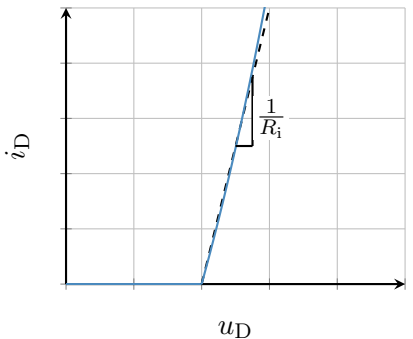

Fig. 1.23: Qualitative diode characteristic in the forward direction

Why is knowledge about power electronics important?

Power electronics are an essential pillar of the modern society

Power electronics are the key technology for the efficient conversion of electrical energy. They are used in a wide range of applications, such as renewable energy systems, electric vehicles, industrial automation, computing and communication systems as well as a wide range of consumer electronics. Hence, power electronics are an essential pillar of the modern society.

Energy efficiency and sustainability is key

Electricity as a share of primary energy is current at $20\,\%$ and is expected to further increase (source: Ember and Energy Institute). Power electronics convert a major share of the worldwide electrical energy as they are used on the generation, transmission, storage and load side. Increasing the conversion and resource efficiency of power electronics direct reduces the primary energy consumption and the environmental impact of the energy system.

Table of contents

Learning objectives

- Understand the electrical energy conversion principles of power electronics.
- Differentiate the main converter application types:
  - DC-DC converters.
  - DC-AC inverters.
  - AC-DC rectifiers.
  - AC-AC converters.
  - And their plentiful realization variants ...
- Analyze the operation of power electronics:
  - in steady state and
  - in transient conditions.
- Understand modulation techniques for switching actuators.
- Have fun learning about power electronics.

Necessary prior knowledge for this course

You should have a basic understanding of the following topics:

- Linear differential equations (modeling, solution techniques),
- Linear algebra basics (e.g., vector and matrix operations),
- Basic signal theory knowledge (e.g., signal properties like root mean square),
- Basic knowledge of electrical circuit theory,
- Basic knowledge of semiconductor physics.

What we will not cover, that is, you do not need to know (covered in separate courses):

- Control engineering (design converter controllers),
- Specific load characteristics (e.g., electric drives or batteries).

Recommended reading

- R. Erickson and D. Maksimovic, Fundamentals of Power Electronics, Vol. 3, Springer, 2020, https://doi.org/10.1007/978-3-030-43881-4
- J. Kassakian et al, Principles of Power Electronics, Vol. 2, Cambridge University Press, 2023, https://doi.org/10.1017/9781009023894
- J. Specovius, Grundkurs Leistungselektronik (in German), Vol. 10, Springer, 2020, https://doi.org/10.1007/978-3-658-21169-1
- F. Zach, Leistungselektronik (in German), Vol. 6, Springer, 2022, https://doi.org/10.1007/978-3-658-31436-1
- D. Schröder and R. Marquardt, Leistungselektronische Schaltungen (in German), Vol. 4, Springer, 2019, https://doi.org/10.1007/978-3-662-55325-1

Table of contents

Step-down converter: overview and assumptions

We consider the following assumptions:

- The switch is ideal, that is, infinitely fast.
- The input voltage is constant: $u_1(t) = U_1$.
- The output voltage is constant: $u_2(t) = U_2$.
- The input voltage is greater than the output voltage: $U_1 > U_2$.

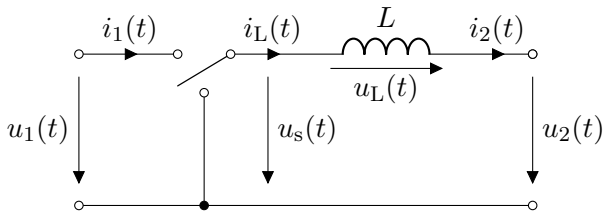

Fig. 2.1: Step-down converter (aka buck converter, ideal switch representation)

Step-down converter: switch states

The voltage at the switch is given by

$$u_{\mathrm{s}}(t) = \begin{cases} U_1, & t \in [kT_{\mathrm{s}}, kT_{\mathrm{s}} + T_{\mathrm{on}}], \\ 0, & t \in [kT_{\mathrm{s}} + T_{\mathrm{on}}, (k+1)T_{\mathrm{s}}] \end{cases} \tag{2.1}$$

with $k \in \mathbb{N}$ being the k-th switching period, T_{s} the switching period time interval, and T_{on} the switch-on time.

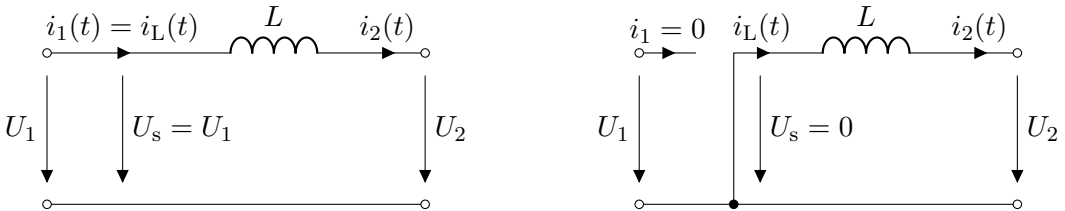

(a) Switch-on time

(b) Switch-off time

Fig. 2.2: Switch states of the step-down converter

Basic terms and definitions

T_{on}	Switch-on time	T_{off}	Switch-off time
$T_{\mathrm{s}} = T_{\mathrm{on}} + T_{\mathrm{off}}$	Switching period	$f_{\mathrm{s}} = 1/T_{\mathrm{s}}$	Switching frequency
$D = T_{\mathrm{on}}/T_{\mathrm{s}}$	Duty cycle		

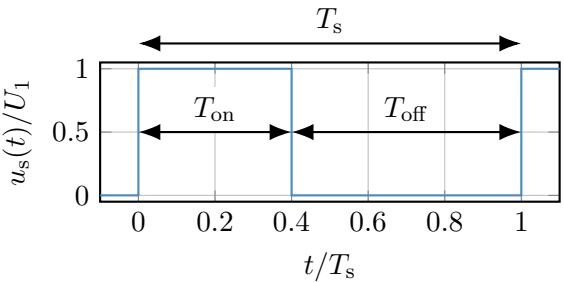

Steady-state analysis

The inductor current from Fig. 2.1 is represented by the differential equation

$$L\frac{\mathrm{d}i_\mathrm{L}(t)}{\mathrm{d}t} = u_\mathrm{L}(t) = u_\mathrm{s}(t) - U_2. \tag{2.2}$$

During the switch-on period we have

$$\begin{aligned} i_\mathrm{L}(t) &= i_\mathrm{L}(kT_\mathrm{s}) + \frac{1}{L}\int_{kT_\mathrm{s}}^{t} u_\mathrm{L}(\tau)\mathrm{d}\tau \\ &= i_\mathrm{L}(kT_\mathrm{s}) + \frac{U_1 - U_2}{L}(t - kT_\mathrm{s}), \quad t \in [kT_\mathrm{s}, kT_\mathrm{s} + T_\mathrm{on}] \end{aligned} \tag{2.3}$$

and during the switch-off period we receive

$$\begin{aligned} i_\mathrm{L}(t) &= i_\mathrm{L}(kT_\mathrm{s} + T_\mathrm{on}) + \frac{1}{L}\int_{kT_\mathrm{s}+T_\mathrm{on}}^{t} u_\mathrm{L}(\tau)\mathrm{d}\tau = i_\mathrm{L}(kT_\mathrm{s} + T_\mathrm{on}) - \frac{U_2}{L}(t - kT_\mathrm{s} - T_\mathrm{on}) \\ &= i_\mathrm{L}(kT_\mathrm{s}) + \frac{U_1 - U_2}{L}T_\mathrm{on} - \frac{U_2}{L}(t - kT_\mathrm{s} - T_\mathrm{on}), \quad t \in [kT_\mathrm{s} + T_\mathrm{on}, (k+1)T_\mathrm{s}]. \end{aligned} \tag{2.4}$$

Steady-state analysis (cont.)

In steady state the inductor current is periodic with period T_s, that is,

$$i_\mathrm{L}(t) = i_\mathrm{L}(t + T_\mathrm{s}).$$

From (2.4) we obtain for $t = kT_\mathrm{s}$

$$\begin{aligned} \overbrace{i_\mathrm{L}(kT_\mathrm{s})}^{\text{Start of period}} &= \overbrace{i_\mathrm{L}(kT_\mathrm{s}) + \frac{U_1 - U_2}{L} T_\mathrm{on} - \frac{U_2}{L}(T_\mathrm{s} - T_\mathrm{on})}^{\text{End of period}} \\ \Leftrightarrow \quad 0 &= \frac{U_1 - U_2}{L} T_\mathrm{on} - \frac{U_2}{L}(T_\mathrm{s} - T_\mathrm{on}) \\ \Leftrightarrow \quad 0 &= U_1 T_\mathrm{on} - U_2 T_\mathrm{s}. \end{aligned} \tag{2.5}$$

Rewriting delivers the output voltage as

$$U_2 = \frac{T_\mathrm{on}}{T_\mathrm{s}} U_1 = D U_1. \tag{2.6}$$

Step-down converter: steady-state time-domain behavior

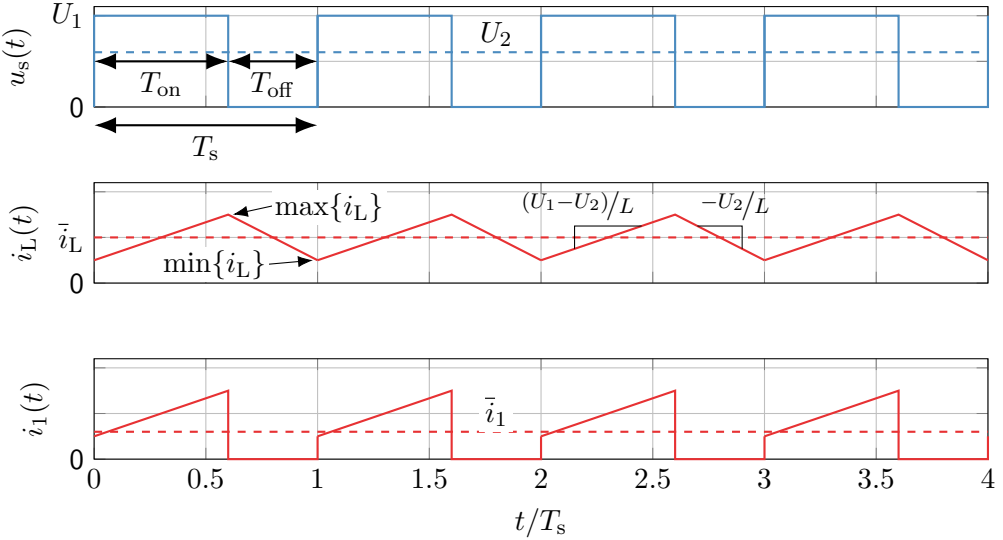

Alternative steady-state analysis: average values

From the previous slide we know that the average inductor voltage is zero in steady state

$$\overline{u}_{\mathrm{L}} = \frac{1}{T_{\mathrm{s}}} \int_0^{T_{\mathrm{s}}} u_{\mathrm{L}}(t)\mathrm{d}t = \overline{u}_{\mathrm{L}} = 0, \tag{2.7}$$

since otherwise the average inductor current would change between periods, compare

$$L\frac{\mathrm{d}i_{\mathrm{L}}(t)}{\mathrm{d}t} = u_{\mathrm{L}}(t).$$

From Fig. 2.1 we can apply Kirchhoff's voltage law to obtain

$$u_{\mathrm{s}}(t) = u_{\mathrm{L}}(t) + u_2(t) \quad \Rightarrow \quad \overline{u}_{\mathrm{s}} = \overline{u}_{\mathrm{L}} + U_2 \quad \Leftrightarrow \quad \overline{u}_{\mathrm{s}} = U_2. \tag{2.8}$$

The average switch voltage is given by

$$\overline{u}_{\mathrm{s}} = \frac{1}{T_{\mathrm{s}}} \int_0^{T_{\mathrm{s}}} u_{\mathrm{s}}(t)\mathrm{d}t = \frac{1}{T_{\mathrm{s}}} \int_0^{T_{\mathrm{on}}} U_1\mathrm{d}t = U_1\frac{T_{\mathrm{on}}}{T_{\mathrm{s}}} = U_1 D. \tag{2.9}$$

Alternative steady-state analysis: average values (cont.)

Combining (2.8) and (2.9) we obtain the voltage transfer ratio

$$\frac{U_2}{U_1} = D. \tag{2.10}$$

In addition, we can calculate the average input current as

$$\bar{i}_1 = \frac{1}{T_\mathrm{s}} \int_0^{T_\mathrm{s}} i_1(t)\mathrm{d}t = \frac{1}{T_\mathrm{s}} \int_0^{T_\mathrm{on}} i_\mathrm{L}(t)\mathrm{d}t = \frac{T_\mathrm{on}}{T_\mathrm{s}} \bar{i}_\mathrm{L} = D\bar{i}_\mathrm{L}. \tag{2.11}$$

Since $i_2(t) = i_\mathrm{L}(t)$ applies, we can conclude

$$\frac{U_2}{U_1} = \frac{\bar{i}_1}{\bar{i}_2} = D. \tag{2.12}$$

Hence, the duty cycle D has a similar interpretation for the DC-DC step-down converter as the turn ratio for an ideal transformer in the AC domain.

Stationary averaged model of the step-down converter

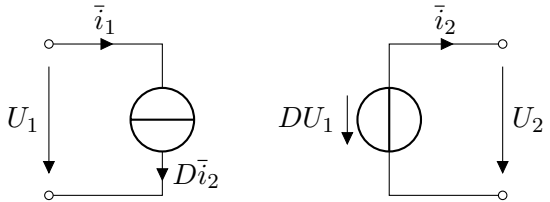

Fig. 2.3: Stationary averaged model of the step-down converter

Switching vs. linear power conversion

In contrast to the linear power conversion approaches from Fig. 1.13 and Fig. 1.14, the switching step-down converter transforms the current and voltage levels with the same factor D which results from the (idealized) loss-less transformation of energy.

Current ripple

Due to the switching operation of the step-down converter, the inductor current exhibits an inherent ripple. The peak-to-peak current ripple is given by

$$\begin{aligned}\Delta i_{\mathrm{L}} &= \max\{i_{\mathrm{L}}(t)\} - \min\{i_{\mathrm{L}}(t)\} = i_{\mathrm{L}}(t = T_{\mathrm{on}}) - i_{\mathrm{L}}(t = T_{\mathrm{s}}) \\ &= \frac{U_1 - U_2}{L} T_{\mathrm{on}} = \frac{U_2}{L} T_{\mathrm{off}} \\ &= \frac{D(1-D)T_{\mathrm{s}}}{L} U_1.\end{aligned} \tag{2.13}$$

The current ripple has two main implications:

- The output power is not constant but varies with the current ripple.
- The root mean square (RMS) current is higher than the average current.

The latter point should be investigated in more detail as it influences the design and loss characteristics of the converter.

Current ripple (cont.)

We define

$$\Delta I_{\mathrm{L}} = \sqrt{\frac{1}{T_{\mathrm{s}}} \int_0^{T_{\mathrm{s}}} \left(i_{\mathrm{L}}(t) - \bar{i}_{\mathrm{L}} \right)^2 \mathrm{d}t} \tag{2.14}$$

as the RMS deviation of the inductor current from its average value. As the average-corrected inductor current has a triangular shape (cf. Fig. 2.4) we can calculate the RMS current as

$$\Delta I_{\mathrm{L}} = \frac{1}{\sqrt{3}} \frac{\Delta i_{\mathrm{L}}}{2} = \frac{D(1-D) T_{\mathrm{s}} U_1}{2\sqrt{3} L}. \tag{2.15}$$

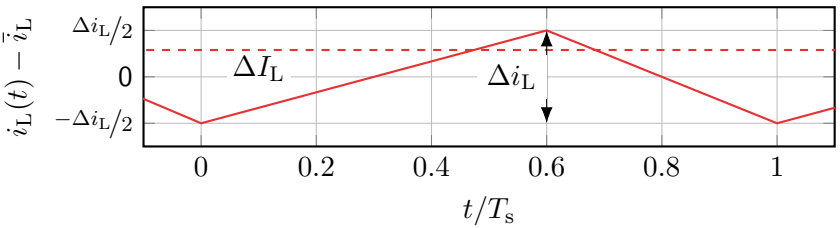

Fig. 2.4: Inductor current ripple

Current ripple (cont.)

The (total) RMS value of the inductor current (triangular signal with offset) is given by

$$I_\mathrm{L} = \sqrt{\bar{i}_\mathrm{L}^2 + \Delta I_\mathrm{L}^2}. \tag{2.16}$$

Considering the internal resistance R_i of the inductor, the ohmic power loss in the inductor is

$$P_\mathrm{L} = R_\mathrm{i} I_\mathrm{L}^2 = R_\mathrm{i} \left(\bar{i}_\mathrm{L}^2 + \Delta I_\mathrm{L}^2 \right). \tag{2.17}$$

The power loss in the inductor is thus composed of a constant part $\overline{P}_\mathrm{L} = R_\mathrm{i} \bar{i}_\mathrm{L}^2$, which is related to the power transfer from input to output, and a ripple part $\Delta P_\mathrm{L} = R_\mathrm{i} \Delta I_\mathrm{L}^2$.

Current ripple and power losses

The current ripple produces additional losses in the inductor. From (2.15) it seems tempting to increase the switching frequency f_s to reduce the ripple, but this will increase switching losses (compare Fig. 1.18). Hence, there is a trade-off decision between switching and conduction losses.

Current ripple and duty cycle

Rewriting the current ripple expression

$$\Delta i_\mathrm{L} = \frac{D(1-D)T_\mathrm{s}}{L} U_1 = (D - D^2)\frac{T_\mathrm{s} U_1}{L}$$

and calculating the derivative with respect to the duty cycle D delivers

$$\frac{\mathrm{d}\Delta i_\mathrm{L}}{\mathrm{d}D} = \frac{T_\mathrm{s} U_1}{L} - 2D\frac{T_\mathrm{s} U_1}{L}. \tag{2.18}$$

Setting the derivative to zero, we find the duty cycle D_max as

$$\frac{\mathrm{d}\Delta i_\mathrm{L}}{\mathrm{d}D} = 0 \quad \Leftrightarrow \quad D_\mathrm{max} = \frac{1}{2} \tag{2.19}$$

which is associated with the maximum current ripple since the second derivative

$$\frac{\mathrm{d}^2\Delta i_\mathrm{L}}{\mathrm{d}D^2} = -\frac{2T_\mathrm{s} U_\mathrm{on}}{L} \tag{2.20}$$

is negative.

Current ripple and duty cycle (cont.)

From (2.19) we can conclude that the maximum current ripple is given by

$$\Delta i_{\mathrm{L,max}} = \frac{1}{4}\frac{T_{\mathrm{s}} U_1}{L} \quad \Rightarrow \quad \Delta i_{\mathrm{L}} = 4D(1-D)\Delta i_{\mathrm{L,max}}. \tag{2.21}$$

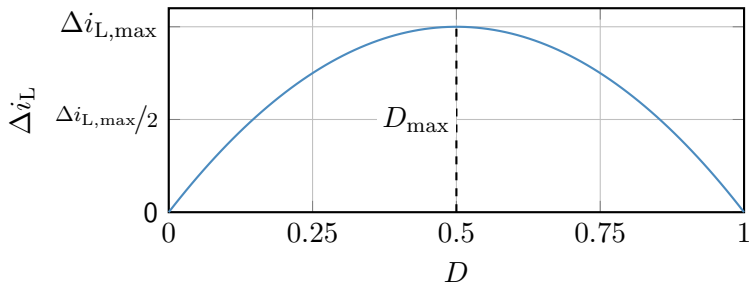

Fig. 2.5: Inductor current ripple as a function of the duty cycle

Table of contents

Step-down converter with output capacitor: overview and assumption

We consider the following assumptions:

- The switch is ideal, that is, infinitely fast.
- The input voltage is constant: $u_1(t) = U_1$.
- The output current is constant: $i_2(t) = I_2$.
- The input voltage is greater than the output voltage: $U_1 > u_2(t)$.

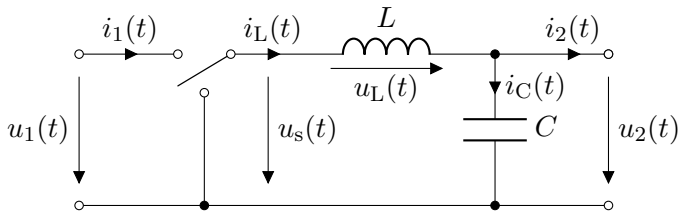

Fig. 2.6: Step-down converter (ideal switch representation) with output capacitor

Steady-state analysis

From (2.3) we know that the inductor current during the switch-on period is given by

$$i_{\mathrm{L}}(t) = i_{\mathrm{L}}(kT_{\mathrm{s}}) + \frac{U_1 - u_{\mathrm{C}}(t)}{L}(t - kT_{\mathrm{s}}), \quad t \in [kT_{\mathrm{s}}, kT_{\mathrm{s}} + T_{\mathrm{on}}].$$

Note that the inductor current is now dependent on $u_{\mathrm{C}}(t)$:

- Formally, we need to consider the impact of the varying output capacitor voltage.
- This would lead to a second-order differential equation which is more complex to solve.
- We will simplify the analysis by assuming that the impact of the output capacitor voltage variation on the inductor current is negligible: $u_{\mathrm{C}}(t) \approx U_2 = \overline{u}_{\mathrm{c}}$.

Simplification comment

The above assumption is valid for sufficiently large output capacitors with only small voltage ripples. Otherwise, the output voltage ripple and the inductor current ripple will be significantly coupled and require a more thoughtful analysis.

Steady-state analysis (cont.)

The capacitor's voltage differential equation is given by

$$C\frac{\mathrm{d}u_{\mathrm{C}}(t)}{\mathrm{d}t} = i_{\mathrm{C}}(t) = i_{\mathrm{L}}(t) - I_2. \tag{2.22}$$

While I_2 is considered a known constant, we first need to determine the inductor current $i_{\mathrm{L}}(t)$. Combining (2.3) and (2.13) we obtain

$$i_{\mathrm{L}}(kT_{\mathrm{s}}) = I_2 - \frac{\Delta i_{\mathrm{L}}}{2} = I_2 - \frac{U_1 - U_2}{L}\frac{T_{\mathrm{on}}}{2} \tag{2.23}$$

and

$$i_{\mathrm{L}}(kT_{\mathrm{s}} + T_{\mathrm{on}}) = I_2 + \frac{\Delta i_{\mathrm{L}}}{2} = I_2 + \frac{U_1 - U_2}{L}\frac{T_{\mathrm{on}}}{2} \tag{2.24}$$

as the initial conditions for the inductor current in steady state.

Steady-state analysis (cont.)

The capacitor's current during the switch-on period is given by

$$\begin{aligned} i_{\mathrm{C}}(t) &= i_{\mathrm{L}}(t) - I_2 = \frac{U_1 - U_2}{L}\left(t - \frac{T_{\mathrm{on}}}{2} - kT_{\mathrm{s}}\right) \\ &= -\frac{\Delta i_{\mathrm{L}}}{2} + \frac{U_1 - U_2}{L}(t - kT_{\mathrm{s}}), \quad t \in [kT_{\mathrm{s}}, kT_{\mathrm{s}} + T_{\mathrm{on}}] \end{aligned} \tag{2.25}$$

and during the switch-off period we receive

$$\begin{aligned} i_{\mathrm{C}}(t) &= i_{\mathrm{L}}(t) - I_2 = \frac{U_1 - U_2}{L}\frac{T_{\mathrm{on}}}{2} - \frac{U_2}{L}(t - kT_{\mathrm{s}} - T_{\mathrm{on}}) \\ &= \frac{\Delta i_{\mathrm{L}}}{2} - \frac{U_2}{L}(t - kT_{\mathrm{s}} - T_{\mathrm{on}}), \quad t \in [kT_{\mathrm{s}} + T_{\mathrm{on}}, (k+1)T_{\mathrm{s}}]. \end{aligned} \tag{2.26}$$

Steady-state analysis (cont.)

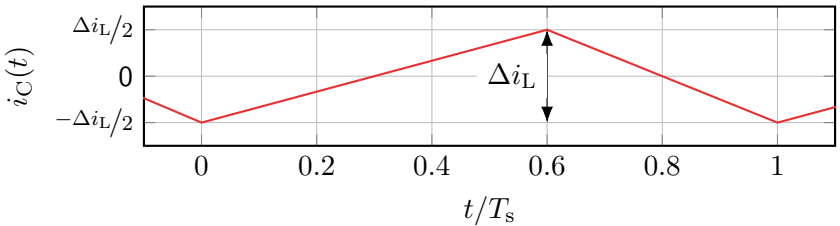

Current ripples through the capacitor and inductor

Based on the made assumptions, the capacitor's current is raising and falling linearly during the switch-on and switch-off periods, that is, it corresponds to the previously considered inductor current ripple.

Steady-state analysis (cont.)

Inserting (2.25) in (2.22) and integrating the differential equation delivers the capacitor voltage during the switch-on period as

$$\begin{aligned} u_{\mathrm{C}}(t) &= u_{\mathrm{C}}(kT_{\mathrm{s}}) + \frac{1}{C}\int_{kT_{\mathrm{s}}}^{t} i_{\mathrm{C}}(\tau)\mathrm{d}\tau, \quad t \in [kT_{\mathrm{s}}, kT_{\mathrm{s}} + T_{\mathrm{on}}] \\ &= u_{\mathrm{C}}(kT_{\mathrm{s}}) + \frac{1}{C}\int_{kT_{\mathrm{s}}}^{t} -\frac{\Delta i_{\mathrm{L}}}{2} + \frac{U_1 - U_2}{L}(\tau - kT_{\mathrm{s}})\mathrm{d}\tau \\ &= u_{\mathrm{C}}(kT_{\mathrm{s}}) + \frac{1}{C}\left[-\frac{\Delta i_{\mathrm{L}}}{2}\tau + \frac{U_1 - U_2}{L}(\frac{1}{2}\tau^2 - kT_{\mathrm{s}}\tau)\right]_{kT_{\mathrm{s}}}^{t} \\ &= u_{\mathrm{C}}(kT_{\mathrm{s}}) - \frac{\Delta i_{\mathrm{L}}}{2C}(t - kT_{\mathrm{s}}) + \frac{U_1 - U_2}{LC}\left[t(\frac{t}{2} - kT_{\mathrm{s}}) + \frac{(kT_{\mathrm{s}})^2}{2}\right]. \end{aligned} \tag{2.27}$$

Here, $u_{\mathrm{C}}(kT_{\mathrm{s}})$ is the initial capacitor voltage at the beginning of the switch-on period.

Steady-state analysis (cont.)

At the end of the switch-on period, the capacitor voltage is given by

$$\begin{aligned} u_{\mathrm{C}}(kT_{\mathrm{s}} + T_{\mathrm{on}}) &= u_{\mathrm{C}}(kT_{\mathrm{s}}) - \frac{\Delta i_{\mathrm{L}}}{2C}(kT_{\mathrm{s}} + T_{\mathrm{on}} - kT_{\mathrm{s}}) \\ &\quad + \frac{U_1 - U_2}{LC}\left[(kT_{\mathrm{s}} + T_{\mathrm{on}})(\frac{kT_{\mathrm{s}} + T_{\mathrm{on}}}{2} - kT_{\mathrm{s}}) + \frac{(kT_{\mathrm{s}})^2}{2}\right] \\ &= u_{\mathrm{C}}(kT_{\mathrm{s}}) - \frac{\Delta i_{\mathrm{L}}}{2C}T_{\mathrm{on}} + \frac{\Delta i_{\mathrm{L}}}{2C}T_{\mathrm{on}} \\ &= u_{\mathrm{C}}(kT_{\mathrm{s}}), \end{aligned} \tag{2.28}$$

i.e., the capacitor voltage at the end of the switch-on period is equal to the voltage at the beginning of the switch-on period. Since the capacitor voltage needs to be continuous over time, this also marks the initial condition for the switch-off period.

Steady-state analysis (cont.)

Inserting (2.26) in (2.22) and integrating the differential equation delivers the capacitor voltage during the switch-off period as

$$\begin{aligned} u_{\mathrm{C}}(t) &= u_{\mathrm{C}}(kT_{\mathrm{s}} + T_{\mathrm{on}}) + \frac{1}{C}\int_{kT_{\mathrm{s}}+T_{\mathrm{on}}}^{t} i_{\mathrm{C}}(\tau)\mathrm{d}\tau, \quad t \in [kT_{\mathrm{s}} + T_{\mathrm{on}}, (k+1)T_{\mathrm{s}}] \\ &= u_{\mathrm{C}}(kT_{\mathrm{s}}) + \frac{1}{C}\int_{kT_{\mathrm{s}}+T_{\mathrm{on}}}^{t} \frac{\Delta i_{\mathrm{L}}}{2} - \frac{U_2}{L}(\tau - kT_{\mathrm{s}} - T_{\mathrm{on}})\mathrm{d}\tau \\ &= u_{\mathrm{C}}(kT_{\mathrm{s}}) + \left[\frac{\Delta i_{\mathrm{L}}}{2}\tau - \frac{U_2}{L}(\frac{1}{2}\tau^2 - kT_{\mathrm{s}}\tau - T_{\mathrm{on}}\tau)\right]_{kT_{\mathrm{s}}+T_{\mathrm{on}}}^{t} \\ &= u_{\mathrm{C}}(kT_{\mathrm{s}}) + \frac{\Delta i_{\mathrm{L}}}{2C}(t - kT_{\mathrm{s}} - T_{\mathrm{on}}) - \frac{U_2}{LC}\left[t(\frac{t}{2} - kT_{\mathrm{s}} - T_{\mathrm{on}}) + \frac{(kT_{\mathrm{s}} + T_{\mathrm{on}})^2}{2}\right]. \end{aligned} \tag{2.29}$$

Here, $u_{\mathrm{C}}(kT_{\mathrm{s}} + T_{\mathrm{on}}) = u_{\mathrm{C}}(kT_{\mathrm{s}})$ is the initial capacitor voltage at the beginning of both the switch-on and switch-off period.

Steady-state time-domain behavior

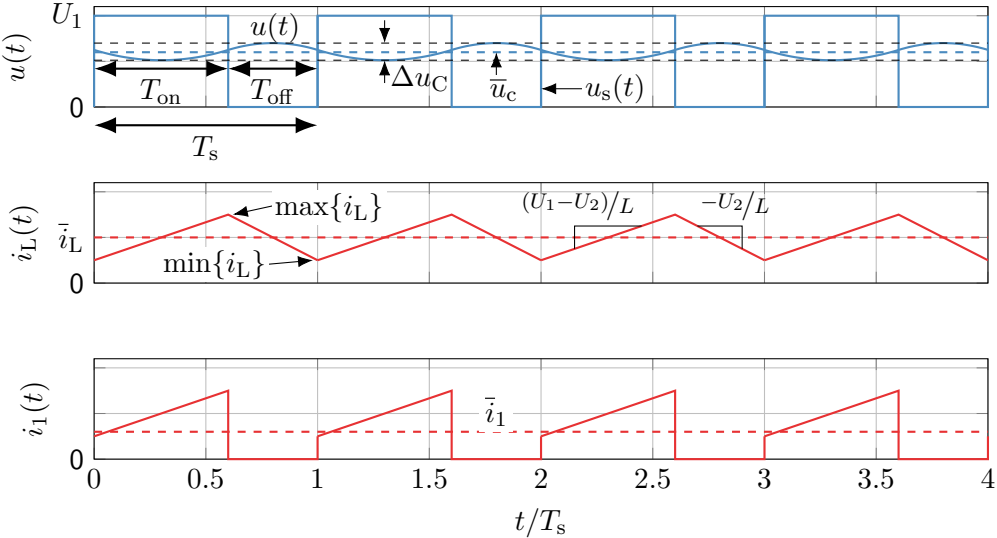

Output voltage ripple

Utilizing (2.27) and calculating the derivative with respect to t we obtain

$$\begin{aligned}\frac{\mathrm{d}u_\mathrm{C}(t)}{\mathrm{d}t} &= -\frac{\Delta i_\mathrm{L}}{2C} + \frac{U_1 - U_2}{LC}t \\ &= -\frac{U_1 - U_2}{LC}\frac{T_\mathrm{on}}{2} + \frac{U_1 - U_2}{LC}(t - kT_\mathrm{s}), \quad t \in [kT_\mathrm{s}, kT_\mathrm{s} + T_\mathrm{on}].\end{aligned} \tag{2.30}$$

Setting the derivative to zero, we find the time t_min at which the minimum voltage occurs as

$$\frac{\mathrm{d}u_\mathrm{C}(t)}{\mathrm{d}t} = 0 \quad \Rightarrow \quad t_\mathrm{min} = \frac{T_\mathrm{on}}{2} + kT_\mathrm{s} \tag{2.31}$$

since the second derivative is positive. Inserting (2.31) in (2.27) reveals the minimum voltage as

$$u_\mathrm{C}(t_\mathrm{min}) = u_\mathrm{C}(kT_\mathrm{s}) - \frac{U_1 - U_2}{LC}\frac{T_\mathrm{on}^2}{8} = u_\mathrm{C}(kT_\mathrm{s}) - \Delta i_\mathrm{L}\frac{T_\mathrm{on}}{8C}. \tag{2.32}$$

Output voltage ripple (cont.)

Likewise, calculating the derivative of (2.29) leads to

$$\begin{aligned}\frac{\mathrm{d}u_\mathrm{C}(t)}{\mathrm{d}t} &= \frac{\Delta i_\mathrm{L}}{2C} - \frac{U_2}{LC}(t - kT_\mathrm{s} - T_\mathrm{on}) \\ &= \frac{U_1 - U_2}{LC}\frac{T_\mathrm{on}}{2} - \frac{U_2}{LC}(t - kT_\mathrm{s} - T_\mathrm{on}), \quad t \in [kT_\mathrm{s} + T_\mathrm{on}, (k+1)T_\mathrm{s}].\end{aligned} \tag{2.33}$$

Setting the derivative to zero, we find the time t_max at which the maximum voltage occurs as

$$\frac{\mathrm{d}u_\mathrm{C}(t)}{\mathrm{d}t} = 0 \quad \Rightarrow \quad t_\mathrm{max} = \frac{T_\mathrm{off}}{2} + T_\mathrm{on} + kT_\mathrm{s} \tag{2.34}$$

since the second derivative is negative. The maximum voltage is then given by

$$u_\mathrm{C}(t_\mathrm{max}) = u_\mathrm{C}(kT_\mathrm{s}) + \Delta i_\mathrm{L}\frac{T_\mathrm{off}}{8C}. \tag{2.35}$$

Output voltage ripple (cont.)

The voltage ripple is then given by

$$\begin{aligned}\Delta u_{\mathrm{C}} &= u_{\mathrm{C}}(t_{\max}) - u_{\mathrm{C}}(t_{\min}) = \Delta i_{\mathrm{L}} \frac{T_{\mathrm{off}}}{8C} + \Delta i_{\mathrm{L}} \frac{T_{\mathrm{on}}}{8C} \\ &= \Delta i_{\mathrm{L}} \frac{T_{\mathrm{s}}}{8C} = \frac{D(1-D) T_{\mathrm{s}}^2 U_1}{8LC}.\end{aligned} \tag{2.36}$$

The voltage ripple is proportionally depending on the inductor current ripple. Hence, the maximum voltage ripple occurs at the same characteristic duty cycle $D_{\max}$ and is given by

$$D_{\max} = \frac{1}{2} \quad \Rightarrow \quad \Delta u_{\mathrm{C,max}} = \frac{T_{\mathrm{s}}^2 U_1}{32LC}. \tag{2.37}$$

Hence, we can rewrite the voltage ripple as

$$\Delta u_{\mathrm{C}} = 4D(1-D)\Delta u_{\mathrm{C,max}}. \tag{2.38}$$

The voltage ripple is associated with additional losses in the output capacitor and the load, that is, an important stress parameter.

Output voltage ripple: alternative via charge balance

If one is not interested in the specific signal shape $u_\mathrm{C}(t)$, the output voltage ripple can be derived from the charge balance over half a period (cf. Fig. 2.7):

$$\Delta Q = \frac{1}{2}\frac{\Delta i_\mathrm{L}}{2}\frac{T_\mathrm{s}}{2}. \qquad (2.39)$$

From

$$\frac{1}{C}\int i_\mathrm{C}(t)\mathrm{d}t = u_\mathrm{C}(t) + u_\mathrm{C}(0)$$

we receive

$$\Delta u_\mathrm{C} = \frac{\Delta Q}{C} = \frac{\Delta i_\mathrm{L} T_\mathrm{s}}{8C}. \qquad (2.40)$$

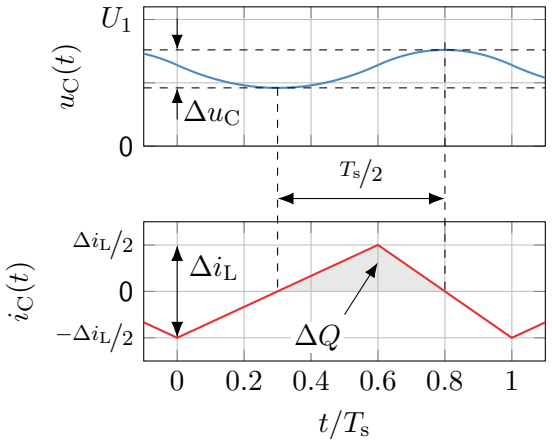

Fig. 2.7: Voltage ripple derivation via charge balance

Average and initial capacitor voltage

The initial voltage $u_\mathrm{C}(kT_\mathrm{s})$ at the beginning of a period is still unknown. We can derive it from the capacitor's average voltage over one period. For simplicity, we consider $k = 0$:

$$\overline{u}_\mathrm{c} = \frac{1}{T_\mathrm{s}} \int_0^{T_\mathrm{s}} u_\mathrm{C}(t)\mathrm{d}t = \frac{1}{T_\mathrm{s}} \left(\int_0^{T_\mathrm{on}} u_\mathrm{C}(t)\mathrm{d}t + \int_{T_\mathrm{on}}^{T_\mathrm{s}} u_\mathrm{C}(t)\mathrm{d}t \right) \stackrel{!}{=} DU_1. \tag{2.41}$$

Inserting (2.27) we receive for the first part

$$\begin{aligned} \int_0^{T_\mathrm{on}} u_\mathrm{C}(t)\mathrm{d}t &= \left[u_\mathrm{C}(0)t + \frac{\Delta i_\mathrm{L}}{2C}\frac{t^2}{2} + \frac{U_1 - U_2}{LC}\frac{t^3}{6} \right]_0^{T_\mathrm{on}} = \dots \\ &= u_\mathrm{C}(0)T_\mathrm{on} - \frac{\Delta i_\mathrm{L}}{C}\frac{T_\mathrm{on}^2}{12}. \end{aligned} \tag{2.42}$$

Average and initial capacitor voltage (cont.)

Inserting (2.29) into the second part of (2.41) delivers

$$\int_{T_{\mathrm{on}}}^{T_{\mathrm{s}}} u_{\mathrm{C}}(t)\mathrm{d}t = \left[u_{\mathrm{C}}(0)t + \frac{\Delta i_{\mathrm{L}}}{2C}(\frac{t^2}{2} - T_{\mathrm{on}}t) - \frac{U_2}{LC}(\frac{t^3}{6} - T_{\mathrm{on}}\frac{t^2}{2} + \frac{T_{\mathrm{on}}^2}{2}t)\right]_{T_{\mathrm{on}}}^{T_{\mathrm{s}}} = \ldots$$
$$= u_{\mathrm{C}}(0)T_{\mathrm{off}} + \frac{\Delta i_{\mathrm{L}}}{C}\frac{T_{\mathrm{off}}^2}{12}. \tag{2.43}$$

Combining both parts results in

$$\overline{u}_{\mathrm{c}} = \frac{1}{T_{\mathrm{s}}}\left(u_{\mathrm{C}}(0)T_{\mathrm{s}} + \frac{\Delta i_{\mathrm{L}}}{C}\frac{T_{\mathrm{off}}^2 - T_{\mathrm{on}}^2}{12}\right)$$
$$= u_{\mathrm{C}}(0) + \frac{\Delta i_{\mathrm{L}}}{12C}T_{\mathrm{s}}(1-2D) \stackrel{!}{=} DU_1. \tag{2.44}$$

Solving for $u_{\mathrm{C}}(0)$ we receive the initial capacitor voltage as

$$u_{\mathrm{C}}(0) = DU_1 - \frac{\Delta i_{\mathrm{L}}}{12C}T_{\mathrm{s}}(1-2D). \tag{2.45}$$

Table of contents

Circuit realization

- The ideal (mechanical) switch cannot be operated with high frequency in practice.
- It must be replaced with semiconductor devices to allow for a practical realization.
- In Fig. 2.8 the simplest realization is shown utilizing one transistor and one diode.
- However, this configuration can only provide positive voltages and currents.
- Hence, the converter can operate in the first quadrant only.

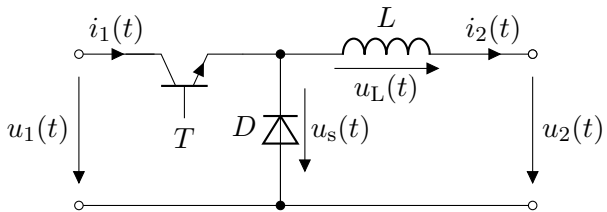

Fig. 2.8: Step-down converter with real components (single quadrant type)

Discontinous conduction mode (DCM)

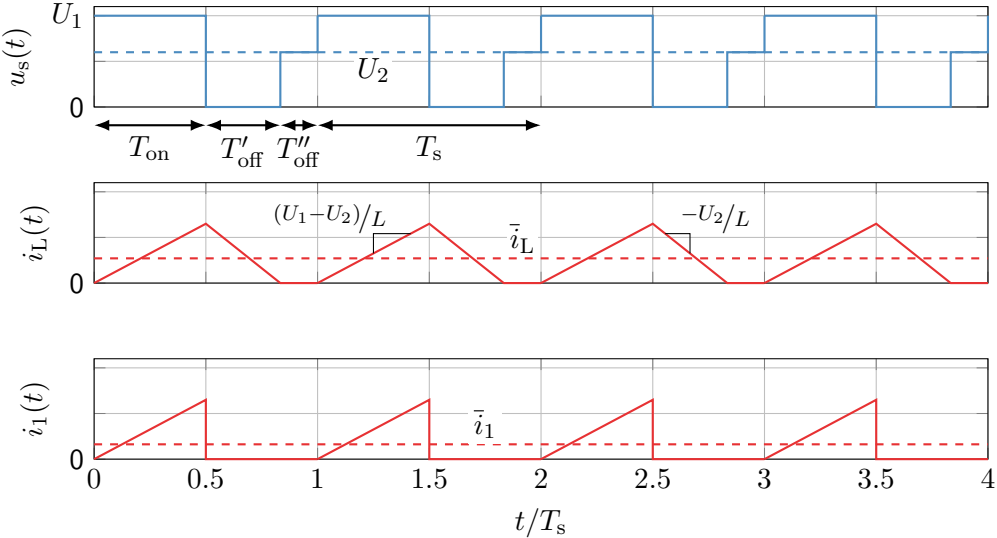

Switch states DCM

In contrast to the previous continuous conduction mode (CCM), the converter traverses three states in the discontinuous conduction mode (DCM):

- Transistor on-time: $T_{\mathrm{on}} = DT_{\mathrm{s}}$,
- Transistor off-time (conducting diode): $T'_{\mathrm{off}} = D'T_{\mathrm{s}}$,
- Transistor off-time (no conduction): $T''_{\mathrm{off}} = T_{\mathrm{s}} - T_{\mathrm{on}} - T'_{\mathrm{off}}$.

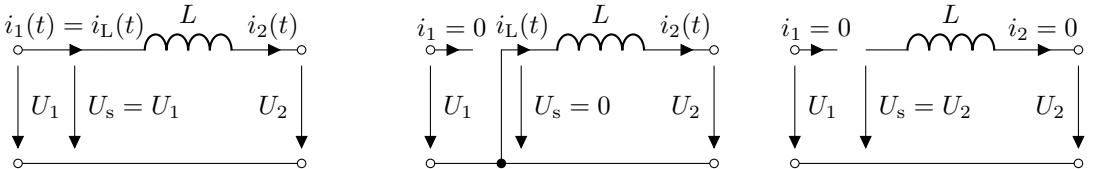

(a) Switch-on time T_{on} (b) Switch-off time T'_{off} (c) Switch-off time T''_{off}

Fig. 2.9: Switch states of the step-down converter including DCM

DCM operation characteristics

The operation in CCM and DCM can be distinguished by the inductor current ripple

$$\bar{i}_{\mathrm{L}} = \bar{i}_2 \begin{cases} \geq \frac{\Delta i_{\mathrm{L}}}{2} = 2D(1-D)\Delta i_{\mathrm{L,max}}: & \text{CCM}, \\ < \frac{\Delta i_{\mathrm{L}}}{2} = 2D(1-D)\Delta i_{\mathrm{L,max}}: & \text{DCM} \end{cases} \tag{2.46}$$

with

$$\Delta i_{\mathrm{L,max}} = \frac{U_1 T_{\mathrm{s}}}{4L}.$$

Hence, the operation mode directly depends on the duty cycle D and average load current $\bar{i}_2$, that is, it can change during runtime. While we have already discussed the operation in CCM, we will now focus on the operation in DCM. Here, it must be noted that

$$U_2 \neq U_1 D \quad \text{(DCM operation)}$$

applies due to the non-conducting diode during T''_{off}.

DCM operation characteristics (cont.)

To find the input-to-output voltage ratio in DCM, we can utilize the current ripple balance:

$$\begin{aligned} \Delta i_{\mathrm{L}} &= \frac{U_1 - U_2}{L} T_{\mathrm{on}} = i_{\mathrm{L}} = \frac{U_1 - U_2}{L} D T_{\mathrm{s}} \quad \text{(rising edge)}, \\ \Delta i_{\mathrm{L}} &= \frac{U_2}{L} T'_{\mathrm{off}} = \frac{U_2}{L} D' T_{\mathrm{s}} \qquad\qquad\quad \text{(falling edge)}. \end{aligned} \tag{2.47}$$

Solving for D' results in

$$D' = \frac{L \Delta i_{\mathrm{L}}}{U_2 T_{\mathrm{s}}} = \frac{U_1 - U_2}{U_2} D = \left(\frac{U_1}{U_2} - 1 \right) D. \tag{2.48}$$

The average load current is

$$\bar{i}_2 = \bar{i}_{\mathrm{L}} = \frac{1}{2} \Delta i_{\mathrm{L}} \frac{T_{\mathrm{on}} + T'_{\mathrm{off}}}{T_{\mathrm{s}}} = \frac{1}{2} \Delta i_{\mathrm{L}} (D + D') \tag{2.49}$$

which is derived from the area under the triangular-shaped current during T_{on} and T'_{off}.

DCM operation characteristics (cont.)

Inserting (2.48) into (2.49) yields

$$\begin{aligned}\bar{i}_2 &= \frac{1}{2}\Delta i_\mathrm{L} D \frac{U_1}{U_2} = \frac{U_1 - U_2}{2L} D T_\mathrm{s} D \frac{U_1}{U_2} \\ &= 2D^2 \left(\frac{U_1}{U_2} - 1 \right) \Delta i_{\mathrm{L,max}}.\end{aligned} \tag{2.50}$$

Solving for the DCM input-to-output voltage ratio results in

$$\frac{U_2}{U_1} = \frac{1}{1 + \frac{\bar{i}_2}{2\Delta i_{\mathrm{L,max}} D^2}}. \tag{2.51}$$

Since $\Delta i_{\mathrm{L,max}}$ also depends on U_1, cf. (2.21), the relation (2.51) only holds for a given U_1. Alternatively, we can utilize (2.50) and solve for U_2 to receive

$$U_2 = \frac{D^2 T_\mathrm{s} U_1^2}{D^2 T_\mathrm{s} U_1 + 2L\bar{i}_2}. \tag{2.52}$$

Step-down converter load curves

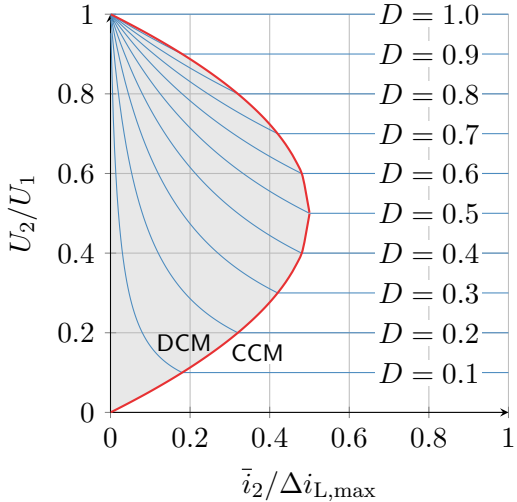

Fig. 2.10: Step-down converter load curves for CCM and DCM

Boundary conduction mode (BCM)

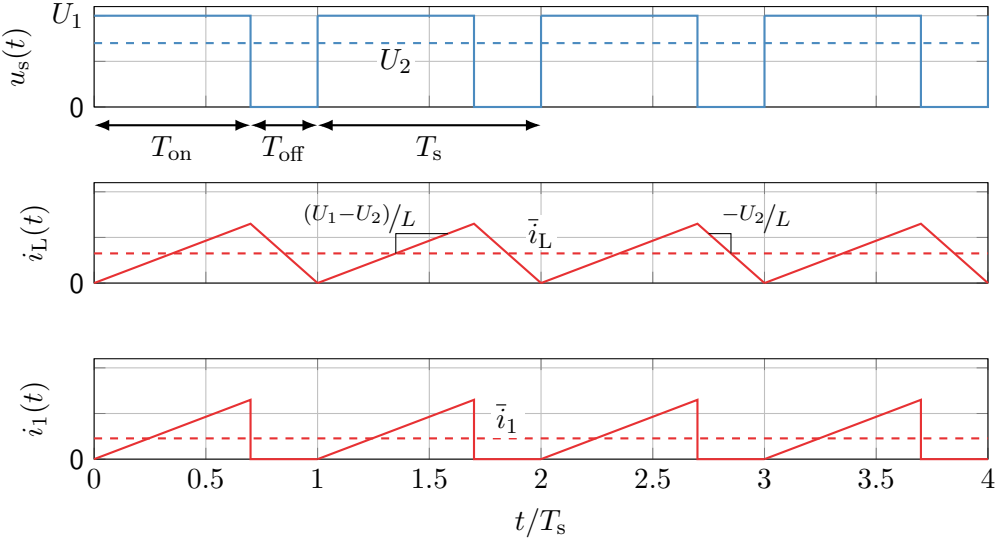

BCM operation characteristics

In the boundary conduction mode (BCM), the average inductor current load is exactly half of the current ripple, that is,

$$\bar{i}_{\mathrm{L}} = \bar{i}_2 = \frac{\Delta i_{\mathrm{L}}}{2} = 2D(1-D)\Delta i_{\mathrm{L,max}}. \tag{2.53}$$

- Diode current becomes zero and then the transistor turns on again.
  - The diode is not hard turned-off but its current naturally decays to zero.
  - Also known as zero current switching (ZCS) or generally soft switching.
- Requires adaptive switching frequency control if load changes. From (2.13) and (2.53) the BCM switching frequency results in

$$f_{\mathrm{s}} = \frac{1}{T_{\mathrm{s}}} = \frac{D(1-2)U_1}{L\Delta i_{\mathrm{L}}} = \frac{D(1-2)U_1}{2L\bar{i}_2}. \tag{2.54}$$

Motivation for BCM: diode reverse recovery

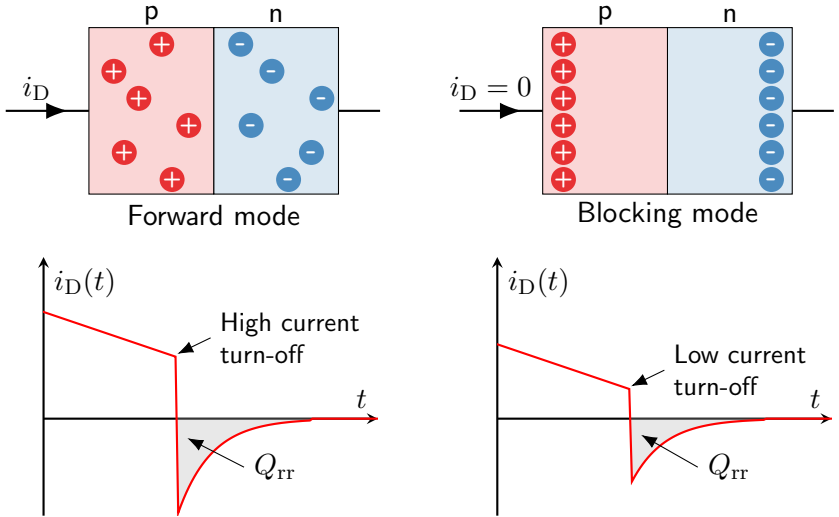

Fig. 2.11: Qualitative and simplified representation of the reverse recovery effect

BCM operation characteristics: comments

Advantages of BCM:

- Reduces the reverse recovery effect, that is, ZCS of the diode during turn on.
- Also allows ZCS transistor turn on.

Limitations of BCM:

- Transistor turn off and diode turn on cannot be soft switched due to topology constraints.
- Ripple current increases with load current: $\Delta i_{\mathrm{L}} = 2\bar{i}_2$.
  - May negatively affects load.
  - Increases conduction losses due to higher RMS current – compare (2.17).
  - High switching frequency required at low loads (switching losses).

Table of contents

Step-up converter: overview and assumptions

We consider the following assumptions:

- The switch is ideal, that is, infinitely fast.
- The input voltage is constant: $u_1(t) = U_1$.
- The output voltage is constant: $u_2(t) = U_2$.
- The input voltage is lower than the output voltage: $U_1 < U_2$.

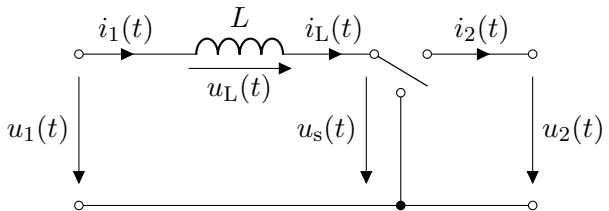

Fig. 2.12: Step-up converter (aka boost converter, ideal switch representation)

Step-up converter: switch states

The voltage at the switch is given by

$$u_{\mathrm{s}}(t) = \begin{cases} 0, & t \in [kT_{\mathrm{s}}, kT_{\mathrm{s}} + T_{\mathrm{on}}], \\ U_2, & t \in [kT_{\mathrm{s}} + T_{\mathrm{on}}, (k+1)T_{\mathrm{s}}]. \end{cases} \tag{2.55}$$

Note: switch on/off definition is reversed compared to the step-down converter.

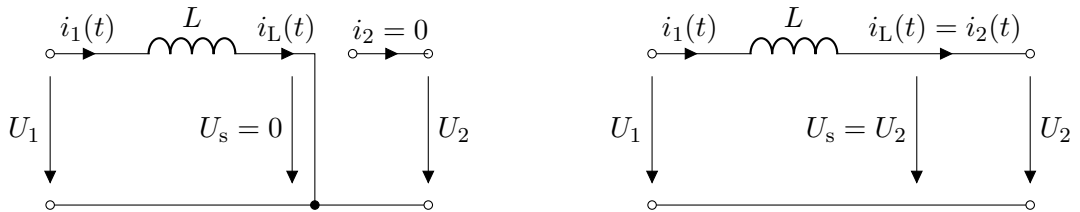

(a) Switch-on time (b) Switch-off time

Fig. 2.13: Switch states of the step-up converter

Step-up converter: steady-state time-domain behavior

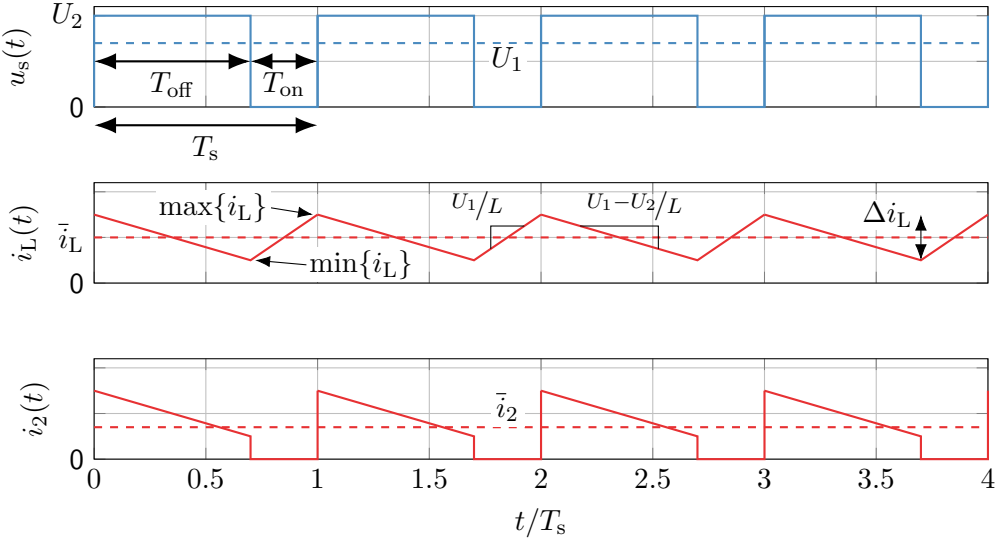

Step-up converter: voltage and current transfer ratios during steady state

In steady state, the absolute voltage-time integral over the inductor must be identical for the switch-on and switch-off interval, that is,

$$\int_0^{T_{\text{off}}} |u_{\text{L}}(t)|\,\mathrm{d}t \stackrel{!}{=} \int_{T_{\text{off}}}^{T_{\text{off}}+T_{\text{on}}} |u_{\text{L}}(t)|\,\mathrm{d}t \tag{2.56}$$

resulting in

$$(U_2 - U_1)T_{\text{off}} = U_1 T_{\text{on}} \quad \Leftrightarrow \quad (U_2 - U_1)(1-D)T_{\text{s}} = U_1 D T_{\text{s}} \tag{2.57}$$

and finally delivering the voltage transfer ratio

$$\frac{U_2}{U_1} = \frac{1}{1-D}. \tag{2.58}$$

Assuming a lossless converter ($P_{\text{in}} = P_{\text{out}}$), the current transfer ratio is

$$\frac{\bar{i}_1}{\bar{i}_2} = \frac{1}{1-D}. \tag{2.59}$$

Step-up converter: current ripple

The inductor current ripple can be found considering the positive slope during T_{on} with

$$\Delta i_{\mathrm{L}} = \frac{U_1}{L} T_{\mathrm{on}} = \frac{U_1}{L} D T_{\mathrm{s}} \tag{2.60}$$

or alternatively evaluating the negative slope during T_{off} with

$$\Delta i_{\mathrm{L}} = \frac{U_2 - U_1}{L} T_{\mathrm{off}} = \frac{U_2 - U_1}{L} (1 - D) T_{\mathrm{s}} = \frac{D(1 - D) T_{\mathrm{s}}}{L} U_2. \tag{2.61}$$

In addition, one can find that the output current and power is changing step-like within the step-up converter, while this is the case for the input side in the step-down converter:

$$\text{step-down:} \quad i_1(t) = \begin{cases} i_{\mathrm{L}}(t), & \text{switch on,} \\ 0, & \text{switch off,} \end{cases} \qquad \text{step-up:} \quad i_1(t) = \begin{cases} i_{\mathrm{L}}(t), & \text{switch on,} \\ i_{\mathrm{L}}(t), & \text{switch off,} \end{cases}$$

$$\text{step-down:} \quad i_2(t) = \begin{cases} i_{\mathrm{L}}(t), & \text{switch on,} \\ i_{\mathrm{L}}(t), & \text{switch off,} \end{cases} \qquad \text{step-up:} \quad i_2(t) = \begin{cases} 0, & \text{switch on,} \\ i_{\mathrm{L}}(t), & \text{switch off.} \end{cases}$$

Step-up converter: current ripple (cont.)

In contrast to the step-down converter, cf. (2.19), the worst-case current ripple of the step-up converter occurs for

$$\Delta i_{\mathrm{L}} = \frac{U_1}{L} D T_{\mathrm{s}} \quad \Rightarrow \quad D_{\max} \to 1. \tag{2.62}$$

This corresponds to the case of an infinitely large output voltage U_2:

$$\lim_{D \to 1} U_2 = \lim_{D \to 1} \frac{1}{1 - D} U_1 = \infty. \tag{2.63}$$

The maximum current ripple is then

$$\Delta i_{\mathrm{L,max}} = \frac{1}{L} U_1 T_{\mathrm{s}}. \tag{2.64}$$

Consequently, we can express the current ripple as:

$$\Delta i_{\mathrm{L}} = D \Delta i_{\mathrm{L,max}}. \tag{2.65}$$

Step-up converter with output capacitor: overview and assumptions

We consider the following assumptions:

- The switch is ideal, that is, infinitely fast.
- The input voltage is constant: $u_1(t) = U_1$.
- The output current is constant: $i_2(t) = I_2$.
- The inductor current $i_\mathrm{L}(t)$ is unaffected by the output voltage ripple (remains triangular).
- The output voltage is greater than the output voltage: $u_2(t) > U_1$.

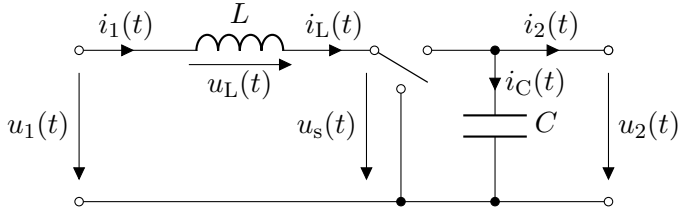

Fig. 2.14: Step-up converter (ideal switch representation) with output capacitor

Step-up converter: capacitor voltage analysis

In contrast to the step-down converter, the capacitor current is changing step-like during the switching event:

$$i_{\mathrm{C}}(t) = \begin{cases} i_{\mathrm{L}}(t) - I_2, & t \in [kT_{\mathrm{s}}, kT_{\mathrm{s}} + T_{\mathrm{off}}], \\ -I_2, & t \in [kT_{\mathrm{s}} + T_{\mathrm{off}}, (k+1)T_{\mathrm{s}}]. \end{cases} \tag{2.66}$$

The steady-state inductor current during the switch-off interval is

$$\begin{aligned} i_{\mathrm{L}}(t) &= \bar{i}_{\mathrm{L}} + \frac{\Delta i_{\mathrm{L}}}{2} - \frac{\Delta i_{\mathrm{L}}}{T_{\mathrm{off}}}(t - kT_{\mathrm{s}}) \\ &= \frac{1}{1-D} I_2 + \Delta i_{\mathrm{L}} \frac{T_{\mathrm{off}} - 2(t - kT_{\mathrm{s}})}{2T_{\mathrm{off}}}, \quad t \in [kT_{\mathrm{s}}, kT_{\mathrm{s}} + T_{\mathrm{off}}]. \end{aligned} \tag{2.67}$$

which follows from the triangular signal shape. Inserting into (2.66) yields

$$i_{\mathrm{C}}(t) = \begin{cases} \frac{D}{1-D} I_2 + \Delta i_{\mathrm{L}} \frac{T_{\mathrm{off}} - 2(t - kT_{\mathrm{s}})}{2T_{\mathrm{off}}}, & t \in [kT_{\mathrm{s}}, kT_{\mathrm{s}} + T_{\mathrm{off}}], \\ -I_2, & t \in [kT_{\mathrm{s}} + T_{\mathrm{off}}, (k+1)T_{\mathrm{s}}]. \end{cases} \tag{2.68}$$

Step-up converter: capacitor voltage analysis (cont.)

The capacitor voltage during the switch-off period is then

$$\begin{aligned} u_{\mathrm{C}}(t) &= u_{\mathrm{C}}(kT_{\mathrm{s}}) + \frac{1}{C}\int_{kT_{\mathrm{s}}}^{t} i_{\mathrm{C}}(\tau)\mathrm{d}\tau, \quad t \in [kT_{\mathrm{s}}, kT_{\mathrm{s}} + T_{\mathrm{off}}] \\ &= u_{\mathrm{C}}(kT_{\mathrm{s}}) + \frac{1}{C}\left(\int_{kT_{\mathrm{s}}}^{t} \frac{D}{1-D} I_2 + \Delta i_{\mathrm{L}} \frac{T_{\mathrm{off}} - 2(\tau - kT_{\mathrm{s}})}{2T_{\mathrm{off}}}\mathrm{d}\tau\right) \\ &= u_{\mathrm{C}}(kT_{\mathrm{s}}) + \left[\frac{D\tau}{(1-D)C} I_2 + \frac{\Delta i_{\mathrm{L}}}{2T_{\mathrm{off}}C}\left(T_{\mathrm{off}}\tau - \tau^2 + 2\tau kT_{\mathrm{s}}\right)\right]_{kT_{\mathrm{s}}}^{t} \\ &= u_{\mathrm{C}}(kT_{\mathrm{s}}) + \frac{D(t - kT_{\mathrm{s}})}{(1-D)C} I_2 + \frac{\Delta i_{\mathrm{L}}}{2T_{\mathrm{off}}C}\left(T_{\mathrm{off}}(t - kT_{\mathrm{s}}) - t(t - 2kT_{\mathrm{s}}) - (kT_{\mathrm{s}})^2\right). \end{aligned} \tag{2.69}$$

The capacitor voltage at the end of the switch-off period is

$$u_{\mathrm{C}}(kT_{\mathrm{s}} + T_{\mathrm{off}}) = u_{\mathrm{C}}(kT_{\mathrm{s}}) + \frac{DI_2}{(1-D)C} T_{\mathrm{off}}. \tag{2.70}$$

Step-up converter: capacitor voltage analysis (cont.)

The capacitor voltage during the switch-on period is then

$$
\begin{aligned}
u_{\mathrm{C}}(t) &= u_{\mathrm{C}}(kT_{\mathrm{s}} + T_{\mathrm{off}}) + \frac{1}{C}\int_{kT_{\mathrm{s}}+T_{\mathrm{off}}}^{t} i_{\mathrm{C}}(\tau)\mathrm{d}\tau, \quad t \in [kT_{\mathrm{s}} + T_{\mathrm{off}}, (k+1)T_{\mathrm{s}}] \\
&= u_{\mathrm{C}}(kT_{\mathrm{s}} + T_{\mathrm{off}}) + \frac{1}{C}\int_{kT_{\mathrm{s}}+T_{\mathrm{off}}}^{t} -I_2\mathrm{d}\tau \\
&= u_{\mathrm{C}}(kT_{\mathrm{s}} + T_{\mathrm{off}}) - \frac{I_2}{C}(t - kT_{\mathrm{s}} - T_{\mathrm{off}}) \\
&= \underbrace{u_{\mathrm{C}}(kT_{\mathrm{s}}) + \frac{DI_2}{(1-D)C}T_{\mathrm{off}}}_{=u_{\mathrm{C}}(kT_{\mathrm{s}}+T_{\mathrm{off}})} - \frac{I_2}{C}(t - kT_{\mathrm{s}} - T_{\mathrm{off}}).
\end{aligned}
\tag{2.71}
$$

Here, $u_{\mathrm{C}}(kT_{\mathrm{s}})$ is the (yet unknown) initial capacitor voltage at the beginning of a period, which will be derived later.

Step-up converter: capacitor voltage analysis (cont.)

In steady state, the capacitor voltage at the end of the switch-on period is identical to the voltage at the beginning of the switch-off period, that is,

$$u_{\mathrm{C}}(kT_{\mathrm{s}}) = u_{\mathrm{C}}((k+1)T_{\mathrm{s}}).$$

Hence, we can identify the voltage ripple from (2.71) as

$$\begin{aligned}\Delta u_{\mathrm{C}} &= \frac{I_2}{C}T_{\mathrm{on}} = \frac{DI_2}{(1-D)C}T_{\mathrm{off}} \\ &= \frac{I_2}{C}DT_{\mathrm{s}} = \frac{\Delta Q}{C}\end{aligned} \tag{2.72}$$

with the charge ripple $\Delta Q = DI_2T_{\mathrm{s}}$.

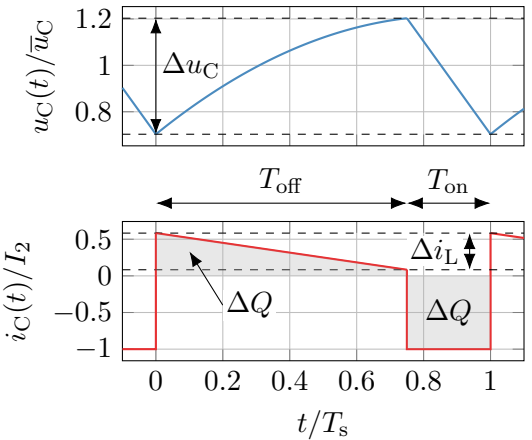

Fig. 2.15: Step-up converter voltage ripple

Step-up converter: capacitor voltage analysis (cont.)

To calculate the initial capacitor voltage $u_\mathrm{C}(kT_\mathrm{s})$, we can utilize

$$\overline{u}_\mathrm{c} = \frac{1}{T_\mathrm{s}} \int_0^{T_\mathrm{s}} u_\mathrm{C}(t)\mathrm{d}t \stackrel{!}{=} \overline{u}_2 = \frac{U_1}{1-D} \tag{2.73}$$

since the average capacitor voltage must be equal to the average output voltage. This yields

$$\begin{aligned} \overline{u}_\mathrm{c} &= \frac{1}{T_\mathrm{s}} \left(\int_0^{T_\mathrm{off}} u_\mathrm{C}(t)\mathrm{d}t + \int_{T_\mathrm{off}}^{T_\mathrm{s}} u_\mathrm{C}(t)\mathrm{d}t \right) \\ &= \dots \\ &= u_\mathrm{C}(kT_\mathrm{s}) + \frac{\Delta u_\mathrm{C}}{2} + \frac{\Delta i_\mathrm{L} T_\mathrm{s}}{12C}(1-D)^2 \end{aligned} \tag{2.74}$$

and finally delivers

$$\begin{aligned} u_\mathrm{C}(kT_\mathrm{s}) &= \frac{U_1}{1-D} - \frac{\Delta u_\mathrm{C}}{2} - \frac{\Delta i_\mathrm{L} T_\mathrm{s}}{12C}(1-D)^2 \\ &= \frac{U_1}{1-D} - \frac{I_2}{2C} D T_\mathrm{s} - \frac{U_1 T_\mathrm{s}^2}{12LC} D(1-D)^2. \end{aligned} \tag{2.75}$$

Circuit realization

- In Fig. 2.16 the simplest realization is shown utilizing one transistor and one diode.
- This configuration can only provide positive voltages and currents (first quadrant).
- The previously made step-up converter's switch-on definition (cf. Fig. 2.13) results from the transistor position in the circuit – difference to the step-down converter.

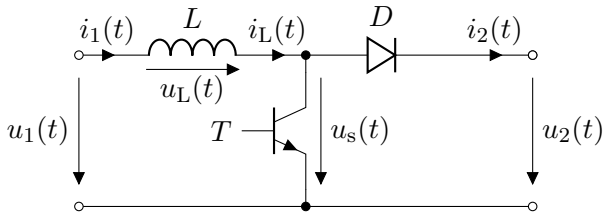

Fig. 2.16: Step-up converter with real components (single quadrant type)

Step-up converter: DCM

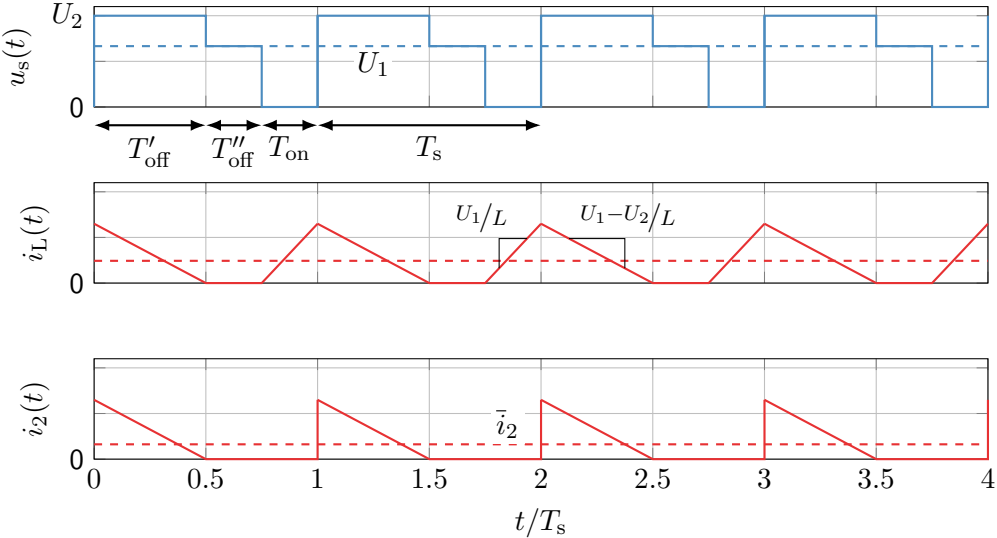

Step-up converter: switch states in DCM

The step-up converter in DCM has three different switch states:

- Transistor on-time: $T_{\mathrm{on}} = DT_{\mathrm{s}}$,
- Transistor off-time (conducting diode): $T'_{\mathrm{off}} = D'T_{\mathrm{s}}$,
- Transistor off-time (no conduction): $T''_{\mathrm{off}} = T_{\mathrm{s}} - T_{\mathrm{on}} - T'_{\mathrm{off}}$.

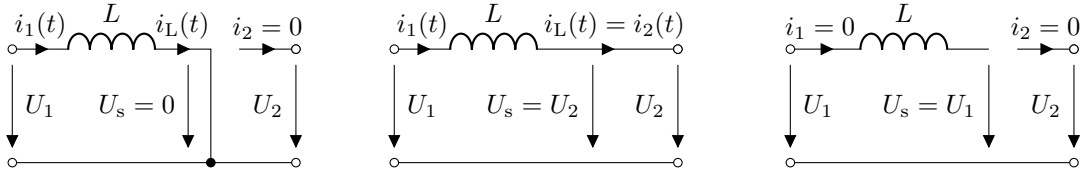

(a) Switch-on time T_{on} (b) Switch-off time T'_{off} (c) Switch-off time T''_{off}

Fig. 2.17: Switch states of the step-up converter including DCM

Step-up converter: DCM operation characteristics

In DCM operation

$$\bar{i}_{\mathrm{L}} = \bar{i}_1 < \frac{\Delta i_{\mathrm{L}}}{2} \quad \Rightarrow \quad U_2 \neq U_1 \frac{1}{1-D}$$

applies due to the non-conducting diode during T''_{off}. To find the input-to-output voltage ratio in DCM, we again utilize the current ripple balance:

$$\begin{aligned} \Delta i_{\mathrm{L}} &= \frac{U_1}{L} T_{\mathrm{on}} = \frac{U_1}{L} D T_{\mathrm{s}} && \text{(rising edge)}, \\ \Delta i_{\mathrm{L}} &= \frac{U_2 - U_1}{L} T'_{\mathrm{off}} = \frac{U_2 - U_1}{L} D' T_{\mathrm{s}} && \text{(falling edge)}. \end{aligned} \tag{2.76}$$

Solving for D' yields

$$D' = \frac{U_1}{U_2 - U_1} D. \tag{2.77}$$

The average load current is

$$\bar{i}_2 = \frac{\Delta i_{\mathrm{L}}}{2} \frac{T'_{\mathrm{off}}}{T_{\mathrm{s}}} = \frac{\Delta i_{\mathrm{L,max}} D}{2} D' = \frac{\Delta i_{\mathrm{L,max}}}{2} \frac{U_1}{U_2 - U_1} D^2. \tag{2.78}$$

Step-up converter: DCM operation characteristics (cont.)

Solving (2.78) delivers the step-up converter voltage gain in DCM as

$$\frac{U_2}{U_1} = 1 + \frac{D^2}{2}\frac{\Delta i_{\mathrm{L,max}}}{\bar{i}_2}. \tag{2.79}$$

Since $\Delta i_{\mathrm{L,max}}$ also depends on U_1, cf. (2.64), the relation (2.79) only holds for a given U_1. Hence, we can insert (2.64) in (2.79) and solve for U_2 to receive

$$U_2 = U_1 + \frac{D^2}{2}\frac{T_{\mathrm{s}}}{L\bar{i}_2}. \tag{2.80}$$

Finally, the step-up converter operates in BCM if

$$\bar{i}_{\mathrm{L}} = \bar{i}_1 = \frac{\Delta i_{\mathrm{L}}}{2} \quad \Leftrightarrow \quad \bar{i}_2 = (1-D)\frac{\Delta i_{\mathrm{L}}}{2}. \tag{2.81}$$

Step-up converter load curves

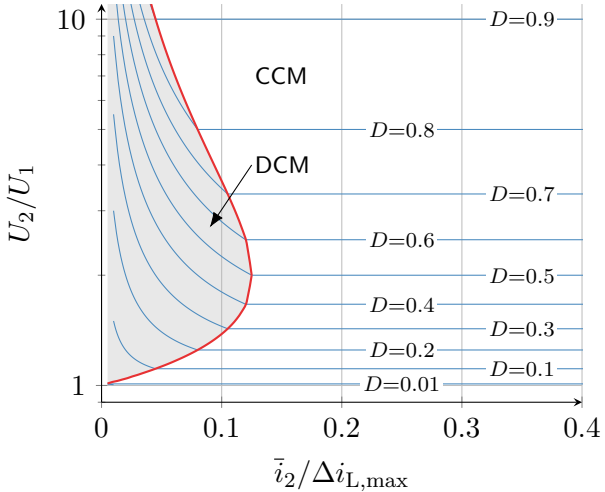

Fig. 2.18: Step-up converter load curves for CCM and DCM (note: logarithmic ordinate)

Table of contents

Buck-boost converter: combining step-up and step-down stages

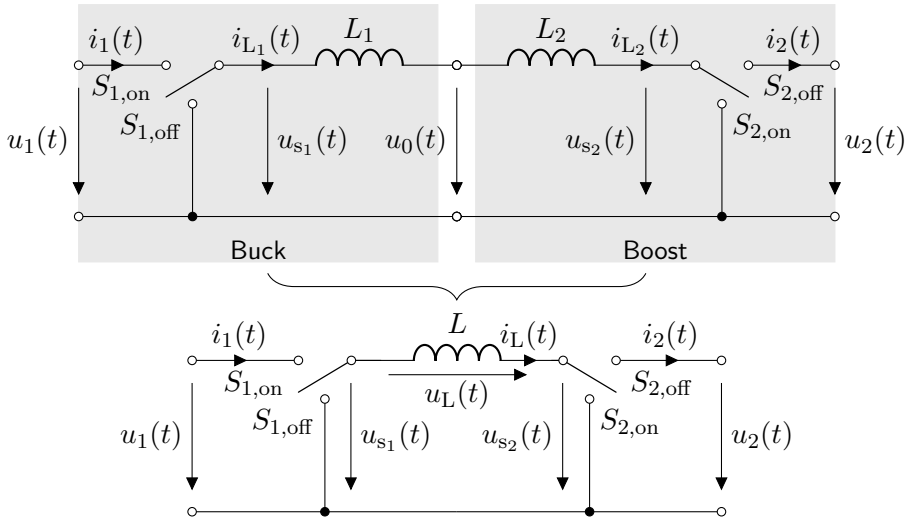

Fig. 2.19: Buck-boost converter (ideal switch representation)

Buck-boost converter: switching states

The buck-boost converter switches are operated synchronously, that is, S_1 and S_2 are either on or off at the same time. Thus, the converter has only two switch states:

$$\begin{aligned} \{S_{1,\mathrm{on}}, S_{2,\mathrm{on}}\} \quad &\rightarrow \quad u_{\mathrm{s}_1}(t) = U_1, u_{\mathrm{s}_2}(t) = 0, \\ \{S_{1,\mathrm{off}}, S_{2,\mathrm{off}}\} \quad &\rightarrow \quad u_{\mathrm{s}_1}(t) = 0, \quad u_{\mathrm{s}_2}(t) = U_2. \end{aligned} \tag{2.82}$$

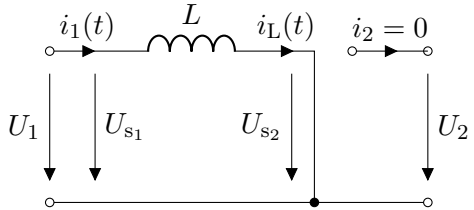

(a) Switch-on time

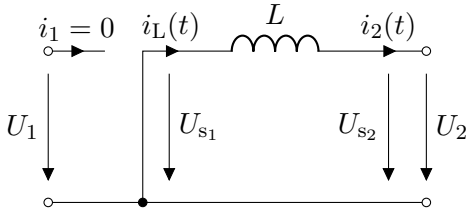

(b) Switch-off time

Fig. 2.20: Switch states of the (synchronous) buck-boost converter

Buck-boost converter: CCM voltage transfer ratio

In CCM, we can derive the voltage transfer ratio directly by the serial connection of the buck and boost stages from Fig. 2.19

$$\frac{U_0}{U_1} = D, \qquad \frac{U_2}{U_0} = \frac{1}{1-D}, \tag{2.83}$$

leading to

$$\frac{U_2}{U_1} = \frac{D}{1-D}. \tag{2.84}$$

Alternatively, we can derive this result from the voltage balance of the inductor L:

$$u_{\mathrm{L}}(t) = \begin{cases} U_1, & t \in [kT_{\mathrm{s}}, kT_{\mathrm{s}} + T_{\mathrm{on}}], \\ -U_2 & t \in [kT_{\mathrm{s}} + T_{\mathrm{on}}, (k+1)T_{\mathrm{s}}]. \end{cases} \tag{2.85}$$

In steady state, the average inductor voltage per period must be zero, yielding

$$U_1 T_{\mathrm{on}} = U_2 T_{\mathrm{off}} \quad \Leftrightarrow \quad U_1 D T_{\mathrm{s}} = U_2 (1-D) T_{\mathrm{s}} \quad \Leftrightarrow \quad \frac{U_2}{U_1} = \frac{D}{1-D}. \tag{2.86}$$

Buck-boost converter: steady-state time-domain behavior

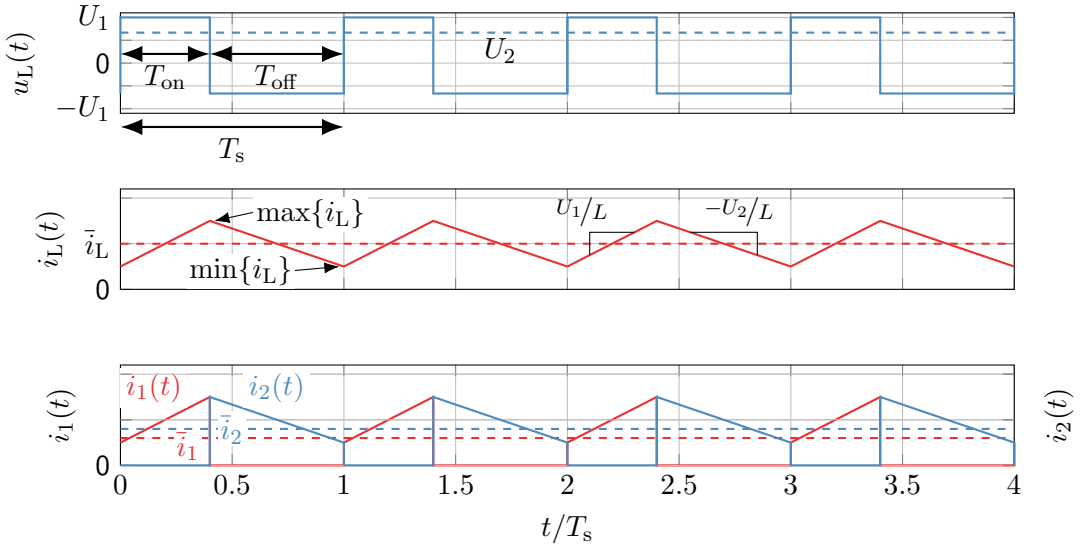

Buck-boost converter: current ripple

The peak-to-peak current ripple of the buck-boost converter is given by

$$\begin{aligned}\Delta i_{\mathrm{L}} &= \max\{i_{\mathrm{L}}(t)\} - \min\{i_{\mathrm{L}}(t)\} = i_{\mathrm{L}}(t = T_{\mathrm{on}}) - i_{\mathrm{L}}(t = T_{\mathrm{s}}) \\ &= \frac{U_1}{L} T_{\mathrm{on}} = \frac{U_2}{L} T_{\mathrm{off}} \\ &= D \frac{T_{\mathrm{s}}}{L} U_1 = D \Delta i_{\mathrm{L,max}}.\end{aligned} \tag{2.87}$$

The buck-boost converter current ripple characteristic matches the previous boost converter behavior – compare (2.62):

- Its minimal for $D \to 0$ since the output voltage becomes zero and the inductor is connected to the output voltage over the entire switching period.
- Its maximal for $D \to 1$ since the inductor is connected to the (non-zero) input voltage over the entire switching period.

Buck-boost converter: output capacitor and voltage ripple

With the usual simplifying assumptions (cf. Fig. 2.14), in particular, a constant output current $i_2(t) = I_2$, the capacitor's current during the switch-on time is given by

$$i_\mathrm{C}(t) = -i_2(t) = -I_2, \quad t \in [kT_\mathrm{s}, kT_\mathrm{s} + T_\mathrm{off}].$$

This is identical to the step-up converter, leading to the same voltage ripple

$$\Delta u_\mathrm{C} = \frac{I_2}{C} T_\mathrm{on} = \frac{I_2}{C} D T_\mathrm{s}.$$

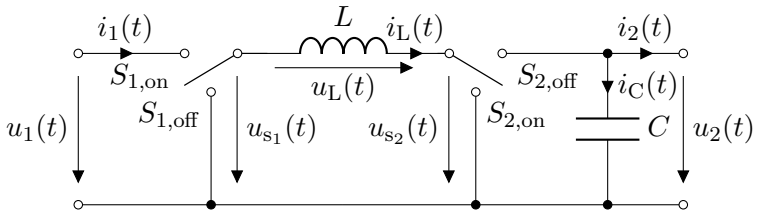

Fig. 2.21: Buck-boost converter with output capacitor

Buck-boost converter: circuit realization

- In Fig. 2.22 the buck-boost converter realization is a direct series circuit combination of Fig. 2.8 and Fig. 2.16.
- This configuration can only provide positive voltages and currents (first quadrant).
- It should be noted that this circuit requires two diodes and two transistors.

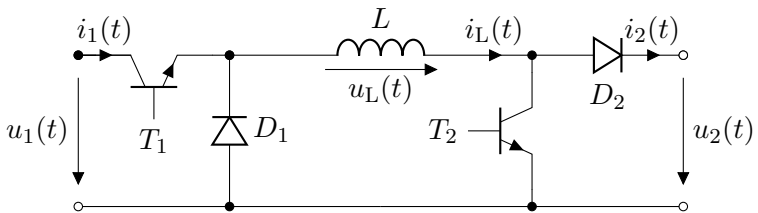

Fig. 2.22: Buck-boost converter with real components (single quadrant type)

Buck-boost converter: switch states in DCM

The buck-boost converter in DCM has three different switch states:

- Transistor on-time: $T_{\mathrm{on}} = DT_{\mathrm{s}}$,
- Transistor off-time (conducting diode): $T'_{\mathrm{off}} = D'T_{\mathrm{s}}$,
- Transistor off-time (no conduction): $T''_{\mathrm{off}} = T_{\mathrm{s}} - T_{\mathrm{on}} - T'_{\mathrm{off}}$.

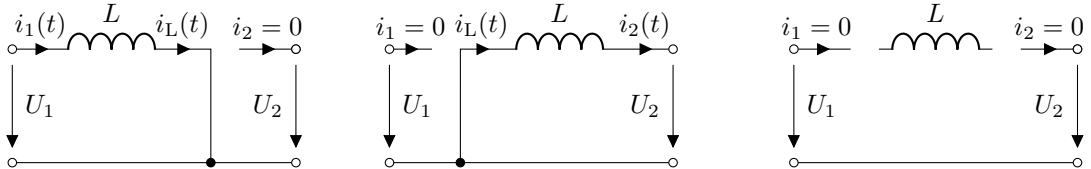

(a) Switch-on time T_{on} (b) Switch-off time T'_{off} (c) Switch-off time T''_{off}

Fig. 2.23: Switch states of the (synchronous) buck-boost converter including DCM

Buck-boost converter: DCM operation characteristics

In DCM operation

$$\bar{i}_{\mathrm{L}} < \frac{\Delta i_{\mathrm{L}}}{2} \quad \Rightarrow \quad U_2 \neq U_1 \frac{D}{1-D}$$

applies due to the non-conducting diode during T''_{off}. To find the input-to-output voltage ratio in DCM, we again utilize the current ripple balance:

$$\begin{aligned} \Delta i_{\mathrm{L}} &= \frac{U_1}{L} T_{\mathrm{on}} = \frac{U_1}{L} D T_{\mathrm{s}} \quad \text{(rising edge)}, \\ \Delta i_{\mathrm{L}} &= \frac{U_2}{L} T'_{\mathrm{off}} = \frac{U_2}{L} D' T_{\mathrm{s}} \quad \text{(falling edge)}. \end{aligned} \tag{2.88}$$

Solving for D' yields

$$D' = \frac{U_1}{U_2} D. \tag{2.89}$$

The average load current is

$$\bar{i}_2 = \frac{\Delta i_{\mathrm{L}}}{2} \frac{T'_{\mathrm{off}}}{T_{\mathrm{s}}} = \frac{\Delta i_{\mathrm{L,max}} D}{2} D' = \frac{\Delta i_{\mathrm{L,max}}}{2} \frac{U_1}{U_2} D^2. \tag{2.90}$$

Buck-boost converter: DCM operation characteristics (cont.)

Solving (2.90) delivers the buck-boost converter voltage gain in DCM as

$$\frac{U_2}{U_1} = \frac{D^2}{2} \frac{\Delta i_{\mathrm{L,max}}}{\bar{i}_2}. \tag{2.91}$$

Since $\Delta i_{\mathrm{L,max}}$ also depends on U_1, the relation (2.91) only holds for a given U_1. Hence, we can insert (2.87) in (2.91) and solve for U_2 to receive

$$U_2 = U_1^2 \frac{D^2}{2} \frac{T_\mathrm{s}}{L \bar{i}_2}. \tag{2.92}$$

Finally, the buck-boost converter operates in BCM if

$$\bar{i}_\mathrm{L} = \frac{\Delta i_\mathrm{L}}{2} \quad \Leftrightarrow \quad \bar{i}_2 = \Delta i_{\mathrm{L,max}} \frac{1}{2} \frac{D}{1-D}. \tag{2.93}$$

Buck-boost converter load curves

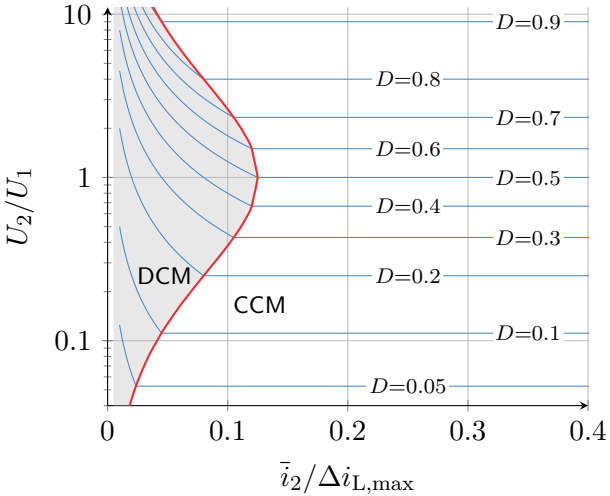

Fig. 2.24: Buck-boost converter load curves for CCM and DCM (note: logarithmic ordinate)

Table of contents

Recap: buck-boost converter switching states

Key characteristic of (synchronous) buck-boost converter

The switching scheme of the (synchronous) buck-boost converter from Fig. 2.20 is realized by two switches and characterized by:

- During switch-on: inductor is connected to $u_1(t)$,
- During switch-off: inductor is connected to $u_2(t)$.

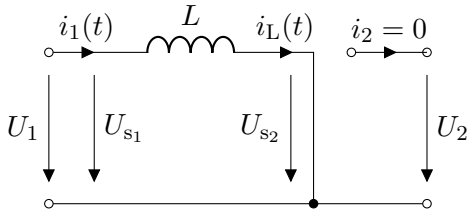

(a) Switch-on time

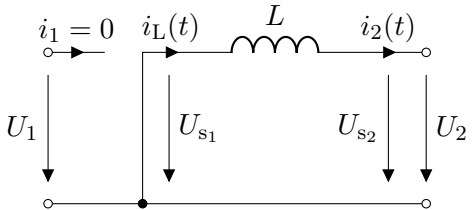

(b) Switch-off time

Inverting buck-boost converter: overview

- Voltage change at the inductor can be also achieved by a single switch which input is connected to the inductor.
- Assuming an ideal, infinitely fast switch, the inductor current $i_{\mathrm{L}}(t)$ remains well-defined (no open switch at inductor).

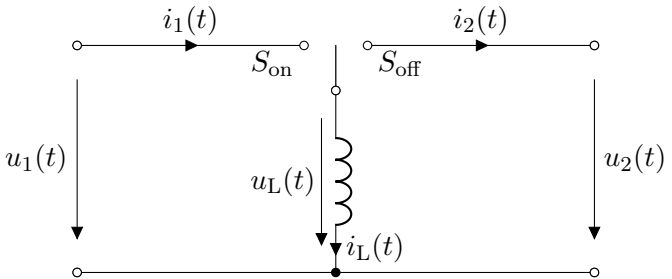

Fig. 2.26: Inverting buck-boost converter (ideal switch representation)

Polarity change of inverting buck-boost converter

- One side of the inductor remains connected to the common connection rail between input and output side.
- The other inductor side switches between the upper input and output rail.
- Consequence: voltage and current directions are inverted between the two switch states.

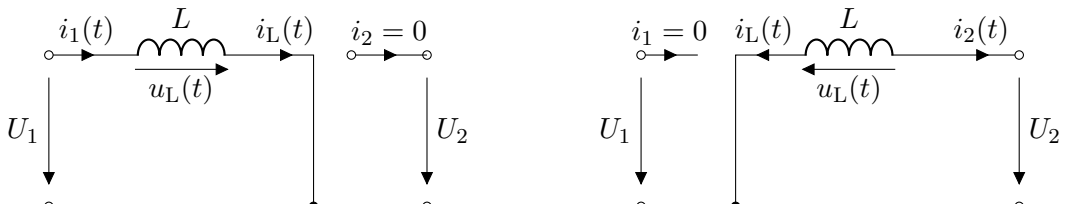

(a) Switch-on time

(b) Switch-off time

Fig. 2.27: Voltage and current definitions of the inverting buck-boost converter

Inverting buck-boost converter: voltage transfer ratios

In CCM, the voltage balance of the inductor L delivers:

$$u_{\mathrm{L}}(t) = \begin{cases} U_1, & t \in [kT_{\mathrm{s}}, kT_{\mathrm{s}} + T_{\mathrm{on}}], \\ U_2 & t \in [kT_{\mathrm{s}} + T_{\mathrm{on}}, (k+1)T_{\mathrm{s}}]. \end{cases} \tag{2.94}$$

In steady state, the average inductor voltage per period must be zero, yielding

$$U_1 T_{\mathrm{on}} = -U_2 T_{\mathrm{off}} \quad \Leftrightarrow \quad U_1 D T_{\mathrm{s}} = -U_2 (1-D) T_{\mathrm{s}} \quad \Leftrightarrow \quad \frac{U_2}{U_1} = -\frac{D}{1-D}. \tag{2.95}$$

Likewise, the analysis of the DCM mode reveals

$$\frac{U_2}{U_1} = -\frac{D^2}{2} \frac{\Delta i_{\mathrm{L,max}}}{\bar{i}_2} \quad \Leftrightarrow \quad U_2 = -U_1^2 \frac{D^2}{2} \frac{T_{\mathrm{s}}}{L \bar{i}_2}. \tag{2.96}$$

Hence, the inverting buck-boost converter has a negative voltage transfer ratio in CCM and DCM, but the same absolute voltage gain as the synchronous buck-boost converter.

Inverting buck-boost converter: circuit realization

- Energy transfer takes place solely indirect by intermediate storage within inductor.
- Further characteristics (current and voltage ripple, operation modes) are analogous to the synchronous buck-boost converter.
- Transistor needs to block up to $|u_1(t)| + |u_2(t)|$, in contrast to step-down/up converter where only the input or output voltage is blocked by the transistor.

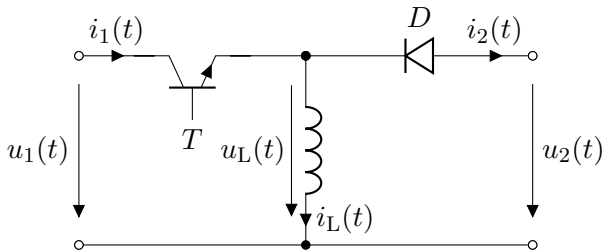

Fig. 2.28: Inverting buck-boost converter with real components (single quadrant type)

Table of contents

Semiconductor utilization

We define the semiconductor utilization as the ratio of the average output power to the transistor (peak) power:

$$\frac{P_2}{P_\mathrm{T}} = \frac{U_2 I_2}{\max\{u_\mathrm{T}\} \cdot \max\{i_\mathrm{T}\}}. \tag{2.97}$$

Background and interpretation:

- Transistor needs to withstand the peak voltage and current (rating requirement).
- The lower the semiconductor utilization, the more costly / bulky the transistor for a given converter power (key parameter for the selection of the power stage).

Assumptions for following calculations:

- Lossless operation in CCM,
- Current and voltage ripple are marginal and can be neglected,
- Given a constant P_2, the duty cycle D is adjusted to achieve the desired output power.

Semiconductor utilization: step-down converter

The step-down converter's transistor peak voltage and current are (cf. Fig. 2.2)

$$\begin{aligned} \max\{u_\mathrm{T}\} &= U_1, \\ \max\{i_\mathrm{T}\} &= \frac{\bar{i}_1}{D} = \frac{I_1}{D}. \end{aligned} \tag{2.98}$$

The transistor must block the (constant) input voltage U_1 and step-like changing current $i_1(t) = i_\mathrm{T}(t)$. The semiconductor utilization is

$$\begin{aligned} \frac{P_2}{P_\mathrm{T}} &= \frac{U_2 I_2}{U_1 \frac{\bar{i}_1}{D}} = \frac{U_1 I_1}{U_1 \frac{I_1}{D}} \\ &= D. \end{aligned} \tag{2.99}$$

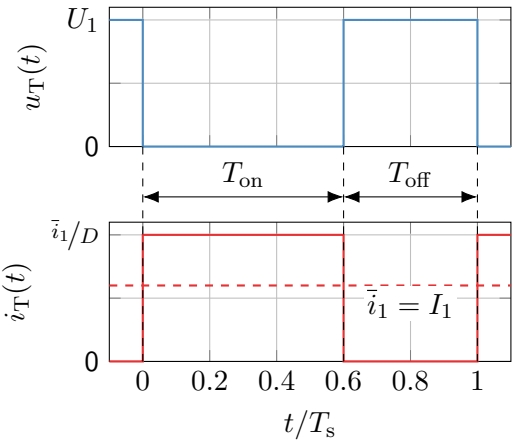

Fig. 2.29: Voltage and current at the step-down converter transistor (w/o current ripple)

Semiconductor utilization: step-up converter

The step-up converter's transistor peak voltage and current are (cf. Fig. 2.13)

$$\begin{aligned} \max\{u_\mathrm{T}\} &= U_2, \\ \max\{i_\mathrm{T}\} &= \max\{i_\mathrm{L}\} = I_1. \end{aligned} \tag{2.100}$$

The transistor must block the (constant) output voltage U_2 and (constant) input current $i_1(t) = i_\mathrm{T}(t)$, which is filtered by the inductor. The semiconductor utilization is

$$\begin{aligned} \frac{P_2}{P_\mathrm{T}} = \frac{U_2 I_2}{U_2 I_1} = \frac{I_2}{I_1} \\ = 1 - D. \end{aligned} \tag{2.101}$$

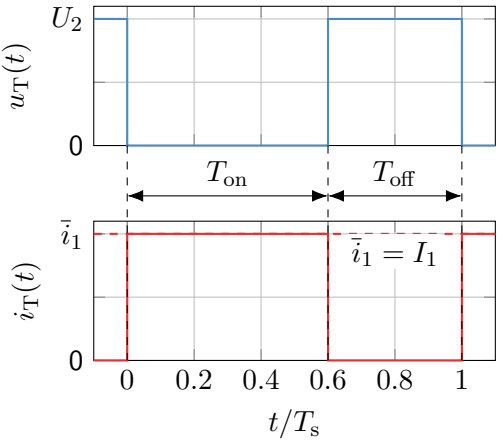

Fig. 2.30: Voltage and current at the step-up converter transistor (w/o current ripple)

Semiconductor utilization: inverting buck-boost converter

The inv. buck-boost converter's transistor peak voltage and current are (cf. Fig. 2.27)

$$\max\{u_\mathrm{T}\} = U_1 - U_2,$$
$$\max\{i_\mathrm{T}\} = \frac{\bar{i}_1}{D} = \frac{I_1}{D}. \qquad (2.102)$$

The transistor must block the (combined) input and output voltage and step-like changing current $i_1(t) = i_\mathrm{T}(t)$. The semiconductor utilization is

$$\frac{P_2}{P_\mathrm{T}} = \frac{U_2 I_2}{(U_1 - U_2)\frac{\bar{i}_1}{D}} = \frac{U_1 I_1}{U_1 \frac{1}{1-D}\frac{I_1}{D}} \qquad (2.103)$$
$$= (1-D)D.$$

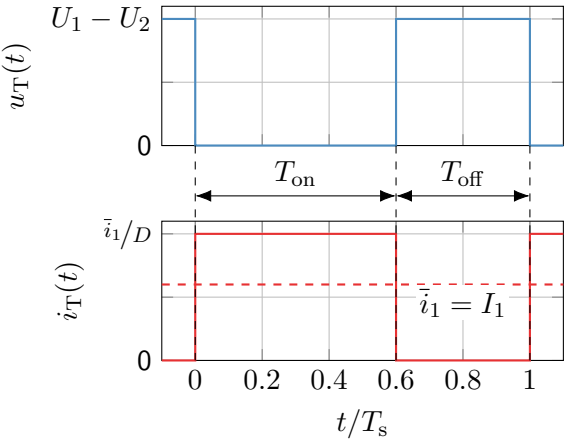

Fig. 2.31: Voltage and current at the inv. buck-boost converter transistor (w/o current ripple)

Semiconductor utilization: summary

- The converters' semiconductor utilization is generally the highest if the input and output voltages are similar:
  - Step-down: $D \to 1$,
  - Step-up: $D \to 0$,
  - Inv. buck-boost: $D \to 0.5$.
- Inverting buck-boost has generally a lower utilization.
- Finding indicates that the inv. buck-boost should be only considered if an application truly requires both step-up and step-down operation.

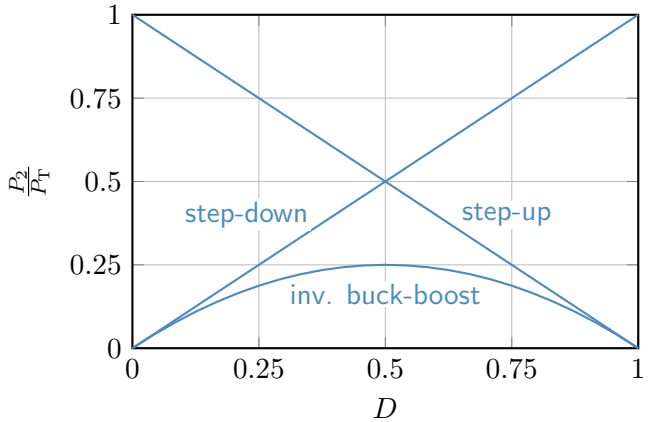

Fig. 2.32: Comparison of the semiconductor utilization for the step-down, step-up, and inv. buck-boost converter

Filter component requirements: step-down converter

Open question regarding filter dimensioning:

- How large do the filter components need to be sized to ensure sufficiently smooth input and output signals?

To answer this, we consider the following assumptions:

- The input and output current are constant: $i_1(t) = I_1$, $i_2(t) = I_2$.
- Additional input capacitor necessary to buffer the pulsating input current.
- Voltage and current ripples do not influence each other (simplified superposition).

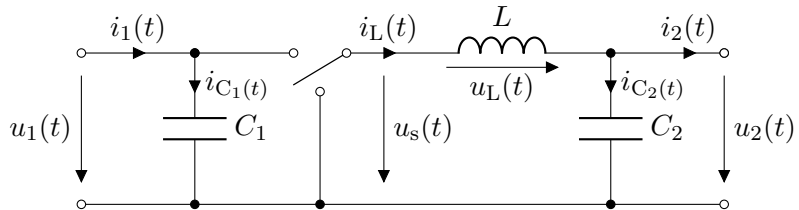

Fig. 2.33: Step-down converter with filter components

Filter component requirements: step-down converter (cont.)

The input voltage ripple is

$$\Delta u_{\mathrm{C}_1} = \frac{I_1(1-D)T_\mathrm{s}}{C_1} \tag{2.104}$$

assuming that the input capacitor is loaded with the input current I_1 during the off-time $T_\mathrm{off} = (1-D)T_\mathrm{s}$. Assuming that there is an input voltage ripple requirement on Δu_{C_1}, that is, an upper limit ripple, the minimum input capacitance is

$$C_1 \geq \frac{I_1(1-D)T_\mathrm{s}}{\Delta u_{\mathrm{C}_1}} = C_{1,\mathrm{min}}. \tag{2.105}$$

The stored input capacitor energy yields

$$E_{\mathrm{C}_1} = \frac{1}{2}C_{1,\mathrm{min}}\left(U_1 + \frac{1}{2}\Delta u_{\mathrm{C}_1}\right)^2 = \frac{1}{2}(1-D)\frac{P_2}{f_\mathrm{s}}\frac{\left(1+\frac{\varepsilon_{u_{\mathrm{C}_1}}}{2}\right)^2}{\varepsilon_{u_{\mathrm{C}_1}}} \tag{2.106}$$

with the normalized ripple factor $\varepsilon_{u_{\mathrm{C}_1}} = {}^{\Delta u_{\mathrm{C}_1}}/_{U_1}$.

Filter component requirements: step-down converter (cont.)

We already know from (2.13) the inductor current ripple being

$$\Delta i_{\mathrm{L}} = \frac{(1-D)U_2 T_{\mathrm{s}}}{L}.$$

Assuming that there is an inductor current ripple requirement on Δi_{L}, that is, an upper limit ripple, the minimum inductance is

$$L \geq \frac{(1-D)U_2 T_{\mathrm{s}}}{\Delta i_{\mathrm{L}}} = L_{\min}. \tag{2.107}$$

The stored inductor energy is

$$E_{\mathrm{L}} = \frac{1}{2} L_{\min} \left(I_2 + \frac{1}{2}\Delta i_{\mathrm{L}} \right)^2 = \frac{1}{2}(1-D)\frac{P_2}{f_{\mathrm{s}}} \frac{\left(1 + \frac{\varepsilon_{i_{\mathrm{L}}}}{2}\right)^2}{\varepsilon_{i_{\mathrm{L}}}} \tag{2.108}$$

with the normalized ripple factor $\varepsilon_{i_{\mathrm{L}}} = {}^{\Delta i_{\mathrm{L}}}/_{I_2}$.

Filter component requirements: step-down converter (cont.)

We already know from (2.36) the output capacitor voltage ripple being

$$\Delta u_{\mathrm{C}_2} = \frac{D(1-D)T_\mathrm{s}^2 U_1}{8LC_2} = \frac{(1-D)}{8LC_2}\frac{U_2}{f_\mathrm{s}^2}.$$

Inserting the inductor sizing (2.107) delivers

$$\Delta u_{\mathrm{C}_2} = \frac{1}{8C_2}\frac{\Delta i_\mathrm{L}}{f_\mathrm{s}} = \frac{\varepsilon_{i_\mathrm{L}}}{8C_2}\frac{I_2}{f_\mathrm{s}}. \tag{2.109}$$

Assuming that there is an output voltage ripple requirement on Δu_{C_2}, that is, an upper limit ripple, the minimum output capacitance is

$$C_2 \geq \frac{\varepsilon_{i_\mathrm{L}} I_2}{8 f_\mathrm{s} \Delta u_{\mathrm{C}_2}} = C_{2,\mathrm{min}}. \tag{2.110}$$

The stored output capacitor energy yields

$$E_{\mathrm{C}_2} = \frac{1}{2}C_{2,\mathrm{min}}\left(U_2 + \frac{1}{2}\Delta u_{\mathrm{C}_2}\right)^2 = \frac{1}{16}\varepsilon_{i_\mathrm{L}}\frac{P_2}{f_\mathrm{s}}\frac{\left(1+\frac{\varepsilon_{u_{\mathrm{C}_2}}}{2}\right)^2}{\varepsilon_{u_{\mathrm{C}_2}}}. \tag{2.111}$$

Filter component requirements: step-down converter interpretation

The stored energy in the filter components is a good proxy for the filter size and weight. All three step-down converter filter components share the following characteristics:

- The stored energy is proportional to the output power P_2.
- The stored energy is inversely proportional to the switching frequency f_s.
- The stored energy is minimal at $\varepsilon_{u_{\mathrm{C}_1}} = \varepsilon_{i_\mathrm{L}} = \varepsilon_{u_{\mathrm{C}_2}} = 1/2$ (i.e., large signal ripples).
  - $\varepsilon_{i_\mathrm{L}} = 1/2$ refers to BCM mode.
  - Increased input voltage ripple and inductor current ripple also increases the transistor requirements, see (2.98).

In addition, E_L and E_{C_1} also scale with

$$(1 - D),$$

that is, are small if the converter's input and output voltage are similar. In the following, we do not analyze the step-up converter in detail, since the findings are analogous.

Filter component requirements: inverting buck-boost converter

Again, we assume the following:

- The input and output current are constant: $i_1(t) = I_1$, $i_2(t) = I_2$.
- Additional capacitors necessary to buffer the pulsating input / output currents.
- Voltage and current ripples do not influence each other (simplified superposition).

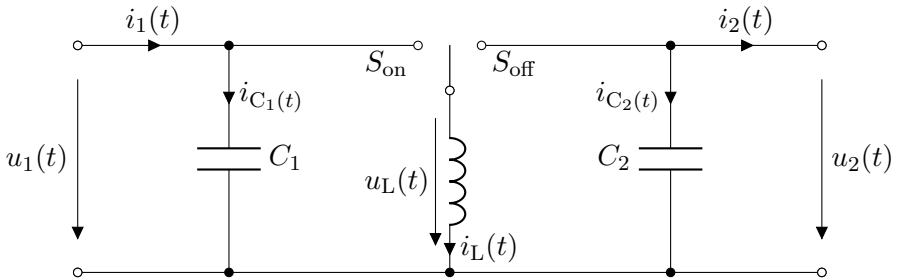

Fig. 2.34: Inverting buck-boost converter with filter components

Filter component requirements: inverting buck-boost converter (cont.)

We further assume an identical normalized input and output voltage ripple requirement

$$\varepsilon_{u_{\mathrm{C}_1}} = \frac{\Delta u_{\mathrm{C}_1}}{U_1} = \varepsilon_{u_{\mathrm{C}_2}} = \frac{\Delta u_{\mathrm{C}_2}}{U_2} = \varepsilon_{u_{\mathrm{C}}}.$$

Following the same derivation as for the step-down converter, the stored filter energies are

$$E_{\mathrm{C}} = E_{\mathrm{C}_1} + E_{\mathrm{C}_2} = \frac{1}{2}\frac{P_2}{f_{\mathrm{s}}}\frac{\left(1+\frac{\varepsilon_{u_{\mathrm{C}}}}{2}\right)^2}{\varepsilon_{u_{\mathrm{C}}}}, \qquad E_{\mathrm{L}} = \frac{1}{2}\frac{P_2}{f_{\mathrm{s}}}\frac{\left(1+\frac{\varepsilon_{i_{\mathrm{L}}}}{2}\right)^2}{\varepsilon_{i_{\mathrm{L}}}}. \tag{2.112}$$

Compared to the step-down converter we can find:

- Same dependence on P_2, f_{s}, and $\varepsilon_{u_{\mathrm{C}}}$ or $\varepsilon_{i_{\mathrm{L}}}$.
- Missing $(1-D)$ scaling factor.
- Result: The inverting buck-boost converter's passive components are generally larger due to the pulsating input and output current which needs to be filtered.

Table of contents

Recap: (inverting) buck-boost converter switching states

Key characteristic drawback of (inverting) buck-boost converter

The switching scheme of the (inverting) buck-boost converter utilizes an indirect inductive energy transfer resulting in pulsating input and output currents which need to be filtered. This leads to larger filter components.

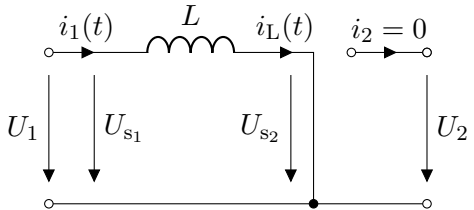

(a) Switch-on time

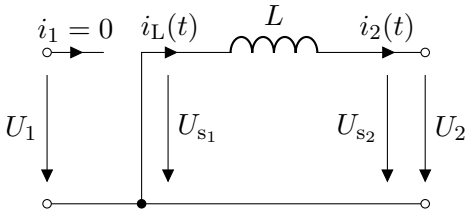

(b) Switch-off time

Ćuk converter: the boost-buck converter with capacative energy transfer

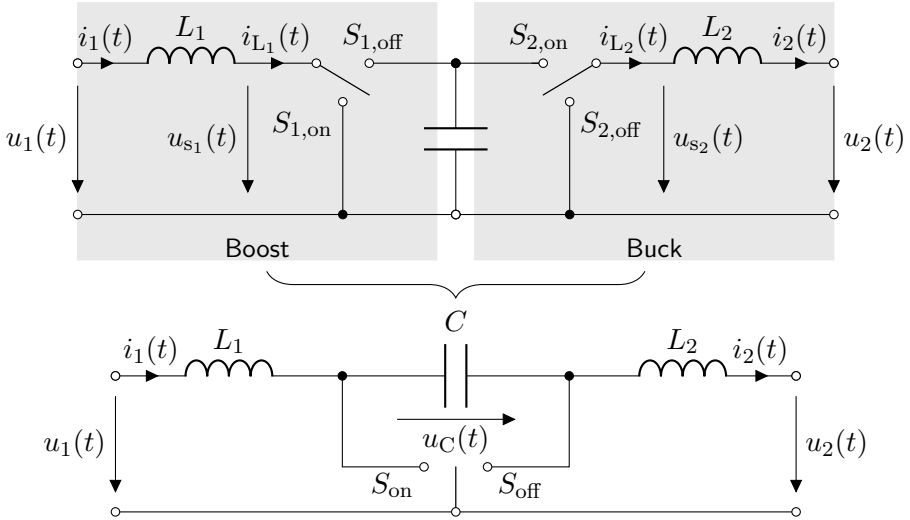

Fig. 2.36: Ćuk converter (ideal switch representation)

Ćuk converter: switching states

- The Ćuk converter uses the capacitor C to transfer energy between the input and output.
- The polarity of C is changed between the two switch states (inverting voltage gain).
- In contrast to the previous topologies, there is no pulsating output or input current thanks to the outer two inductors.

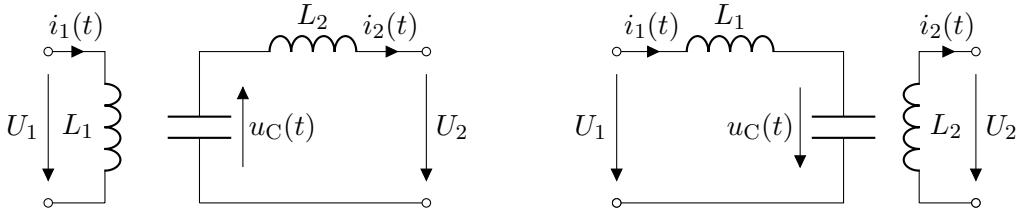

(a) Switch-on time (b) Switch-off time

Fig. 2.37: Switch states of the Ćuk converter

Ćuk converter: voltage gain

In periodic steady-state operation, the voltage balance during a switching period of the two inductors must be fulfilled:

$$L_1: \quad DU_1 + (1-D)(U_1 - U_\mathrm{C}) = 0, \qquad L_2: \quad D(U_2 + U_\mathrm{C}) + (1-D)U_2 = 0. \tag{2.113}$$

Above, U_1, U_2, and U_C are considered constant.From those we can derive:

$$L_1: \quad U_\mathrm{C} = \frac{U_1}{1-D}, \qquad L_2: \quad U_\mathrm{C} = -\frac{U_2}{D}. \tag{2.114}$$

Combining both equations delivers the voltage gain of the Ćuk converter:

$$\frac{U_2}{U_1} = -\frac{D}{1-D}. \tag{2.115}$$

This is the same finding as for the inverting buck-boost converter, which seems quite obvious, as the Ćuk converter just flips the order of the buck and boost parts.

Ćuk converter: circuit realization

- Like the inverting buck-boost, the Ćuk converter only requires one diode and transistor.
- Transistor T needs to block $u_\mathrm{C}(t)$ during the off-time, while it covers both the input and output current during the on-time: semiconductor utilization is also $P_2/P_\mathrm{T} = (1-D)D$ as for the inverting buck-boost (cf. Fig. 2.32).

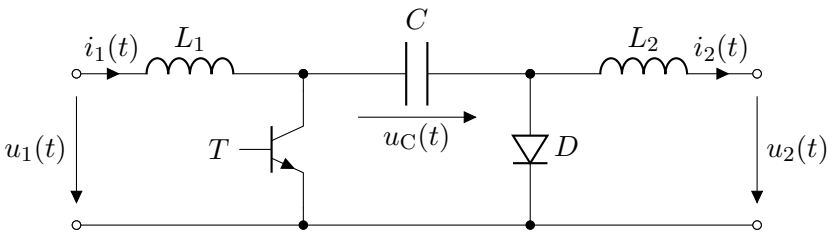

Fig. 2.38: Ćuk converter with real components (single quadrant type)

Single ended primary inductance converter (SEPIC)

- Output inductor and diode change places compared to the Ćuk converter.
- Output current becomes pulsating (compared to Ćuk).
- Input to output gain becomes non-inverting (cf. next slides).

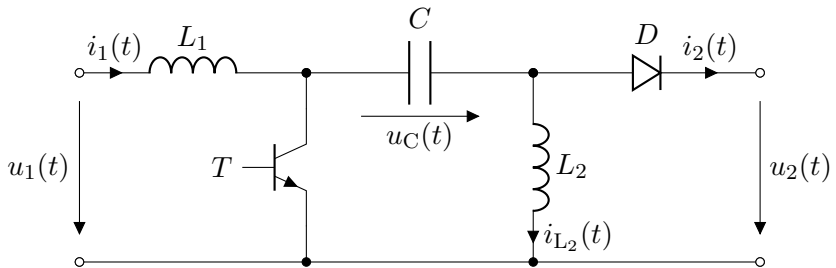

Fig. 2.39: SEPIC with real components (single quadrant type)

SEPIC: switching states

- During switch on-time, the transistor is conducting and the diode is blocking (causing the output current pulsation).
- During switch off-time, the diode is conducting and the transistor is blocking.

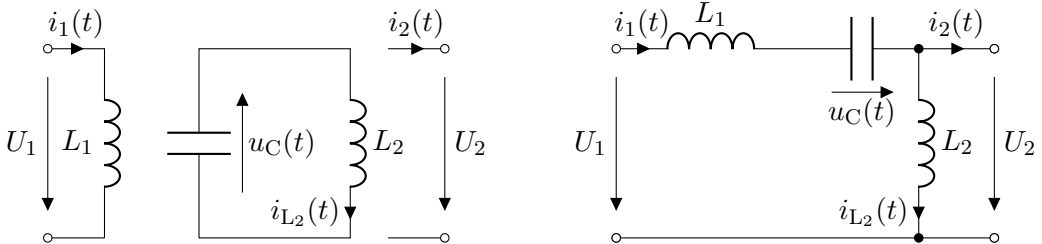

(a) Switch-on time

(b) Switch-off time

Fig. 2.40: Switch states of the SEPIC

SEPIC: voltage gain

In periodic steady-state operation, the voltage balance during a switching period of the two inductors must be fulfilled:

$$L_1: \quad DU_1 + (1-D)(U_1 - U_2 - U_\mathrm{C}) = 0, \qquad L_2: \quad -DU_\mathrm{C} + (1-D)U_2 = 0. \tag{2.116}$$

Above, U_1, U_2, and U_C are considered constant.From those we can derive:

$$L_1: \quad U_\mathrm{C} = \frac{U_1}{1-D} - U_2, \qquad L_2: \quad U_\mathrm{C} = \left(\frac{1}{D} - 1\right) U_2. \tag{2.117}$$

Combining both equations delivers the voltage gain of the SEPIC:

$$\frac{U_2}{U_1} = \frac{D}{1-D}. \tag{2.118}$$

Similar to the synchronous buck-boost, the SEPIC comes with a positive voltage gain, but with the advantages of a single transistor and diode as well as non-pulsating input currents (at the cost of more filter components).

Buck/boost converter for both current polarities

- Previous buck/boost realizations allowed only unidirectional current flow (cf. Fig. 2.8 and Fig. 2.16).
- Right realization with two transistors and body diodes enables both current polarities (two quadrant type).
- No discontinuous current flow (no DCM mode).
- Transistors must be switched complementary to prevent a DC-link short-circuit:
  - T_1: on, T_2: off,
  - T_1: off, T_2: on.

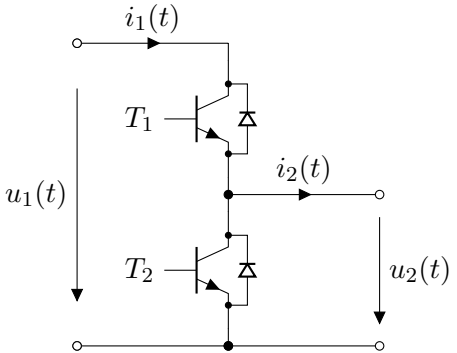

Fig. 2.41: DC-DC converter realization for both current polarities (w/o filter components, aka half-bridge)

Buck/boost converter for both voltage polarities

- Required constraints are:
  - $u_1 > 0$: otherwise DC link short-circuit,
  - $i_2 > 0$: to meet semiconductor capabilities.
- Possible switching states:

T_1	T_2	u_2	i_1
on	off	$+u_1$	$+i_2$
off	on	$-u_1$	$-i_2$
on	on	0	0
off	off	0	0

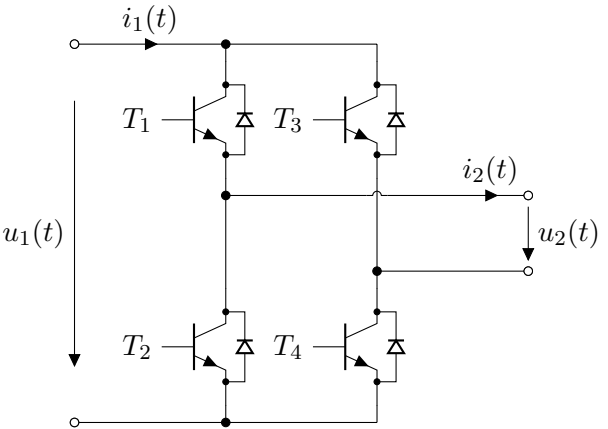

Fig. 2.42: DC-DC converter realization for both voltage polarities (w/o filter components, aka asymmetrical half-bridge)

Buck/boost converter for both current and voltage polarities

- For achieving full four quadrant operation (4Q), we combine the previous half-bridge variants.
- Also requires complementary switching of $\{T_1, T_2\}$ and $\{T_3, T_4\}$ to prevent a DC-link short-circuit.
- Possible (allowed) switching states:

T_1	T_2	T_3	T_4	u_2	i_1
on	off	off	on	$+u_1$	$+i_2$
off	on	on	off	$-u_1$	$-i_2$
on	off	on	off	0	0
off	on	off	on	0	0

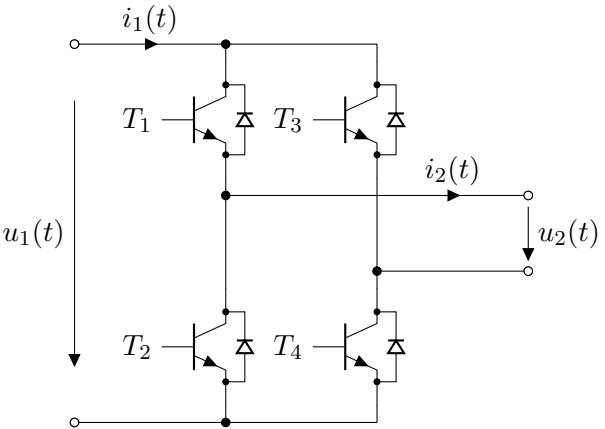

Fig. 2.43: DC-DC converter realization for both current and voltage polarities (w/o filter components, aka full-bridge)

Buck/boost converter for both current and voltage polarities (cont.)

Define duty cycle as relative on-times

$$D = \frac{T_{\mathrm{on}}}{T_{\mathrm{s}}}, \quad \text{for } T_1, T_4,$$

and conversely

$$D' = \frac{T_{\mathrm{on}}}{T_{\mathrm{s}}} = (1 - D), \quad \text{for } T_2, T_3.$$

This leads to the average output voltage of

$$U_2 = (2D - 1)U_1. \tag{2.119}$$

- Also holds 2Q converter from Fig. 2.42.
- Boost mode follows analogously.

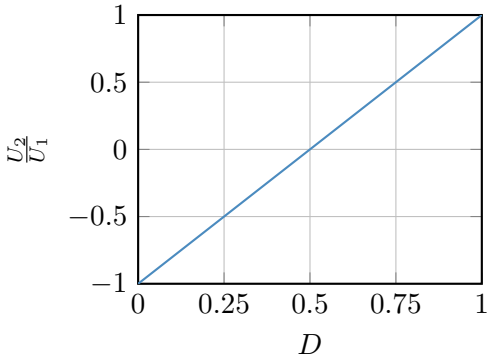

Fig. 2.44: Voltage gain for a buck converter with two voltage polarities

Section summary

This section introduced non-isolated DC-DC converters. The key takeaways are:

- **Buck converter:** step-down voltage conversion, voltage gain $0 \leq D \leq 1$,
- **Boost converter:** step-up voltage conversion, voltage gain $1 \leq \frac{1}{(1-D)}$.

From those basic topologies, we could derive all others:

- **(Inverting) buck-boost converter:** voltage gain $(-)\frac{D}{(1-D)}$,
- **(Inverting) boost-buck / Ćuk converter and SEPIC:** voltage gain $(-)\frac{D}{(1-D)}$.

Finally, we discussed the realization of converters for both current and voltage polarities by using bridge-type switch realizations. Also, we have emphasized the trade-off decisions between

- semiconductor utilization
- filter requirements / sizing,
- applied voltage gain as well as voltage and current signal quality.

Table of contents

Galvanic isolation

A definition

Galvanic isolation is a principle of decoupling functional sections of electrical circuits to prevent a direct current flow from input to output, that is, enabling different ground potentials for the circuit sections.

Typical reasons for requiring galvanic isolation are:

- Safety (prevention of electric shock),
- Noise reduction,
- contact corrosion reduction.

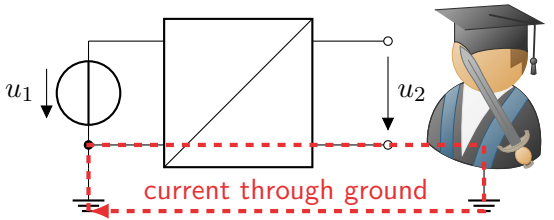

(a) Lack of galvanic isolation

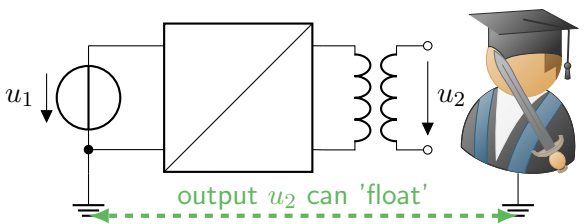

(b) Galvanic isolation via inductive separation

Fig. 3.1: Why galvanic isolation can be useful

Galvanic isolation: technical realization

Capacative

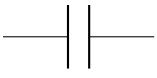

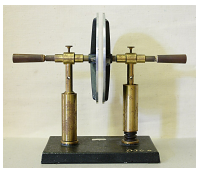

source: Wikimedia Commons, H. Grobe, CC BY 3.0

Optical

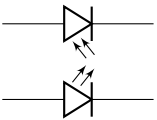

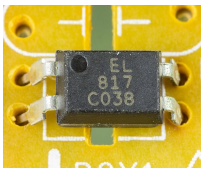

source: Wikimedia Commons, R. Spekking, CC BY-SA 4.0

Inductive

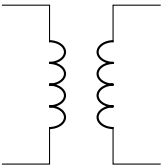

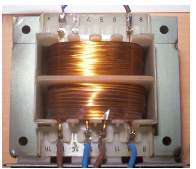

source: Wikimedia Commons, S. Riepl, public domain

Galvanic isolation via transformer

- In power electronics, transformers are mostly used to provide galvanic isolation.
- Reason: the power density per volume and weight is typically higher than for capacitive or optical isolation.
- Assumptions for the following model:
  - Ideal coupling (no leakage flux),
  - no losses,
  - no saturation.

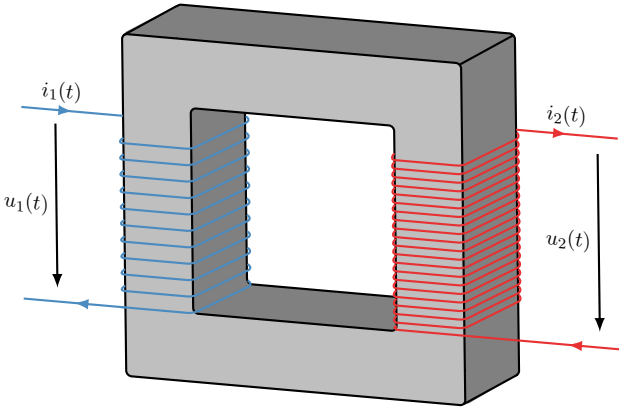

Fig. 3.2: Simple transformer with primary and secondary winding

Simplistic transformer model

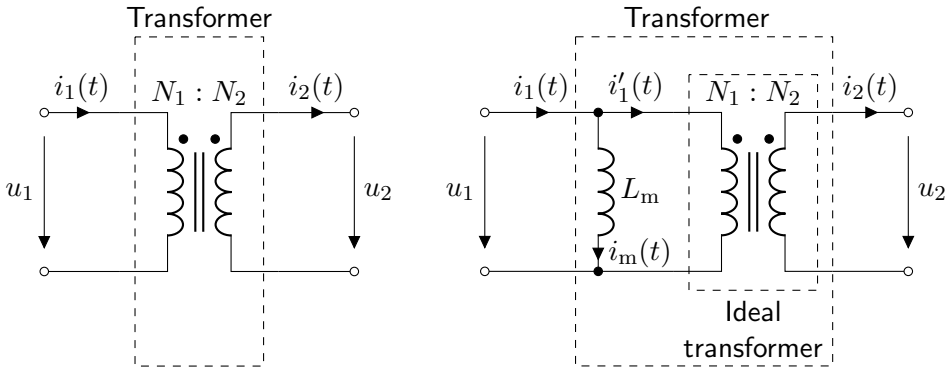

(a) Schematic symbol representation

(b) Equivalent circuit model

Fig. 3.3: Transformer model

Simplistic transformer model (cont.)

Based on Fig. 3.3 we consider the transformer as a combination of an ideal transformer with the conversion ratios

$$\frac{u_1(t)}{u_2(t)} = \frac{N_1}{N_2} \quad \text{and} \quad \frac{i_1'(t)}{i_2(t)} = \frac{N_2}{N_1} \tag{3.1}$$

and an inductor with the magnetizing inductance L_m:

$$u_1(t) = L_\mathrm{m} \frac{\mathrm{d}i_\mathrm{m}(t)}{\mathrm{d}t} \quad \text{and} \quad i_1(t) = i_1'(t) + i_\mathrm{m}(t). \tag{3.2}$$

- L_m models the magnetic energy stored in the transformer.
- Above model is a significant simplification (very first principle approach).
- More details on the transformer model can be found in the Electrical Machines and Drives course material.

Table of contents

Topology derivation based on the inverting buck-boost converter

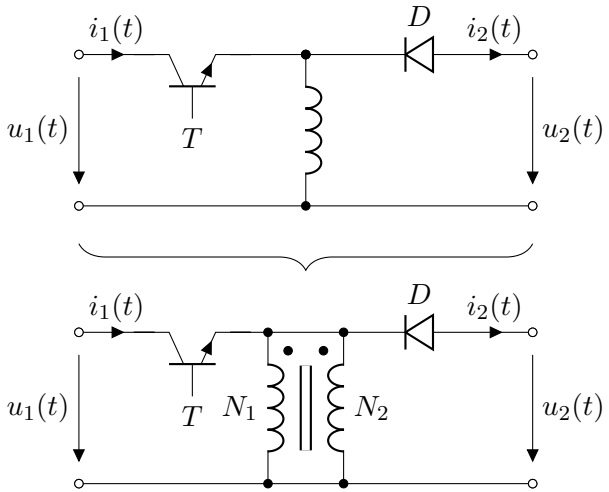

Topology derivation based on the inverting buck-boost converter (cont.)

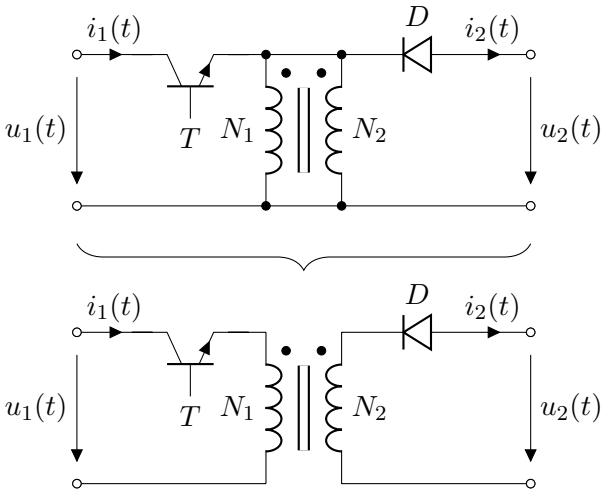

Flyback converter: topology

- Flyback converter = non-inverting, galvanically isolated buck-boost converter.
- Polarity change of primary and secondary transformer windings compensate for the inverting buck-boost characteristic.
- Transistor T is placed below the transformer to enable a fixed emitter / source potential (beneficial for driver).
- Transformer's magnetizing inductance serves as the converter's energy buffer.

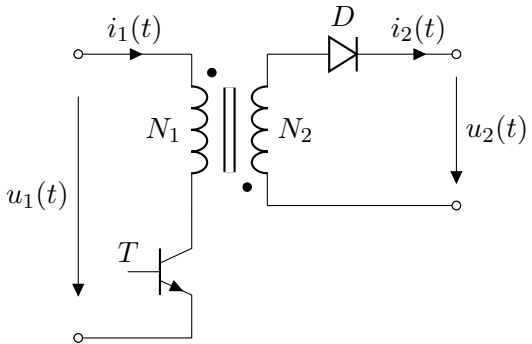

Fig. 3.4: Flyback converter topology

Flyback converter: switching states in CCM

- Switch-on time: rising primary current induces a negative voltage at the transformer's secondary winding leading to blocking diode. Energy is stored in L_m.
- Switch-off time: primary current is blocked by transistor and an equivalent current is induced in the secondary winding. Energy is taken from L_m.

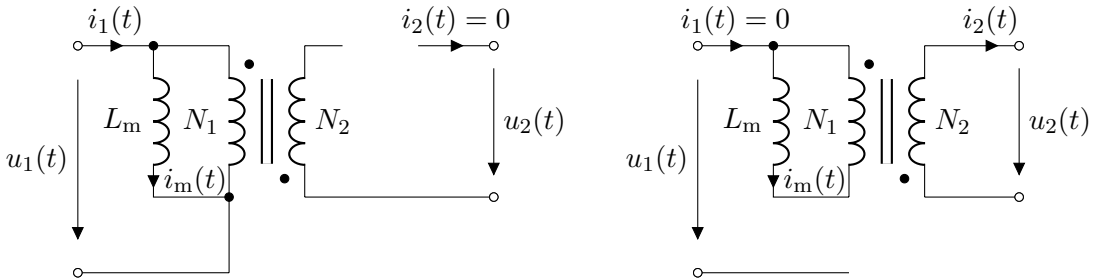

(a) Switch-on time

(b) Switch-off time

Fig. 3.5: Switch states of the flyback converter

Flyback converter: steady-state time-domain behavior in CCM

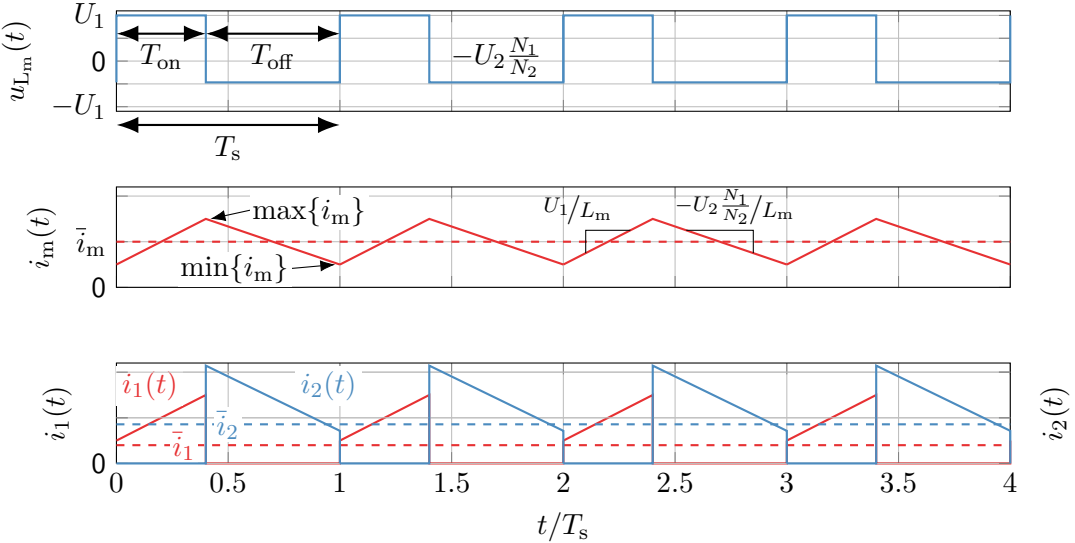

Flyback converter: impact of the transformer turns ratio

The transformer scales the peak input and output current according to the turns ratio N_2/N_1 (with ε being a small time period)

$$i_2(t = T_{\text{on}} + \varepsilon) = \frac{N_1}{N_2} i_1(t = T_{\text{on}} - \varepsilon),$$

i.e., the output side may carry significantly different peak currents than the input. Also, when the transistor blocks it must withstand the voltage

$$u_{\text{T}}(t) = u_1(t) + \frac{N_1}{N_2} u_2(t), \quad t \in [T_{\text{on}}, T_{\text{s}}].$$

Hence, the turn ratio has a significant impact on components' stress factors.

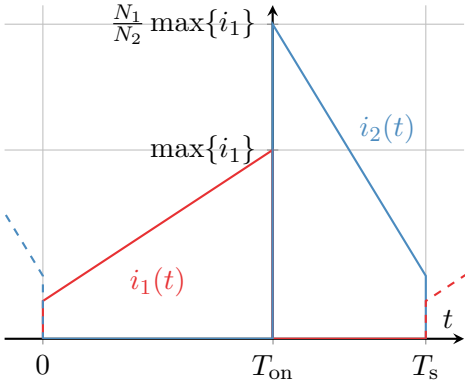

Fig. 3.6: Example of the ratio of the input and output current for $N_2/N_1 = 0.6$

Flyback converter: voltage transfer ratio in CCM

In CCM, the voltage balance of the magnetizing inductor L_m delivers:

$$u_{\mathrm{L_m}}(t) = \begin{cases} U_1, & t \in [kT_\mathrm{s}, kT_\mathrm{s} + T_\mathrm{on}], \\ -\frac{N_1}{N_2} U_2 & t \in [kT_\mathrm{s} + T_\mathrm{on}, (k+1)T_\mathrm{s}]. \end{cases} \tag{3.3}$$

In steady state, the average inductor voltage per period must be zero, yielding

$$U_1 T_\mathrm{on} = \frac{N_1}{N_2} U_2 T_\mathrm{off} \quad \Leftrightarrow \quad U_1 D T_\mathrm{s} = \frac{N_1}{N_2} U_2 (1-D) T_\mathrm{s} \quad \Leftrightarrow \quad \frac{U_2}{U_1} = \frac{N_2}{N_1} \frac{D}{1-D}. \tag{3.4}$$

- Structurally similar result to the (inverting/synchronous) buck-boost converter.
- The voltage transfer ratio is additionally scaled by the turns ratio N_2/N_1.
- The flyback's tranformer enables additional degrees of freedom to achieve a certain voltage transfer ratio via D and N_2/N_1.

Flyback converter: switch states in DCM

The flyback converter in DCM has three different switch states:

- Transistor on-time: $T_{\mathrm{on}} = DT_{\mathrm{s}}$,
- Transistor off-time (conducting diode): $T'_{\mathrm{off}} = D'T_{\mathrm{s}}$,
- Transistor off-time (no conduction): $T''_{\mathrm{off}} = T_{\mathrm{s}} - T_{\mathrm{on}} - T'_{\mathrm{off}}$.

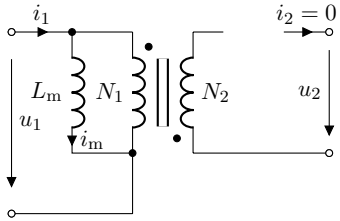

(a) Switch-on time T_{on}

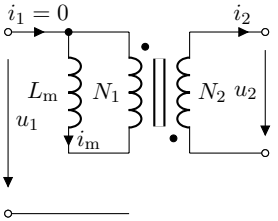

(b) Switch-off time T'_{off}

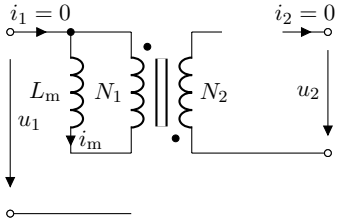

(c) Switch-off time T''_{off}

Fig. 3.7: Switch states of the flyback converter including DCM

Flyback converter: steady-state time-domain behavior in DCM

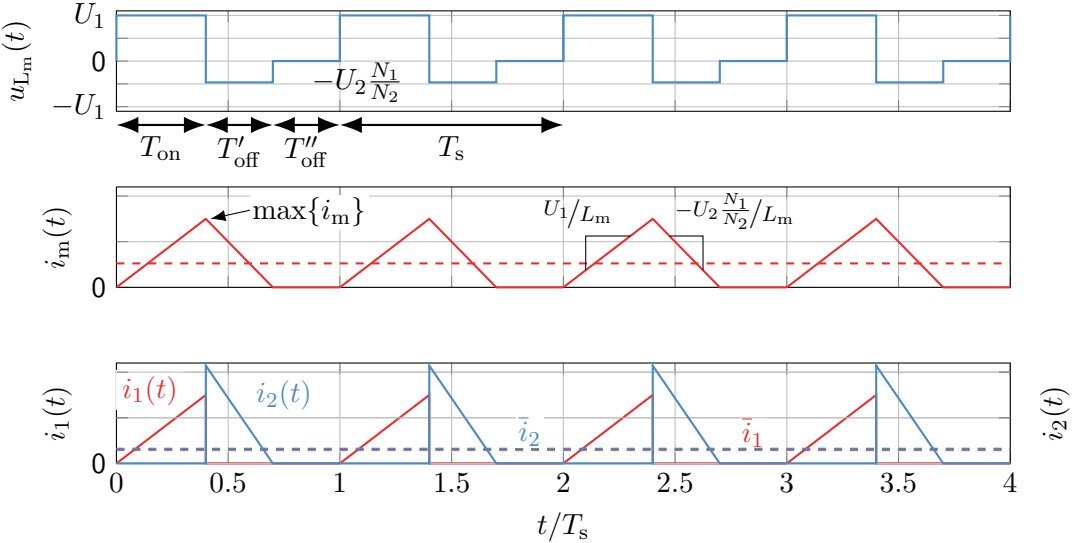

Flyback converter: DCM operation characteristics

In DCM operation

$$\bar{i}_{\mathrm{m}} < \frac{\Delta i_{\mathrm{m}}}{2} \quad \Rightarrow \quad U_2 \neq U_1 \frac{N_2}{N_1} \frac{D}{1-D}$$

applies due to the non-conducting diode during T''_{off}. To find the input-to-output voltage ratio in DCM, we again utilize the current ripple balance:

$$\begin{aligned} \Delta i_{\mathrm{m}} &= \frac{U_1}{L_{\mathrm{m}}} T_{\mathrm{on}} = \frac{U_1}{L_{\mathrm{m}}} D T_{\mathrm{s}} && \text{(rising edge)}, \\ \Delta i_{\mathrm{m}} &= \frac{N_1}{N_2} \frac{U_2}{L_{\mathrm{m}}} T'_{\mathrm{off}} = \frac{N_1}{N_2} \frac{U_2}{L_{\mathrm{m}}} D' T_{\mathrm{s}} && \text{(falling edge)}. \end{aligned} \tag{3.5}$$

Solving for D' yields

$$D' = \frac{N_2}{N_1} \frac{U_1}{U_2} D. \tag{3.6}$$

The average load current is

$$\bar{i}_2 = \frac{N_1}{N_2} \frac{\Delta i_{\mathrm{m}}}{2} \frac{T'_{\mathrm{off}}}{T_{\mathrm{s}}} = \frac{N_1}{N_2} \frac{\Delta i_{\mathrm{m,max}} D}{2} D' = \frac{N_1}{N_2} \frac{\Delta i_{\mathrm{m,max}}}{2} \frac{U_1}{U_2} D^2 \frac{N_2}{N_1} = \frac{\Delta i_{\mathrm{m,max}}}{2} \frac{U_1}{U_2} D^2. \tag{3.7}$$

Flyback converter: DCM operation characteristics (cont.)

Solving (3.7) delivers the flyback converter voltage gain in DCM as

$$\frac{U_2}{U_1} = \frac{D^2}{2} \frac{\Delta i_{\mathrm{m,max}}}{\bar{i}_2}. \tag{3.8}$$

Since $\Delta i_{\mathrm{m,max}}$ also depends on U_1, the relation (3.8) only holds for a given U_1. Hence, we can insert $\Delta i_{\mathrm{m,max}} = {}^{T_\mathrm{s} \cdot U_1}/_{L}$ in (3.7) and solve for U_2 to receive

$$U_2 = U_1^2 \frac{D^2}{2} \frac{T_\mathrm{s}}{L_\mathrm{m} \bar{i}_2}. \tag{3.9}$$

- Interestingly, the voltage gain in DCM seems independent of the turns ratio ${}^{N_2}/_{N_1}$.
- Reason: output voltage U_2 depends on the (average) output current $\bar{i}_2$ which is inversely scaled by the turns ratio – cf. cancelation of ${}^{N_2}/_{N_1}$ in (3.7).
- However, the transformer's magnetizing inductance is actually a function of the turns ratio $L_\mathrm{m}(N_1, N_2)$ (compare Electrical Machines and Drives course material).

Outlook: multi-port (flyback) converter

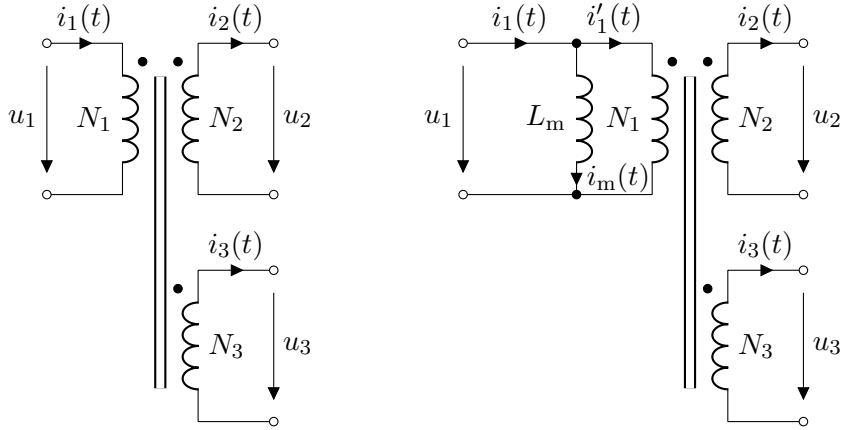

(a) Schematic symbol representation

(b) Equivalent circuit model

Fig. 3.8: Multi-port (flyback) transformer: add multiple secondary windings to a common core to enable different input-to-output voltage ratios

Table of contents

Topology derivation based on the buck converter

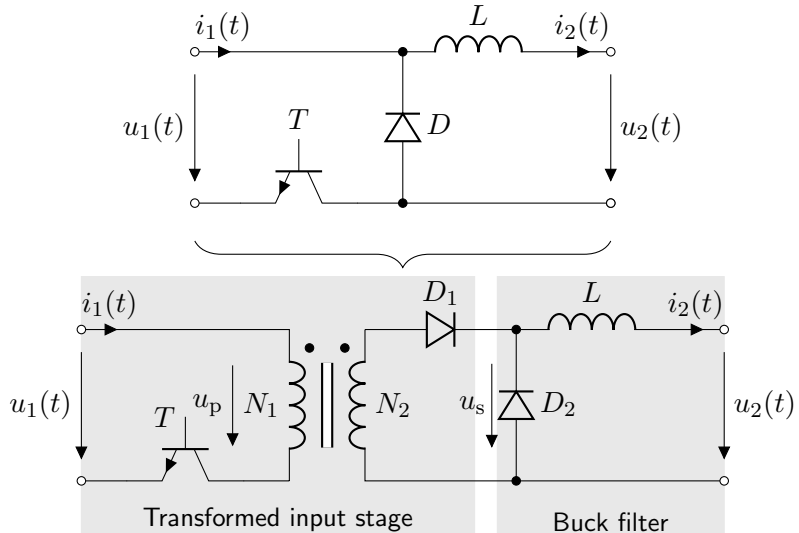

Forward converter: topology

- Forward converter = galvanically isolated buck converter.
- Main energy buffer: inductor L.
- Transformer: galvanic isolation plus voltage scaling:

$$u_\mathrm{s}(t) = \frac{N_2}{N_1} u_\mathrm{p}(t)$$

with $u_\mathrm{p}(t) = u_1(t), t \in [0, T_\mathrm{on}]$.

- Different to flyback, where the transformer's purpose is to provide both energy storage and galvanic isolation.

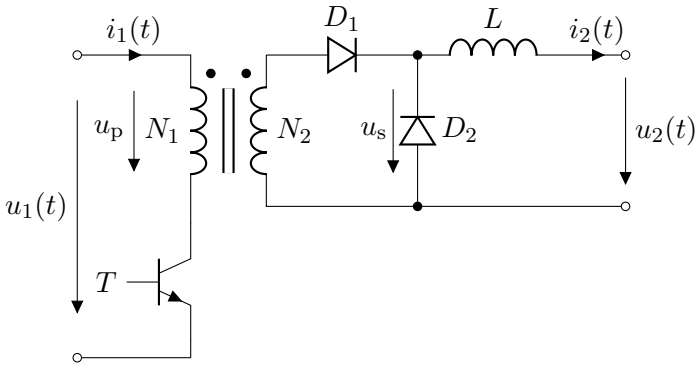

Fig. 3.9: Forward converter topology

Forward converter: steady-state time-domain behavior (ideal transformer)

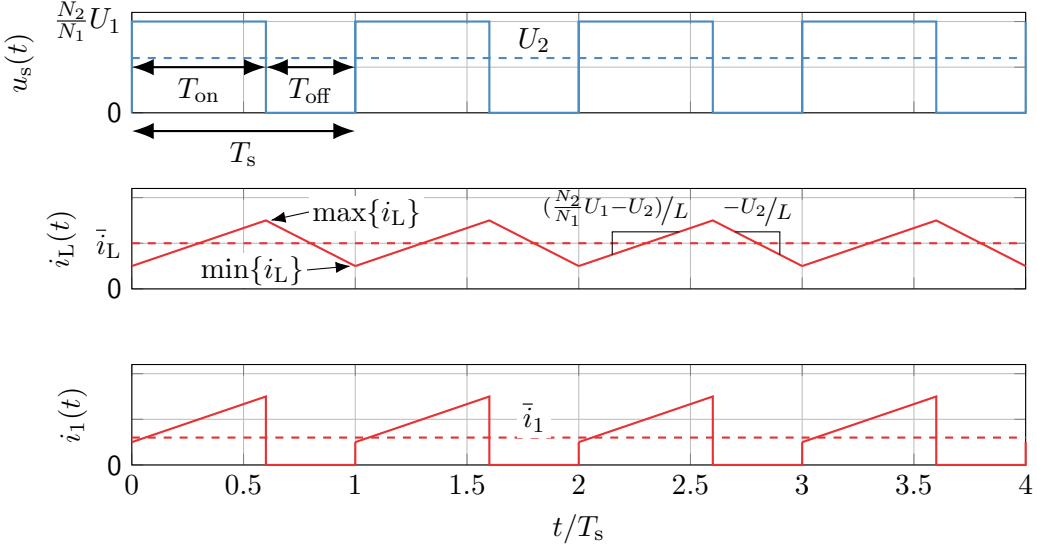

Forward converter: idealized steady-state operation

Assumption:

- The transformer is ideal and does not exhibit a magnetizing inductance.

Consequence:

- The transformer's secondary output voltage $u_\mathrm{s}(t)$ is a N_2/N_1 scaled version of the standard buck converter's switch voltage (compare Fig. 2.8).
- The (idealized) forward converter characteristics are analogous to the buck converter.

Hence, the voltage input-to-output voltage ratios for the (idealized) forward converter are:

$$\text{CCM:}\quad \frac{U_2}{U_1} = \frac{N_2}{N_1} D, \qquad \text{DCM:}\quad U_2 = \frac{N_2^2}{N_1^2} \frac{D^2 T_\mathrm{s} U_1^2}{D^2 T_\mathrm{s} \frac{N_2}{N_1} U_1 + 2L\bar{i}_2}. \tag{3.10}$$

Forward converter: magnetizing inductance issue

Magnetizing inductance

With every switching cycle the primary magnetizing current $i_\mathrm{m}(t)$ increases (i.e., transformer saturates and takes damage).

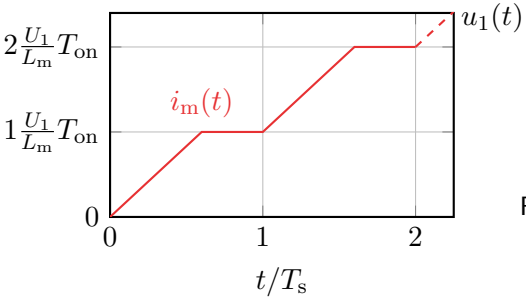

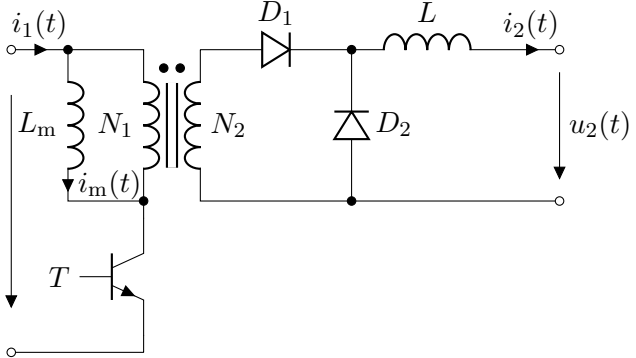

Fig. 3.10: Forward converter topology with primary magnetizing inductance

Forward converter: demagnetization via negative input voltage

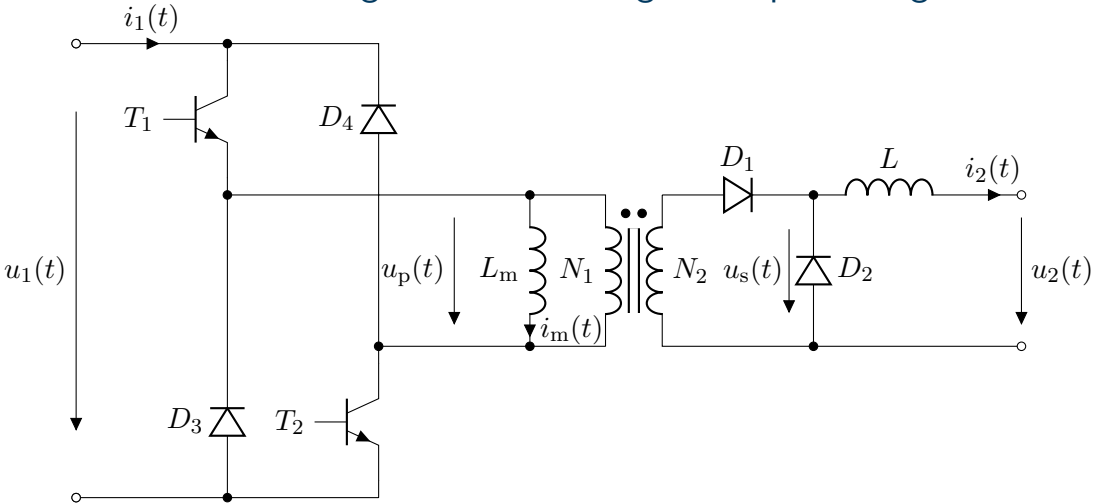

Fig. 3.11: Forward converter topology with an asymmetrical half-bridge

Forward converter: steady-state time-domain behavior (asym. half-bridge)

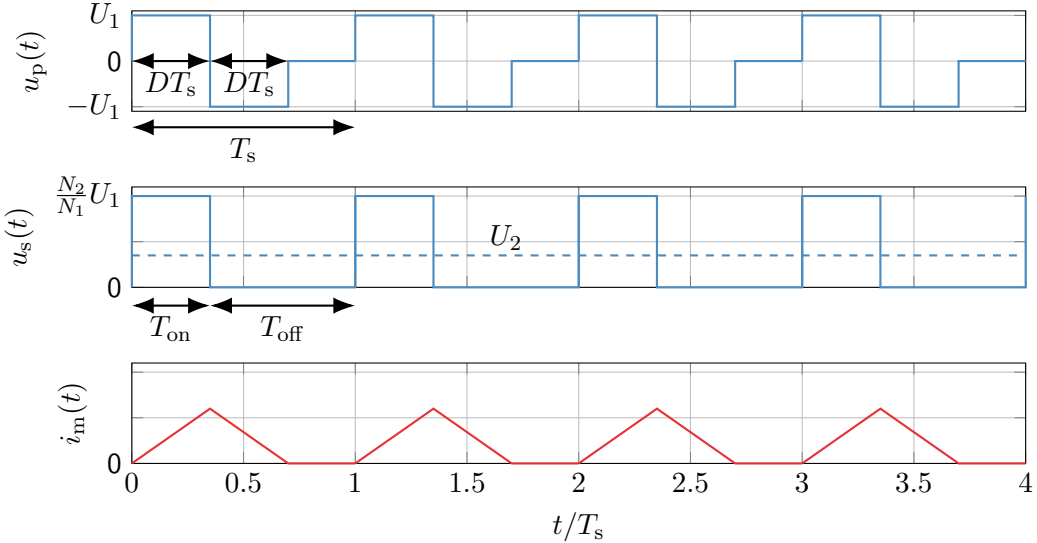

Forward converter with asym. half-bridge input stage

To demagnetize the transformer, the input voltage $u_\mathrm{p}(t)$ is modulated as follows:

$$u_\mathrm{p}(t) = \begin{cases} U_1, & t \in [kT_\mathrm{s}, kT_\mathrm{s} + DT_\mathrm{s}], \quad T_1 = T_2 = \text{on}, \\ -U_1, & t \in [kT_\mathrm{s} + DT_\mathrm{s}, kT_\mathrm{s} + 2DT_\mathrm{s}], \quad T_1 = T_2 = \text{off}, \\ 0, & t \in [kT_\mathrm{s} + 2DT_\mathrm{s}, kT_\mathrm{s} + T_\mathrm{s}], \quad T_1 = \text{on}, \, T_2 = \text{off}. \end{cases} \tag{3.11}$$

Consequently, we have

$$\overline{u}_{\mathrm{L_m}} = \frac{1}{T_\mathrm{s}} \int_0^{T_\mathrm{s}} u_\mathrm{p}(t) \mathrm{d}t = 0 \tag{3.12}$$

and, therefore, the transformer's magnetizing current $i_\mathrm{m}(t)$ does not increase during a pulse period.However, this also limits the applicable duty cycle to

$$D \leq \frac{1}{2}$$

since otherwise (3.12) cannot be fulfilled.

Forward converter: demagnetization via negative input voltage (cont.)

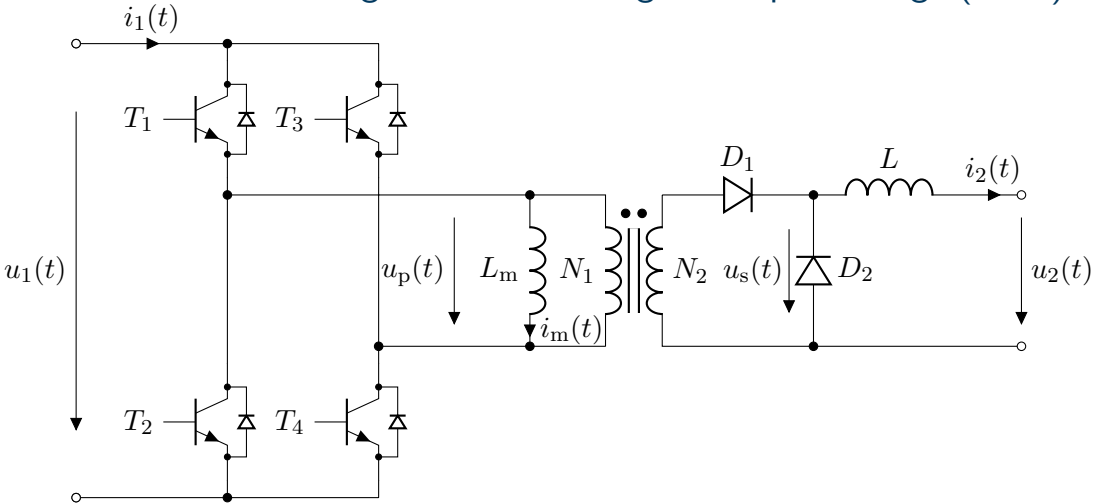

Fig. 3.12: Forward converter topology with a full-bridge

Forward converter: steady-state time-domain behavior (full-bridge)

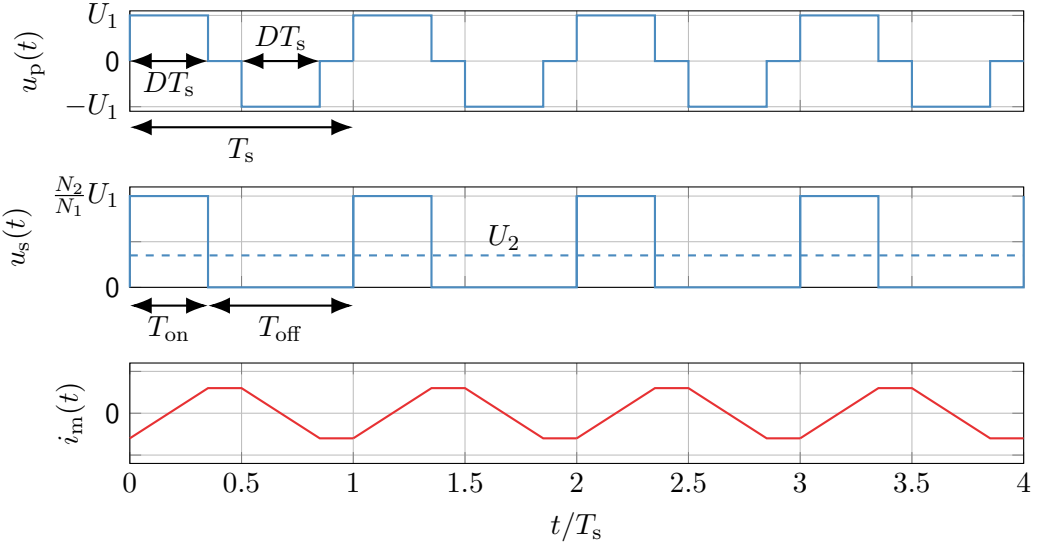

Forward converter: hysteresis curves of the transformer

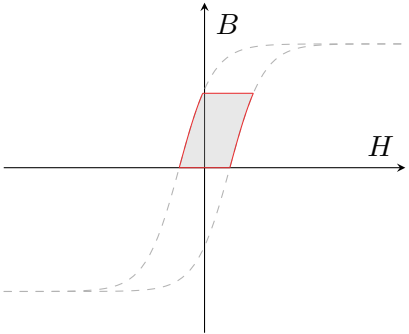

(a) Asym. half-bridge: utilizes only the upper half of the hysteresis curve due to non-negative magnetizing currents

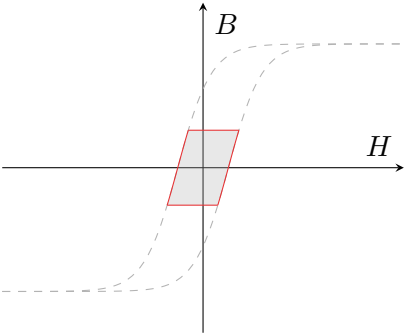

(b) Full-bridge: utilizes both positive and negative hysteresis curve parts due the four-quadrant input stage

Fig. 3.13: Hysteresis curves of the forward converter's transformer with different input stages (qualitative and simplified representation)

Forward converter with full-bridge input stage

The average input voltage $\overline{u}_\mathrm{p}$ of the full-bridge forward converter is conceptually identical to the asym. half-bridge variant and with the constraint

$$\overline{u}_{\mathrm{L_m}} = \frac{1}{T_\mathrm{s}} \int_0^{T_\mathrm{s}} u_\mathrm{p}(t) \mathrm{d}t = 0$$

the duty cycle also remains limited to

$$D \leq \frac{1}{2}.$$

However, the full-bridge realization comes with distinct differences compared to the asym. half-bridge:

- Utilizes magnetic core more efficiently, i.e., core can be made smaller or less winding turns are required.
- Effective switching frequency is doubled allowing for smaller filter components.
- Obvious disadvantage: more complex input stage (costs).

Forward converter with additional demagnetization winding

Alternative: transfer the idea of the flyback converter and add another winding N_3 to the transformer with reversed polarity. When T blocks, the energy stored in the transformer's magnetic field is inherited by N_3 and transferred back to the input.

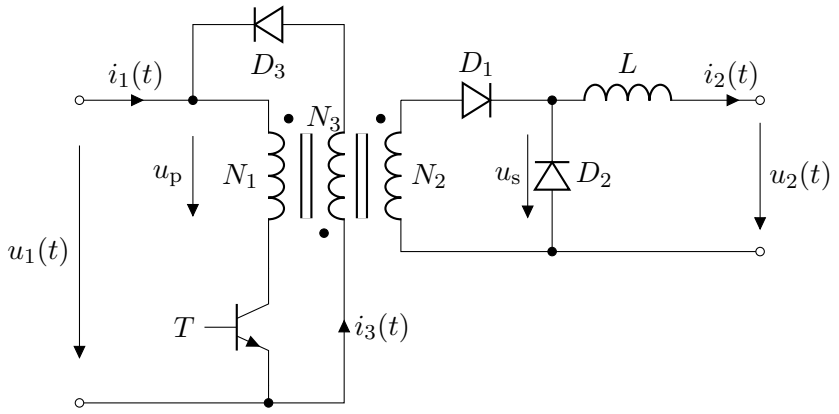

Fig. 3.14: Forward converter with demagnetization winding (aka single-ended forward converter)

Forward converter: steady-state time-domain behavior (demag. winding)

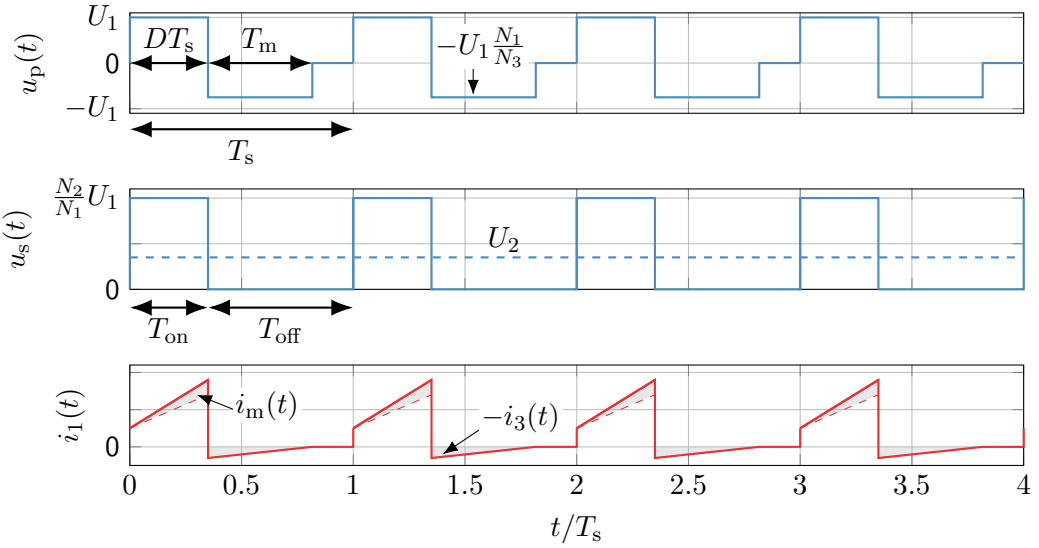

Forward converter with additional demagnetization winding (cont.)

The maximum magnetizing current is

$$\max\{i_{\mathrm{m}}(t)\} = i_{\mathrm{m}}(t = (k+D)T_{\mathrm{s}}) = \frac{U_1}{L_{\mathrm{m}}} D T_{\mathrm{s}} \tag{3.13}$$

which is reached at the end of the turn-on time T_{on}.After switching off the transistor, the winding N_3 takes over the magnetizing current leading to

$$\max\{|i_3(t)|\} = |i_3(t = (k+D)T_{\mathrm{s}})| = \frac{N_1}{N_3} \max\{i_{\mathrm{m}}(t)\} = \frac{N_1}{N_3} \frac{U_1}{L_{\mathrm{m}}} D T_{\mathrm{s}}. \tag{3.14}$$

To ensure that $i_{\mathrm{m}}(t = kT_{\mathrm{s}}) = 0$ holds at the next switch-on event, the voltage balance regarding the magnetizing inductance must be zero:

$$\overline{u}_{\mathrm{L_m}} = \frac{1}{T_{\mathrm{s}}} \int_0^{T_{\mathrm{s}}} u_{\mathrm{p}}(t)\mathrm{d}t = U_1 D T_{\mathrm{s}} - \frac{N_1}{N_3} U_1 T_{\mathrm{m}} = 0. \tag{3.15}$$

Here, T_{m} denotes the demagnetization time interval which results in

$$T_{\mathrm{m}} = \frac{N_3}{N_1} D T_{\mathrm{s}}. \tag{3.16}$$

Forward converter with additional demagnetization winding (cont.)

Since the transistor switch-on time already covers DT_s, the demagnetization time interval T_m is limited to

$$T_\mathrm{m} \leq (1-D)T_\mathrm{s}. \tag{3.17}$$

Combining (3.16) and (3.17) yields

$$\frac{N_3}{N_1} \leq \frac{1-D}{D} \quad \Leftrightarrow \quad D \leq \frac{N_1}{N_1+N_3} \tag{3.18}$$

as a threshold for the turns ratio to enable certain switch-on times.Also, it should be noted that the turns ratio directly influences the maximum blocking voltage of the transistor:

$$\max\{u_\mathrm{T}(t)\} = U_1 + U_1\frac{N_1}{N_3} = U_1\left(1+\frac{N_1}{N_3}\right). \tag{3.19}$$

Hence, to allow relatively high duty cycles by a high N_1 to N_3 ratio, cf. (3.18), the blocking voltage of the transistor increases.

Section summary

This section provided a (very) limited introduction to isolated DC-DC converters with the forward and flyback converters as examples. The key takeaways are:

- The forward converter is a buck-derived topology while the flyback converter is a buck-boost-derived topology.
- A transformer is used to provide galvanic isolation between input and output.
- Limiting the magnetiziation of the transformer is a key aspect in the operation of these converters to prevent saturation (nonlinear behavior, extra losses).

In addition, there are many other isolated topologies that are used in practice, e.g.,

- Push-pull converter,
- Isolated Ćuk / SEPIC variants,
- Boost-derived topologies with full-/half bridge input stages,
- ...

Table of contents

High-level view of the rectification task

Assuming that the input voltage is an ideal sinusoidal signal

$$u_1(t) = \hat{u}_1 \sin(\omega t)$$

with the angular frequency $\omega = 2\pi f$ and the amplitude $\hat{u}_1$, the task of a rectifier is to convert this input into a unidirectional, ideally constant, voltage $u_2(t) \approx u_2$, as shown in Figure 4.1. A typical application is the grid voltage rectification in power supplies.

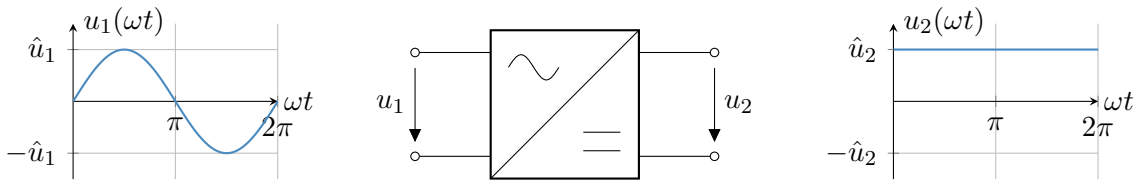

Fig. 4.1: Simplified representation of a single-phase rectifier

Frequency analysis: Fourier series

Often the rectification introduces non-fundamental frequency components, e.g., due to the output voltage rectification or by a load current feedback towards the input side. To analyze the frequency spectrum of a periodic signal $x(t)$, the Fourier series is used:

$$x(t) = \frac{a^{(0)}}{2} + \sum_{k=1}^{\infty} \left(a^{(k)} \cos(k\omega t) + b^{(k)} \sin(k\omega t) \right), \quad k \in \mathbb{N}, \tag{4.1}$$

$$a^{(k)} = \frac{1}{\pi} \int_0^{2\pi} u(t) \cos(k\omega t) \mathrm{d}\omega t, \; k \geq 0, \qquad b^{(k)} = \frac{1}{\pi} \int_0^{2\pi} u(t) \sin(k\omega t) \mathrm{d}\omega t, \; k \geq 1.$$

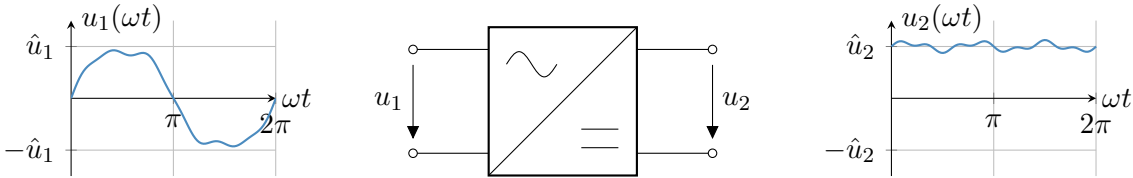

Fig. 4.2: Rectification under distorted conditions

Frequency analysis: Fourier series (cont.)

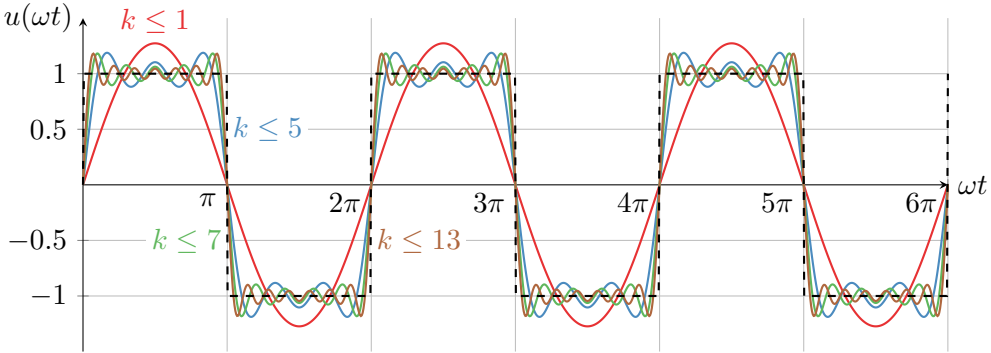

Fig. 4.3: Fourier series example: representation of a square wave signal

M1U uncontrolled rectifier circuit

Based on Fig. 4.4, the output voltage $u_2(t)$ of the M1U rectifier is

$$u_2(t) = \begin{cases} u_1(t) = \hat{u}_1 \sin(\omega t), & 0 \leq \omega t < \pi, \\ 0, & \pi \leq \omega t < 2\pi. \end{cases} \tag{4.2}$$

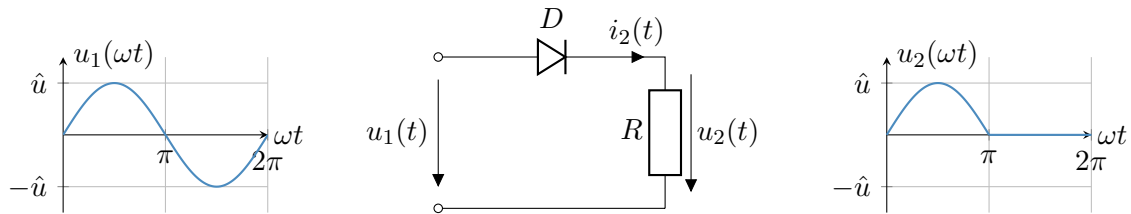

Fig. 4.4: M1U topology (aka single-pulse rectifier) with typical input and output voltage signals feeding a resistive load

M1U uncontrolled rectifier circuit (cont.)

From (4.2), the average output voltage of the M1U rectifier is

$$\begin{aligned}\overline{u}_2 &= \frac{1}{T}\int_0^T u_2(t)\mathrm{d}t = \frac{1}{2\pi}\int_0^{2\pi} u_2(\omega t)\mathrm{d}\omega t = \frac{1}{2\pi}\int_0^{\pi} \hat{u}_1 \sin(\omega t)\mathrm{d}\omega t \\ &= \frac{\hat{u}_1}{2\pi}\left[-\cos(\omega t)\right]_0^{\pi} = \frac{\hat{u}_1}{2\pi}\left(1+1\right) = \frac{\hat{u}_1}{\pi} = \frac{\sqrt{2}U_1}{\pi}\end{aligned} \tag{4.3}$$

with U_1 being the RMS value of the input voltage $u_1(t)$. The RMS value of the output voltage $u_2(t)$ results in

$$\begin{aligned}U_2 &= \sqrt{\frac{1}{2\pi}\int_0^{\pi} \hat{u}_1^2 \sin^2(\omega t)\mathrm{d}\omega t} = \hat{u}_1\sqrt{\frac{1}{2\pi}\left[\frac{1}{2}\omega t - \frac{\sin(2\omega t)}{4}\right]_0^{\pi}} \\ &= \frac{\hat{u}_1}{2} = \frac{U_1}{\sqrt{2}}.\end{aligned} \tag{4.4}$$

M1U uncontrolled rectifier circuit (cont.)

The Fourier coefficients of the output voltage $u_2(t)$ from (4.2) are

$$
\begin{aligned}
a^{(0)} &= \frac{1}{\pi}\int_0^{2\pi} u_2(t)\mathrm{d}\omega t = 2\overline{u}_2 = 2\frac{\hat{u}_1}{\pi},\\
a^{(k)} &= \frac{1}{\pi}\int_0^{2\pi} u_2(t)\cos(k\omega t)\mathrm{d}\omega t = \frac{1}{\pi}\int_0^{\pi} \hat{u}_1\sin(\omega t)\cos(k\omega t)\mathrm{d}\omega t\\
&= \frac{\hat{u}_1}{2\pi}\int_0^{\pi} \sin(\omega t(1-k)) + \sin(\omega t(1+k))\mathrm{d}\omega t = \ldots = \begin{cases} \frac{\hat{u}_1}{\pi}\frac{2}{1-k^2}, & k = 2,4,6,\ldots\\ 0, & \text{otherwise.}\end{cases} \qquad (4.5)\\
b^{(k)} &= \frac{1}{\pi}\int_0^{2\pi} u_2(t)\sin(k\omega t)\mathrm{d}\omega t = \frac{1}{\pi}\int_0^{\pi} \hat{u}_1\sin(\omega t)\sin(k\omega t)\mathrm{d}\omega t\\
&= \frac{\hat{u}_1}{2\pi}\int_0^{\pi} \cos(\omega t(1-k)) - \cos(\omega t(k+1))\mathrm{d}\omega t = \ldots = \begin{cases} \frac{\hat{u}_1}{2}, & k = 1,\\ 0, & k \geq 2.\end{cases}
\end{aligned}
$$

Above, $a^{(0)}$ represents a DC component, while the $a^{(k)} \neq 0$ coefficients indicate harmonics.

M1U uncontrolled rectifier circuit (cont.)

From (4.5) the Fourier series of $u_2(t)$ results in

$$u_2(t) = \hat{u}_1 \left(\frac{1}{\pi} + \frac{1}{2} \sin(\omega t) + \sum_{k=2,4,6,\ldots} \frac{2}{\pi(1-k^2)} \cos(k\omega t) \right). \tag{4.6}$$

For a resistive load, the output current has the same harmonic spectrum:

$$i_2(t) = \frac{\hat{u}_1}{R} \left(\frac{1}{\pi} + \frac{1}{2} \sin(\omega t) + \sum_{k=2,4,6,\ldots} \frac{2}{\pi(1-k^2)} \cos(k\omega t) \right). \tag{4.7}$$

Resulting observations are:

- Non-fundamental current frequency components can distort the input side.
- Higher frequency harmonics decrease with $\sim 1/(1-k^2)$.

Transformer input filtering

To reduce the input side distortion, a transformer can be used to filter out the harmonics:

- Impedance of magnetizing inductance L_m is zero for DC components, i.e., the transformer blocks the DC current from the input (cf. dotted red line for $\bar{i}_2$ below).
- With higher frequency harmonics, the impedance of L_m increases, i.e., filtering out the harmonics less effectively.

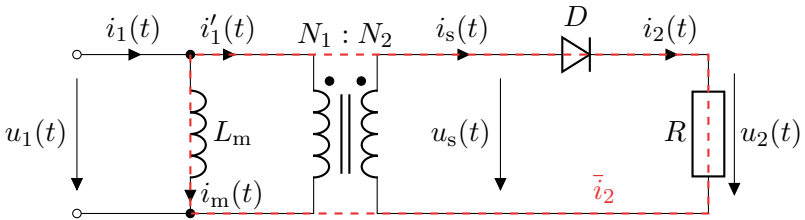

Fig. 4.5: M1U topology with input transformer and DC current path (red dotted line)

Transformer input filtering (cont.)

While the transformer can help out filter unwanted harmonics, the output DC current also introduces an offset magnetization to the transformer's core. Issues related with this are:

- **Core utilization:** To prevent core saturation, the transformer must be oversized.
- **Core losses:** The magnetization offset can increase the core losses.

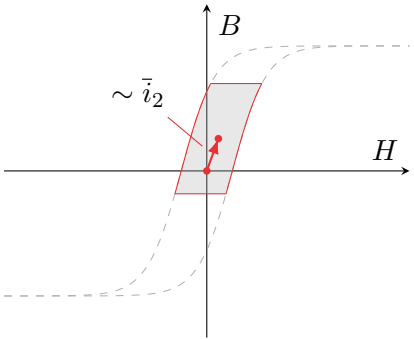

Fig. 4.6: Shift of the hysteresis curve due to the DC magnetization

Capacitive output filtering

To smooth the output voltage $u_2(t)$, a capacitor C is added. The initial charging voltage is

$$u_2(t) = \begin{cases} u_1(t) = \hat{u}_1 \sin(\omega t), & 0 \leq \omega t < \pi/2, \\ \hat{u}_1, & \omega t > \pi/2 \end{cases} \tag{4.8}$$

with the capacitor current $i_2(t)$ being

$$i_2(t) = \begin{cases} C\mathrm{d}u_2(t)/\mathrm{d}t = \hat{i}_2 \cos(\omega t) = C\omega\hat{u}_1 \cos(\omega t), & 0 \leq \omega t < \pi/2, \\ 0, & \omega t > \pi/2. \end{cases} \tag{4.9}$$

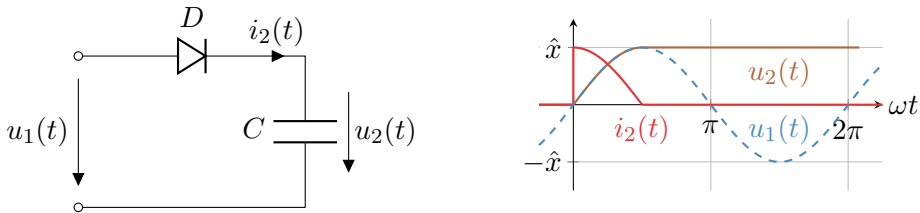

Fig. 4.7: M1U topology with output capacitor (unloaded and idealized charging curve)

Capacitive output filtering (cont.)

If the rectified output is loaded, the capacitor voltage ripples:

- If $u_2(t) \leq u_1(t)$: diode conducts, capacitor charges (follows input voltage).
- If $u_2(t) > u_1(t)$: diode blocks, capacitor discharges via I_0.

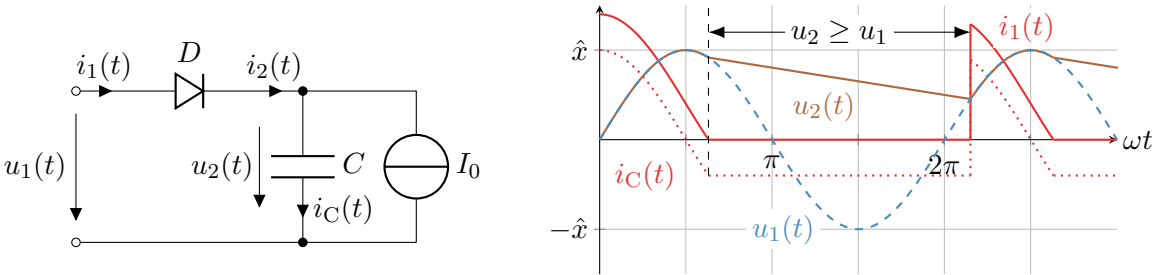

Fig. 4.8: M1U topology with output capacitor and constant load current

Table of contents

M2U uncontrolled rectifier circuit

The previous M1U topology only rectified half of a cycle resulting in a reduced output voltage utilization and increased voltage ripple. By adding another diode and utilizing a center-tapped transformer, the circuit can be extended towards a full-cycle rectifier.

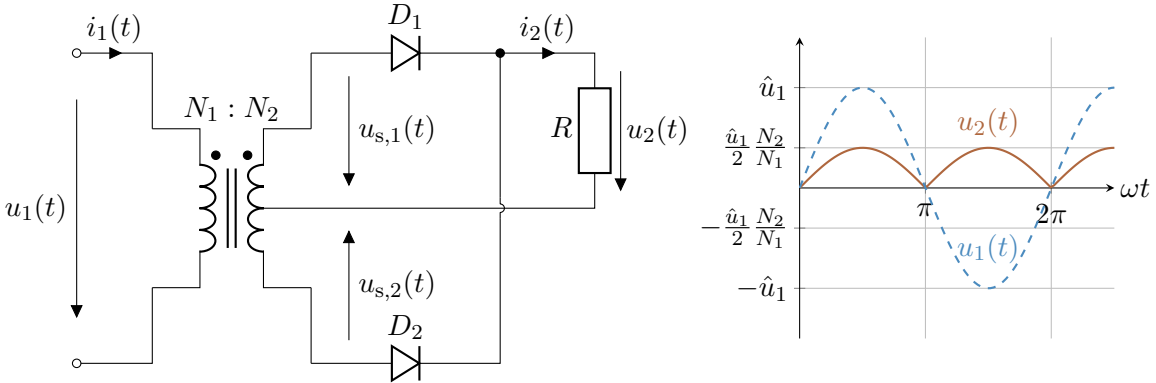

Fig. 4.9: M2U topology (aka two-pulse mid-point rectifier) with center-tapped transformer

M2U uncontrolled rectifier circuit (cont.)

From Fig. 4.9 we can conclude the following:

- During the positive half-cycle of $u_1(t)$: D_1 conducts, D_2 blocks, and $u_2(t) = u_{\mathrm{s},1}(t)$.
- During the negative half-cycle of $u_1(t)$: D_2 conducts, D_1 blocks, and $u_2(t) = u_{\mathrm{s},2}(t)$.

The output voltages of the center-tapped transformer are

$$u_{\mathrm{s},1}(t) = \frac{1}{2}\frac{N_2}{N_1}\hat{u}_1 \sin(\omega t) \quad \text{and} \quad u_{\mathrm{s},2}(t) = -\frac{1}{2}\frac{N_2}{N_1}\hat{u}_1 \sin(\omega t). \tag{4.10}$$

Here, it should be noted that both $u_{\mathrm{s},1}(t)$ and $u_{\mathrm{s},2}(t)$ are utilizing only half of the secondary winding turns due to the central tapping.The output voltage results in

$$u_2(t) = \frac{1}{2}\frac{N_2}{N_1}\left|u_1(t)\right| = \frac{1}{2}\frac{N_2}{N_1}\hat{u}_1 \left|\sin(\omega t)\right|. \tag{4.11}$$

M2U uncontrolled rectifier circuit (cont.)

From (4.11), the average output voltage of the M2U rectifier is

$$\begin{aligned}\overline{u}_2 &= \frac{1}{T}\int_0^T u_2(t)\mathrm{d}t = \frac{1}{2\pi}\int_0^{2\pi}\frac{1}{2}\frac{N_2}{N_1}\hat{u}_1\left|\sin(\omega t)\right|\mathrm{d}\omega t = \frac{1}{\pi}\int_0^{\pi}\frac{1}{2}\frac{N_2}{N_1}\hat{u}_1\sin(\omega t)\mathrm{d}\omega t \\ &= \frac{1}{2\pi}\frac{N_2}{N_1}\hat{u}_1\left[-\cos(\omega t)\right]_0^{\pi} = \frac{1}{2\pi}\frac{N_2}{N_1}\hat{u}_1\left(1+1\right) = \frac{1}{\pi}\frac{N_2}{N_1}\hat{u}_1.\end{aligned} \tag{4.12}$$

Not considering the transformer conversion via N_2/N_1, this is twice as much as in the M1U case, compare (4.3). The RMS value of the output voltage $u_2(t)$ results in

$$\begin{aligned}U_2 &= \sqrt{\frac{1}{2\pi}\frac{1}{2^2}\frac{N_2^2}{N_1^2}\hat{u}_1^2\int_0^{2\pi}\sin^2(\omega t)\mathrm{d}\omega t} = \frac{1}{2}\frac{N_2}{N_1}\hat{u}_1\sqrt{\frac{1}{\pi}\int_0^{\pi}\sin^2(\omega t)\mathrm{d}\omega t} \\ &= \frac{1}{2}\frac{N_2}{N_1}\hat{u}_1\sqrt{\frac{1}{2\pi}\left[\frac{1}{2}\omega t - \frac{\sin(2\omega t)}{4}\right]_0^{\pi}} = \frac{N_2}{N_1}\frac{\hat{u}_1}{\sqrt{2}} = \frac{N_2}{N_1}U_1.\end{aligned} \tag{4.13}$$

M2U uncontrolled rectifier circuit (cont.)

The Fourier coefficients of the output voltage $u_2(t)$ from (4.11) are

$$
\begin{aligned}
a^{(0)} &= \frac{1}{\pi}\int_0^{2\pi} u_2(t)\mathrm{d}\omega t = 2\overline{u}_2 = \frac{2}{\pi}\frac{N_2}{N_1}\hat{u}_1, \\
a^{(k)} &= \frac{1}{\pi}\int_0^{2\pi} u_2(t)\cos(k\omega t)\mathrm{d}\omega t = \frac{1}{2\pi}\frac{N_2}{N_1}\left(\int_0^{\pi}\hat{u}_1\sin(\omega t)\cos(k\omega t)\mathrm{d}\omega t\right. \\
&\quad \left.+\int_{\pi}^{2\pi}(-1)\hat{u}_1\sin(\omega t)\cos(k\omega t)\mathrm{d}\omega t\right) = \ldots = \begin{cases} \frac{\hat{u}_1}{\pi}\frac{N_2}{N_1}\frac{2}{1-k^2}, & k = 2,4,6,\ldots \\ 0, & \text{otherwise.} \end{cases} \qquad (4.14) \\
b^{(k)} &= \frac{1}{\pi}\int_0^{2\pi} u_2(t)\sin(k\omega t)\mathrm{d}\omega t = \frac{1}{2\pi}\frac{N_2}{N_1}\left(\int_0^{\pi}\hat{u}_1\sin(\omega t)\sin(k\omega t)\mathrm{d}\omega t\right. \\
&\quad \left.+\int_{\pi}^{2\pi}(-1)\hat{u}_1\sin(\omega t)\sin(k\omega t)\mathrm{d}\omega t\right) = \ldots = 0.
\end{aligned}
$$

These coefficients also indicate significant harmonics, which are in particular scaled by the transformer turns ratio.

Table of contents

B2U uncontrolled rectifier circuit

The B2U circuit also allows full-cycle rectification but without the need for a center-tapped transformer, that is, fully utilizes the input voltage without halving it on the output side.

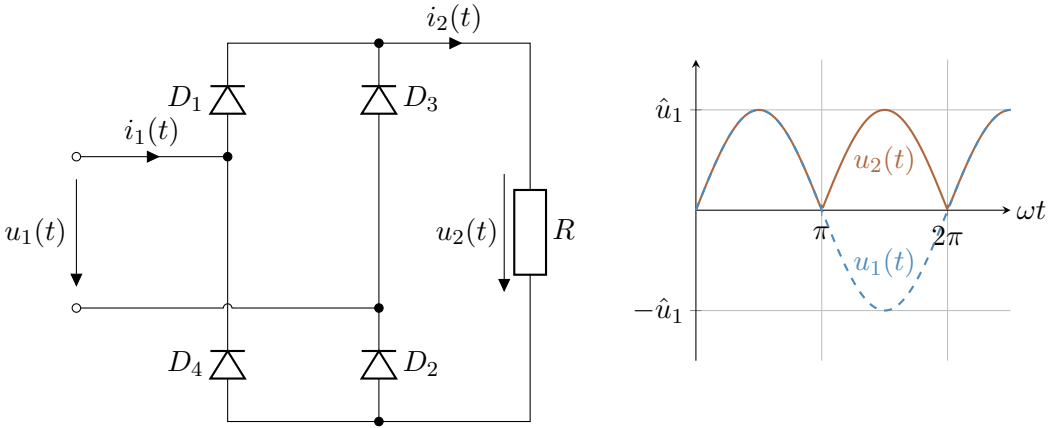

Fig. 4.10: B2U topology (aka two-pulse bridge rectifier) with resistive load

B2U uncontrolled rectifier circuit (cont.)

For a purely resistive load as in Fig. 4.10 the output voltage $u_2(t)$ is

$$u_2(t) = |u_1(t)| = \hat{u}_1 \left|\sin(\omega t)\right| . \tag{4.15}$$

Here, following diodes are conducting:

- Positive half-cycle: D_1 and D_2,
- Negative half-cycle: D_3 and D_4.

The average output voltage $\overline{u}_2$ is

$$\overline{u}_2 = \frac{1}{T}\int_0^T u_2(t)\mathrm{d}t = \frac{1}{2\pi}\int_0^{2\pi} \hat{u}_1 \left|\sin(\omega t)\right| \mathrm{d}\omega t = \ldots = \frac{2}{\pi}\hat{u}_1. \tag{4.16}$$

The Fourier coefficients of the output voltage $u_2(t)$ are analogous to the M2U case, compare (4.14) with appropriate scaling considering the lack of the center-tapped transformer.

B2U uncontrolled rectifier circuit with capacitive output filtering

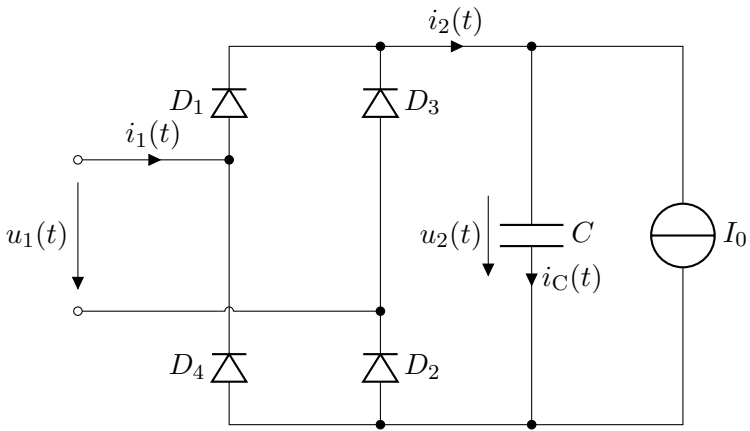

Fig. 4.11: B2U topology with output capacitor and constant load

B2U uncontrolled rectifier circuit with capacitive output filtering (cont.)

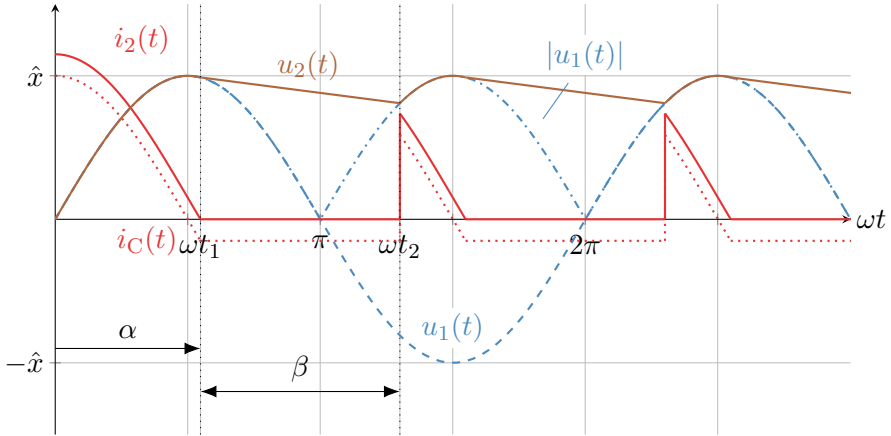

Fig. 4.12: Typical signal curves for B2U topology with output capacitor and constant load

B2U uncontrolled rectifier circuit with capacitive output filtering (cont.)

The filter capacitor current $i_\mathrm{C}(t)$ is

$$i_\mathrm{C}(t) = \begin{cases} -I_0, & i_2(t) = 0, \\ C\frac{\mathrm{d}}{\mathrm{d}t}u_2(t), & i_2(t) > 0, \end{cases} \tag{4.17}$$

that is, if the output current $i_2(t)$ is zero, the diode bridge blocks and the capacitor discharges via the load. Contrary, if the output current is positive, the diodes conduct and the capacitor voltage is determined by the rectified input voltage.The output current is given by

$$i_2(t) = i_\mathrm{C}(t) + I_0. \tag{4.18}$$

Inserting (4.17) in (4.18) delivers the output current during the conduction phase:

$$i_2(t) = C\omega\hat{u}_1 \cos(\omega t) + I_0, \quad 0 \leq \omega t < \omega t_1. \tag{4.19}$$

B2U uncontrolled rectifier circuit with capacitive output filtering (cont.)

The conduction phase lasts until $\omega t_1 = \alpha$ which can be determined from (4.19):

$$\alpha = \arccos\left(-\frac{I_0}{C\omega\hat{u}_1}\right). \tag{4.20}$$

For $\alpha < \omega t < \omega t_2$ the capacitor discharges via the load:

$$\begin{aligned} u_2(t) &= u_2(\omega t_1) + \int_{t_1}^{t} -\frac{I_0}{C}\mathrm{d}\tau = u_2(\alpha) + \int_{\alpha}^{\omega t} -\frac{I_0}{\omega C}\mathrm{d}\omega\tau \\ &= u_2(\alpha) - \frac{I_0}{\omega C}(\omega t - \alpha), \quad \omega t_1 \leq \omega t < \omega t_2. \end{aligned} \tag{4.21}$$

The blocking phase lasts until $\omega t_2 = \alpha + \beta$, that is, the rectified input voltage is equal to the capacitor voltage (note: not solvable for ωt_2 in closed-form, requires numerical methods):

$$u_2(\omega t_2) = u_2(\alpha) - \frac{I_0}{\omega C}(\omega t_2 - \alpha) \stackrel{!}{=} \hat{u}_1|\sin(\omega t_2)| = |u_1(\omega t_2)|. \tag{4.22}$$

B2U rectifier with capacitive output filtering and grid impedance

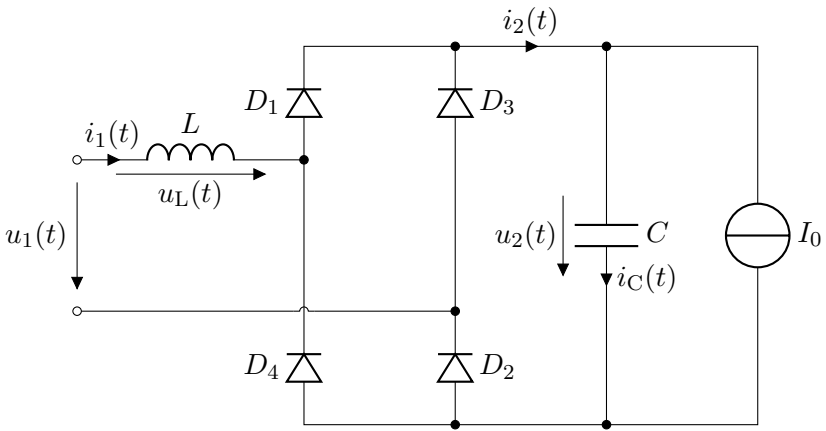

Fig. 4.13: B2U topology considering an output capacitor, constant load, and grid impedance

B2U rectifier with capacitive output filtering and grid impedance (cont.)

For the modified scenario form (4.13) we assume an infinite capacitance capacitor, i.e.,

$$u_2(t) \approx U_2$$

to keep the analysis simple. Like before, the diode bridge conduction is determined by the output current $i_2(t)$:

- $i_2(t) > 0$: diode bridge conducts, $u_{\mathrm{L}}(t) = |u_1(t)| - U_2$,
- $i_2(t) = 0$: diode bridge blocks, $u_{\mathrm{L}}(t) = \max\{0, |u_1(t)| - U_2\}$.

Hence, the B2U rectifier behavior is driven by the grid impedance current and the dynamics introduced by L. Similar to the previous analysis on DC-DC converters, the discontinuous conduction mode (DCM) and the boundary conduction mode (BCM) will be differentiated in the following.

B2U rectifier with capacitive output filtering and grid impedance (cont.)

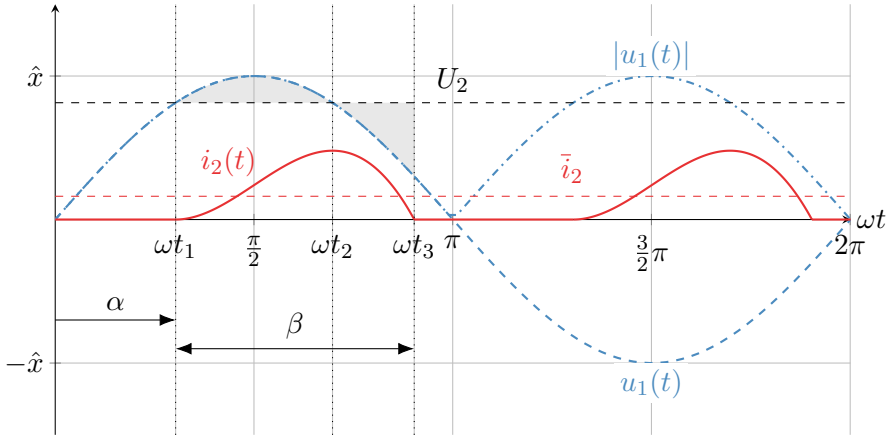

Fig. 4.14: Typical signal curves for B2U topology feeding a constant load from the grid and an infinite output capacitance in DCM

B2U rectifier with capacitive output filtering and grid impedance (cont.)

In steady-state DCM the output current is zero for

$$i_2(\omega t) = 0, \quad 0 \leq \omega t < \omega t_1. \tag{4.23}$$

Until then the diode bridge is in blocking mode and disconnects the input from the output. At $\omega t_1 = \alpha$ the diodes start conducting since the input voltage exceeds the output voltage:

$$u_1(\omega t_1 = \alpha) = \hat{u}_1 \sin(\alpha) \stackrel{!}{=} U_2 \quad \Leftrightarrow \quad \alpha = \arcsin\left(\frac{U_2}{\hat{u}_1}\right). \tag{4.24}$$

At this point, the output current is rising due to the positive inductor voltage:

$$\begin{aligned} i_2(\omega t) &= \frac{1}{L}\int_{t_1}^{t} u_1(t) - U_2 \mathrm{d}\tau = \frac{1}{\omega L}\int_{\omega t_1}^{\omega t} u_1(\omega\tau) - U_2 \mathrm{d}\omega\tau = \frac{1}{\omega L}\int_{\omega t_1}^{\omega t} \hat{u}_1 \sin(\omega\tau) - U_2 \mathrm{d}\omega\tau \\ &= \frac{\hat{u}_1}{\omega L}\left(\cos(\alpha) - \cos(\omega t) - \frac{U_2}{\hat{u}_1}(\omega t - \alpha)\right), \quad \omega t_1 \leq \omega t < \omega t_3. \end{aligned} \tag{4.25}$$

B2U rectifier with capacitive output filtering and grid impedance (cont.)

At $\omega t_2 = \alpha + \beta$ the current reaches zero again and the diode bridge blocks again:

$$\begin{aligned} i_2(\omega t_2) = \frac{\hat{u}_1}{\omega L}\left(\cos(\alpha) - \cos(\omega t_2) - \frac{U_2}{\hat{u}_1}(\omega t_2 - \alpha)\right) &\stackrel{!}{=} 0 \\ \Leftrightarrow \cos(\alpha) - \cos(\alpha+\beta) - \beta\sin(\alpha) &= 0. \end{aligned} \tag{4.26}$$

For a given α, this equation is not solvable in closed-form w.r.t. β and requires numerical methods. However, if β is known, α can be determined leading to

$$\alpha = \arctan\left(\frac{1-\cos(\beta)}{\beta - \sin(\beta)}\right). \tag{4.27}$$

The average output current in DCM is

$$\bar{i}_2 = \frac{1}{T}\int_0^T i_2(t)\mathrm{d}t = \frac{1}{\pi}\int_\alpha^{\alpha+\beta} i_2(\omega t)\mathrm{d}\omega t = \ldots = \frac{\hat{u}_1}{\pi\omega L}\left(\frac{\hat{u}_1}{U_2}(1-\cos(\beta)) - \frac{U_2}{\hat{u}_1}\frac{\beta^2}{2}\right). \tag{4.28}$$

B2U rectifier with capacitive output filtering and grid impedance (cont.)

For a better representation in the following, the average current is normalized:

$$\bar{i}_2' = \frac{\bar{i}_2}{\frac{2}{\pi}\frac{\hat{u}_1}{\omega L}} = \frac{1}{2}\left(\frac{\hat{u}_1}{U_2}(1-\cos(\beta)) - \frac{U_2}{\hat{u}_1}\frac{\beta^2}{2}\right). \tag{4.29}$$

Here, the denominator $2/\pi \cdot \hat{u}_1/\omega L$ is the absolute average value of the inductor current in case of a grid short circuit.

Based on the correlations found, the operating characteristics in DCM of the rectifier can be visualized, which has been implemented in Fig. 4.16 (left part):

- In DCM, $\beta \in [0, \pi[$ holds, i.e., the diode bridge is conducting for $0 \ldots 100\,\%$ per half cycle.
- At $\beta = \pi$ the diode bridge is conducting for the full half cycle (i.e., entering BCM).
- In order to achieve a commutation of the current between the diode pairs D1/D4 and D2/D3, the current gets zero (for a short time) so that the rectifier operates in BCM.

B2U rectifier with capacitive output filtering and grid impedance (cont.)

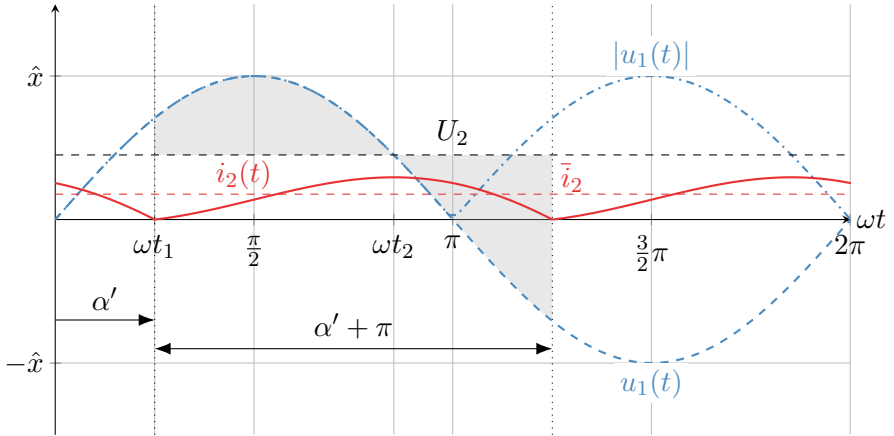

Fig. 4.15: Typical signal curves for B2U topology feeding a constant load from the grid and an infinite output capacitance in BCM

B2U rectifier with capacitive output filtering and grid impedance (cont.)

In steady-state BCM, the output current is analogous to the DCM as from (4.25) leading to

$$i_2(\omega t) = \frac{\hat{u}_1}{\omega L}\left(\cos(\alpha') - \cos(\omega t) - \frac{U_2}{\hat{u}_1}(\omega t - \alpha')\right), \quad \alpha' \leq \omega t < \alpha' + \pi \tag{4.30}$$

with α' being the phase angle at which the diodes start conducting in BCM – cf. Fig. 4.15. After a half cycle, the current reaches zero for a short moment enabling the diode bridge to commutate the current between the diode pairs:

$$i_2(\omega t = \alpha' + \pi) = 0 \quad \Leftrightarrow \quad \cos(\alpha') - \cos(\alpha' + \pi) - \frac{U_2}{\hat{u}_1}\pi = 0 \tag{4.31}$$

from which

$$\frac{U_2}{\hat{u}_1} = \frac{2}{\pi}\cos(\alpha') \tag{4.32}$$

follows after some intermediate calculation steps.

B2U rectifier with capacitive output filtering and grid impedance (cont.)

The average output current in BCM follows as

$$\begin{aligned}\bar{i}_2 &= \frac{1}{T}\int_0^T i_2(t)\mathrm{d}t = \frac{1}{\pi}\int_{\alpha'}^{\alpha'+\pi} i_2(\omega t)\mathrm{d}\omega t = \ldots \\ &= \frac{2}{\pi}\frac{\hat{u}_1}{\omega L}\sin(\alpha').\end{aligned} \tag{4.33}$$

Applying the same normalization as (4.29) leads to

$$\bar{i}_2' = \frac{\bar{i}_2}{\frac{2}{\pi}\frac{\hat{u}_1}{\omega L}} = \sin(\alpha'). \tag{4.34}$$

Combining (4.32) and (4.34) reveals

$$\frac{U_2}{\hat{u}_1} = \frac{2}{\pi}\cos(\arcsin(\bar{i}_2')). \tag{4.35}$$

The resulting load curve for the BCM is also depicted in Fig. 4.16 (right part).

B2U rectifier with capacitive output filtering and grid impedance (cont.)

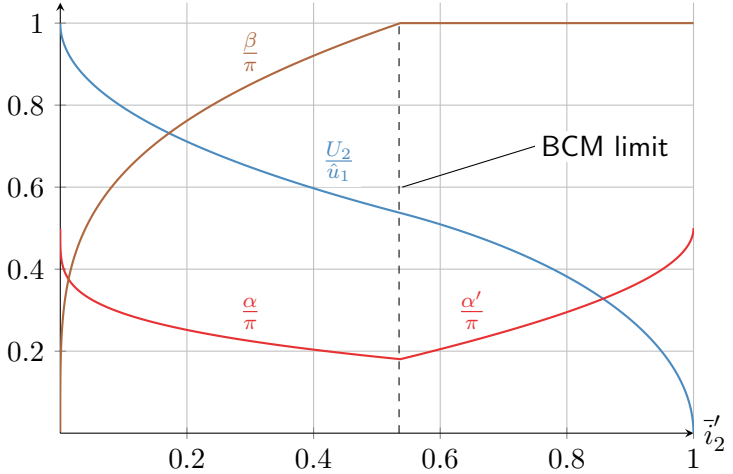

Fig. 4.16: Load curve of the B2U rectifier with capacitive output filtering and grid impedance

B2U rectifier with capacitive output filtering and grid impedance (cont.)

Assuming DCM, the input current of the B2U rectifier is

$$i_1(t) = \begin{cases} i_2(t), & \alpha \leq \omega t < \alpha + \beta, \\ -i_2(t), & \pi + \alpha \leq \omega t < \pi + \alpha + \beta. \end{cases} \tag{4.36}$$

The minus sign during the second half-cycle results from the conducting diodes D3/D4 reversing the current direction in the inductor – cf. Fig. 4.13. The input current can be decomposed into its fundamental and harmonic components:

$$i_1(t) = \underbrace{a_1 \cos(\omega t) + b_1 \sin(\omega t)}_{=i_1^{(1)}(t)} + \underbrace{\sum_{k=2}^{\infty} \Big(a^{(k)} \cos(k\omega t) + b^{(k)} \sin(k\omega t) \Big)}_{i_1^{(\mathrm{h})}(t)}, \quad k \in \mathbb{N}. \tag{4.37}$$

As will be discussed in the following, the harmonic components $i_1^{(\mathrm{h})}(t)$ are considered distortions negatively impacting the grid quality.

B2U rectifier with capacitive output filtering and grid impedance (cont.)

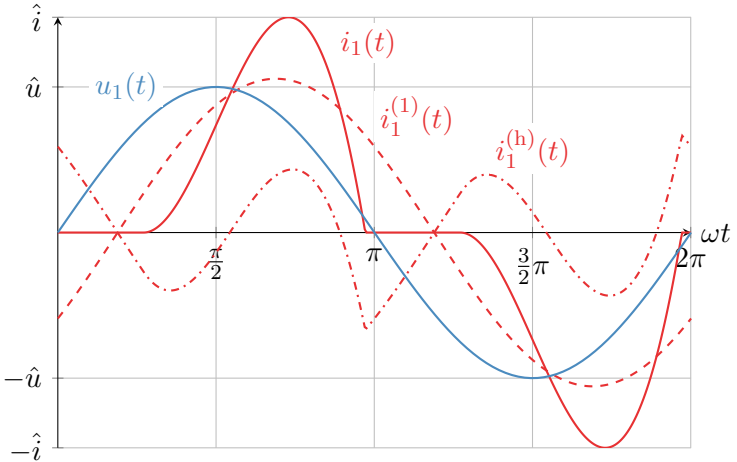

Fig. 4.17: Input current decomposition of the B2U rectifier with $i_1^{(1)}(t)$ being the fundamental and $i_1^{(\mathrm{h})}(t)$ harmonic components

Recap: active, reactive, and apparent power in sinusoidal steady-state

The complex power is defined as

$$\underline{S} = \underline{U} \cdot \underline{I}^* = P + \mathrm{j}Q = Se^{\mathrm{j}\varphi}, \tag{4.38}$$

with the active power P, the reactive power Q, and the apparent power S as well as $\underline{U}$ and $\underline{I}$ being the complex voltage and current phasors.From (4.38) directly follows:

$$S = |\underline{S}| = \sqrt{P^2 + Q^2}. \tag{4.39}$$

The power factor λ is defined as

$$\lambda = \cos(\varphi) = \frac{P}{S}. \tag{4.40}$$

Typically, one tries to operate power converters with a unity power factor $\lambda \approx 1$ to avoid reactive power transfer (i.e., additional reactive currents leading to more losses in the grid).

Active power transfer considering harmonics

The active power can be alternatively expressed as the average of the instantaneous power:

$$P = \frac{1}{T}\int_0^T p(t)\mathrm{d}t = \frac{1}{2\pi}\int_0^{2\pi} u(\omega t)i(\omega t)\mathrm{d}\omega t. \tag{4.41}$$

To generalize the analysis for arbitrary voltage and current harmonics, we consider both Fourier decompositions

$$u(\omega t) = \overline{u} + \sum_{k=1}^{\infty} \hat{u}^{(k)} \cos(k\omega t - \varphi_u^{(k)}), \quad i(\omega t) = \overline{i} + \sum_{k=1}^{\infty} \hat{i}^{(k)} \cos(k\omega t - \varphi_i^{(k)}) \tag{4.42}$$

with $\overline{u}$ and $\overline{i}$ being the DC components, $\hat{u}^{(k)}$ and $\hat{i}^{(k)}$ the amplitudes of the k-th harmonic and $\varphi_u^{(k)}$ and $\varphi_i^{(k)}$ the phase angles of the voltage and current harmonics.This amplitude-phase representation is analogous to (4.1) with the relations:

$$\hat{x}^{(k)} = \sqrt{(a^{(k)})^2 + (b^{(k)})^2}, \quad \varphi_x^{(k)} = -\arccos\left(\frac{a^{(k)}}{\hat{x}^{(k)}}\right) \cdot \operatorname{sign}\left(b^{(k)}\right). \tag{4.43}$$

Active power transfer considering harmonics (cont.)

Substituting the Fourier series of $u_1(\omega t)$ and $i_1(\omega t)$ into the instantaneous power expression delivers:

$$\begin{aligned} p(t) &= u(\omega t) i(\omega t) \\ &= \left(\overline{u} + \sum_{k=1}^{\infty} \hat{u}^{(k)} \cos(k\omega t - \varphi_u^{(k)}) \right) \left(\overline{i} + \sum_{m=1}^{\infty} \hat{i}^{(m)} \cos(m\omega t - \varphi_i^{(m)}) \right). \end{aligned}$$

Expanding this product yields:

$$\begin{aligned} p(t) = \overline{u}\overline{i} &+ \overline{u} \sum_{m=1}^{\infty} \hat{i}^{(m)} \cos(m\omega t - \varphi_i^{(m)}) + \overline{i} \sum_{k=1}^{\infty} \hat{u}^{(k)} \cos(k\omega t - \varphi_u^{(k)}) \\ &+ \sum_{k=1}^{\infty} \sum_{m=1}^{\infty} \hat{u}^{(k)} \hat{i}^{(m)} \cos(k\omega t - \varphi_u^{(k)}) \cos(m\omega t - \varphi_i^{(m)}). \end{aligned}$$

Active power transfer considering harmonics (cont.)

Using the trigonometric identities the last term becomes:

$$\sum_{k=1}^{\infty}\sum_{m=1}^{\infty}\hat{u}^{(k)}\hat{i}^{(m)}\cos(k\omega t-\varphi_u^{(k)})\cos(m\omega t-\varphi_i^{(m)})$$
$$=\sum_{k=1}^{\infty}\sum_{m=1}^{\infty}\hat{u}^{(k)}\hat{i}^{(m)}\frac{1}{2}\left[\cos((k-m)\omega t+\varphi_i^{(k)}-\varphi_u^{(m)})+\cos((k+m)\omega t-\varphi_u^{(k)}-\varphi_i^{(m)})\right].$$

Hence, we receive integral terms of the form

$$\int_0^{2\pi}\cos(n\omega t+\varphi)\mathrm{d}\omega t=\begin{cases}2\pi\cos(\varphi), & n=0,\\ 0 & n\neq 0\end{cases}$$

with $n=k-m\in\mathbb{Z}$ or $n=k+m\in\mathbb{Z}$, respectively. Due to the periodicity and symmetry of the cosine function, the integral over a full period is zero for $n\neq 0$.

Conclusion: Cross-frequency terms ($k\neq m$) cancel due to their oscillatory nature, leaving only contributions from voltage and current harmonics of the same order ($k=m$).

Active power transfer considering harmonics (cont.)

Summarizing the previous considerations, the active power can be expressed as:

$$P = \frac{1}{T}\int_0^T p(t)\,\mathrm{d}t = \sum_{k=1}^{\infty} \frac{\hat{u}^{(k)}\hat{i}^{(k)}}{2}\cos(\varphi_i^{(k)} - \varphi_u^{(k)}). \tag{4.44}$$

Inserting the B2U ideal input voltage assumption $u(t) = u_1(t) = \hat{u}_1 \sin(\omega t)$, this boils down to:

$$P = \frac{\hat{u}_1\hat{i}_1^{(1)}}{2}\cos(\varphi_i^{(1)} - \varphi_u^{(1)}) = U_1 I_1^{(1)}\cos(\varphi_i^{(1)} - \varphi_u^{(1)}) \tag{4.45}$$

with U_1 and $I_1^{(1)}$ being the RMS values of the fundamental voltage and current component and $\varphi_i^{(1)}$ the phase angle between the fundamental voltage and current component. The power factor results in

$$\lambda = \frac{P}{S} = \frac{U_1 I_1^{(1)}}{U_1 I_1}\cos(\varphi_i^{(1)} - \varphi_u^{(1)}) = \frac{I_1^{(1)}}{I_1}\cos(\varphi_i^{(1)} - \varphi_u^{(1)}). \tag{4.46}$$

i.e., the harmonics increase the apparent power S but do not contribute to the active power P. Consequently, the B2U's power factor is typically limited to $70\,\%$ or lower.

Total harmonic distortion (THD)

Another important measure for the quality of the input current is the total harmonic distortion (THD):

$$\mathrm{THD}(i_1) = \frac{\sqrt{\sum_{k=2}^{\infty} \left(I_1^{(k)}\right)^2}}{I_1^{(1)}} = \frac{I_1^{(\mathrm{h})}}{I_1^{(1)}}. \tag{4.47}$$

The THD quantifies the ratio of the RMS value of the harmonic components to the RMS value of the fundamental component.Rewriting the decomposition (4.37) in the RMS form

$$I_1^2 = \left(I_1^{(1)}\right)^2 + \left(I_1^{(\mathrm{h})}\right)^2, \tag{4.48}$$

and inserting (4.47) in the power factor expression (4.46) leads to

$$\lambda = \frac{1}{\sqrt{1 + \mathrm{THD}^2(i_1)}} \cos(\varphi_i^{(1)} - \varphi_u^{(1)}). \tag{4.49}$$

Hence, the larger the THD, the more the power factor deviates from unity.

B2U rectifier: THD and power factor

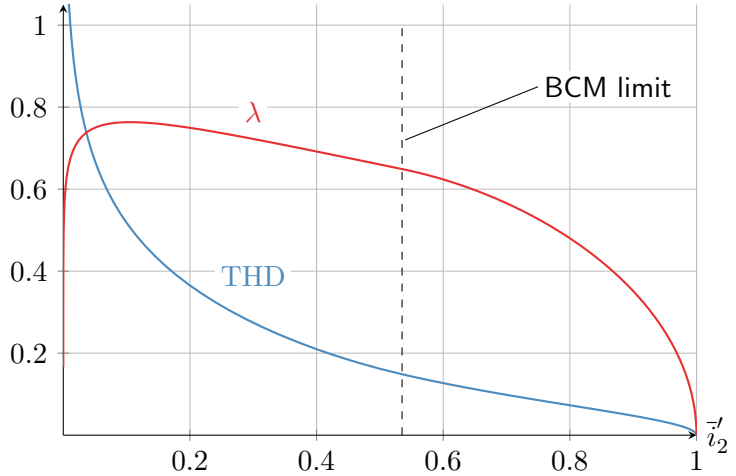

Fig. 4.18: THD and power factor of the B2U rectifier with capacitive output filtering and grid impedance

B2U rectifier impact on the grid voltage

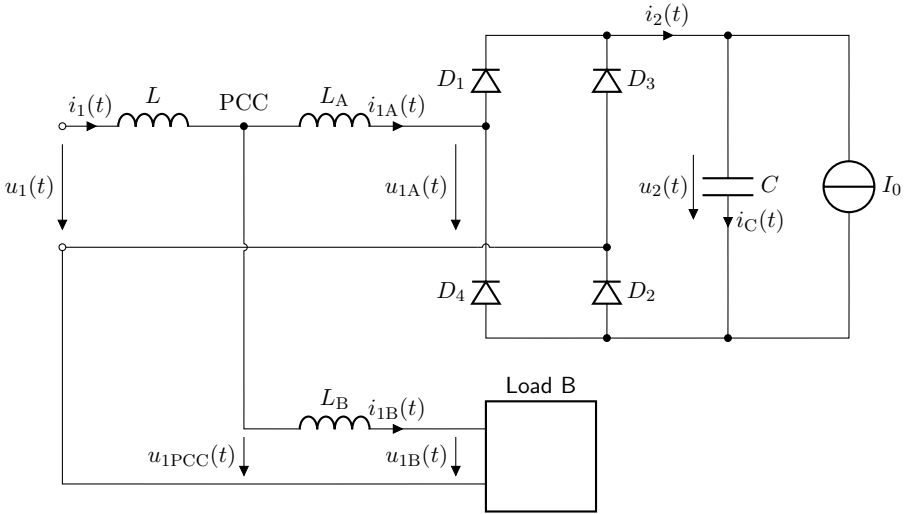

Fig. 4.19: B2U rectifier and a second load connected to the grid

B2U rectifier impact on the grid voltage (cont.)

In Fig. 4.19 the B2U rectifier and a second load are connected to the grid $u_1(t)$ with

- L being the grid inductance (at the point of common coupling – PCC),
- L_A being the inductance of the cable connecting the B2U rectifier to the PCC,
- L_B being the inductance of the cable connecting the second load to the PCC.

Assuming $i_{1\mathrm{B}}(t) = 0$ for the sake of simplicity, the inductive voltage divider rule yields

$$\frac{u_1(t) - u_{1\mathrm{PCC}}(t)}{u_1(t) - u_{1\mathrm{A}}(t)} = \frac{L}{L + L_\mathrm{A}} \tag{4.50}$$

and, therefore, the voltage at the second load's PCC $u_{1\mathrm{PCC}}(t)$ is

$$u_{1\mathrm{PCC}}(t) = u_1(t) - \frac{L}{L + L_\mathrm{A}}(u_1(t) - u_{1\mathrm{A}}(t)). \tag{4.51}$$

B2U rectifier impact on the grid voltage (cont.)

Assuming again a constant output voltage $u_2(t) = U_2$ (due to an infinite filter capacitance), the B2U's input voltage is

$$u_{1\mathrm{A}}(t) = \begin{cases} u_1(t), & i_{1\mathrm{A}}(t) = 0 \\ \mathrm{sign}(i_2(t)) \cdot U_2, & i_{1\mathrm{A}}(t) \neq 0. \end{cases} \tag{4.52}$$

Hence, the voltage at the second load's PCC is

$$u_{1\mathrm{PCC}}(t) = \begin{cases} u_1(t), & i_{1\mathrm{A}}(t) = 0 \\ u_1(t)\left(1 - \frac{L}{L+L_\mathrm{A}}\right) + \frac{L}{L+L_\mathrm{A}}\mathrm{sign}(i_2(t)) \cdot U_2, & i_{1\mathrm{A}}(t) \neq 0. \end{cases} \tag{4.53}$$

As on can see on the next slide, the B2U rectifier operation leads to a distorted grid voltage $u_{1\mathrm{PCC}}(t)$ which might impair the operation of the second load. Increasing the input inductance L_A by an explicit filter inductor can mitigate this issue, however, at the expense of volume, weight and cost as well as voltage drop associated with the input filter inductor.

B2U rectifier impact on the grid voltage (cont.)

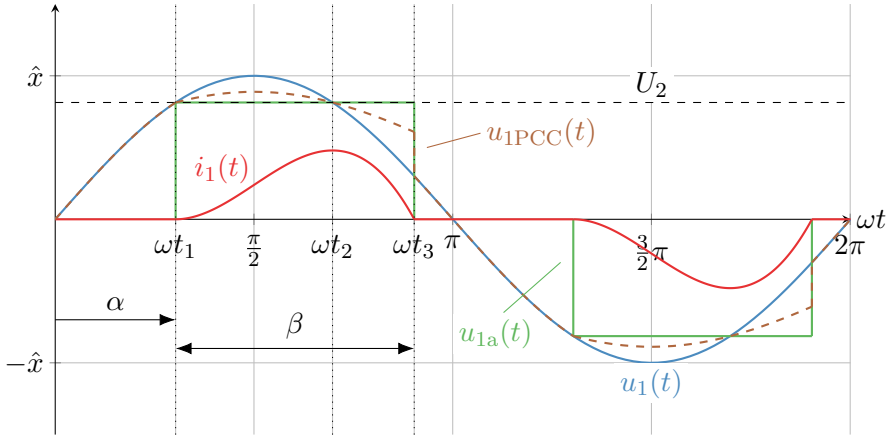

Fig. 4.20: Relevant signals of the scenario from (4.19) with B2U in DCM

B2U rectifier impact on the neutral line in three-phase grid

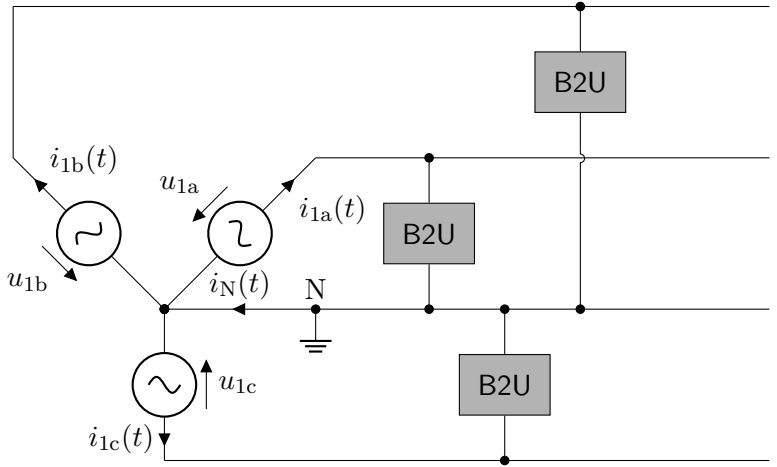

Fig. 4.21: Three-phase grid with single-phase rectifiers connected to neutral

B2U rectifier impact on the neutral line in three-phase grid (cont.)

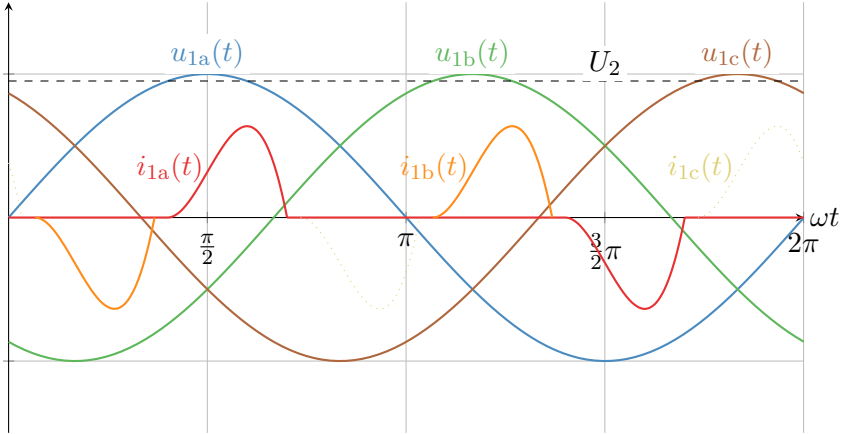

Fig. 4.22: Relevant signals of the scenario from (4.21) assuming identical operation conditions for all single-phase rectifiers

B2U rectifier impact on the neutral line in three-phase grid (cont.)

The neutral conductor current is the sum of the phase currents:

$$i_{\mathrm{N}}(t) = i_{1\mathrm{a}}(t) + i_{1\mathrm{b}}(t) + i_{1\mathrm{c}}(t). \tag{4.54}$$

In the example from Fig. 4.22 the neutral conductor current corresponds to the enveloping curve over the phase currents shown in the figure:

- The B2U rectifier represents a nonlinear load such that the three-phase currents do not cancel each other out.
- The neutral conductor current leads to power losses in the neutral conductor and can cause overheating.

Need for grid-friendly rectification

The shown analysis of the B2U rectifier highlights its negative impact on the grid, especially if multiple B2U rectifiers are connected to the same grid. Therefore, grid-friendly rectification alternatives are essential to ensure the stable operation of the grid and the connected loads.

Table of contents

General PFC circuit structure

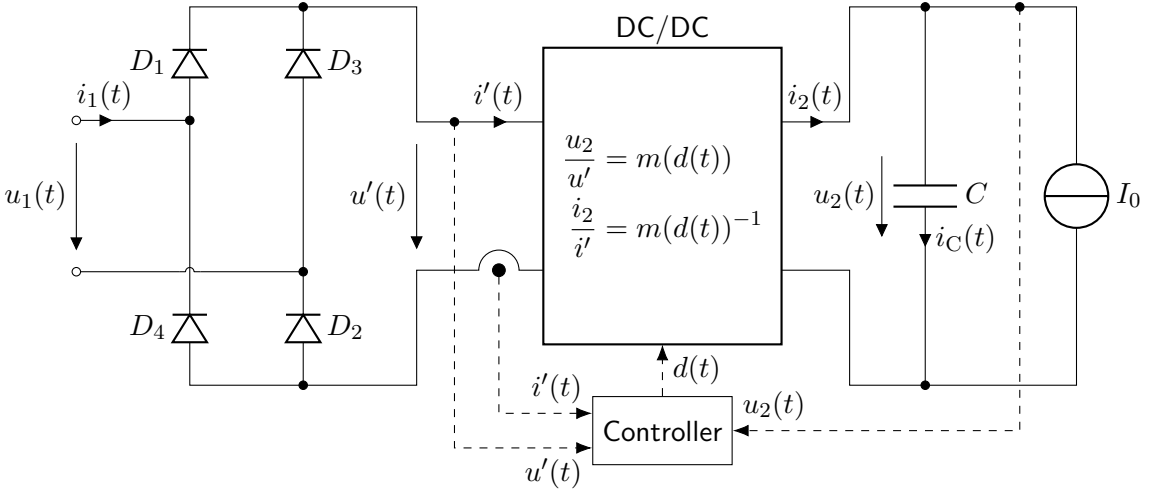

Fig. 4.23: Rectifier with power factor correction (PFC) realized as a combination of a single-phase diode bridge and a cascaded DC/DC converter with voltage / current transfer ratio $m(t)$

Idealized PFC rectifier signals in the time domain (steady state)

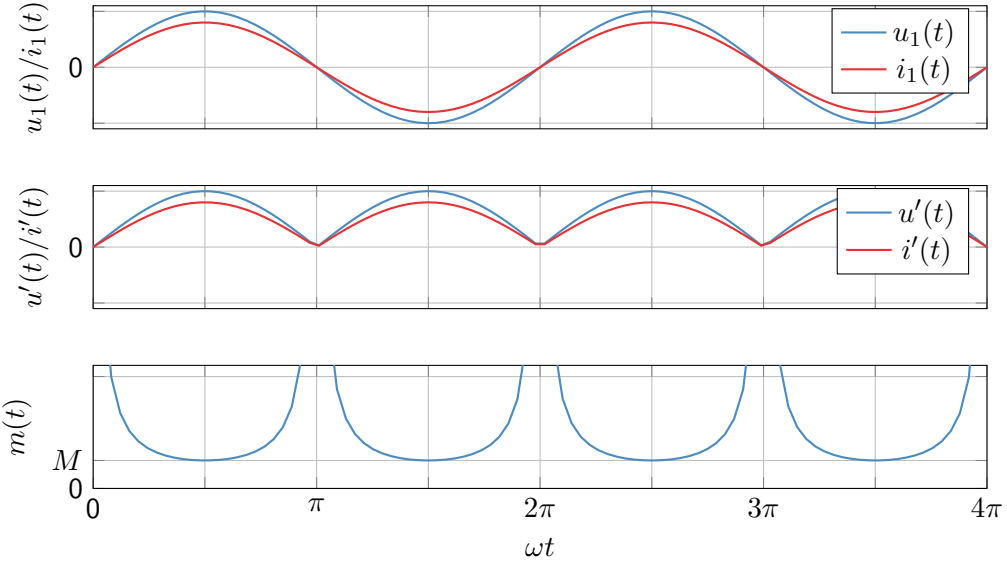

Operation concept and assumptions for the PFC rectifier

Main idea: utilize a DC/DC converter to control the input current $i_1(t)$ such that it follows the input voltage $u_1(t)$ in phase:

$$i_1(t) = \hat{i}_1 \sin(\omega t) \sim \hat{u}_1 \sin(\omega t) = u_1(t). \tag{4.55}$$

Assumptions for the following PFC rectifier analysis:

- The input voltage $u_1(t)$ is an ideal sinusoidal signal with amplitude $\hat{u}_1$ and frequency ω.
- The output voltage is considered constant: $u_2(t) \approx U_2$.
- The grid impedance is neglected for the sake of simplicity.
  - The grid impedance as in Fig. 4.13 would (mainly) introduce a phase shift between $|u_1(t)|$ and $u'(t)$ which can be compensated by the control setup.

Based on these assumptions and the objective (4.55), the voltages and currents in front of the DC/DC converter must be proportional to each other (to achieve unity power factor):

$$\frac{u_1(t)}{i_1(t)} = \frac{u'(t)}{i'(t)}. \tag{4.56}$$

Voltage transfer ratio

Considering an ideal DC/DC converter with a voltage transfer ratio $m(t)$, the converter must deliver a rectified-sinusoidal $u'(t)$ given some constant U_2:

$$u'(t) = \frac{U_2}{m(t)} \quad \Leftrightarrow \quad \hat{u}_1 |\sin(\omega t)| = \frac{U_2}{m(t)}. \tag{4.57}$$

Hence, the voltage transfer ratio $m(t)$ is given by

$$m(t) = \frac{U_2}{u'(t)} = \frac{U_2}{\hat{u}_1 |\sin(\omega t)|} \tag{4.58}$$

which varies between

$$\begin{aligned} \max_{u'}\{m(t)\} &= \infty, & \arg\max_{u'}\{m(t)\} &= 0, \\ \min_{u'}\{m(t)\} &= \frac{U_2}{\hat{u}_1} = M, & \arg\min_{u'}\{m(t)\} &= \hat{u}_1. \end{aligned} \tag{4.59}$$

One can conclude that the DC/DC converter must be able to deliver a voltage transfer ratio of

$$m(t) \in [M, \ldots, \infty].$$

Voltage transfer ratio (cont.)

The above voltage transfer ratio range restricts the possible topologies accordingly, e.g.:

- Standard boost converter: $m(t) = {}^{1}/_{(1-d(t))}$,
- Buck-boost converter or SEPIC: $m(t) = {}^{d(t)}/_{(1-d(t))}$.

Due to its simplicity and low component count, the boost converter is the most common choice for PFC applications leading to the reference duty cycle (assuming CCM operation):

$$d(t) = \frac{U_2 - \hat{u}_1 |\sin(\omega t)|}{U_2} = 1 - \frac{1}{M} |\sin(\omega t)|. \tag{4.60}$$

Remark on nomenclature and steady state

In contrast to the previous DC/DC converter section, the duty cycle $d(t)$ is now a function of time and not a constant (small d instead of capital D). However, the voltage transfer to duty cycle ratio was derived in steady state, i.e., (4.60) only holds approximately for $f_s >> f = {}^{\omega}/_{2\pi}$ (so-called quasi steady state).

PFC rectifier with boost converter

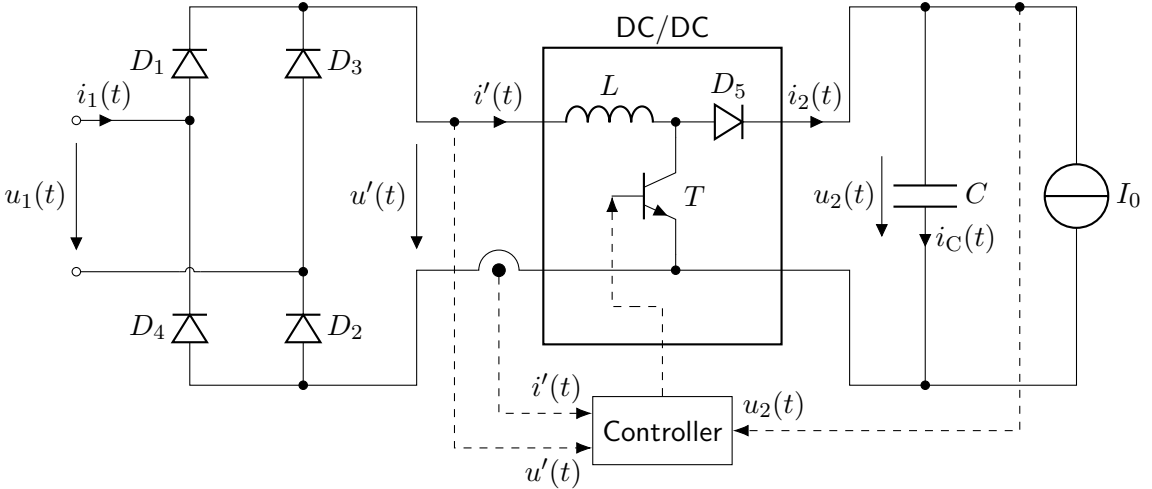

Fig. 4.24: PFC rectifier realized as a combination of a single-phase diode bridge and a cascaded DC/DC boost converter

PFC rectifier with boost converter (cont.)

The duty cycle from (4.60) does not consider the inner voltage demand of the boost converter, in particular of its filter inductor L:

$$\begin{aligned} u_{\mathrm{L}}(t) &= L\frac{\mathrm{d}}{\mathrm{d}t}i'(t) = L\frac{\mathrm{d}}{\mathrm{d}t}\left(\hat{i}_1|\sin(\omega t)|\right) \\ &= \hat{i}_1\omega L\cos(\omega t)\mathrm{sgn}(\sin(\omega t)). \end{aligned} \tag{4.61}$$

Within one switching period of the boost converter the voltage balance must hold:

$$\begin{aligned} & u'(t) = u_{\mathrm{L}}(t) + U_2(1-d(t)) \\ \Leftrightarrow \quad & \hat{u}_1|\sin(\omega t)| = \hat{i}_1\omega L\cos(\omega t)\mathrm{sgn}(\sin(\omega t)) + M\hat{u}_1(1-d(t)). \end{aligned} \tag{4.62}$$

Rearranging towards the duty cycle $d(t)$ yields

$$d(t) = 1 - \frac{1}{M}|\sin(\omega t)| + \frac{\hat{i}_1\omega L}{M\hat{u}_1}\cos(\omega t)\mathrm{sgn}(\sin(\omega t)). \tag{4.63}$$

PFC rectifier with boost converter (cont.)

Evaluating (4.63) for $\omega t = \varepsilon$ with $\varepsilon \in \mathbb{R} > 0$ being an infinitesimally small value, one obtains

$$d(\varepsilon/\omega) = 1 - \sin(\varepsilon) + \frac{\hat{i}_1 \omega L}{M \hat{u}_1} \cos(\varepsilon) \mathrm{sgn}(\sin(\varepsilon)) \approx 1 + \frac{\hat{i}_1 \omega L}{M \hat{u}_1} > 1.$$

Hence, the additional voltage demand of the boost converter inductor L leads to a duty cycle exceeding unity, that is, exceeding the feasible range and, therefore, the boost converter is not able to deliver the required voltage transfer ratio $m(t)$:

- The boost converter is not able to exactly track the input current reference $i_1(t) = \hat{i}_1 \sin(\omega t)$ (especially at the beginning and end of a half period).
- The lower L the less the negative impact of the inductor voltage demand.
- Consequently, one wants to keep the inductance L as low as possible which on the other hand requires a high switching frequency f_s to keep the current ripple within acceptable bounds.

Pulse width modulation (PWM)

As seen on the previous slides, the duty cycle $d(t)$ is a function of time. To generate a switching signal $s(t)$ for the boost converter, a pulse width modulation (PWM) scheme is used:

$$s(t) = \begin{cases} 1 & \text{(transistor } T \text{ on)}, \quad \text{if } d(t) > c(t), \\ 0 & \text{(transistor } T \text{ off)}, \quad \text{otherwise} \end{cases} \tag{4.64}$$

with a (high frequency) carrier signal $c(t)$, e.g., a triangular or sawtooth signal.

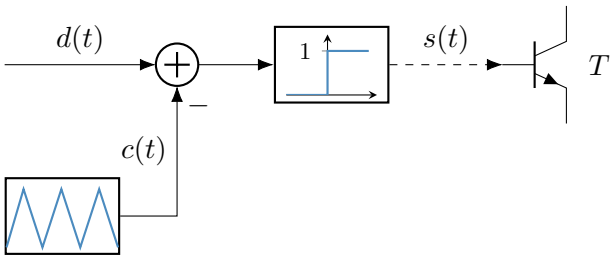

Fig. 4.25: Pulse width modulation with triangular carrier to actuate a transistor

PWM-based switching signals

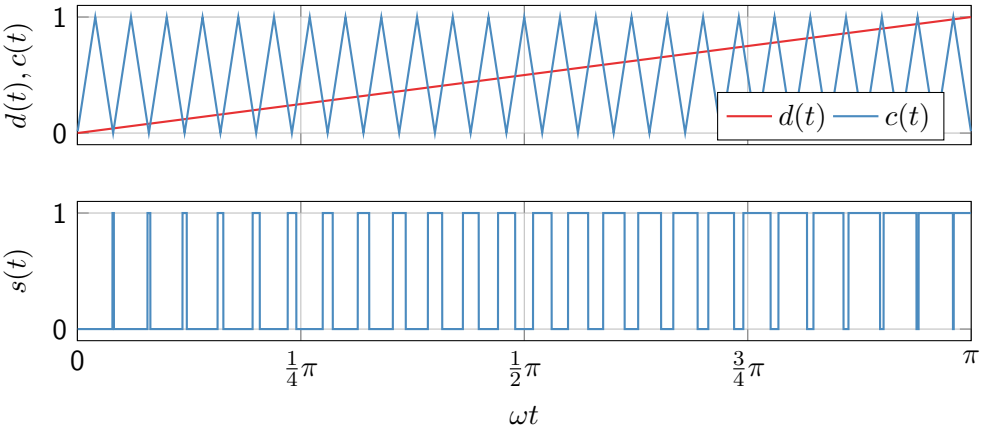

Fig. 4.26: Qualitative illustration of a PWM-based switching signal with a triangular carrier signal

PWM-based switching signals (cont.)

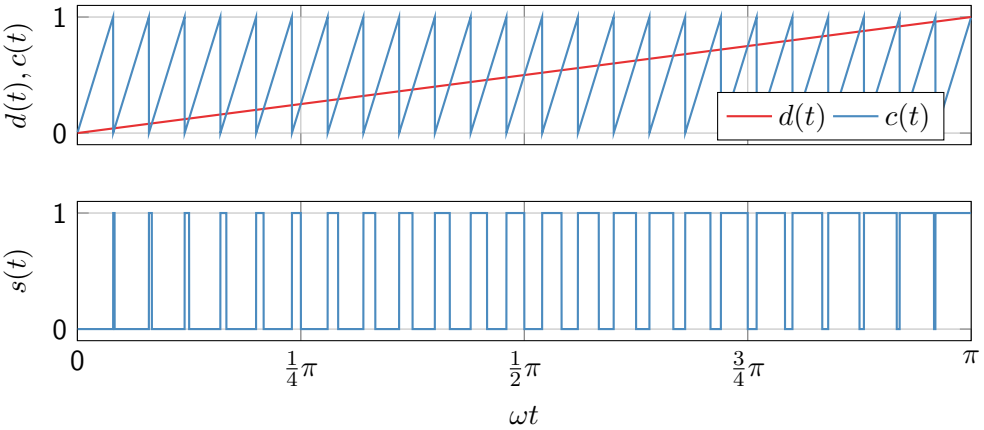

Fig. 4.27: Qualitative illustration of a PWM-based switching signal with a sawtooth carrier signal

PWM-based open-loop control of the boost converter PFC rectifier

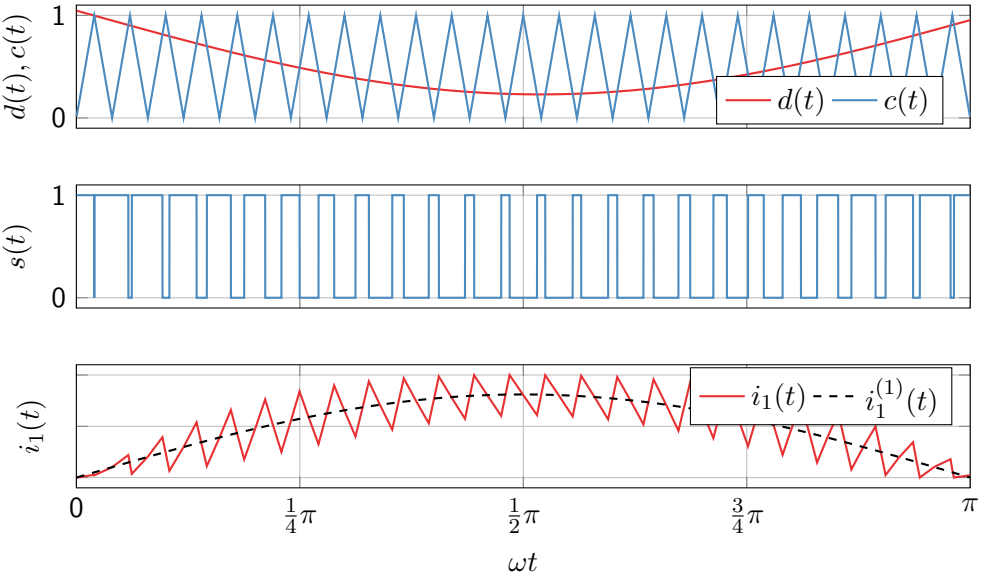

PWM-based PFC rectifier current ripple

Due to the switching behavior of the boost converter, the input current $i_1(t)$ exhibits a current ripple. The boost inductor voltage during a switching period is:

$$u_{\mathrm{L}}(t) = \begin{cases} \hat{u}_1 \sin(\omega t), & 0 < t \leq dT_{\mathrm{s}} \\ \hat{u}_1 \sin(\omega t) - U_2, & dT_{\mathrm{s}} < t \leq T_{\mathrm{s}}. \end{cases} \tag{4.65}$$

We assume that

$$T_{\mathrm{s}} << {}^{2\pi}/_{\omega}$$

such that the input voltage and duty cycle are approximately constant within one switching period.The ripple current envelope $\Delta i_1(t)$ is then defined as the moving difference between the actual input current $i_1(t)$ and its fundamental component $i_1^{(1)}(t)$:

$$\Delta i_1(t) = \pm\frac{1}{2} \max_{\tau \in [t \pm \frac{T_{\mathrm{s}}}{2}]} |i_1(\tau) - i_1^{(1)}(\tau)|. \tag{4.66}$$

One should note that this ripple definition is different from the one used in the previous DC/DC converter section.

PWM-based PFC rectifier current ripple (cont.)

Assuming CCM operation and a sufficiently small switching time interval T_s, the ripple current can be approximated by the current rise during the on-time of the boost converter:

$$\begin{aligned}\Delta i_1(t) &= \pm\frac{1}{2L}\int_0^{dT_\mathrm{s}} u_\mathrm{L}(\tau)\mathrm{d}\tau = \pm\frac{1}{2L}\int_0^{dT_\mathrm{s}} \hat{u}_1\sin(\omega t)\mathrm{d}\tau \\ &\approx \pm\frac{\hat{u}_1\sin(\omega t)}{2L}\int_0^{dT_\mathrm{s}} 1\mathrm{d}\tau = \pm\frac{\hat{u}_1\sin(\omega t)}{2L}dT_\mathrm{s}.\end{aligned} \tag{4.67}$$

Inserting $d(t)$ from (4.63) in a quasi steady-state fashion yields

$$\Delta i_1(t) = \pm\frac{\hat{u}_1 T_\mathrm{s}\sin(\omega t)}{2L}\left(1 - \frac{1}{M}|\sin(\omega t)| + \frac{\hat{i}_1\omega L}{M\hat{u}_1}\cos(\omega t)\mathrm{sgn}(\sin(\omega t))\right). \tag{4.68}$$

Due to the varying input voltage and duty cycle, the ripple current is not constant but also varies with time (cf. next slide).

PWM-based PFC rectifier current ripple (cont.)

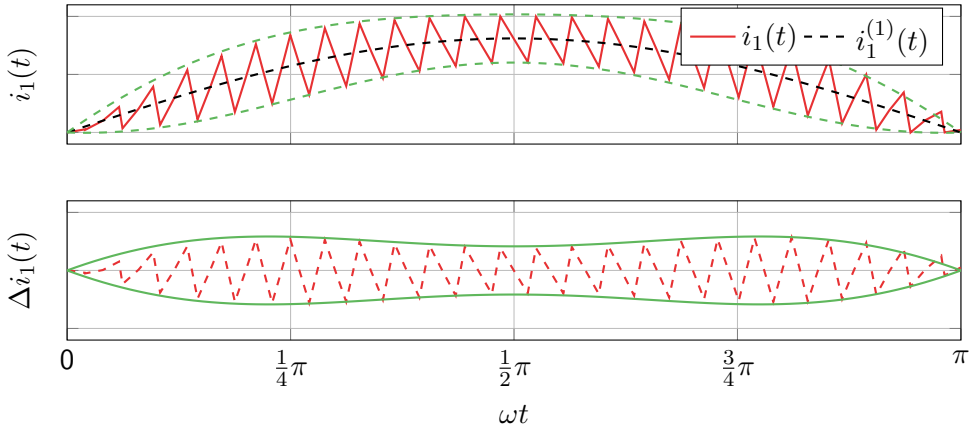

PFC rectifier with boost converter: closed-loop control structure

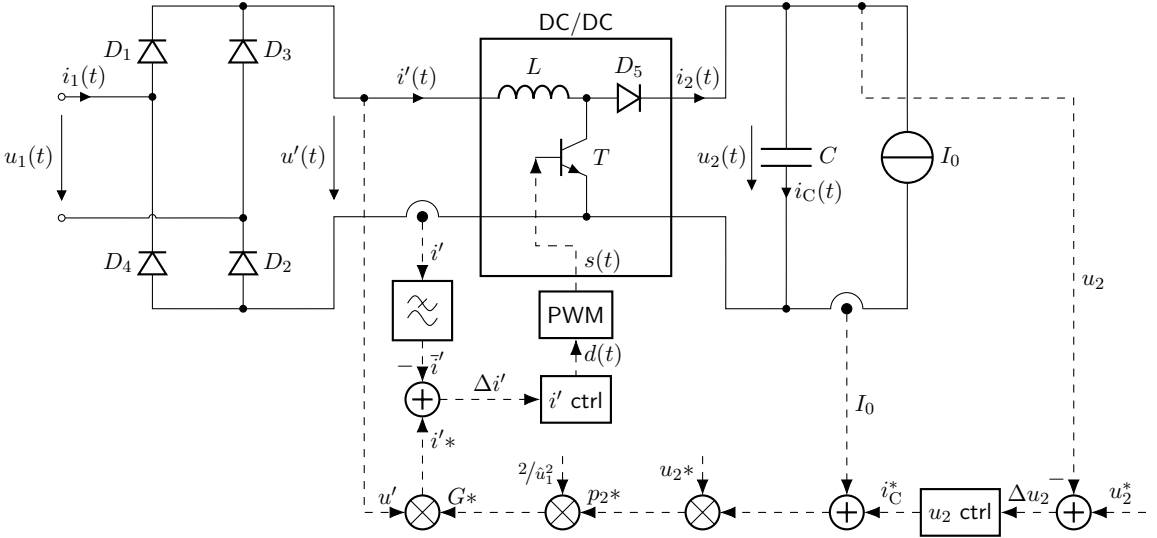

Fig. 4.28: Control structure of PFC rectifier with boost DC/DC converter

PFC rectifier with boost converter: closed-loop control structure (cont.)

Reasons for closed-loop control:

- Mismatches between the actual system and the plant model behavior result in (steady-state) control errors.
- Faster transient response to load changes.
- Robustness against further disturbances (e.g., input voltage variations).

Central idea of the closed-loop control: given some required load power

$$p_2(t) = u_2(t) i_2(t) = u_2(t) \left(I_0 + i_{\mathrm{C}}(t) \right)$$

operate the boost converter such that the load power is represented by a (virtual) conductance at the input of the boost converter:

$$g(t) = \frac{p_1(t)}{\hat{u}_1^2} = \frac{p_2(t)}{\hat{u}_1^2} = \frac{U_2 \left(I_0 + i_{\mathrm{C}}(t) \right)}{\hat{u}_1^2}.$$

PFC rectifier with boost converter: closed-loop control structure (cont.)

The required conductance $g(t)$ is calculated by the outer voltage controller:

- If $u_2(t) < U_2^*$: increase $p_2(t)$ by increasing the conductance $g(t)$.
- If $u_2(t) > U_2^*$: decrease $p_2(t)$ by decreasing the conductance $g(t)$.

With

$$\hat{i}'(t) = \hat{u}_1 g(t)$$

the required reference input current for the inner current controller can be calculated.

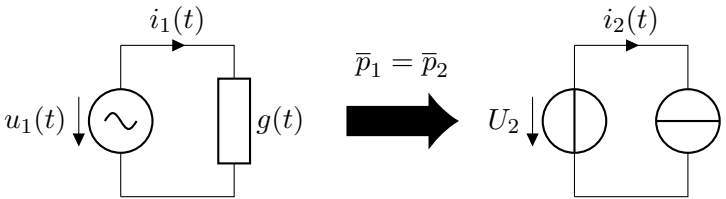

Fig. 4.29: Interpretation of the closed-loop control of a PFC rectifier as a variable conductance tuning

PFC rectifier with boost converter: capacitor sizing

Based on the previous assumption $u_2(t) \approx U_2$ the question is raised how the output capacitor C of the boost converter must be sized to keep the output voltage ripple within acceptable bounds justifying the assumption. For a lossless converter, the instantaneous power is:

$$p_2(t) = p_1(t) = u_1(t) i_1(t).$$

Assuming that the input voltage and current are both ideally sinusoidal and in phase (i.e., the PFC rectifier operates perfectly), the instantaneous power is:

$$p_2(t) = \hat{u}_1 \hat{i}_1 \sin(\omega t) \sin(\omega t) = \frac{\hat{u}_1 \hat{i}_1}{2} \left(1 - \cos(2\omega t)\right). \tag{4.69}$$

Hence, we can decompose the instantaneous power into a constant term and a harmonic term with twice the frequency of the input voltage/current:

$$p_2(t) = \underbrace{\frac{\hat{u}_1 \hat{i}_1}{2}}_{\overline{p}_2} \underbrace{- \frac{\hat{u}_1 \hat{i}_1}{2} \cos(2\omega t)}_{p_2^{(\mathrm{h})}(t)}. \tag{4.70}$$

PFC rectifier with boost converter: capacitor sizing (cont.)

The resulting harmonic output current component is (approximately)

$$i_2^{(\mathrm{h})}(t) \approx \frac{p_2^{(\mathrm{h})}(t)}{\overline{u}_2} = -\frac{\hat{u}_1 \hat{i}_1}{2\overline{u}_2}\cos(2\omega t) = -\frac{\overline{p}_2}{\overline{u}_2}\cos(2\omega t). \tag{4.71}$$

If the load current I_0 is (approximately) constant, the harmonic current is entirely flowing into the output capacitor $i_2^{(\mathrm{h})}(t) = i_\mathrm{C}(t)$ leading to the voltage ripple:

$$\Delta u_2(t) = \frac{1}{C}\int i_\mathrm{C}(t)\mathrm{d}t = -\underbrace{\frac{\overline{p}_2}{\overline{u}_2}\frac{1}{2\omega C}}_{\Delta\hat{u}_2}\sin(2\omega t). \tag{4.72}$$

To limit the output voltage ripple to a certain amplitude value $\Delta\hat{u}_2$, the output capacitor C must exhibit a minimal capacitance value:

$$C > \frac{\overline{p}_2}{\overline{u}_2}\frac{1}{2\omega\Delta\hat{u}_2}. \tag{4.73}$$

PFC rectifier with boost converter: capacitor sizing (cont.)

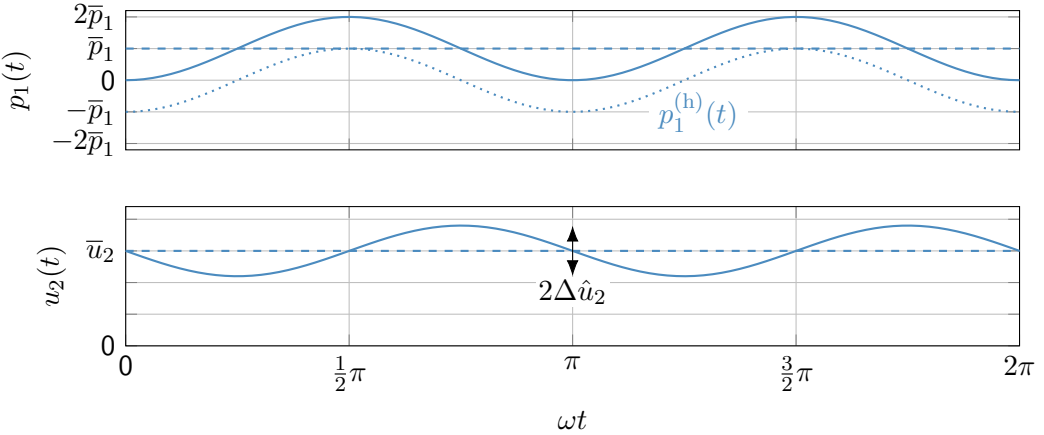

Fig. 4.30: Power and voltage oscillations in the PFC rectifier in quasi steady-state operation

Table of contents

M3U uncontrolled rectifier circuit

The M3U rectifier addresses three-phase systems and typically utilizes an input transformer to mitigate offset phase currents and further harmonics (compare Fig. 4.5). To simplify things, we assume that the input transformer delivers an ideal three-phase voltage source:

$$u_{1\mathrm{a}}(t) = \hat{u}_1 \sin(\omega t), \quad u_{1\mathrm{b}}(t) = \hat{u}_1 \sin(\omega t - 2\pi/3), \quad u_{1\mathrm{c}}(t) = \hat{u}_1 \sin(\omega t + 2\pi/3).$$

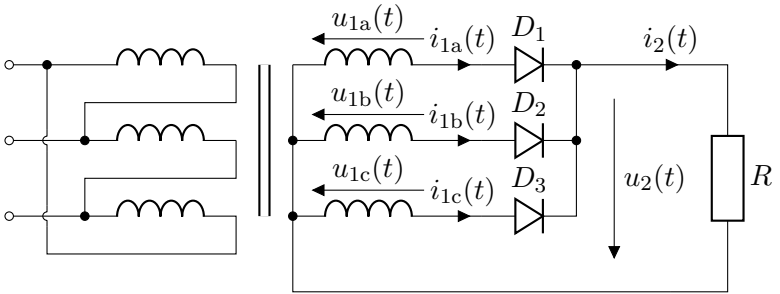

Fig. 4.31: M3U topology (aka three-pulse mid-point rectifier) with an input three-phase transformer and a resistive load

M3U rectifier resistive load operation

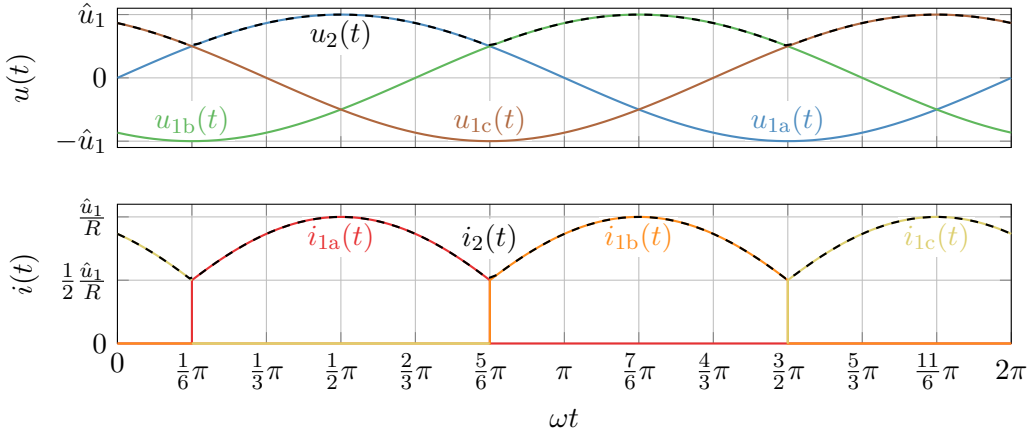

Fig. 4.32: M3U characteristic voltage and current curves for a resistive load

M3U rectifier resistive load operation: average output voltage

With a resistive load, the M3U rectifier's output is always determined by the transformer phase with the highest voltage:

$$u_2(t) = \max\left\{u_{1\mathrm{a}}(t), u_{1\mathrm{b}}(t), u_{1\mathrm{c}}(t)\right\}. \tag{4.74}$$

- Assume $u_{1\mathrm{a}}(t)$ has the highest voltage for some time t.
- Hence, there is a negative voltage difference between the phases b-a and c-a.
- These can be only compensated by the diodes D_2 and D_3, which are in blocking mode while D_1 is conducting.

The average output voltage can be found by evaluating the conduction interval of one phase, e.g., $u_{1\mathrm{a}}(t)$:

$$\bar{u}_2 = \frac{3}{2\pi}\int_{\frac{1}{6}\pi}^{\frac{5}{6}\pi} \hat{u}_1 \sin(\omega t)\mathrm{d}\omega t = \frac{3}{2\pi}\left[-\hat{u}_1\cos(\omega t)\right]_{\frac{1}{6}\pi}^{\frac{5}{6}\pi} = \frac{3}{2\pi}\hat{u}_1 2\frac{\sqrt{3}}{2} = \frac{3\sqrt{3}}{2\pi}\hat{u}_1. \tag{4.75}$$

M3U rectifier with output filter

To filter both the output voltage and current, an output filter can be added to the M3U rectifier circuit (Fig. 4.33). The filter consists of a series inductor L and a capacitor C in parallel. In steady state

$$\overline{u}_{\mathrm{C}} = \overline{u}_2 = \frac{3\sqrt{3}}{2\pi}\hat{u}_1 \tag{4.76}$$

holds as the average inductor voltage must be zero to prevent a current run away.

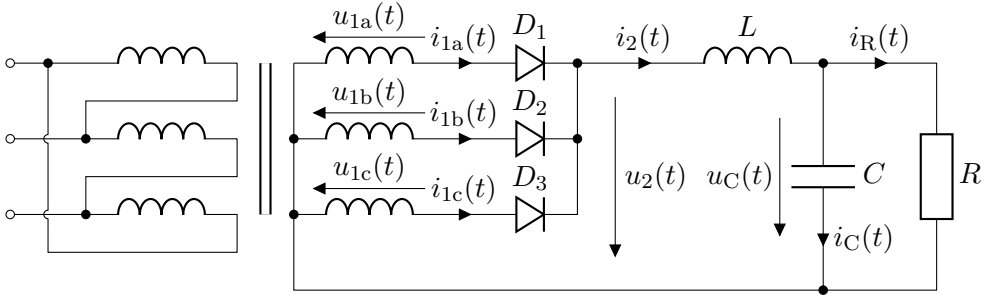

Fig. 4.33: M3U topology with an input three-phase transformer, a resistive load and output filter

M3U rectifier with output filter (cont.)

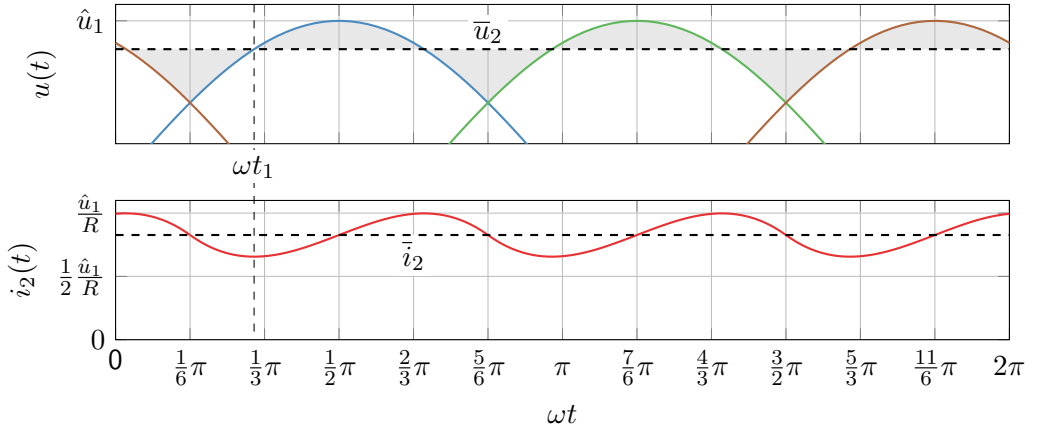

Fig. 4.34: M3U characteristic voltage and current curves considering an idealized output filter with $u_\mathrm{C}(t) = \overline{u}_2 = \text{const.}$

M3U rectifier with output filter (cont.)

From Fig. 4.34 one can observe that

$$u_2(t) = u_{1a}(t) = \hat{u}_1 \sin(\omega t), \quad \omega t \in \left[\frac{1}{6}\pi, \frac{5}{6}\pi\right] \tag{4.77}$$

holds. At $\omega t = \omega t_1$ the phase voltage $u_{1a}(t)$ is equal to the average output voltage $\overline{u}_2$:

$$\overline{u}_2 = \frac{3\sqrt{3}}{2\pi}\hat{u}_1 = \hat{u}_1 \sin(\omega t_1) \quad \Leftrightarrow \quad \omega t_1 = \arcsin\left(\frac{3\sqrt{3}}{2\pi}\right). \tag{4.78}$$

Based on this, the current $i_2(t)$ can be calculated as

$$\begin{aligned} i_2(t) &= i_2(\omega t_1) + \frac{1}{\omega L}\int_{\omega t_1}^{\omega t} (u_2(\omega\tau) - \overline{u}_2)\,\mathrm{d}\omega\tau \\ &= i_2(\omega t_1) + \frac{1}{\omega L}\int_{\omega t_1}^{\omega t} (\hat{u}_1 \sin(\omega\tau) - \hat{u}_1 \sin(\omega t_1))\,\mathrm{d}\omega\tau, \quad \omega t \in \left[\frac{1}{6}\pi, \frac{5}{6}\pi\right] \end{aligned} \tag{4.79}$$

with $i_2(\omega t_1)$ being the initial (yet unknown) current at ωt_1.

M3U rectifier with output filter (cont.)

Solving the integral in (4.79) yields

$$\begin{aligned} i_2(t) &= i_2(\omega t_1) + \frac{\hat{u}_1}{\omega L}\left[-\cos(\omega\tau) - \omega\tau\sin(\omega t_1)\right]_{\omega t_1}^{\omega t} \\ &= i_2(\omega t_1) + \frac{\hat{u}_1}{\omega L}\left[-\cos(\omega t) + \cos(\omega t_1) - \sin(\omega t_1)\,(\omega t - \omega t_1)\right]. \end{aligned} \tag{4.80}$$

To determine the initial current $i_2(\omega t_1)$, one can utilize the fact that the average inductor current must be identical to the average load current since otherwise the output capacitor would be charged or discharged indefinitely:

$$\bar{i}_2 \stackrel{!}{=} \bar{i}_\mathrm{R} = \frac{\overline{u}_2}{R} = \frac{\hat{u}_1\sin(\omega t_1)}{R}. \tag{4.81}$$

M3U rectifier with output filter (cont.)

The average inductor current can be calculated as

$$\begin{aligned}\bar{i}_2 &= \frac{3}{2\pi}\int_{\frac{1}{6}\pi}^{\frac{5}{6}\pi} i_2(\omega\tau)\mathrm{d}\omega\tau = \frac{3}{2\pi}\int_{\frac{1}{6}\pi}^{\frac{5}{6}\pi} i_2(\omega t_1)\mathrm{d}\omega\tau \\ &+ \frac{3}{2\pi}\int_{\frac{1}{6}\pi}^{\frac{5}{6}\pi} \frac{\hat{u}_1}{\omega L}\left[-\cos(\omega\tau)+\cos(\omega t_1)-\sin(\omega t_1)\left(\omega\tau-\omega t_1\right)\right]\mathrm{d}\omega\tau \\ &= \dots \\ &= i_2(\omega t_1) + \frac{\hat{u}_1}{\omega L}\left[\cos(\omega t_1)+\sin(\omega t_1)(\omega t_1-\frac{\pi}{2})\right].\end{aligned} \tag{4.82}$$

Inserting into (4.81) and solving for $i_2(\omega t_1)$ yields

$$i_2(\omega t_1) = \frac{\hat{u}_1}{R}\sin(\omega t_1) - \frac{\hat{u}_1}{\omega L}\left[\cos(\omega t_1)+\sin(\omega t_1)(\omega t_1-\frac{\pi}{2})\right]. \tag{4.83}$$

With this result, the current $i_2(t)$ can be calculated using (4.80).

M3U rectifier with output filter: CCM vs. DCM

The previous analysis only holds for CCM as otherwise all diodes would be blocking simultaneously. From (4.80) one can find that the minimum current $i_2(t)$ is reached when $\omega t = \omega t_1$, i.e.,

$$\min\{i_2(t)\} = i_2(\omega t_1) = \frac{\hat{u}_1}{R}\sin(\omega t_1) - \frac{\hat{u}_1}{\omega L}\left[\cos(\omega t_1) + \sin(\omega t_1)(\omega t_1 - \frac{\pi}{2})\right]. \tag{4.84}$$

The boundary between CCM and DCM can be found by setting $\min\{i_2(t)\} = 0$ leading to $i_2(\omega t_1) = 0$. In this boundary case, the average output current is

$$\begin{aligned} \bar{i}_2 &= \frac{\hat{u}_1}{\omega L}\left[\cos(\omega t_1) + \sin(\omega t_1)(\omega t_1 - \frac{\pi}{2})\right] \\ &= \frac{\overline{u}_2}{\omega L}\left[\tan(\omega t_1) + \omega t_1 - \frac{\pi}{2}\right]. \end{aligned} \tag{4.85}$$

One can also reinterpret this result for designing the filter inductor L to ensure CCM operation:

$$L \geq \frac{\overline{u}_2}{\omega \bar{i}_2}\left[\tan(\omega t_1) + \omega t_1 - \frac{\pi}{2}\right]. \tag{4.86}$$

Table of contents

B6U uncontrolled rectifier circuit

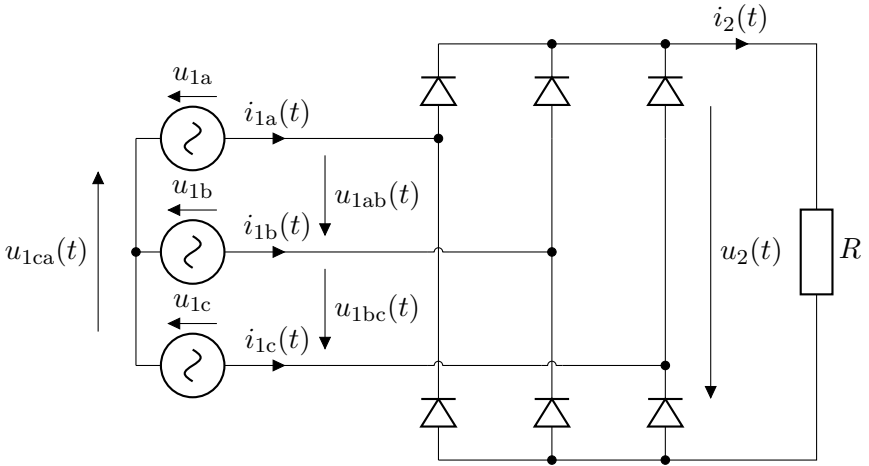

Fig. 4.35: B6U topology (aka six-pulse bridge rectifier) with resistive load

B6U rectifier resistive load operation

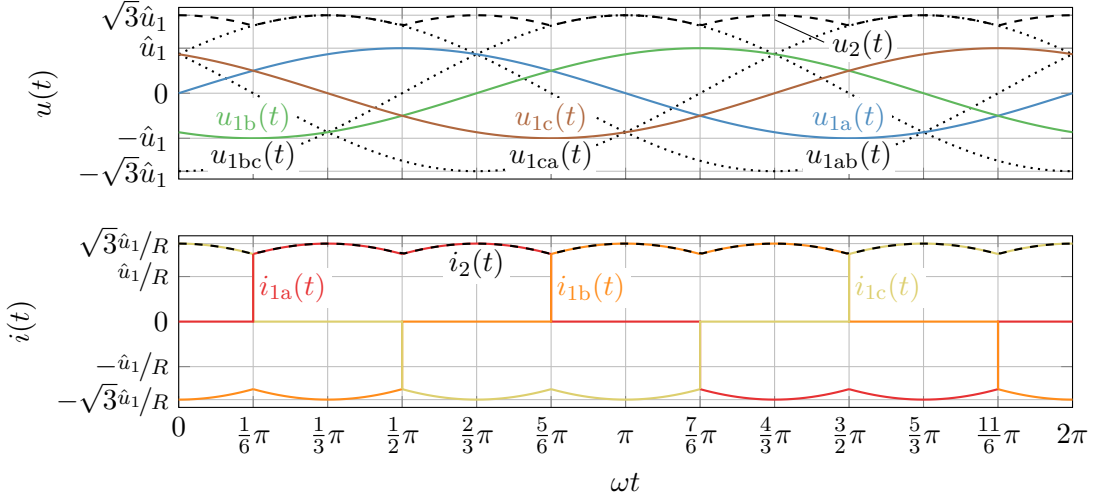

Fig. 4.36: B6U characteristic voltage and current curves for a resistive load

B6U rectifier resistive load operation (cont.)

In the B6U bridge with a resistive load the upper output potential is determined by the highest phase voltage while the lower output potential is determined by the lowest phase voltage. The output voltage $u_2(t)$ is given by

$$u_2(t) = \max\{u_{1a}(t), u_{1b}(t), u_{1c}(t)\} - \min\{u_{1a}(t), u_{1b}(t), u_{1c}(t)\}. \tag{4.87}$$

Alternatively, we can evaluate the line-to-line voltages

$$\begin{aligned} u_{1ab}(t) &= u_{1a}(t) - u_{1b}(t) & u_{1bc}(t) &= u_{1b}(t) - u_{1c}(t) & u_{1ca}(t) &= u_{1c}(t) - u_{1a}(t) \\ &= \sqrt{3}\hat{u}_1 \sin(\omega t + \frac{1}{6}\pi), & &= \sqrt{3}\hat{u}_1 \sin(\omega t - \frac{1}{2}\pi), & &= \sqrt{3}\hat{u}_1 \sin(\omega t + \frac{5}{6}\pi) \end{aligned}$$

and find that the B6U output voltage is given by

$$u_2(t) = \max\{u_{1ab}(t), u_{1bc}(t), u_{1ca}(t)\}. \tag{4.88}$$

B6U rectifier resistive load operation (cont.)

The average output voltage $\overline{u}_2$ is given by

$$\begin{aligned}\overline{u}_2 =& \frac{3}{\pi}\int_{\frac{1}{6}\pi}^{\frac{1}{2}\pi} u_{1\mathrm{ab}}(\omega t)\mathrm{d}\omega t = \frac{3}{\pi}\int_{\frac{1}{6}\pi}^{\frac{1}{2}\pi} \sqrt{3}\hat{u}_1 \sin(\omega t + \frac{1}{6}\pi)\mathrm{d}\omega t \\ =& \frac{3\sqrt{3}}{\pi}\hat{u}_1 \left[-\cos(\omega t + \frac{1}{6}\pi)\right]_{\frac{1}{6}\pi}^{\frac{1}{2}\pi} = \frac{3\sqrt{3}}{\pi}\hat{u}_1.\end{aligned} \tag{4.89}$$

Compared to the M3U rectifier average voltage from (4.75), the B6U average output voltage is doubled – this is an analogous finding to the single phase case where the B2U rectifier has a doubled average output voltage compared to the M2U rectifier.

Impact of further filter elements

The impact of filters elements, e.g., the line impedance from Fig. 4.13 or an LC output filter as in Fig. 4.33, can be analyzed in a similar manner for the B6U rectifier. While such filter elements are common in practice, they are not explicitly treated for the B6U rectifier in the following due to time constraints.

Table of contents

12-pulse rectifier: B6U-2S topology

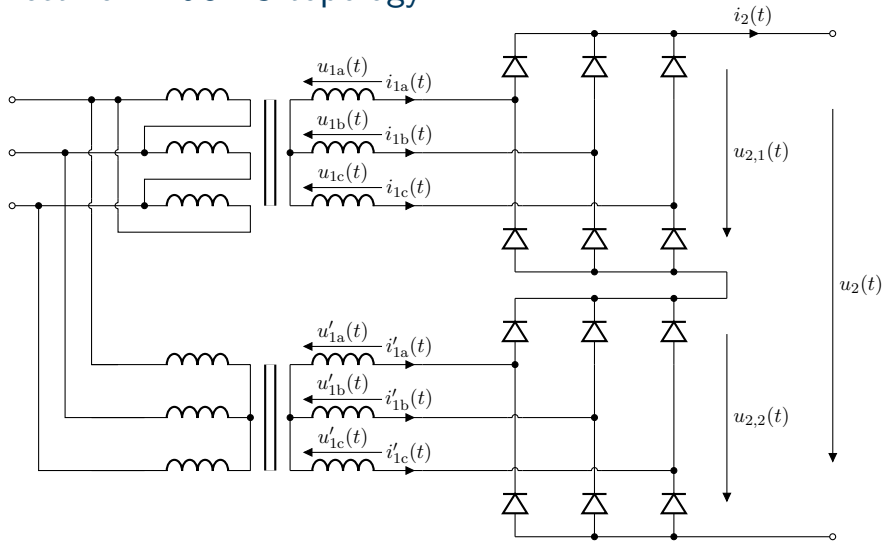

Fig. 4.37: 12-pulse recitifier with B6U-2S topology: two B6U rectifiers connected in series

12-pulse rectifier: B6U-2S topology (cont.)

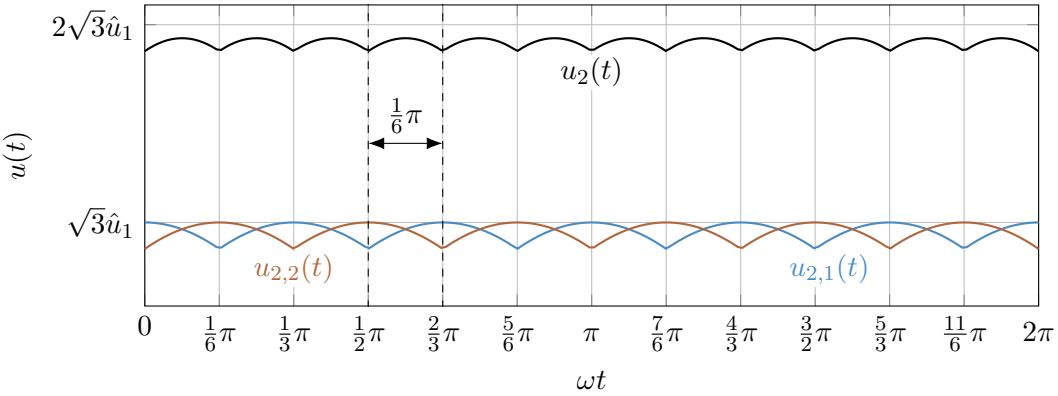

Fig. 4.38: B6U-2S output voltage characteristic: voltage output ripple is reduced by shifting the phase of the second rectifier by $1/6 \cdot \pi$ utilizing different transformer winding schemes at the input

12-pulse rectifier: B6U-2P topology

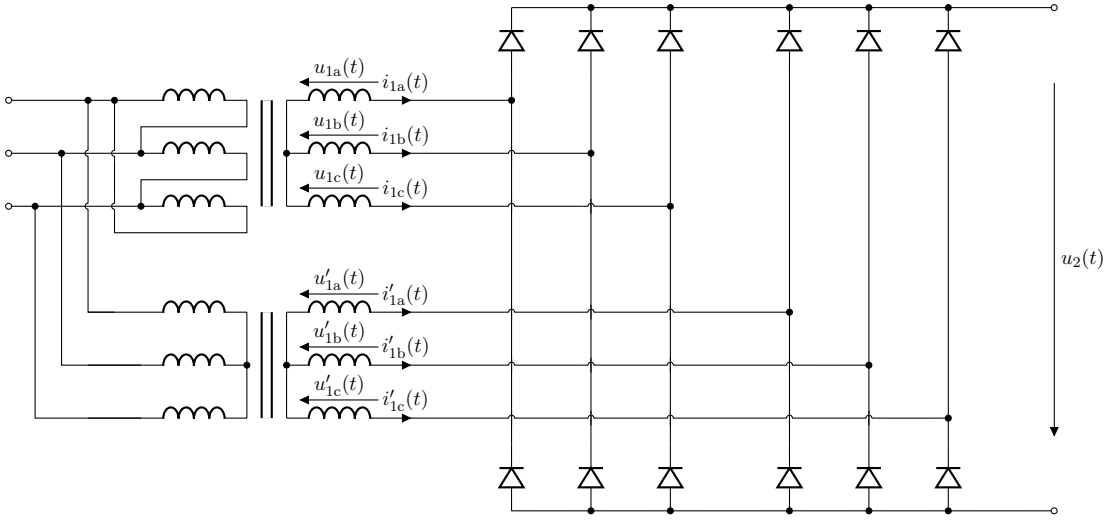

Fig. 4.39: 12-pulse recitifier with B6U-2P topology: two B6U rectifiers connected in parallel

12-pulse rectifier: B6U-2P topology (cont.)

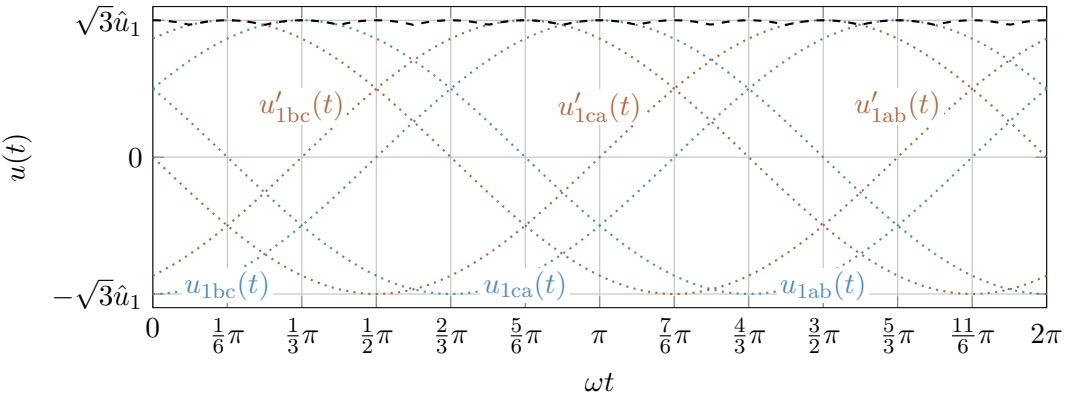

Fig. 4.40: B6U-2P output voltage characteristic: simplified representation as displacement currents between the transformers are not taken into account

Comparison of output voltage ripple characteristics

From the previous analyses of the considered three-phase rectifiers one can find

$$\Delta u_2 = \max\{u_2(t)\} - \min\{u_2(t)\} = \left(1 - \cos\left(\frac{\pi}{p}\right)\right)\hat{u}_2 \tag{4.90}$$

with p being the number of pulses. For the considered rectifiers, the output voltage is given by

$$\hat{u}_2 = \begin{cases} \hat{u}_1, & \text{for M3U,} \\ \sqrt{3}\hat{u}_1, & \text{for B6U and B6U-2P,} \end{cases} \quad \text{and} \quad \overline{u}_2 = \begin{cases} \frac{3\sqrt{3}}{2\pi}\hat{u}_1, & \text{for M3U,} \\ \frac{3\sqrt{3}}{\pi}\hat{u}_1, & \text{for B6U and B6U-2P} \end{cases}$$

leading to the normalized output voltage ripple being defined as

$$\frac{\Delta u_2}{\overline{u}_2} = \begin{cases} \frac{2\pi}{3\sqrt{3}}\left(1 - \cos\left(\frac{\pi}{3}\right)\right) = 60.46\,\%, & \text{for M3U,} \\ \frac{\pi}{3}\left(1 - \cos\left(\frac{\pi}{6}\right)\right) = 14.03\,\%, & \text{for B6U,} \\ \frac{\pi}{3}\left(1 - \cos\left(\frac{\pi}{12}\right)\right) = 3.57\,\%, & \text{for B6U-2P.} \end{cases} \tag{4.91}$$

Takeaway: the higher the recitifier's pulse number, the lower the output voltage ripple, that is, there is a trade-off between the number of semiconductors and the filter effort.

Section summary

This section provided an introduction to diode-based rectifiers. Not considering the active PFC extension, those are also coined passive rectifiers. The key takeaways are:

- All considered rectifiers operate exclusively unidirectional.
- There is a complex interaction between semiconductor effort and filter effort to provide a DC voltage with a certain signal quality.
- Without active PFC, any diode-based rectifier will introduce significant distortions at the primary side due to harmonics and phase shifts between input voltage and current.
- Active PFC can be used to provide a near-unity power factor, which is required in many applications due to industrial / legal regulations.

In addition, there are further topologies that are not covered in this course, such as

- M6U rectifier,
- very high pulse number rectifiers (e.g., 18 or 24-pulse rectifiers) requiring more complex transformer winding schemes to achieve the desired phase shift on the secondary side,
- three-phase rectifiers with an integrated PFC stage (e.g., Vienna rectifier).

Table of contents

Thyristor: an externally switchable power electronic component

- Can block voltage in both directions (when off)
  - Different to diode (only blocks reverse voltage)
- Can conduct current in only one direction (when on)
  - Identical to diode
- Turn-on: via gate signal
- Turn off: via current drop below holding current (i.e., depends on load characteristics and input voltage)

Application area

While transistors are used for high-frequency converters due to their favorable turn-on/off characteristics and have replaced thyristors in many cases, the latter are still used in low switching frequency applications (mostly energy grid) due to their favorable high voltage / current ratings.

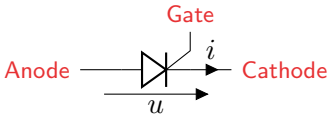

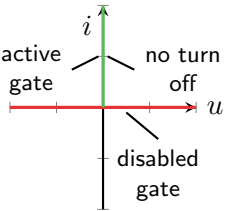

Fig. 5.1: Idealized thyristor characteristics and circuit symbol

Thyristor examples

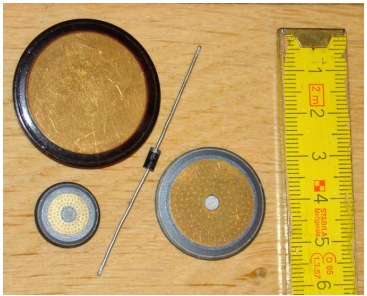

(a) Top left: $1000\,\mathrm{V}/200\,\mathrm{A}$ (diode); bottom left: $1500\,\mathrm{V}/20\,\mathrm{A}$; right: $1500\,\mathrm{V}/120\,\mathrm{A}$; 1N4007 (diode) (source: Wikimedia Commons, CC0 1.0)

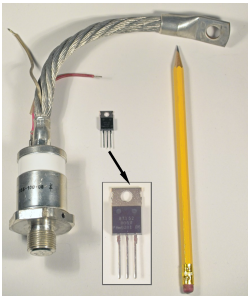

(b) Left: $800\,\mathrm{V}/100\,\mathrm{A}$; right: $800\,\mathrm{V}/13\,\mathrm{A}$ (source: Wikimedia Commons, Julo, CC0 BY-SA 3.0)

Fig. 5.2: Thyristor examples with different voltage and current ratings

M1 rectifier comparison

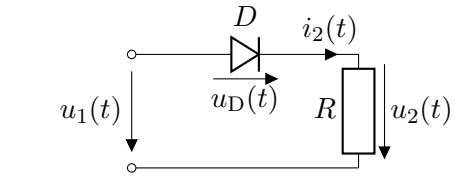

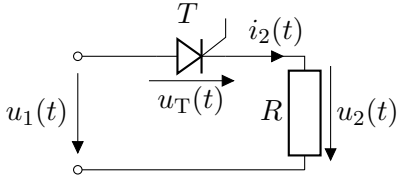

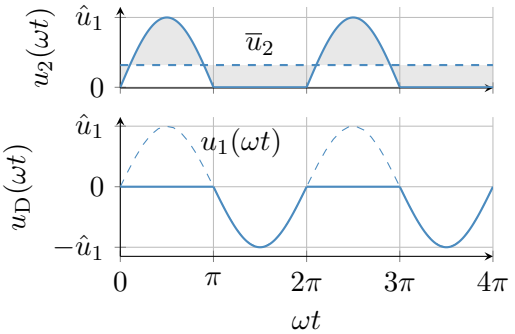

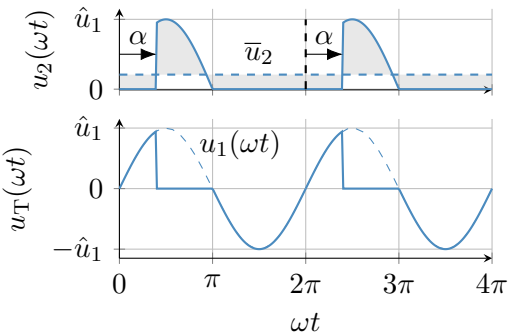

M1C rectifier

The average output voltage of the M1C circuit, i.e., the M1 rectifier with a thyristor, for a resistive load is given by

$$\overline{u}_2 = \frac{1}{2\pi}\int_{\alpha}^{\pi} \hat{u}_1 \sin(\omega t)\mathrm{d}\omega t = \frac{\hat{u}_1}{2\pi}\left[-\cos(\omega t)\right]_{\alpha}^{\pi} = \frac{\hat{u}_1}{2\pi}\left(1+\cos(\alpha)\right). \tag{5.1}$$

Here, α denotes the phase angle at which the thyristor is triggered (aka firing angle). In the M1C case, the feasible range for α is $[0, \pi]$ as the thyristor requires a positive forward voltage to start conducting, that is, if $u_\mathrm{T} < 0$ a firing impulse would not change its conduction state. The RMS value of the output voltage is given by

$$U_2 = \sqrt{\frac{1}{2\pi}\int_{\alpha}^{\pi} \hat{u}_1^2 \sin^2(\omega t)\mathrm{d}\omega t} = \ldots = \frac{\hat{u}_1}{2}\sqrt{\frac{\pi - \alpha + \sin(\alpha)\cos(\alpha)}{\pi}}. \tag{5.2}$$

In contrast to the M1U rectifier from (4.3), the M1C rectifier allows for controlling the output voltage by adjusting the firing angle α.

M1C rectifier: Fourier series

The Fourier coefficients of the output voltage $u_2(t)$ for the M1C converter are

$$
\begin{aligned}
a^{(0)} &= \frac{1}{\pi}\int_0^{2\pi} u_2(t)\mathrm{d}\omega t = \frac{1}{\pi}\int_\alpha^{\pi} \hat{u}_1 \sin(\omega t)\mathrm{d}\omega t = 2\overline{u}_2 = \frac{\hat{u}_1}{\pi}(1+\cos(\alpha)),\\
a^{(k)} &= \frac{1}{\pi}\int_0^{2\pi} u_2(t)\cos(k\omega t)\mathrm{d}\omega t = \frac{1}{\pi}\int_\alpha^{\pi} \hat{u}_1 \sin(\omega t)\cos(k\omega t)\mathrm{d}\omega t = \ldots\\
&= \begin{cases} \frac{\hat{u}_1}{\pi}\frac{2}{1-k^2}, & k=1\\ \frac{1}{2\pi}\left(\frac{\cos(\alpha(k-1))+\cos(k\pi)}{k-1} - \frac{\cos(\alpha(k+1))+\cos(k\pi)}{k+1}\right), & k\geq 2. \end{cases} \qquad (5.3)\\
b^{(k)} &= \frac{1}{\pi}\int_0^{2\pi} u_2(t)\sin(k\omega t)\mathrm{d}\omega t = \frac{1}{\pi}\int_\alpha^{\pi} \hat{u}_1 \sin(\omega t)\sin(k\omega t)\mathrm{d}\omega t = \ldots\\
&= \begin{cases} \frac{-\alpha+\pi+\cos(\alpha)\sin(\alpha)}{2\pi}, & k=1,\\ \frac{1}{2\pi}\left(\frac{\sin(\alpha(k-1))+\sin(k\pi)}{k-1} - \frac{\sin(\alpha(k+1))+\sin(k\pi)}{k+1}\right), & k\geq 2. \end{cases}
\end{aligned}
$$

In contrast to the M1U rectifier, one can observe additional harmonic components due to additional distortion of the output voltage caused by the thyristor switching.

Table of contents

M2C converter

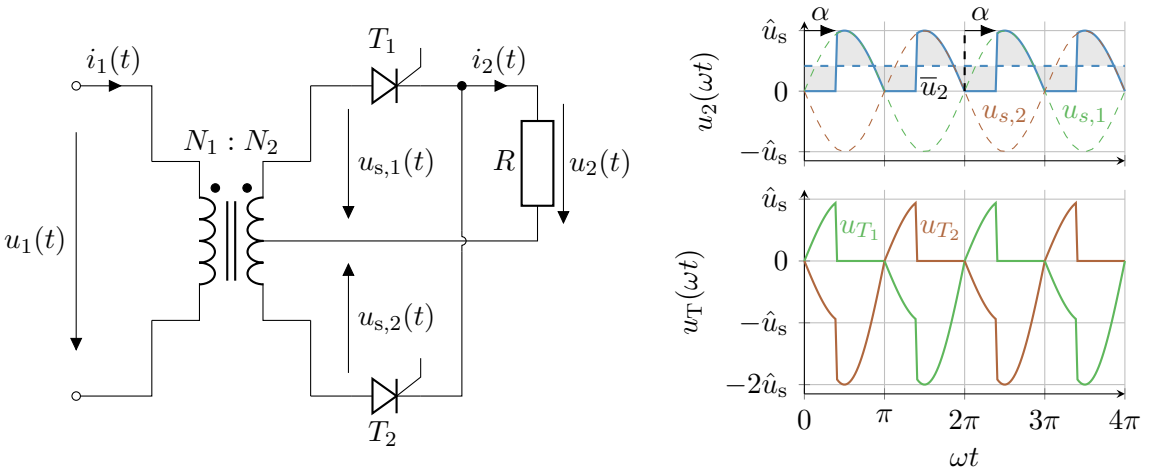

Fig. 5.3: M2C topology (aka two-pulse mid-point converter) with center-tapped transformer and a resistive load

M2C converter: resistive load

The average output voltage of the M2C converter for a resistive load is given by

$$\overline{u}_2 = \frac{1}{\pi}\int_{\alpha}^{\pi} \hat{u}_\mathrm{s}\sin(\omega t)\mathrm{d}\omega t = \frac{\hat{u}_\mathrm{s}}{\pi}\left[-\cos(\omega t)\right]_{\alpha}^{\pi} = \frac{\hat{u}_\mathrm{s}}{\pi}\left(1+\cos(\alpha)\right). \tag{5.4}$$

The RMS value of the output voltage results in

$$U_2 = \sqrt{\frac{1}{\pi}\int_{\alpha}^{\pi} \hat{u}_\mathrm{s}^2\sin^2(\omega t)\mathrm{d}\omega t} = \ldots = \frac{\hat{u}_\mathrm{s}}{\sqrt{2}}\sqrt{\frac{\pi-\alpha+\sin(\alpha)\cos(\alpha)}{\pi}}. \tag{5.5}$$

The primary to secondary voltage ratio of the center-tapped transformer yields

$$\frac{\hat{u}_\mathrm{s}}{\hat{u}_1} = \frac{1}{2}\frac{N_2}{N_1}.$$

It should be noted that in the case of a resistive load, the M2C's output voltage is always positive for the feasible firing angle range $\alpha \in [0, \pi]$.

M2C converter with an output filter

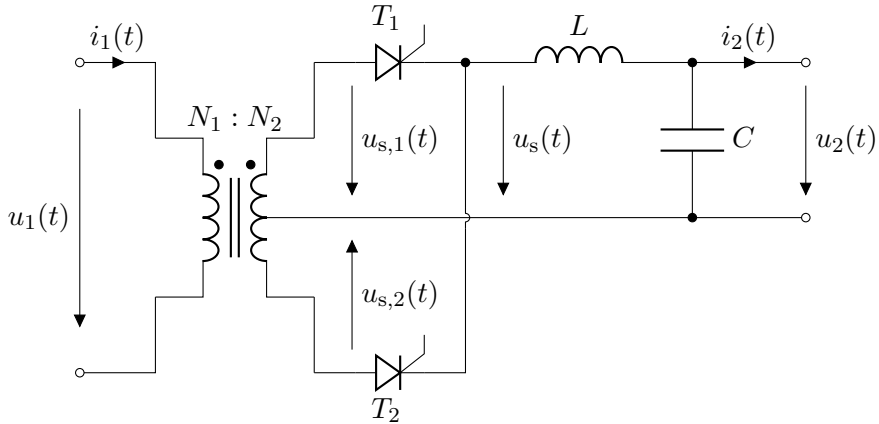

Fig. 5.4: M2C converter with an output filter assuming $u_2(t) = U_2 = \text{const.}$

M2C converter with an output filter (cont.)

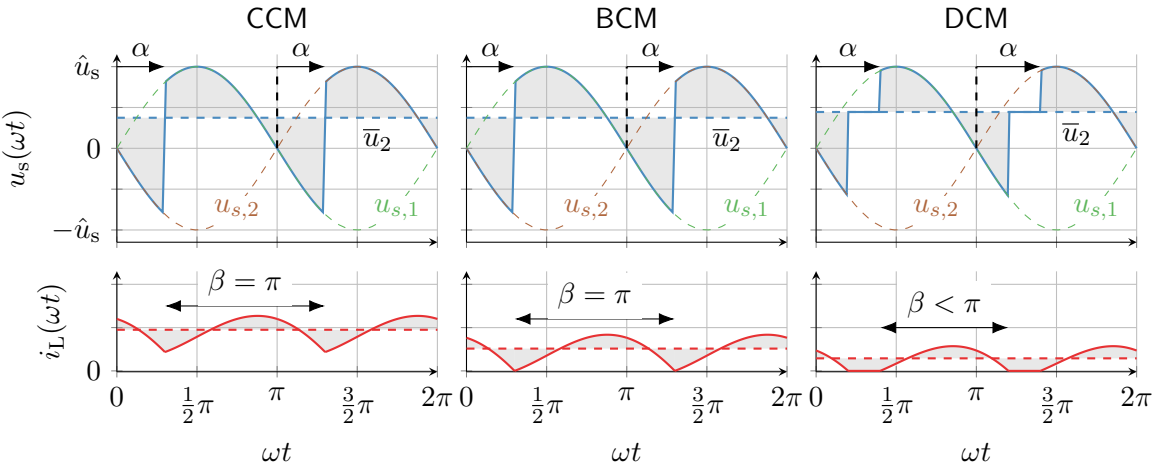

Fig. 5.5: M2C topology with an output filter and different average load currents

M2C converter with an output filter (cont.)

Due to the output filter, the secondary voltage $u_\mathrm{s}(t)$ can become negative since the current flow is maintained by the inductor and, therefore, a thyristor is remaining in the conducting state (until the next thyristor is triggered). The average output voltage in CCM (and BCM) is given by

$$\begin{aligned}\overline{u}_2 &= \frac{1}{\pi}\int_{\alpha}^{\alpha+\pi} \hat{u}_\mathrm{s}\sin(\omega t)\mathrm{d}\omega t = \frac{\hat{u}_\mathrm{s}}{\pi}\left[-\cos(\omega t)\right]_{\alpha}^{\alpha+\pi} = \frac{\hat{u}_\mathrm{s}}{\pi}\left(-\cos(\alpha+\pi)+\cos(\alpha)\right)\\ &= \hat{u}_\mathrm{s}\frac{2}{\pi}\cos(\alpha).\end{aligned} \tag{5.6}$$

In DCM the conduction interval β is less than π and the average output voltage is given by

$$\begin{aligned}\overline{u}_2 &= \frac{1}{\pi}\int_{\alpha}^{\alpha+\beta} \hat{u}_\mathrm{s}\sin(\omega t)\mathrm{d}\omega t = \frac{\hat{u}_\mathrm{s}}{\pi}\left[-\cos(\omega t)\right]_{\alpha}^{\alpha+\beta} = \frac{\hat{u}_\mathrm{s}}{\pi}\left(\cos(\alpha)-\cos(\alpha+\beta)\right)\\ &= \hat{u}_\mathrm{s}\frac{2}{\pi}\sin\left(\frac{\beta}{2}\right)\sin\left(\alpha+\frac{\beta}{2}\right).\end{aligned} \tag{5.7}$$

M2C converter with an active load

Analyzing (5.6) for the feasible firing angle range $\alpha \in [0, \pi]$ reveals

$$\overline{u}_2 \begin{cases} \geq 0, & \alpha \in [0, \pi/2], \\ < 0, & \alpha \in (\pi/2, \pi], \end{cases} \tag{5.8}$$

that is, the output voltage can become negative for $\alpha > \pi/2$ in CCM and BCM (analogous observation can be also made for DCM). Assuming an average output current $\overline{i}_2 > 0$, which can be only positive due to the thyristor unipolar current capability, the average output power is in the range of (for CCM and BCM)

$$\overline{p}_2 \begin{cases} \geq 0, & \alpha \in [0, \pi/2], \\ < 0, & \alpha \in (\pi/2, \pi]. \end{cases} \tag{5.9}$$

Hence, the M2C can transfer energy from the load to the source which requires an active load (e.g., battery or generator) to maintain this reversed energy flow. Consequently, the M2C can be used as a bidirectional energy transfer system operating both as a rectifier and an inverter.

M2C converter with an active load (cont.)

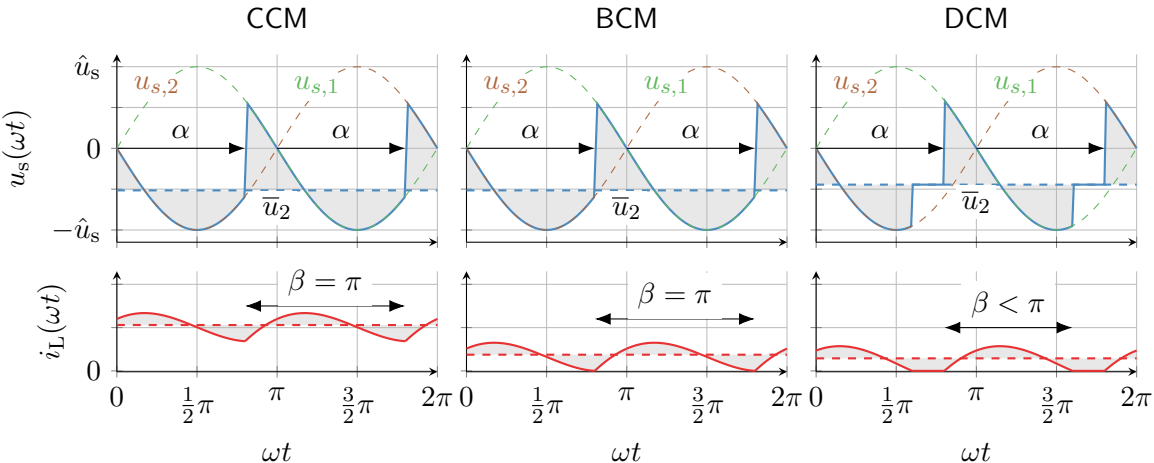

Fig. 5.6: M2C topology with a negative output voltage delivering energy to the source side

M2C output voltage overview

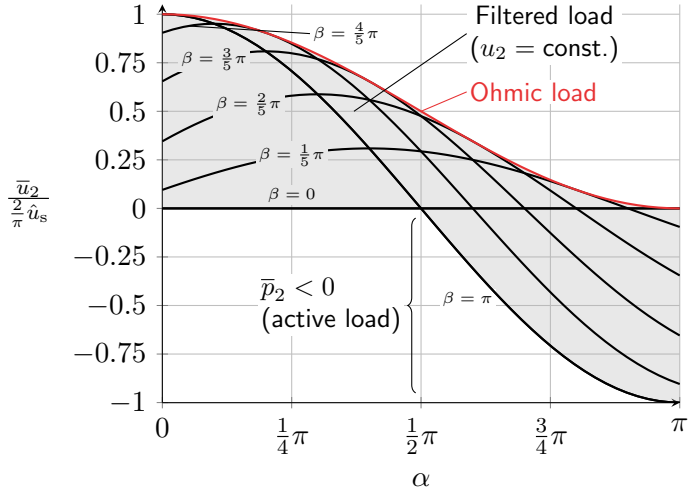

Fig. 5.7: M2C output voltage overview

Table of contents

M2C: complex power analysis

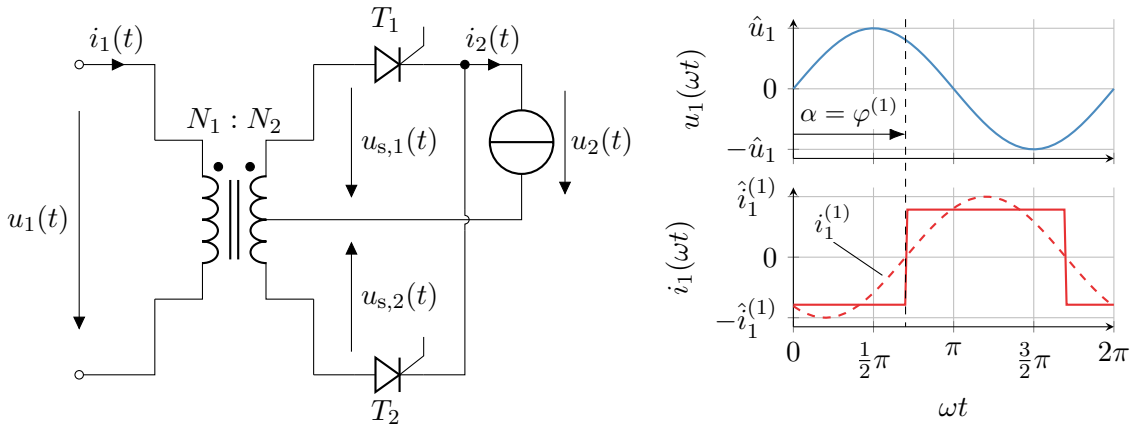

Fig. 5.8: Input voltage and current of the M2C converter with idealized filtered, constant output current (represented by a current source) and an idealized transformer

M2C: complex power analysis (cont.)

Based on the setup form Fig. 5.8 one can observe that the phase angle $\varphi^{(1)}$ between the input voltage $u_1(t)$ and the fundamental input current $i_1^{(1)}(t)$ is given by the firing angle α:

$$\varphi^{(1)} = \alpha.$$

Considering the center-tapped transformer, the input current fundamental amplitude is

$$i_1^{(1)} = \frac{4}{\pi}\frac{1}{2}\frac{N_2}{N_1}I_2 = \frac{2}{\pi}\frac{N_2}{N_1}I_2, \tag{5.10}$$

where I_2 is constant output current and $4/\pi$ represents the first Fourier coefficient of the square-shaped input current $i_1(t)$. The latter is formed by the thyristors applying the positive and negative output current to the transformer's secondary side. The RMS value of the fundamental component $I_1^{(1)}$ and the RMS value of the input current I_1 are

$$I_1^{(1)} = \frac{\sqrt{2}}{\pi}\frac{N_2}{N_1}I_2, \qquad I_1 = \frac{1}{2}\frac{N_2}{N_1}I_2. \tag{5.11}$$

The latter can be found by considering that the RMS value of a symmetrical block-shaped signal is its amplitude.

M2C: complex power analysis (cont.)

Assuming an ideal sinusoidal input voltage, the active power is only transferred based on its fundamental component

$$P_1 = P_1^{(1)} = I_1^{(1)} U_1 \cos(\varphi^{(1)}) \tag{5.12}$$

with U_1 being the RMS value of the input voltage – compare (4.45). Assuming idealized, lossless components the active input power must be equal to the average output power

$$P_1 = \overline{p}_2 = I_2 \overline{u}_2 = I_2 \hat{u}_\mathrm{s} \frac{2}{\pi} \cos(\alpha) = I_2 \hat{u}_{\mathrm{s}0} \cos(\alpha) \tag{5.13}$$

with $\hat{u}_{\mathrm{s}0} = \hat{u}_\mathrm{s} \cdot 2/\pi$ being the maximum reachable output voltage (for $\alpha = 0$). From (5.12) the fundamental reactive power can be determined as

$$Q_1^{(1)} = I_1^{(1)} U_1 \sin(\varphi^{(1)}) = I_2 \hat{u}_{\mathrm{s}0} \sin(\alpha) \tag{5.14}$$

and the fundamental apparent power is given by

$$S_1^{(1)} = I_1^{(1)} U_1 = I_2 \hat{u}_{\mathrm{s}0} = \text{const.} \tag{5.15}$$

M2C: reactive power diagram

Rewriting the fundamental apparent power in terms of the active and reactive power yields:

$$\left(S_1^{(1)}\right)^2 = \left(P_1\right)^2 + \left(Q_1^{(1)}\right)^2 = I_2^2 \hat{u}_{\mathrm{s0}}^2 \quad \Leftrightarrow \left(\frac{Q_1^{(1)}}{I_2 \hat{u}_{\mathrm{s0}}}\right)^2 + \left(\frac{P_1^2}{I_2 \hat{u}_{\mathrm{s0}}}\right)^2 = 1. \tag{5.16}$$

Inserting $P_1 = I_2 \hat{u}_{\mathrm{s0}} \cos(\alpha)$ from (5.13) finally yields the following circular equation

$$\left(\frac{Q_1^{(1)}}{I_2 \hat{u}_{\mathrm{s0}}}\right)^2 + \left(\cos(\alpha)\right)^2 = 1 \quad \Leftrightarrow \quad \left(\frac{Q_1^{(1)}}{S_1^{(1)}}\right)^2 + \left(\frac{\overline{u}_2}{\hat{u}_{\mathrm{s0}}}\right)^2 = 1 \tag{5.17}$$

which can be visualized as a reactive power diagram of the M2C converter – compare the upcoming Fig. 5.9.

M2C: reactive power diagram (cont.)

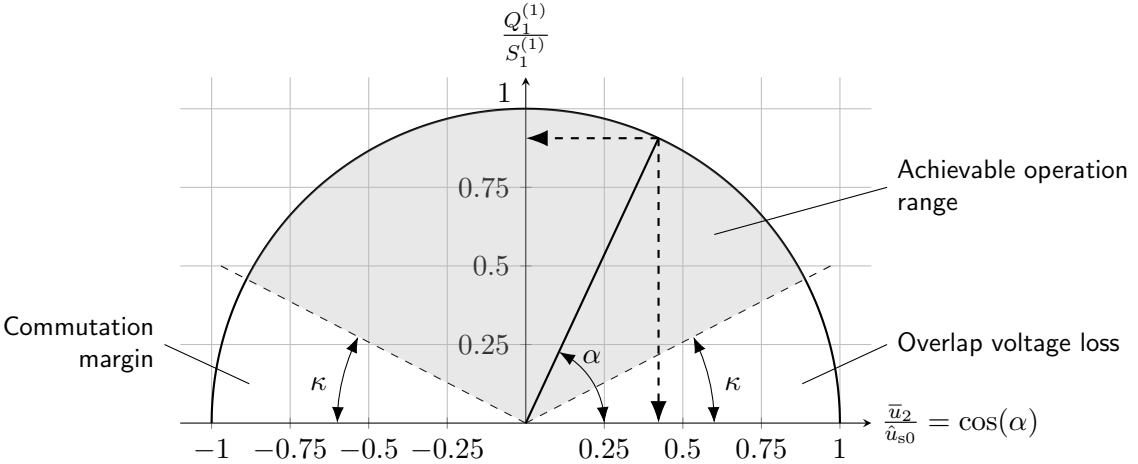

Fig. 5.9: Fundamental reactive power demand at some constant output current

M2C: complex power analysis incl. harmonics

Extending the previous analysis of the complex power fundamental components to the total complex power, one can determine the total apparent power as

$$S_1 = I_1 U_1 = \frac{1}{2}\frac{N_2}{N_1} I_2 U_1 = \frac{\pi}{2\sqrt{2}} S_1^{(1)} \approx 1.11 \cdot S_1^{(1)}. \tag{5.18}$$

Interestingly, the apparent power is independent of the firing angle α. The total reactive power is given by

$$Q_1 = \sqrt{S_1^2 - P_1^2} = S_1^{(1)} \sqrt{\frac{\pi^2}{8} - \cos^2(\alpha)} = \frac{\sqrt{2}}{\pi}\frac{N_2}{N_1} I_2 U_1 \sqrt{\frac{\pi^2}{8} - \cos^2(\alpha)}. \tag{5.19}$$

Alternatively, one could also determine the harmonic reactive power

$$Q_1^{(\mathrm{h})} = \sqrt{\left(S_1\right)^2 - \left(S_1^{(1)}\right)^2} = S_1^{(1)} \sqrt{\frac{\pi^2 - 8}{8}} = \frac{\sqrt{2}}{\pi}\frac{N_2}{N_1} I_2 U_1 \sqrt{\frac{\pi^2 - 8}{8}}. \tag{5.20}$$

first and then determine the total reactive power as

$$Q_1 = \sqrt{\left(Q_1^{(1)}\right)^2 + \left(Q_1^{(\mathrm{h})}\right)^2} = S_1^{(1)} \sqrt{\sin^2(\alpha) + \frac{\pi^2 - 8}{8}} = \frac{\sqrt{2}}{\pi}\frac{N_2}{N_1} I_2 U_1 \sqrt{\sin^2(\alpha) + \frac{\pi^2 - 8}{8}}.$$

Table of contents

Commutation

Idealized, instantaneous commutation

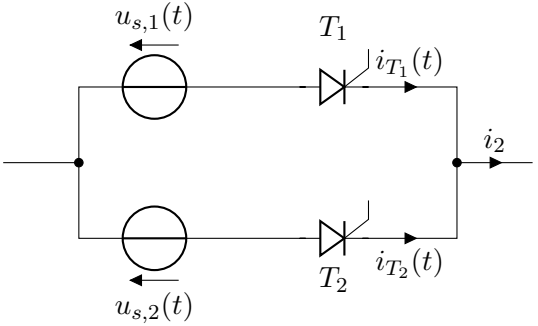

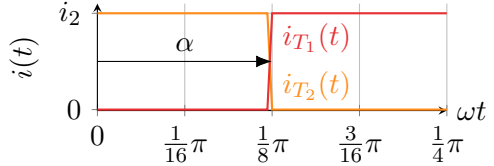

Actual commutation (with overlap)

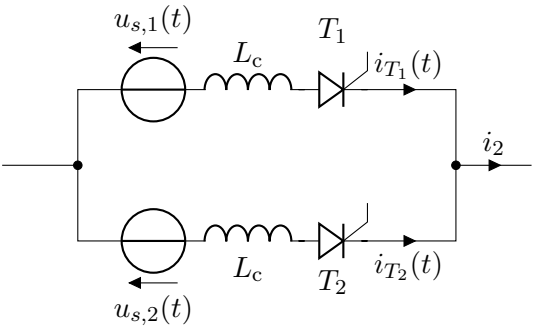

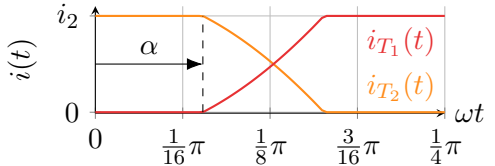

Commutation (cont.)

So far we have considered an idealized, instantaneous commutation of the thyristors. In practice, the commutation process is not instantaneous and the thyristors overlap for a certain period due to the commutation inductance L_c, which can originate from:

- Stray inductance of the feeding transformer,
- Parasitic inductance of the thyristor package,
- Parasitic inductance of the circuit layout.

Kirchhoff's voltage law for the commutation loop yields

$$u_\mathrm{c}(t) = u_{\mathrm{s},1}(t) - u_{\mathrm{s},2}(t) = 2L_\mathrm{c}\frac{\mathrm{d}}{\mathrm{d}t}i_{T_2}(t) = -2L_\mathrm{c}\frac{\mathrm{d}}{\mathrm{d}t}i_{T_1}(t) \tag{5.21}$$

with the commutation voltage $u_\mathrm{c}(t)$ and the thyristor currents $i_{T_1}(t)$ and $i_{T_2}(t)$.

Commutation (cont.)

From (5.21) the thyristor currents can be expressed as

$$i_{T_1}(t) = i_{T_1}(k\pi+\alpha) - \frac{1}{2L_\mathrm{c}\omega}\int_{k\pi+\alpha}^{\omega t} u_\mathrm{c}(\tau)\mathrm{d}\tau = i_{T_1}(k\pi+\alpha) + \frac{u_\mathrm{s}}{L_\mathrm{c}\omega}\left(\cos(k\pi+\alpha) - \cos(\omega t)\right),$$

$$i_{T_2}(t) = i_{T_2}(k\pi+\alpha) + \frac{1}{2L_\mathrm{c}\omega}\int_{k\pi+\alpha}^{\omega t} u_\mathrm{c}(\tau)\mathrm{d}\tau = i_{T_2}(k\pi+\alpha) - \frac{u_\mathrm{s}}{L_\mathrm{c}\omega}\left(\cos(k\pi+\alpha) - \cos(\omega t)\right).$$

Here, $i_{T_1}(k\pi+\alpha)$ and $i_{T_2}(k\pi+\alpha)$ are the thyristor currents at the beginning of the commutation process during the k-th half cycle. One can distinguish two cases:

$$i_{T_1}(k\pi+\alpha) = 0, \quad i_{T_2}(k\pi+\alpha) = i_2, \quad \text{commutation from } T_2 \text{ to } T_1,$$
$$i_{T_1}(k\pi+\alpha) = i_2, \quad i_{T_2}(k\pi+\alpha) = 0, \quad \text{commutation from } T_1 \text{ to } T_2.$$

The commutation process ends when the thyristor currents reach i_2 and zero, respectively.

Commutation: overlap angle and feasible firing angle range

To determine the commutation overlap angle κ, we consider $k = 0$ and the commutation from T_2 to T_1, that is, $i_{T_1}(\alpha) = 0$. The commutation ends when $i_{T_1}(\alpha + \kappa) = i_2$, which yields

$$i_{T_1}(\alpha + \kappa) = i_2 \stackrel{!}{=} \frac{u_\mathrm{s}}{L_\mathrm{c}\omega} \left(\cos(\alpha) - \cos(\alpha + \kappa)\right). \tag{5.22}$$

Solving for the overlap angle κ results in

$$\kappa = \arccos\left(\cos(\alpha) - \frac{i_2 L_\mathrm{c}\omega}{u_\mathrm{s}}\right) - \alpha. \tag{5.23}$$

To ensure a successful commutation $\alpha + \kappa < \pi$ must hold: Otherwise the commutation voltage changes its sign and the commutation fails. Hence, the achievable firing angle is determined by

$$\alpha + \kappa < \pi \quad \Leftrightarrow \quad \arccos\left(\cos(\alpha) - \frac{i_2 L_\mathrm{c}\omega}{u_\mathrm{s}}\right) < \pi \tag{5.24}$$

leading to

$$\alpha < \arccos\left(\frac{i_2 L_\mathrm{c}\omega}{u_\mathrm{s}} - 1\right). \tag{5.25}$$

Commutation: successful and unsuccessful examples

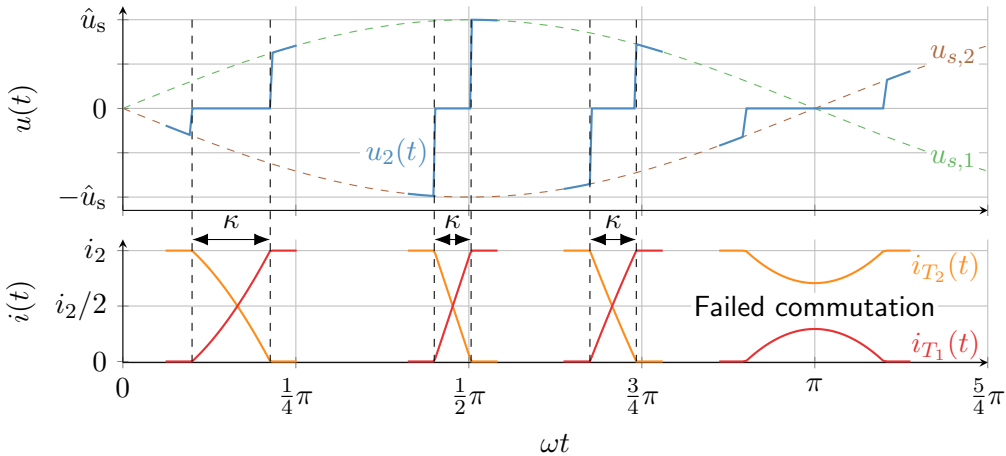

Fig. 5.10: Commutation process for different firing angles α

Commutation: output voltage deviation

As seen in Fig. 5.10, the output voltage of the thyristor stage is zero during the commutation process as the transformer's secondary side is temporarily short-circuited during the overlap period (since both thyristors are conducting):

$$u_\mathrm{s}(\omega t) = 0, \qquad \omega t \in [k\pi + \alpha, k\pi + \alpha + \kappa]. \tag{5.26}$$

The output voltage loss due to commutation corresponds to

$$\Delta u = \frac{1}{\pi}\int_{\alpha}^{\alpha+\kappa} \hat{u}_\mathrm{s}\sin(\omega t)\mathrm{d}(\omega t) = \frac{\hat{u}_\mathrm{s}}{\pi}\left[-\cos(\omega t)\right]_{\alpha}^{\alpha+\kappa} = \frac{\hat{u}_\mathrm{s}}{\pi}\left[\cos(\alpha) - \cos(\alpha+\kappa)\right]. \tag{5.27}$$

Inserting (5.23) for κ yields

$$\begin{aligned}\Delta u &= \frac{\hat{u}_\mathrm{s}}{\pi}\left[\cos(\alpha) - \cos\left(\alpha + \arccos\left(\cos(\alpha) - \frac{i_2 L_\mathrm{c}\omega}{\hat{u}_\mathrm{s}}\right) - \alpha\right)\right] \\ &= \frac{i_2 L_\mathrm{c}\omega}{\pi}.\end{aligned} \tag{5.28}$$

Hence, the average output voltage is deviating by Δu due to the commutation process.

Table of contents

M3C converter

The previous diode-based rectifiers with higher-pulse numbers can be directly transferred to their controlled counterparts using thyristors, such as the 3-pulse converter shown in Fig. 5.11.

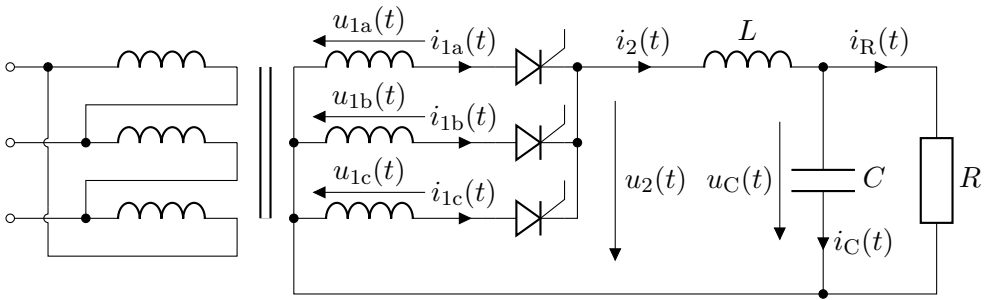

Fig. 5.11: M3C topology with an input three-phase transformer, a resistive load and output filter

M3C converter (cont.)

The M3C converter's firing angle α starts at the crossing of two adjacent input voltages, that is, where the voltage over the next thyristor becomes positive. For CCM and neglecting commutation and other parasitic effects, the M3C's average output voltage is

$$\begin{aligned}\overline{u}_2 &= \frac{3}{2\pi}\int_{\frac{1}{6}\pi+\alpha}^{\frac{5}{6}\pi+\alpha} \hat{u}_1 \sin(\omega t)\mathrm{d}\omega t \\ &= \frac{3}{2\pi}\hat{u}_1\left[-\cos(\omega t)\right]_{\frac{1}{6}\pi+\alpha}^{\frac{5}{6}\pi+\alpha} = \ldots \\ &= \frac{3\sqrt{3}}{2\pi}\hat{u}_1\cos(\alpha).\end{aligned} \tag{5.29}$$

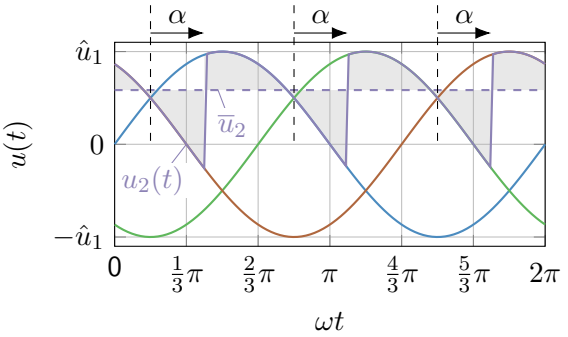

Fig. 5.12: Examplary firing angle for the M3C converter

B6C converter

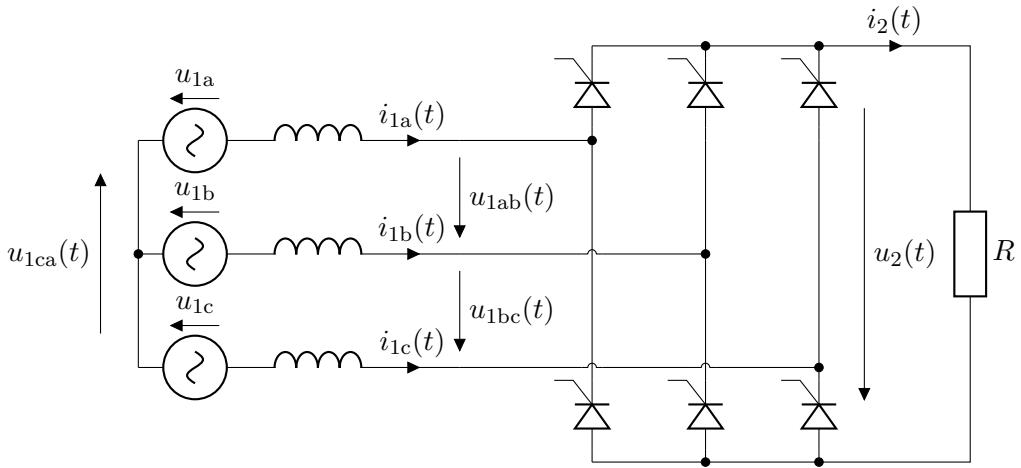

Fig. 5.13: B6C topology with line chokes and a resistive load

Output voltage of a thyristor bridge converter with p pulses

The average output voltage (under idealized CCM operation) of a thyristor bridge converter with p pulses is given by

$$\begin{aligned}\overline{u}_2 &= \frac{p}{2\pi}\int_{\alpha-\frac{\pi}{p}}^{\alpha+\frac{\pi}{p}} \hat{u}\cos(\omega t)\mathrm{d}\omega t \\ &= \hat{u}\frac{p}{2\pi}\left[\sin\left(\alpha+\frac{\pi}{p}\right)-\sin\left(\alpha-\frac{\pi}{p}\right)\right] \\ &= \hat{u}\frac{p}{\pi}\sin\left(\frac{\pi}{p}\right)\cos(\alpha). \qquad (5.30)\end{aligned}$$

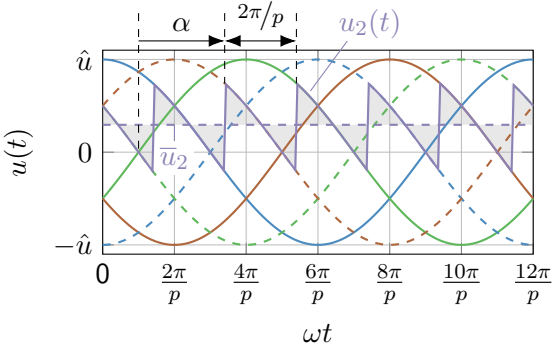

Fig. 5.14: Generalized firing angle representation for a thyristor bridge converter with p pulses and $\hat{u}$ being the line-to-line voltage amplitude

Here, the maximum achievable voltage

$$\max_{\alpha}\overline{u}_2 = \hat{u}\frac{p}{\pi}\sin\left(\pi/p\right) \qquad (5.31)$$

increases with the number of pulses p.

Section summary

This section provided an introduction to thyristor-based converters. The key takeaways are:

- In contrast to diode-based rectifiers:
  - Are controllable by varying the firing angle α (within its feasible range).
  - Can transfer power in both directions (rectifier and inverter operation).
- Likewise diode-based rectifiers:
  - Introduce harmonics in the output voltage and input current (i.e., require filters).
  - Typically, do not operate at unity power factor (require reactive power).
  - Are line-commutated, as the external grid voltage is required to achieve the commutation.

Previous analyses based on diodes or thyristor-based converters were dealt with in varying detail level, but as they can be transferred analogously they are not explicitly shown due to time constraints. In addition, there are further interesting thyristor-based applications such as

- four quadrant thyristor converters (e.g., cycloconverters) covering both voltage and current polarities,
- specialized stacked topologies for high-voltage DC transmission.

Table of contents

Transistor-based AC/DC converters: self-commutated converters

Up to now:

- Diode-based converters
  - Rectification only
  - No control
- Thyristor-based converters
  - Rectification and inversion
  - Limited control / line commutation

Extension in this section:

- Transistor-based converters
  - Rectification and inversion
  - Fully controllable / self-commutated

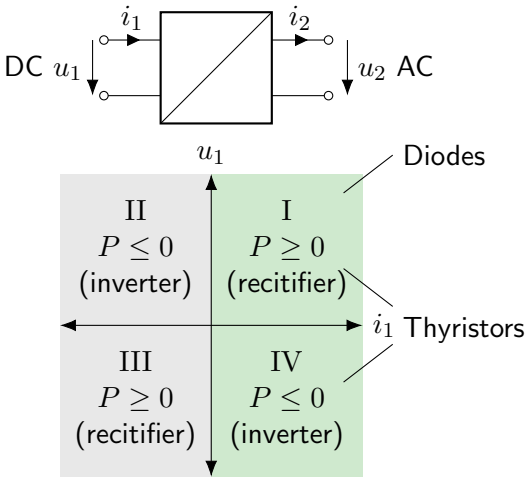

Idealized switch representation of a single-phase AC/DC bridge converter

Define switching function:

$$s_i(t) = \begin{cases} +1 & \text{upper position,} \\ -1 & \text{lower position.} \end{cases} \tag{6.1}$$

Output voltage considering a voltage source at the input is:

$$u_2(t) = \underbrace{\frac{1}{2}\left(s_1(t) - s_2(t)\right)}_{s(t)} u_1(t). \tag{6.2}$$

Input current assuming a current source at the output results in:

$$i_1(t) = s(t) i_2(t). \tag{6.3}$$

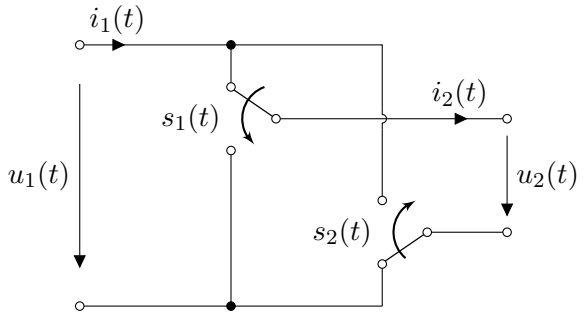

Fig. 6.1: Idealized switch representation of a single-phase AC/DC bridge converter

Circuit realization

- Remember: complementary switching of $\{T_1, T_2\}$ and $\{T_3, T_4\}$ to prevent a DC-link short-circuit.
- Possible (allowed) switching states:

T_1	T_2	T_3	T_4	s_1	s_2	s
on	off	off	on	$+1$	-1	$+1$
off	on	on	off	-1	$+1$	-1
on	off	on	off	$+1$	$+1$	0
off	on	off	on	-1	-1	0

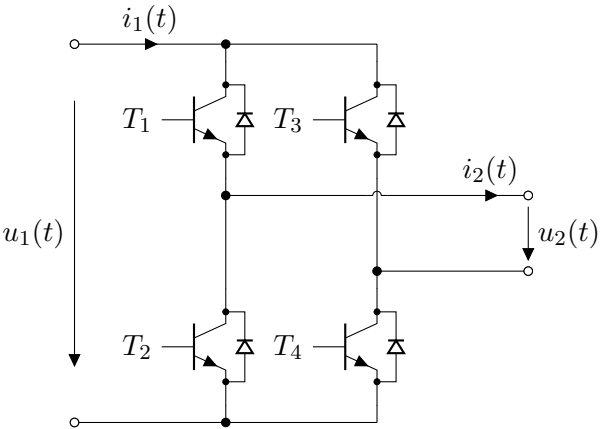

Fig. 6.2: Full-bridge single-phase AC/DC converter (identical to the one used in the DC/DC section in Fig. 2.43)

Pulse width modulation (PWM) options

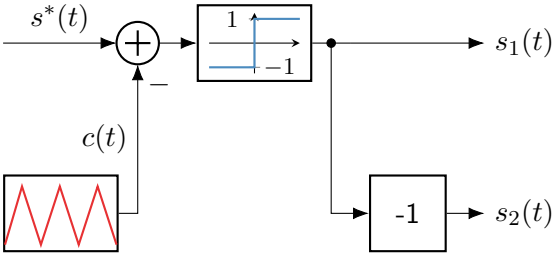

Fig. 6.3: PWM with complementary switching

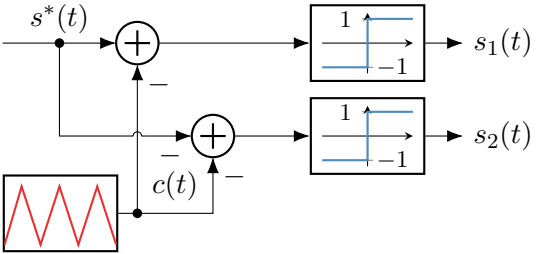

Fig. 6.4: PWM with interleaved switching

PWM example with complementary switching

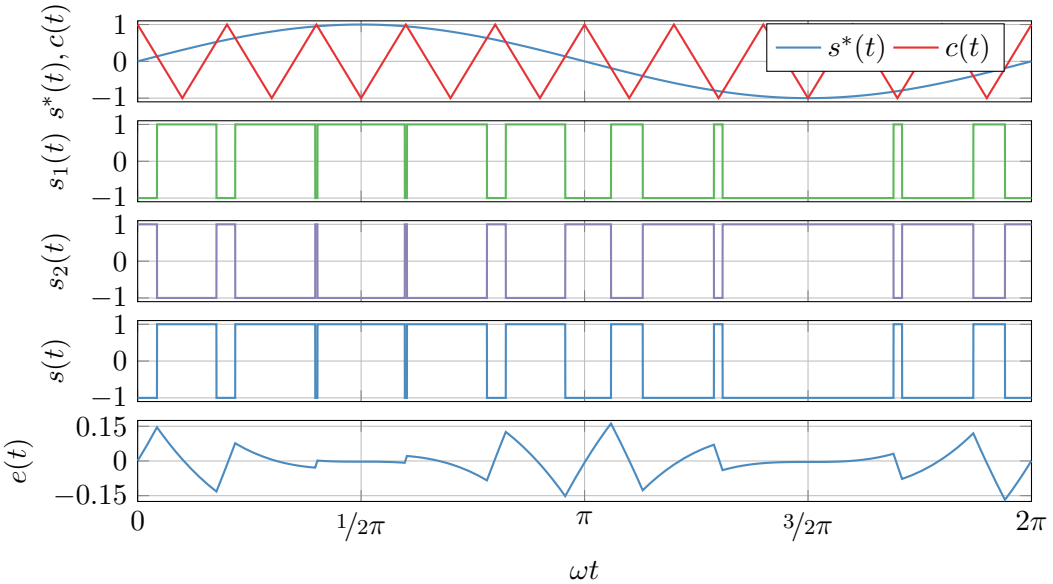

PWM example with interleaved switching

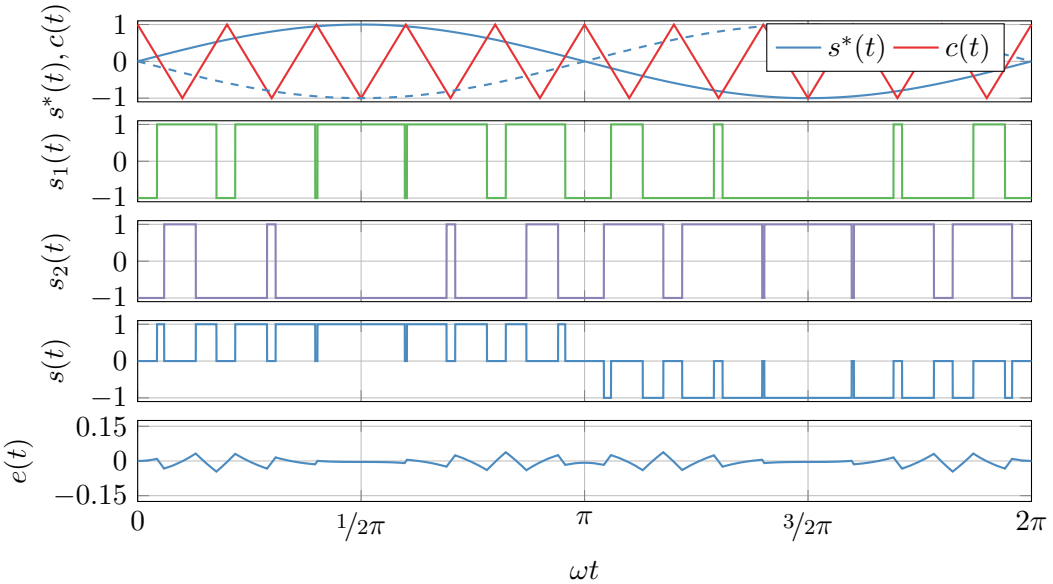

PWM approximation error analysis

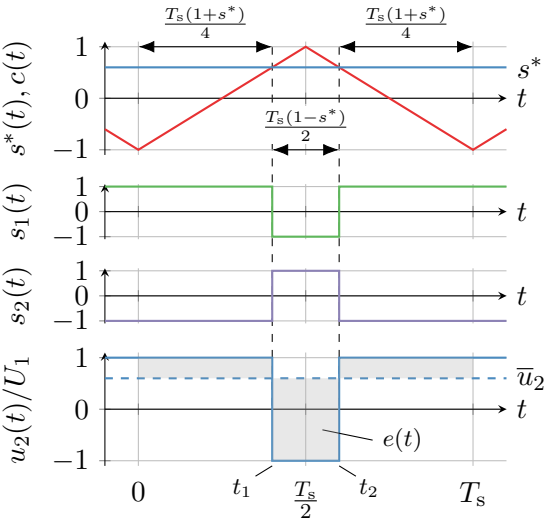

Fig. 6.5: Pulse pattern for complementary PWM

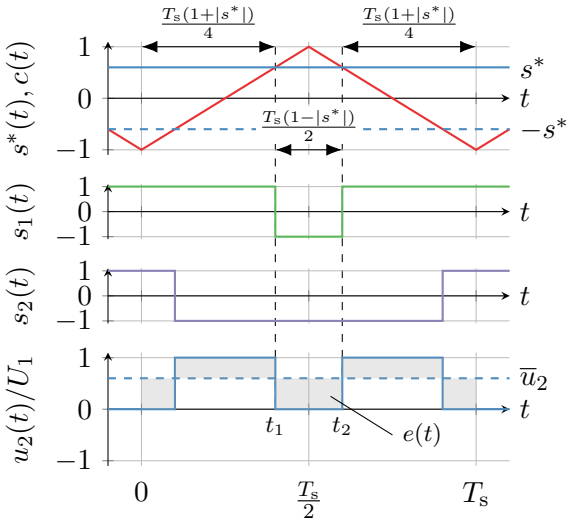

Fig. 6.6: Pulse pattern for interleaved PWM

PWM approximation error analysis (cont.)

To evaluate the error between the reference $s^*(t)$ and the switched output voltage $u_2(t)$, we introduce the following normalized integral difference:

$$e(t) = \frac{1}{T_\mathrm{s}} \int_{t_0}^{t} \left(s^*(\tau) - s(\tau)\right) \mathrm{d}\tau. \tag{6.4}$$

This error can be interpreted as the resulting current ripple assuming a pure inductive load L at a constant input voltage $u_1(t) = U_1$:

$$\Delta i_2(t) = \frac{T_\mathrm{s} U_1}{2L} \left|e(t)\right|. \tag{6.5}$$

For a constant reference $s^*(t) = s^*$, the biggest error corresponds to the integral over the time interval $[t_1, t_2]$ as can be seen in Fig. 6.5 and Fig. 6.6:

$$\begin{aligned} &\text{complimentary switching (cs):} && \max_t e_\mathrm{cs}(t) = \frac{1}{T_s} \left(s^* + 1\right) \left(t_2 - t_1\right) = \frac{1}{2} \left(s^* + 1\right) \left(1 - s^*\right), \\ &\text{interleaved switching (is):} && \max_t e_\mathrm{is}(t) = \frac{1}{T_s} \left|s^*\right| \left(t_2 - t_1\right) = \frac{1}{2} \left|s^*\right| \left(1 - \left|s^*\right|\right). \end{aligned} \tag{6.6}$$

PWM approximation error analysis (cont.)

Further, analyzing (6.6)

$$\frac{\mathrm{d}}{\mathrm{d}s^*}\left(\max_t e_{\mathrm{cs}}(t)\right) = -2s^*, \qquad \frac{\mathrm{d}}{\mathrm{d}s^*}\left(\max_t e_{\mathrm{is}}(t)\right) = \mathrm{sgn}(s^*) - 2s^* \tag{6.7}$$

reveals the worst case deviation at a switching reference of:

$$\arg\max_{s^*}\left\{\max_t e_{\mathrm{cs}}(t)\right\} = 0, \qquad \arg\max_{s^*}\left\{\max_t e_{\mathrm{is}}(t)\right\} = \pm\frac{1}{2}. \tag{6.8}$$

Inserting this finding into (6.5) delivers

$$\begin{aligned} \Delta i_{2,\mathrm{cs}} &= (1-s^*)(1+s^*)\Delta i_{2,\mathrm{cs,max}} \quad \text{with} \quad \Delta i_{2,\mathrm{cs,max}} = \frac{T_{\mathrm{s}}U_1}{2L}, \\ \Delta i_{2,\mathrm{is}} &= 4\,|s^*|\,(1-|s^*|)\Delta i_{2,\mathrm{is,max}} \quad \text{with} \quad \Delta i_{2,\mathrm{is,max}} = \frac{T_{\mathrm{s}}U_1}{8L}. \end{aligned} \tag{6.9}$$

Hence, the current ripple of the interleaved PWM is only $1/4$ of the complementary PWM.

PWM approximation error analysis (cont.)

Reasons for current ripple reduction of interleaved vs. complimentary PWM:

- Effective pulse number doubled:
  - CS: $f_\mathrm{p} = f_\mathrm{s}$
  - IS: $f_\mathrm{p} = 2f_\mathrm{s}$
- Output voltage steps halved:
  - CS: $\Delta u_2 = \pm 2U_1$
  - IS: $\Delta u_2 = \pm U_1$

Note on applicability

This analysis only holds for $s^* = \mathrm{const.}$ and can be transferred only approximately for $s^*(t) = f(\omega)$ if $T_s << \frac{2\pi}{\omega}$.

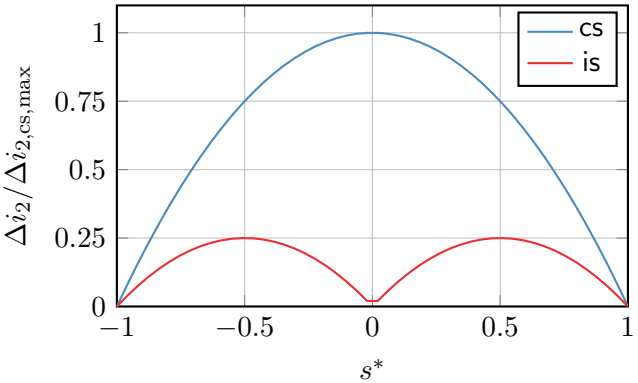

Fig. 6.7: Current ripple as a function of the single-phase AC/DC normalized reference output voltage s^*

Overmodulation

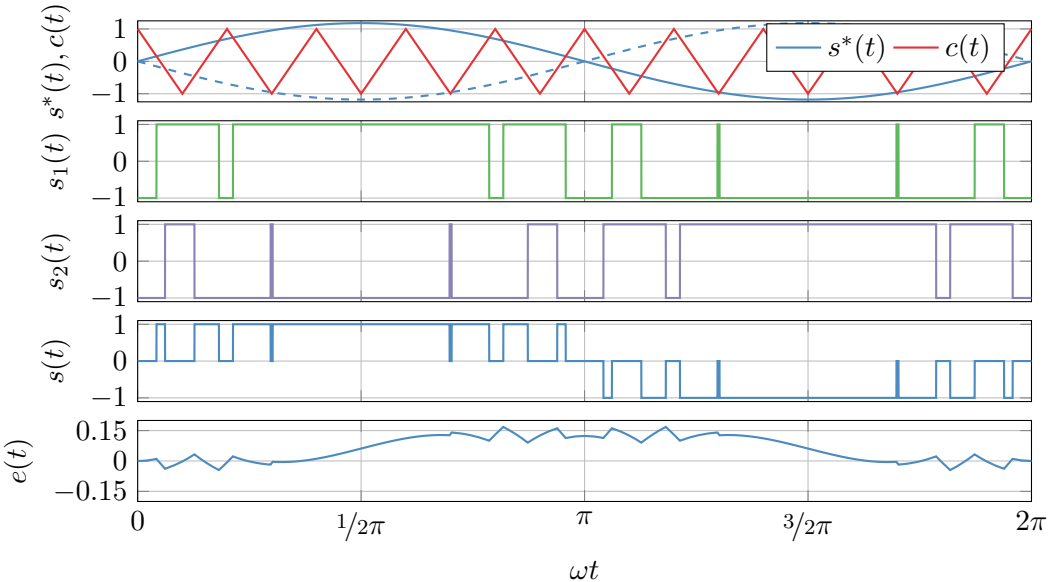

Overmodulation (cont.)

Considering a normalized input reference

$$s^*(t) = m \sin(\omega t) = \frac{\hat{u}_2^*}{U_1} \sin(\omega t)$$

with the modulation ratio m one can distinguish two PWM operation areas:

- $m \leq 1$: linear modulation,
- $m > 1$: overmodulation.

Harmonics

While the normalized output voltage fundamental can be increased beyond unity via overmodulation, increased voltage harmonics must be accepted.

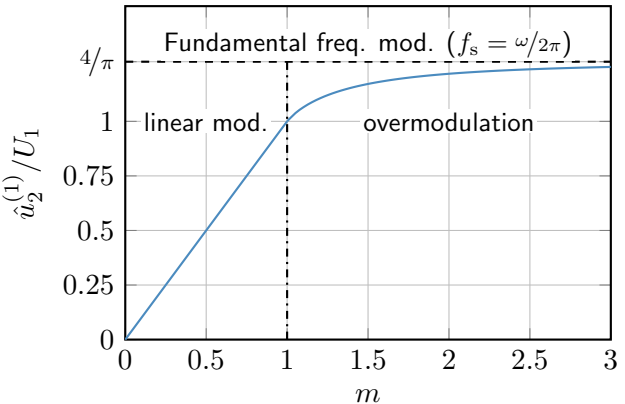

Fig. 6.8: Reference amplitude to output voltage fundamental amplitude

Overmodulation (cont.)

Due to the converter's constraints, the reference voltage is limited to

$$s^*_{\mathrm{lim}}(t) = \begin{cases} 1 & \text{if } s^*(t) > 1, \\ s^*(t) & \text{if } -1 \leq s^*(t) \leq 1, \\ -1 & \text{if } s^*(t) < -1. \end{cases}$$

Hence, from ωt_0 to ωt_1 the converter's output voltage is clipped for $m > 1$. With

$$m \sin(\omega t_0) \stackrel{!}{=} 1$$

one can find

$$\omega t_0 = \arcsin\left(\frac{1}{m}\right). \tag{6.10}$$

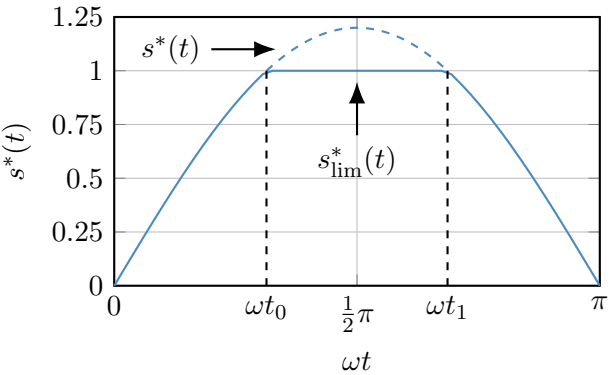

Fig. 6.9: Exemplary time series between average reference and actual voltage in the overmodulation range

Overmodulation (cont.)

To calculate the resulting fundamental output voltage during overmodulation, a Fourier analysis is performed while utilizing the quarter-wave symmetry of the output voltage signal:

$$\begin{aligned}\frac{u_2^{(1)}}{U_1} &= \frac{1}{\pi}\int_0^{2\pi} s_{\lim}^*(\omega\tau)\sin(\omega\tau)\mathrm{d}\omega\tau \\ &= \frac{4}{\pi}\left(\int_0^{\omega t_0} m\sin^2(\omega\tau)\mathrm{d}\omega\tau + \int_{\omega t_0}^{\frac{\pi}{2}} 1\sin(\omega\tau)\mathrm{d}\omega\tau\right) \\ &= \frac{4}{\pi}\left[\frac{m}{2}\left(\omega t_0 - \frac{1}{2}\sin(2\omega t_0)\right) + \cos(\omega t_0)\right].\end{aligned} \tag{6.11}$$

Inserting ωt_0 from (6.10) and applying trigonometric identities yields:

$$\frac{u_2^{(1)}}{U_1} = \frac{2}{\pi}\left[m\arcsin\left(\frac{1}{m}\right) + \sqrt{1-\frac{1}{m^2}}\right] \in \left[1, \frac{4}{\pi}\right] \quad \text{for} \quad m \geq 1. \tag{6.12}$$

Fundamental frequency modulation (aka square wave modulation)

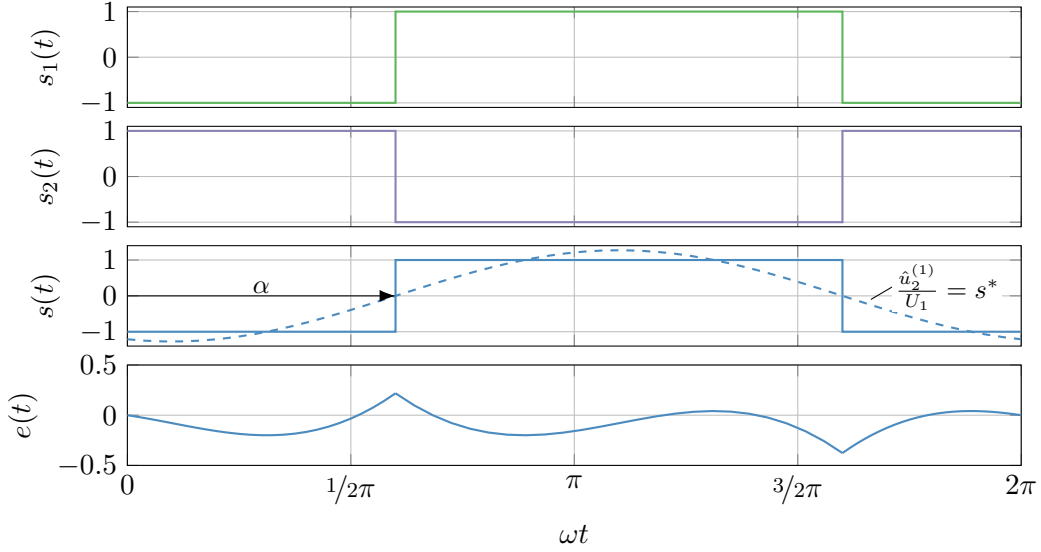

Fundamental frequency modulation (cont.)

The fundamental frequency modulation leads to a pulse pattern synchronized with the fundamental output voltage $\hat{u}_2^{(1)}(t)$, i.e., the switching frequency matches the fundamental voltage frequency

$$f_\mathrm{s} = \frac{\omega}{2\pi}.$$

The fundamental output voltage amplitude can be derived from the corresponding Fourier coefficient

$$\begin{aligned}\frac{u_2^{(k)}}{U_1} &= \frac{1}{\pi}\int_\alpha^{\alpha+\pi} \frac{u_2(t)}{U_1}\sin(k(\omega t-\alpha))\mathrm{d}\omega t = \frac{2}{\pi}\int_0^{\pi/2}\sin(k\omega t)\mathrm{d}\omega t \\ &= \frac{2}{\pi}\left[-\frac{1}{k}\cos(k\omega t)\right]_0^{\pi/2} = \frac{2}{\pi}\left[\frac{1}{k}\left(\cos(0)-\cos(k\frac{\pi}{2})\right)\right] \\ &= \frac{4}{\pi}\frac{1}{k}, \quad k=1,3,5,7,\ldots\end{aligned} \tag{6.13}$$

The fundamental output voltage amplitude is thus given by $\hat{u}_2^{(1)} = 4/\pi \cdot U_1$ which is fixed due to fundamental frequency modulation while only the phase angle α can be adjusted.

Blanking / interlocking time

When the i-th half bridge is actuated, i.e., changes it switching state, an interlocking / blanking time t_0 is introduced to avoid short-circuiting the DC link:

- First: turn off conducting transistor,
- Second: wait t_0 (ensure safe turn off),
- Third: turn on the other transistor.

Background

Signal delays or component tolerances lead to varying switch on/off times, which is why the interlock ensures an orderly switching process.

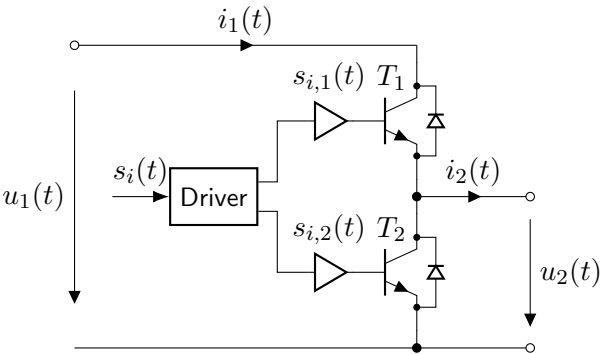

Fig. 6.10: Actuation of one half-bridge branch

Current paths depending on the switching state and current flow direction

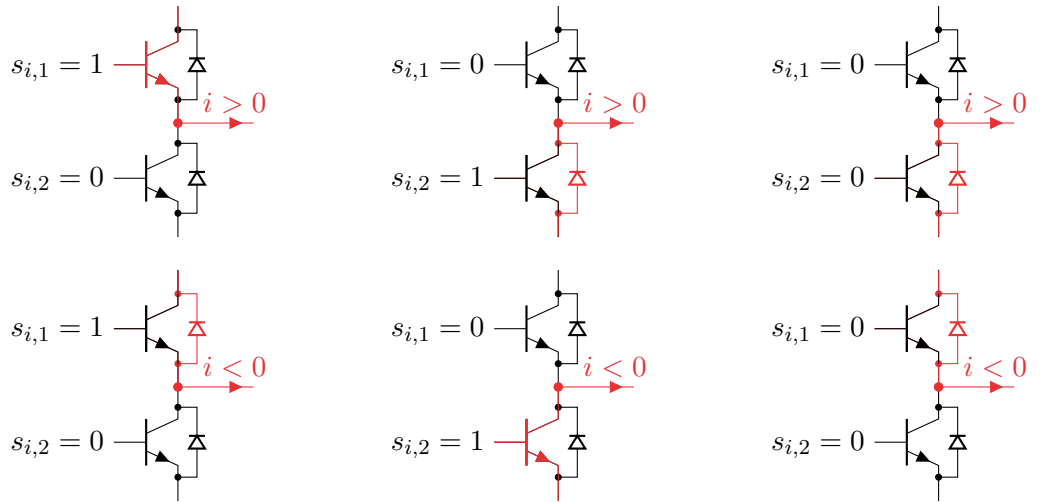

(a) Upper transistor on

(b) Lower transistor on

(c) Both transistors off

Blanking / interlocking time: positive load current

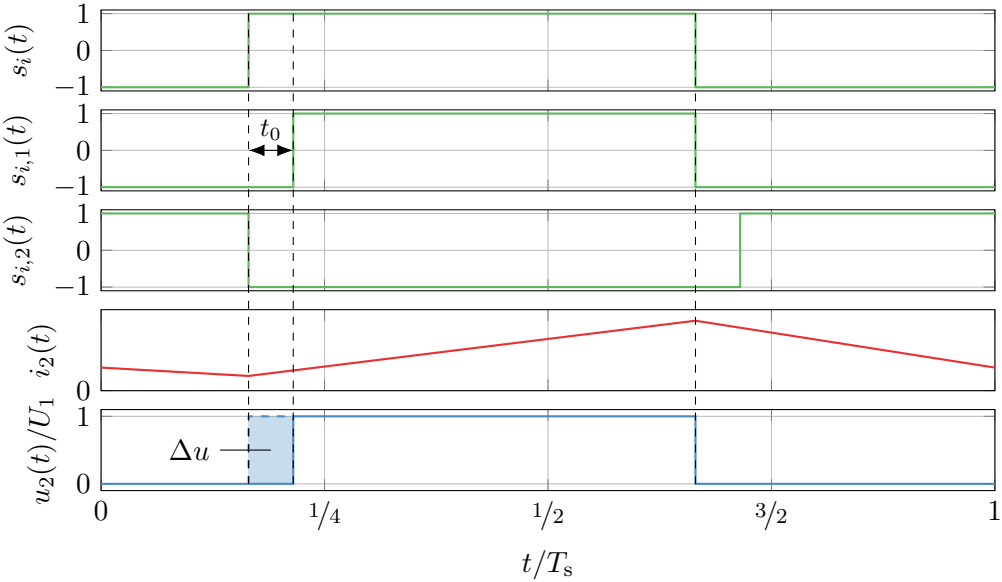

Blanking / interlocking time: negative load current

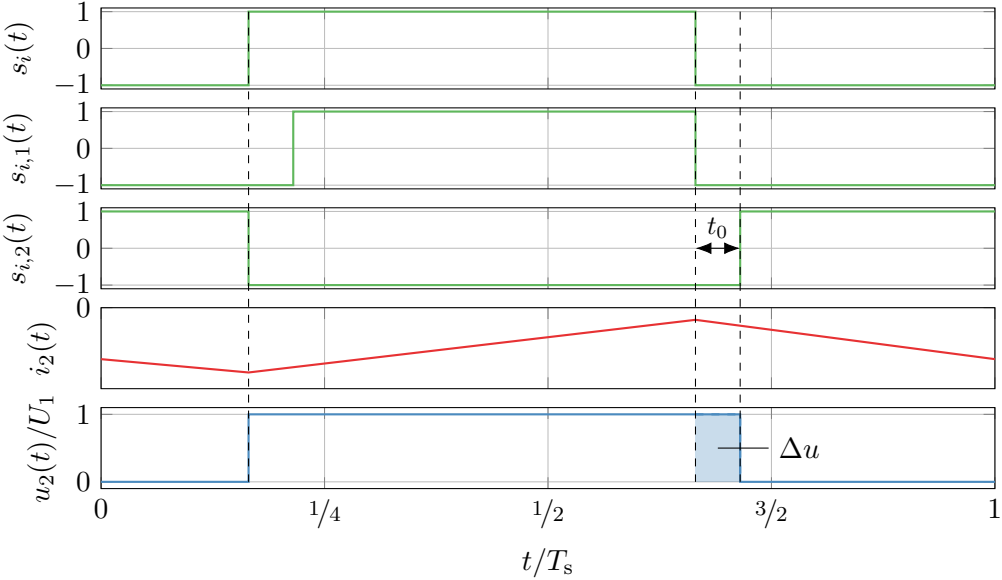

Blanking / interlocking time: discontinuous conduction

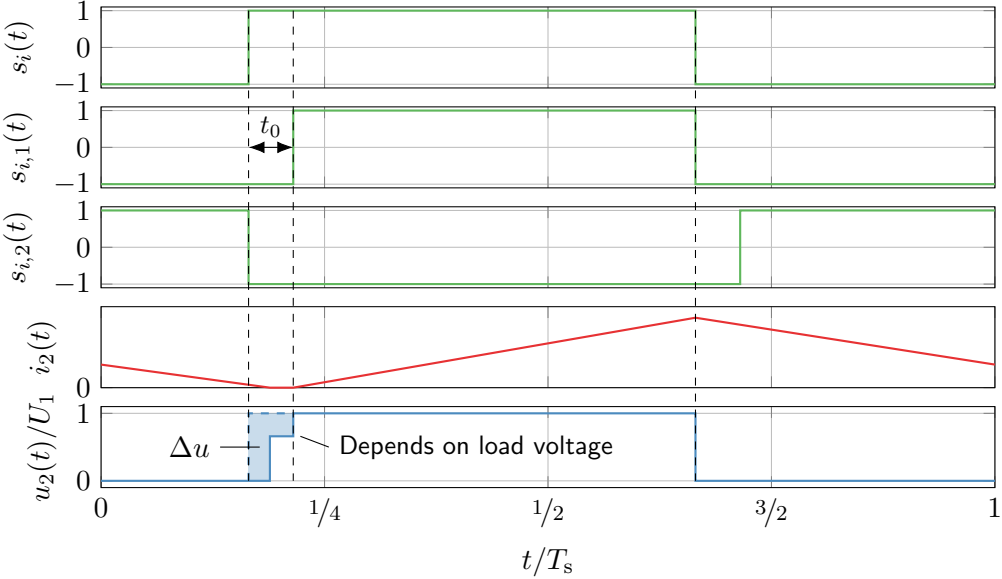

Blanking / interlocking time (cont.)

For the continuous conduction case, the voltage error Δu due to the interlocking time t_0 is given by

$$\Delta u = \overline{u}_2 - U_1 s^* = -\mathrm{sgn}(i_2)\frac{t_0}{T_\mathrm{s}}U_1 = -\mathrm{sgn}(i_2)t_0 f_\mathrm{s} U_1. \tag{6.14}$$

Hence, the error depends on the relative duration of the interlocking time t_0 compared to the switching period T_s which is a device-specific parameter (cf. below).

Device type	t_0	f_s
GTO	$10\,\mu\mathrm{s} - 30\,\mu\mathrm{s}$	$200\,\mathrm{Hz} - 500\,\mathrm{Hz}$
IGBT	$2\,\mu\mathrm{s} - 4\,\mu\mathrm{s}$	$5\,\mathrm{kHz} - 20\,\mathrm{kHz}$
MOSFET	$\leq 1\,\mu\mathrm{s}$	$20\,\mathrm{kHz} - 1000\,\mathrm{kHz}$

Tab. 6.1: Typical interlocking times and switching frequencies for different power semiconductor devices

Outlook: multi-level converters

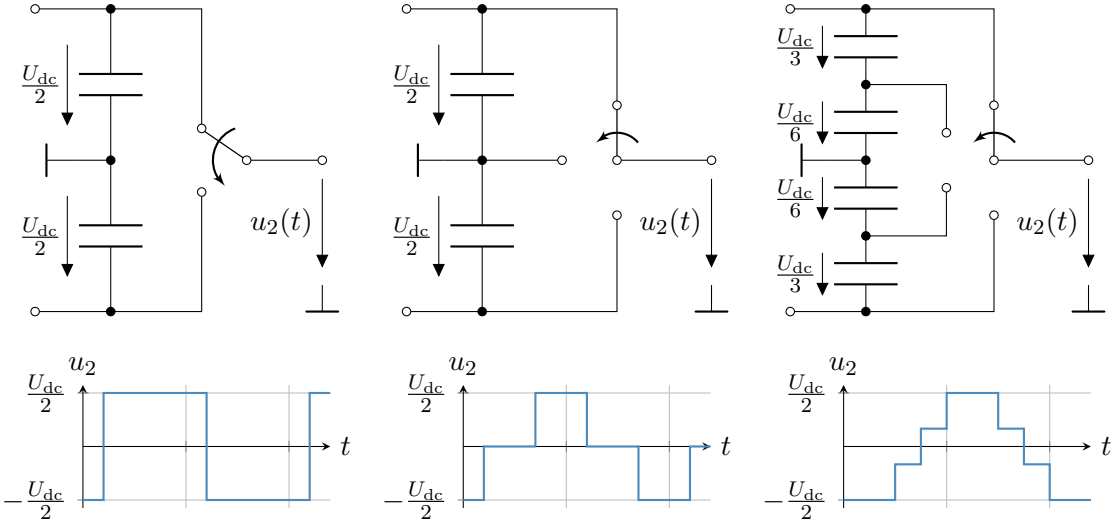

(a) 2-level half bridge (b) 3-level half bridge (c) 4-level half bridge

Table of contents

Rectifier application setup

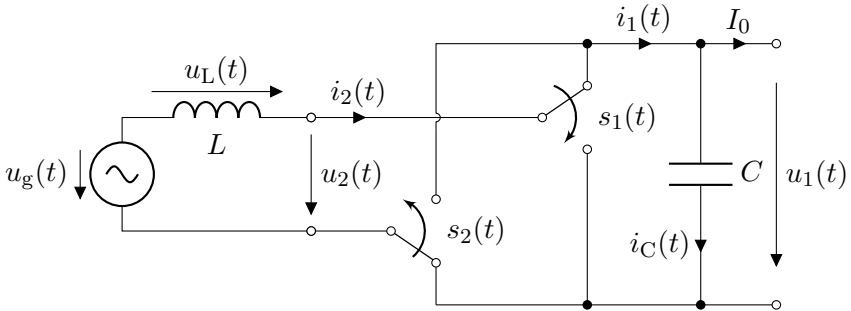

Fig. 6.13: Single-phase grid rectification: full bidirectional operation possible (e.g., for electrical rail vehicles with a $15\,\mathrm{kV}$, $16\frac{2}{3}\,\mathrm{Hz}$ grid). Note: converter topology is flipped to align u_2 with the AC grid side while u_1 is the DC output. Also known as active front end (AFE) rectifier.

Steady-state operation

Assuming steady state, the grid side input loop from Fig. 6.13 can be described with complex phasors:

$$\underline{\hat{u}}_2 = \underline{\hat{u}}_\mathrm{g} - \mathrm{j}\omega L \underline{\hat{i}}_2. \qquad (6.15)$$

The converter's input voltage amplitude is

$$\hat{u}_2 = \sqrt{\hat{u}_\mathrm{g}^2 + \left(\omega L \hat{i}_2\right)^2}. \qquad (6.16)$$

As the converter boosts the grid voltage towards the DC-link, the following condition must apply:

$$u_1(t) \approx U_\mathrm{dc} \geq \hat{u}_2 = \sqrt{\hat{u}_\mathrm{g}^2 + \left(\omega L \hat{i}_2\right)^2}. \qquad (6.17)$$

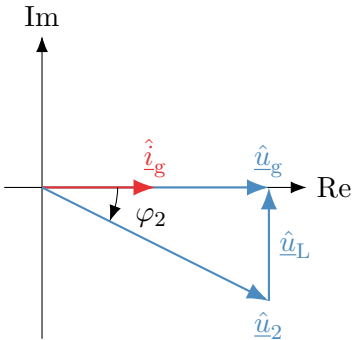

Fig. 6.14: Steady-state phasor diagram assuming $\cos(\varphi) = 1$ operation (enforced via some supervisory control)

Steady-state operation (cont.)

With the assumption of $\cos(\varphi) = 1$ operation and a lossless converter, the following relations hold:

$$P = P_1 = P_2 = P_\mathrm{g} = U_\mathrm{g} I_\mathrm{g} = \frac{1}{2} \hat{u}_\mathrm{g} \hat{i}_\mathrm{g}. \tag{6.18}$$

While there is no reactive power exchange with the grid, the converter needs to supply the reactive power Q_2 to compensate for the line inductance demand:

$$Q_2 = \omega L I_\mathrm{g}^2. \tag{6.19}$$

The resulting apparent power S_2 is

$$S_2 = \sqrt{P^2 + Q_2^2} = \sqrt{P^2 + \left(\omega L I_\mathrm{g}^2\right)^2} = \sqrt{P^2 + \left(\frac{\omega L}{U_\mathrm{g}^2} P^2\right)^2} = P \sqrt{1 + \left(\frac{\omega L}{U_\mathrm{g}^2} P\right)^2}. \tag{6.20}$$

Steady-state operation (cont.)

Neglecting the switching-induced current and voltage ripples, the instantaneous grid power is

$$p_\mathrm{g}(t) = u_\mathrm{g}(t) i_\mathrm{g}(t) = \hat{u}_\mathrm{g} \hat{i}_\mathrm{g} \cos^2(\omega t) = P + P\cos(2\omega t). \tag{6.21}$$

The instantaneous converter power at its AC input is

$$\begin{aligned} p_2(t) = u_2(t) i_2(t) &= \left(u_\mathrm{g}(t) + u_\mathrm{L}(t)\right) i_\mathrm{g}(t) = \left(u_\mathrm{g}(t) + L\frac{\mathrm{d}}{\mathrm{d}t} i_\mathrm{g}(t)\right) i_\mathrm{g}(t) \\ &= \hat{u}_\mathrm{g} \hat{i}_\mathrm{g} \cos^2(\omega t) + \omega L \hat{i}_\mathrm{g}^2 \sin(\omega t)\cos(\omega t) \\ &= P\left(1 + \cos(2\omega t)\right) + Q_2 \sin(2\omega t) = P + S_2 \cos(2\omega t - 2\varphi_2) \end{aligned} \tag{6.22}$$

with φ_2 being the phase angle between $i_2(t)$ and $u_2(t)$. Hence, the converter power oscillates at twice the grid frequency with an amplitude of S_2. As $S_2 > P$ applies, the instantaneous output power gets temporarily negative as a result of the reactive power compensation on the grid input side.

Steady-state operation (cont.)

Assuming a nearly constant DC-link voltage $u_1(t) \approx U_{\mathrm{dc}}$, the converter DC-side current $i_1(t)$ oscillates as well:

$$i_1(t) = \frac{p_1(t)}{U_{\mathrm{dc}}} = \frac{p_2(t)}{U_{\mathrm{dc}}} = \frac{P}{U_{\mathrm{dc}}} + \frac{S_2}{U_{\mathrm{dc}}} \cos(2\omega t - 2\varphi_2). \tag{6.23}$$

For a constant load current

$$I_0 = \frac{P}{U_{\mathrm{dc}}},$$

the converter's output current can be rewritten as

$$i_1(t) = I_0 \left(1 + \sqrt{1 + \left(\frac{\omega L U_{\mathrm{dc}}}{U_{\mathrm{g}}^2} \right)^2} \cos(2\omega t - 2\varphi_2) \right). \tag{6.24}$$

Consequently, the DC-link capacitor carries the harmonic current content:

$$i_{\mathrm{C}}(t) = i_1(t) - I_0 = I_0 \sqrt{1 + \left(\frac{\omega L U_{\mathrm{dc}}}{U_{\mathrm{g}}^2} \right)^2} \cos(2\omega t - 2\varphi_2). \tag{6.25}$$

Steady-state operation (cont.)

Assuming that the voltage ripple of the DC-link capacitor does not significantly affect the output current, the voltage oscillation amplitude can be approximated as:

$$\hat{u}_\mathrm{C} = \hat{u}_1 \approx \frac{\hat{i}_1}{2\omega C} = \frac{I_0}{2C}\sqrt{1 + \left(\frac{\omega L U_\mathrm{dc}}{U_\mathrm{g}^2} I_0\right)^2}. \tag{6.26}$$

This relation results from the complex phasor analysis of the capacitor's impedance given the current ripple (6.25). From (6.26) one can

- derive the required DC-link capacitance for a given voltage ripple,
- estimate the voltage ripple for a given DC-link capacitance.

Steady-state operation (cont.)

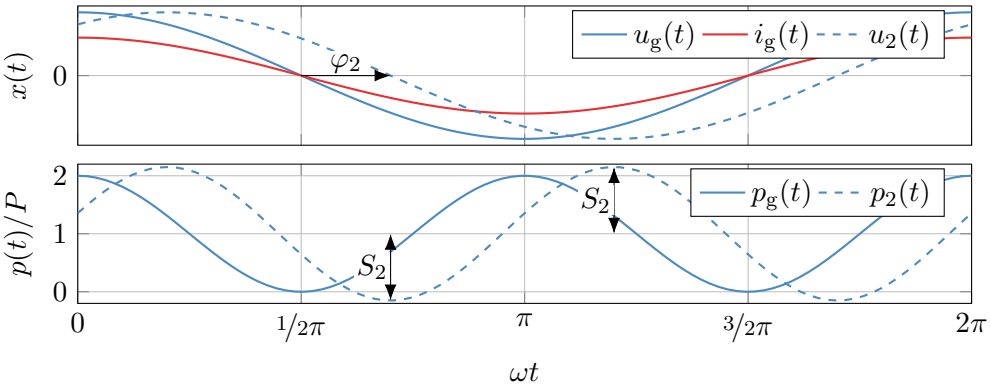

Fig. 6.15: Steady-state operation of the single-phase four-quadrant rectifier: (top) individual signals and (bottom) power oscillations at twice the grid frequency

Table of contents

Idealized switch representation of a three-phase AC/DC bridge converter

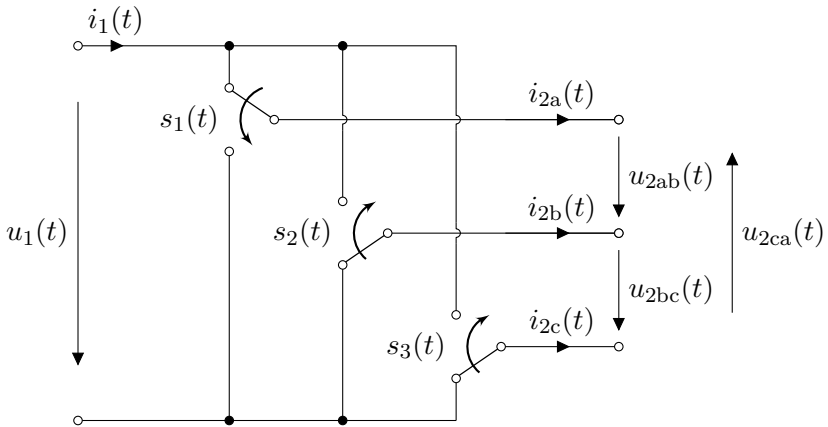

Fig. 6.16: Idealized switch representation of a three-phase two-level AC/DC bridge converter

Circuit realization

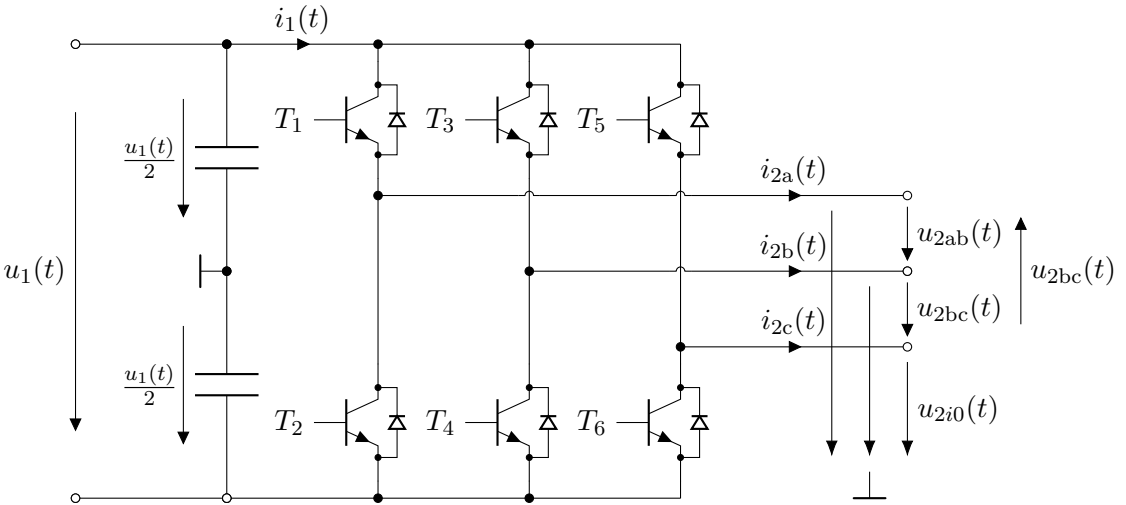

Fig. 6.17: Three-phase two-level AC/DC converter

Switching states and load-independent output voltages

Reutilizing the switching function definition (6.1), the line-to-line voltages can be expressed as

$$\begin{aligned} u_{2\mathrm{ab}}(t) &= \frac{1}{2}\left(s_{\mathrm{a}}(t) - s_{\mathrm{b}}(t)\right) u_1(t), \\ u_{2\mathrm{bc}}(t) &= \frac{1}{2}\left(s_{\mathrm{b}}(t) - s_{\mathrm{c}}(t)\right) u_1(t), \\ u_{2\mathrm{ca}}(t) &= \frac{1}{2}\left(s_{\mathrm{c}}(t) - s_{\mathrm{a}}(t)\right) u_1(t). \end{aligned} \tag{6.27}$$

The line-to-ground voltages are given by

$$\begin{aligned} u_{2\mathrm{a0}}(t) &= \frac{1}{2} s_{\mathrm{a}}(t) u_1(t), \\ u_{2\mathrm{b0}}(t) &= \frac{1}{2} s_{\mathrm{b}}(t) u_1(t), \\ u_{2\mathrm{c0}}(t) &= \frac{1}{2} s_{\mathrm{c}}(t) u_1(t). \end{aligned} \tag{6.28}$$

Three-phase converter with symmetric load in star connection

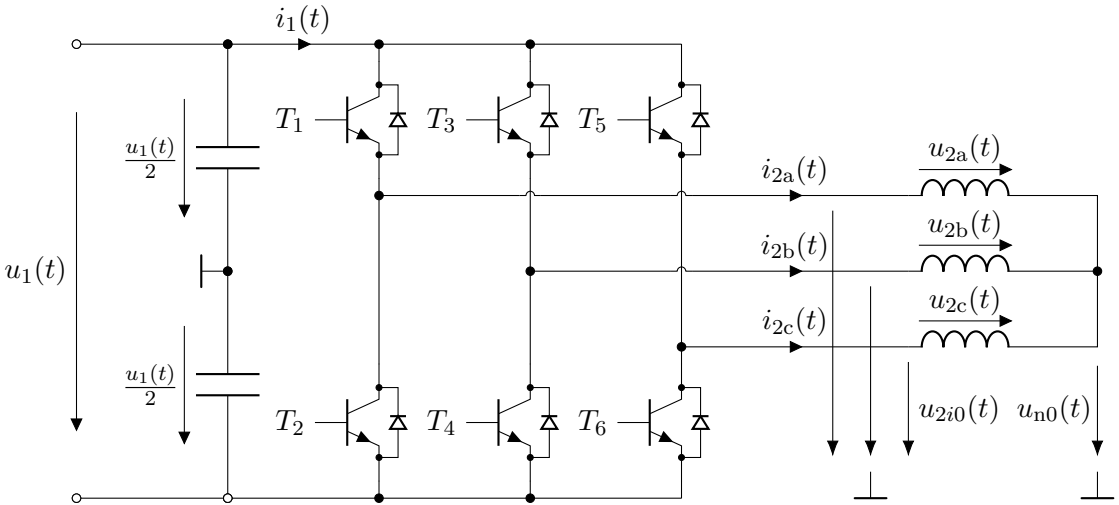

Fig. 6.18: Three-phase two-level AC/DC converter with symmetric load in star connection

Three-phase converter with symmetric load in star connection (cont.)

Assuming a star-connected load, the three-phase currents sum up to zero:

$$i_{2\mathrm{a}}(t) + i_{2\mathrm{b}}(t) + i_{2\mathrm{c}}(t) = 0. \tag{6.29}$$

If the star point is not connected to ground, $u_{\mathrm{n}0}(t) \neq 0$ may occur leading to a load voltage of

$$u_{2\mathrm{a}}(t) = u_{2\mathrm{a}0}(t) - u_{\mathrm{n}0}(t), \quad u_{2\mathrm{b}}(t) = u_{2\mathrm{b}0}(t) - u_{\mathrm{n}0}(t), \quad u_{2\mathrm{c}}(t) = u_{2\mathrm{c}0}(t) - u_{\mathrm{n}0}(t). \tag{6.30}$$

To calculate $u_{\mathrm{n}0}(t)$ one can utilize the load equation (assuming an inductive load):

$$u_{2i}(t) = L\frac{\mathrm{d}}{\mathrm{d}t} i_{2i}(t) + u_{\mathrm{n}0}(t) \tag{6.31}$$

summing up to

$$3u_{\mathrm{n}0}(t) + L\frac{\mathrm{d}}{\mathrm{d}t}\left(i_{2\mathrm{a}}(t) + i_{2\mathrm{b}}(t) + i_{2\mathrm{c}}(t)\right) = u_{2\mathrm{a}0}(t) + u_{2\mathrm{b}0}(t) + u_{2\mathrm{c}0}(t) \tag{6.32}$$

and finally delivering the star-to-ground voltage as

$$u_{\mathrm{n}0}(t) = \frac{1}{3}\left(u_{2\mathrm{a}0}(t) + u_{2\mathrm{b}0}(t) + u_{2\mathrm{c}0}(t)\right). \tag{6.33}$$

Three-phase converter with symmetric load in star connection (cont.)

No.	s_a	s_b	s_c	$\frac{u_{2\mathrm{a}0}}{u_1}$	$\frac{u_{2\mathrm{b}0}}{u_1}$	$\frac{u_{2\mathrm{c}0}}{u_1}$	$\frac{u_{2\mathrm{a}}}{u_1}$	$\frac{u_{2\mathrm{b}}}{u_1}$	$\frac{u_{2\mathrm{c}}}{u_1}$	$\frac{u_{\mathrm{ab}}}{u_1}$	$\frac{u_{\mathrm{bc}}}{u_1}$	$\frac{u_{\mathrm{ca}}}{u_1}$	$\frac{u_{\mathrm{n}0}}{u_1}$
0	-1	-1	-1	$-\frac{1}{2}$	$-\frac{1}{2}$	$-\frac{1}{2}$	0	0	0	0	0	0	$-\frac{1}{2}$
1	$+1$	-1	-1	$+\frac{1}{2}$	$-\frac{1}{2}$	$-\frac{1}{2}$	$+\frac{2}{3}$	$-\frac{1}{3}$	$-\frac{1}{3}$	$+1$	0	-1	$-\frac{1}{6}$
2	$+1$	$+1$	-1	$+\frac{1}{2}$	$+\frac{1}{2}$	$-\frac{1}{2}$	$+\frac{1}{3}$	$+\frac{1}{3}$	$-\frac{2}{3}$	0	$+1$	-1	$+\frac{1}{6}$
3	-1	$+1$	-1	$-\frac{1}{2}$	$+\frac{1}{2}$	$-\frac{1}{2}$	$-\frac{1}{3}$	$+\frac{2}{3}$	$-\frac{1}{3}$	-1	$+1$	0	$-\frac{1}{6}$
4	-1	$+1$	$+1$	$-\frac{1}{2}$	$+\frac{1}{2}$	$+\frac{1}{2}$	$-\frac{2}{3}$	$+\frac{1}{3}$	$+\frac{1}{3}$	-1	0	$+1$	$+\frac{1}{6}$
5	-1	-1	$+1$	$-\frac{1}{2}$	$-\frac{1}{2}$	$+\frac{1}{2}$	$-\frac{1}{3}$	$-\frac{1}{3}$	$+\frac{2}{3}$	0	-1	1	$-\frac{1}{6}$
6	$+1$	-1	$+1$	$+\frac{1}{2}$	$-\frac{1}{2}$	$+\frac{1}{2}$	$+\frac{1}{3}$	$-\frac{2}{3}$	$+\frac{1}{3}$	1	-1	0	$+\frac{1}{6}$
7	$+1$	$+1$	$+1$	$+\frac{1}{2}$	$+\frac{1}{2}$	$+\frac{1}{2}$	0	0	0	0	0	0	$+\frac{1}{2}$

Tab. 6.2: Switching states and resulting voltages of the three-phase two-level AC/DC converter with symmetric load in star connection (with $2^3 = 8$ possible switching states)

Three-phase fundamental frequency modulation (aka six-step mode)

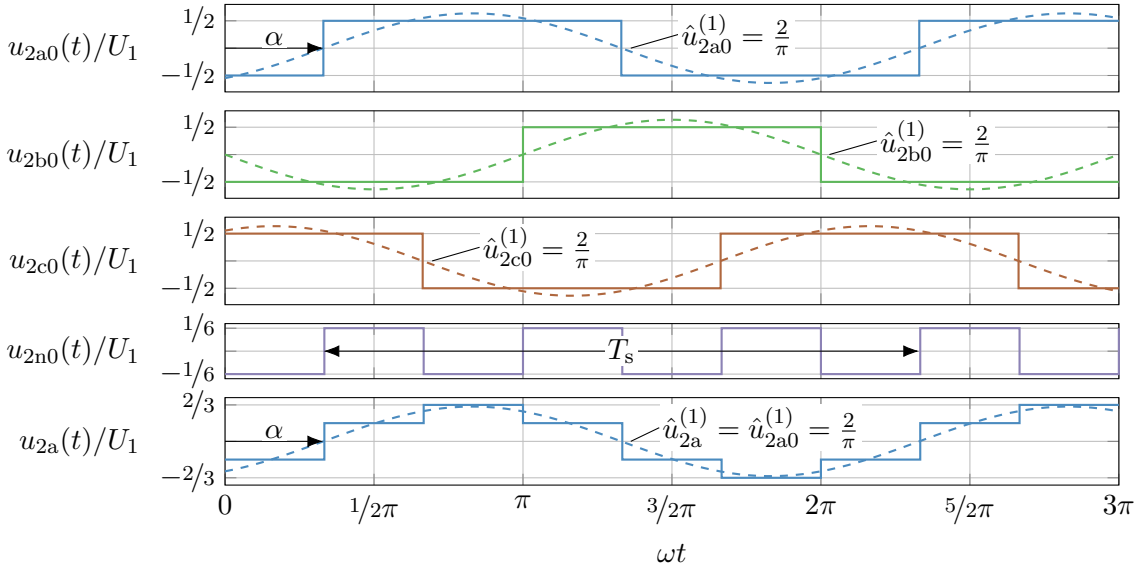

Three-phase fundamental frequency modulation (cont.)

From the previous figure and voltage equations, we can summarize the following observations:

- Due to the fundamental frequency modulation, the switching frequency of the inverter is identical to the fundamental frequency: $f_\mathrm{s} = \omega/2\pi$.
- The star-to-ground voltage $u_{\mathrm{n}0}(t)$ shows a rectangular signal pattern with triple fundamental frequency.
- Consequently, it does not influence the fundamental output voltage, that is, the fundamental components of the line-to-ground voltage $u_{2i0}(t)$ as well as the load voltage $u_{2i}(t)$ are identical: $\hat{u}_{2i0}^{(1)} = \hat{u}_{2i}^{(1)}$.

Note on the star point

The previous analysis assumed a non-connected star point, which comes with certain advantages, e.g., on the rejection of current harmonics. If, however, the star point would be connected, the three-phase converter can be interpreted and analyzed as three independent single-phase converters (each driven by a half bridge).

Three-phase pulse width modulation (PWM)

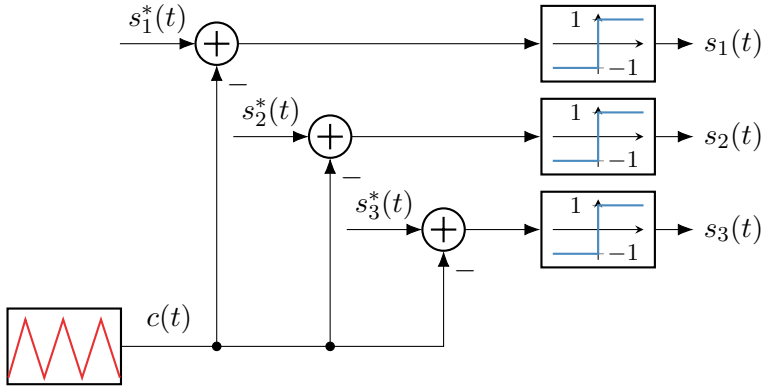

Fig. 6.19: Three-phase PWM (note: a distinction between interleaved and complementary PWM is not relevant here, as the three-phase converter operates on a half-bridge basis while the previously considered single-phase converter was based on a full bridge. While independent and phase-shifted carriers per phase could be also used in the three-phase converter, this is typically not utilized due to increasing current harmonics.)

Three-phase PWM example (with ref. modulation index $m = 0.5$)

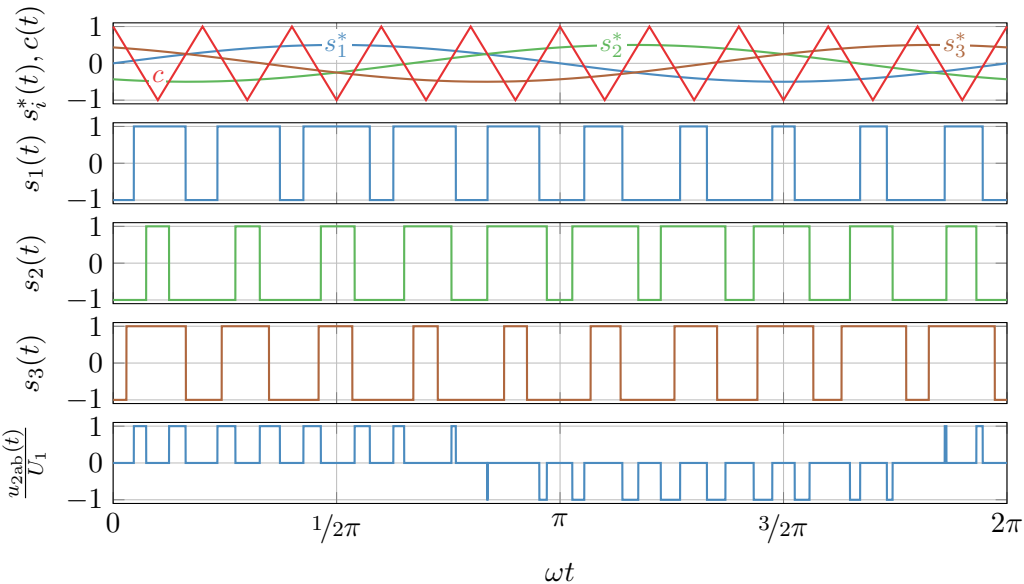

Three-phase PWM example (with ref. modulation index $m = 1$)

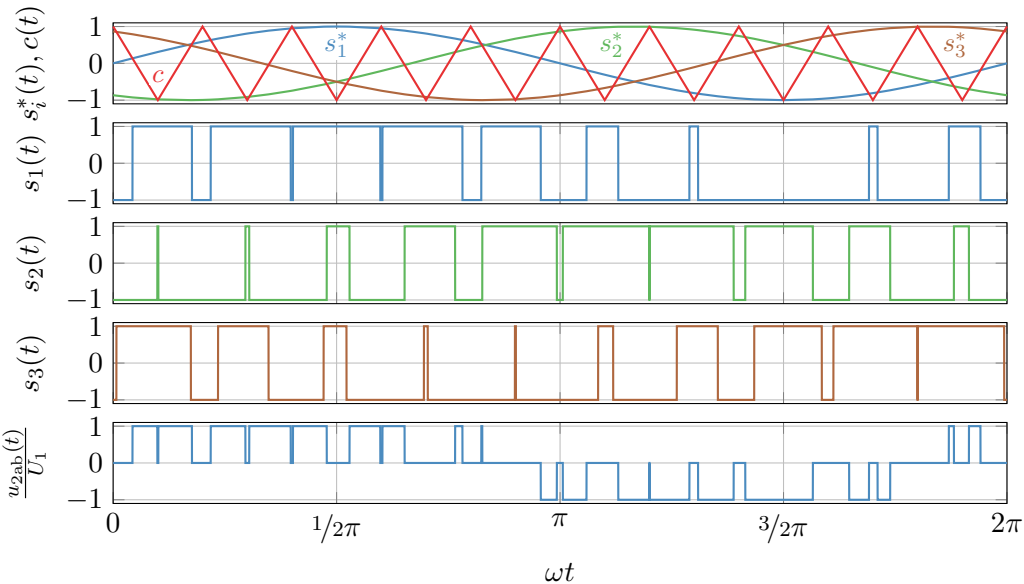

Three-phase PWM example (with ref. modulation index $m = 1.18$)

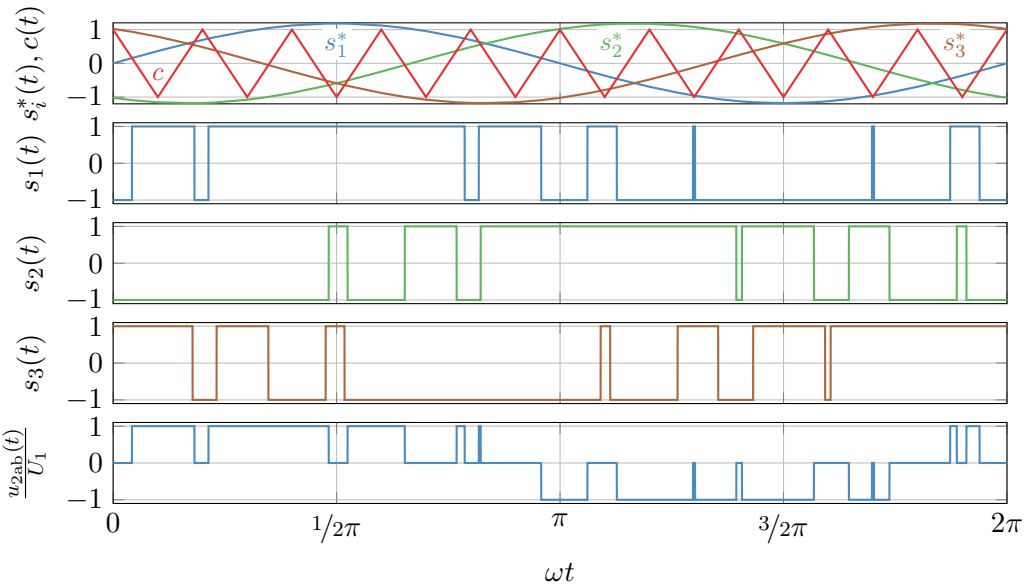

Section summary

This section provided an introduction to transistor-based AC/DC converters. The key takeaways are:

- They render themselves (half/full) bridge topologies as already known from the DC/DC converter context.
- Can transfer power in both directions and handle all four quadrants on the AC side.
- Require modulation strategies to generate the desired output voltage:
  - High switching frequency PWM (low harmonics, below maximum conv. utilization) or
  - Low switching frequency fundamental modulation (max. utilization, but high harmonics).
- The output voltage amplitude and phase angle can be adjusted to achieve arbitrary power factors for grid operation or to supply various loads such as DC or AC motors.

While this section only covered a very brief overview about these self-commutated converters, the following aspects are, among other, important for practical applications:

- closed-loop control,
- Further modulation strategies (e.g., space vector modulation or optimized pulse pattern),
- converters with a current source (instead of voltage source) within the DC link.

Table of contents

English-German dictionary I

active power	Wirkleistung
angle	Winkel
apparent power	Scheinleistung
average	Mittelwert
boundary conduction mode (BCM)	Lückgrenzbetrieb
bridge	Brücke / Brückenschaltung
capacitance	Kapazität [Größe]
capacitor	Kondensator [Bauelement]
choke	Drossel / Spule
circuit	Schaltkreis
commutation	Kommutierung

English-German dictionary II

continuous conduction mode (CCM)	Nicht-lückender Betrieb
converter	Umrichter
copper	Kupfer
current	Strom
derivative	Ableitung
differential equation	Differentialgleichung
discontinuous conduction mode (DCM)	Lückbetrieb
duty cycle	Tastgrad
efficiency	Wirkungsgrad
energy	Energie
fan	Lüfter
firing angle	Zünd- / Steuerwinkel

English-German dictionary III

flyback converter	Sperrwandler
forward converter	Durchflusswandler
frequency	Frequenz
fundamental frequency modulation	Grundfrequenz-/Blocktaktung
galvanic isolation	Galvanische Trennung
hard switching	Hartes Schalten (unter Last)
heat	Wärme
inductance	Induktivität [Größe]
inductor	Spule [Bauelement]
interlocking time	Wechselrichtersperrzeit
inverter	Wechselrichter
line choke	Netzdrossel

English-German dictionary IV

load	Last / Belastung
losses	Verluste
modulation ratio	Aussteuergrad
nameplate	Typenschild
overmodulation	Übermodulation
point of common coupling	Ankopplungs-/Verknüpfungspunkt
power	Leistung
power electronics	Leistungselektronik
power factor	Leistungsfaktor
power factor correction (PFC)	Leistungsfaktorkorrekturfilter
reactive power	Blindleistung

English-German dictionary V

rectifier	Gleichrichter
resistance	Widerstand [Größe]
resistor	Widerstand [Bauelement]
ripple	Schwankung
root mean square (RMS)	Effektivwert
semiconductor	Halbleiter
soft switching	Weiches Schalten (lastlos)
steady state	Stationärer Zustand
step-down / buck converter	Tiefsetzsteller
step-up / boost converter	Hochsetzsteller
switch	Schalter
terminal	Anschlussfeld

English-German dictionary VI

total harmonic distortion (THD)	Oberschwingungsgesamtverzerrung
transformer	Transformator
transient	Transienter Zustand
unit	Maßeinheit
voltage	Spannung
work	Arbeit
zero current switching	Nullstromschalten
zero voltage switching	Nullspannungsschalten

Nomenclature I

$x(t)$	time-dependent, scalar quantity
$\hat{x}$	(fundamental) amplitude of a signal $x(t)$
$\hat{x}^{(k)}$	k-th harmonic amplitude of a signal $x(t)$
$\boldsymbol{x}(t)$	time-dependent, vectorial quantity
X	constant, scalar quantity (e.g., root mean square value)
$\boldsymbol{X}$	matrix
$\overline{x}$	average
$\overline{x}(t)$	dynamic average ($t \in [-T_\mathrm{s}/2, +T_\mathrm{s}/2]$)
$\underline{X}$	complex quantity
$\underline{X}^*$	complex conjugate
$\frac{\mathrm{d}}{\mathrm{d}t}x(t)$	derivative (first derivative w.r.t. time)